TESIS DOCTORAL

2018

ANÁLISIS DE LA EVOLUCIÓN NEUROCRANEAL EN LA RADIACIÓN TEMPRANA DE EUSUCHIA

ALEJANDRO SERRANO MARTÍNEZ

PROGRAMA DE DOCTORADO EN CIENCIAS

FRANCISCO ORTEGA COLOMA
FABIEN FLORENT KNOLL

RESUMEN

El de los crocodilomorfos es un linaje de gran éxito evolutivo, abarcando 230 millones de años desde su origen, a finales del Triásico, hasta la actualidad. Los restos de estos animales son comunes en yacimientos mesozoicos y cenozoicos de todo el globo, mostrando una gran diversidad y abundancia en estos ecosistemas pretéritos. Entre estos, destaca el yacimiento de Lo Hueco (Cretácico Superior, Fuentes, Cuenca), por la cantidad y preservación de restos de crocodilomorfo hallados. Los especímenes extraídos en el yacimiento de Lo Hueco presentan caracteres morfológicos que han permitido establecer tres morfotipos de eusuquios basales, dos de ellos atribuidos a nuevas especies endémicas de este yacimiento: *Lohuecosuchus megadontos*, *Agaresuchus fontisensis* y Allodaposuchidae indeterminado.

En la presente tesis doctoral se reconstruyen y describen las cavidades intracraneanas de varios de los ejemplares de eusuquio basal procedentes del yacimiento de Lo Hueco. Los especímenes fueron escaneados mediante Tomografía Axial Computerizada (TAC), lo que permite acceder al interior de la pieza para reconstruir las cavidades internas, incluyendo el encéfalo, el oído interno, y los sistemas de senos faringotimpánicos y paranasales. Estas cavidades alojaron también algunos de los órganos sensoriales de estos animales, y mediante una serie de medidas lineales y volumétricas de estas regiones se ha podido estimar las capacidades neurosensoriales y cognitivas que tenían estos animales en vida. Estos datos se han comparado con los de varios ejemplares de crocodilios actuales de distintos tamaños, así como taxones externos a Crocodylomorpha, como aves, escamosos o tortugas.

Los resultados obtenidos muestran que las cavidades intracraneanas de los cocodrilomorfos son estructuras muy conservadoras, siendo las de los taxones actuales muy similares a los ya presentes en las formas basales del grupo. Sin embargo, se han encontrado algunos caracteres que parecen seguir un patrón filogenético, como la forma de la superficie dorsocaudal del cerebro, la forma de los divertículos intertimpánicos o la longitud relativa del seno faríngeo medio. Los resultados también confirman que las capacidades neurosensoriales y cognitivas presentes en las especies actuales de crocodilios, como un agudo sentido del olfato y la vista o una adaptación auditiva a frecuencias bajas, ya estaban presentes en los miembros basales de Eusuchia.

ABSTRACT

Crocodylomorpha is a very successful lineage, spanning 230 million years from its origin, in the Late Triassic, to present day. Crocodylomorph remains are common in Mesozoic and Cenozoic fossil sites across the world, showing a high diversity and abundance in these remote ecosystems. The fossil site of Lo Hueco (Upper Cretaceous, Cuenca, Spain) is noteworthy because of the number and preservation of the crocodylomorph remains found. The Lo Hueco specimens have morphological characters that allow establishing three basal eusuchian morphotypes, two of them diagnosed as new endemical species: *Lohuecosuchus megadontos*, *Agaresuchus fontisensis* and indeterminate Allodaposuchidae.

The main aim of this PhD dissertation is to reconstruct and describe the inner skull cavities of several of the basal eusuchian samples from the Lo Hueco fossil site. The specimens were scanned using the CT-Technology, which allows to observe the interior of the specimen and reconstruct its inner cavities, including the brain itself, inner ear and pharyngotympanic and paranasal sinus systems. The inner cavities also housed some of the neurosensorial organs of these animals. These regions have been linearly and volumetrically measured to estimate the neurosensorial and cognitive capabilities of these animals. These data were compared to those of several extant crocodylians of different sizes, and to those of some specimens from the outgroup of Crocodylomorpha, such as birds, squamates and turtles.

The results show that the inner skull cavities of crocodylomorphs are very conservative structures, being those of the extant specimens very similar to the inner skull cavities of the basal members of the group. However, there are some characters that varies during the course of evolution, such as the shape of the caudodorsal region of the cerebrum, the shape of the intertympanic diverticula or the relative length of the median pharyngeal sinus. Our results also suggest that the neurosensory and cognitive capabilities of extant crocodylians, such as a sharp olfactory and visual acuity, or an adaptation to low-frequence hearing, were already present in early members of Eusuchia.

AGRADECIMIENTOS

Son muchas las personas que han contribuido, consciente o inconscientemente, a la realización de esta tesis doctoral, y por ello os habéis ganado no solo un huequito en este trabajo, sino uno bien grande en mi corazón. Probablemente me deje a gente, pero a todos los que estáis leyendo esto os digo: no agradeceré a la mitad de vosotros ni la mitad de lo que querría, y lo que yo querría es menos de la mitad de lo que la mitad de vosotros merecéis.

Las primeras personas a las que quiero incluir en este apartado son mis directores, que han hecho posible todo esto. A Fabien le debo mucho, ya que me ofreció la posibilidad de continuar en mundo de la paleontología tras terminar la carrera, en un momento en el que no veía nada claro poder seguir en este campo al no encontrar ninguna opción para el Proyecto Fin de Máster. Me acogió y rebuscó hasta conseguir un material para estudiar que se adecuase a mis preferencias. Y vaya si lo logró. Una colección de dientes de dinosaurio terópodo de Níger, todo un sueño para mi dinofriki interior. Y no solo eso; con este trabajo empecé a atisbar todo lo que conlleva la investigación: no solo emoción al descubrir algo nuevo, sino también el trabajo que conlleva tener que repetir los análisis estadísticos una y otra vez porque hay un dato mal puesto, la constante búsqueda de bibliografía actualizada o todo lo que hay que hacer y rellenar para hacer público tu trabajo. Y cuando terminé el máster, me ofreció la posibilidad de continuar trabajando en paleoneuroanatomía con él. Me ayudó a buscar un puesto para poder empezar a hacer reconstrucciones en el Museo Nacional de Ciencias Naturales hasta conseguir una beca, y me llevó a diversas instituciones, como el ESRF en Grenoble, a hacer TACs a varias piezas. No olvidaré que estoy aquí gracias a que tú me abriste las puertas.

Y si Fabien fue el que me abrió la puerta, Francisco Ortega, Patxi, fue la persona que me permitió quedarme. Él fue el que me cedió el material de Níger, dándome una primera oportunidad que superaba con creces mis expectativas. Y al cerrar este estudio, decidió mantenerme a su lado al sugerir analizar las cavidades internas de la gran colección de cráneos de cocodrilo hallados en el yacimiento de Lo Hueco, al mismo tiempo que no paró hasta que conseguí obtener una beca para quedarme en el grupo de investigación. A partir de entonces, Patxi siempre me ha hecho sentir una parte importante del grupo, confiándome tareas que no habría creído ser capaz de hacer. Ser un buen jefe de grupo, dirigiendo y coordinando todos los temas que trata su equipo ya es difícil. Pero el compaginarlo con preocuparse de la situación de los miembros de su equipo, moviendo cielo y tierra hasta conseguir los medios para estos

puedan continuar con su investigación es algo propio de muy pocos, y agradezco enormemente que tú seas uno de ellos.

También quiero mencionar a José Luis Sanz, Pepelu, una persona que, si bien no ha tenido que ver en la redacción de este trabajo, ha influido enormemente en él, ya que me inspiró (a mí y a toda una generación) para dedicarme a esta pasión que tengo desde que soy pequeño.

Centrándome ya en el Grupo de Biología Evolutiva, no puedo dejar de mencionar al "consejo de sabios", que han supuesto un referente para mí. A Fer le conocí en mi primer año en Las Hoyas, y ya entonces me impresionó su buen rollo combinado con una profesionalidad apabullante. Allí también conocí a Iván-o-Chicho, mi mentor en el tema de cocodrilos, cuyo ingenio en la chanza solo es comparable con su altruismo, estando dispuesto a ayudarme siempre que lo necesitaba. ¡Una cerveza por vosotros! Adán, la persona más trabajadora que conozco, con la que siempre puedes contar en temas paleontológicos y ajenos, como salir a cenar a un asturiano por el centro, una sesión de películas lamentables o una partida de Catán. Fátima, nuestra superpreparadora y compañera de TACs, con la que es imposible aburrirse. Creo que es esencial remarcar que sin ti y tu equipo (Ana, Natalia, Susana L., Susana B., Marta, Javier, Elena, Irene), ni esta ni ninguna de las tesis de este grupo habría salido adelante. También quiero mencionar a J. M. Gasulla, un grande con el que me encantaría seguir compartiendo excavaciones en Morella (y donde haga falta), a Andrea Arcucci, de la que he aprendido muchísimo y que siempre me ha hecho sentir valorado, y a Santiago Martín, con quien he compartido pocos pero muy interesantes debates sobre paleontología.

También quiero agradecer a mis compañeros desde el origen de esta loca idea que es la paleontología, a quienes me acerqué durante mis primeras excavaciones en Las Hoyas, y con quienes he acabado compartiendo todas y cada una de mis experiencias paleontológicas: mis compañeros Trilobiteens™. A Carlos, al que considero un alma gemela, y con quien tuve la gran suerte de juntarme ya en los últimos años de carrera. Todo esto hubiera sido mucho más duro sin nuestras payasadas (falla hombre, falla). Y Dani, porque hablar contigo siempre hace que saque lo mejor de mí, científica y personalmente. Creo con sinceridad que es muy difícil encontrar a alguien tan grande y tan dispuesto a ayudar como tú. ¡Espero que compartamos muchas más excavaciones juntos!

Y lo mejor es que esto solo fue el comienzo, el inicio de un club llamado por las malas (y sabias) lenguas "malditos teenagers®", y con sede en L'Europee, al que se fué añadiendo más y más gente, cada uno añadiendo algo a este cóctel de paleofrikis: Nacho, con quien también

coincidí en Las Hoyas, y que pese a acabar fuera de la paleo y viéndonos menos, cada vez que nos juntamos es como si nos viésemos todos los días. Pedro, que dio ese puntito internacional que todo buen grupo debe tener para hacer humor a base de malentendidos “portuñoleses”, y que tanto me ayudó con el máster. Y no contento con eso, contó conmigo en 2014 para la campaña en Casal da Costa, donde excavé mi primer dinosaurio (y vaya dinosaurio). Elena-chan y su eterna sonrisa, por muy malas que vengan, que tantísimo me ayudó cuando estaba totalmente perdido en eso que llaman “solicitar correctamente una FPU”. Si he llegado hasta aquí, es en una gran parte por ti. Adrián, un crack en todos los aspectos. Alguien capaz de juntarte un análisis estadístico de nombre impronunciable, una canción de Iron Maiden y un montaje sacado de los rincones más oscuros de internet es alguien a quien nunca deberías alejar de tu lado. Sori (aka Marcos), mi alumno en este ingrato mundo que son los TACs, que ha aprendido todo lo que yo sé, pero obviando mi mala suerte al obtener resultados decentes. Pak, incombustible e indesmoralizable, que su lucha por hacer lo que le gusta, cueste lo que cueste, me ha servido de referencia en muchísimas ocasiones para no rendirme. Elisabete, con quien me junté por culpa de los análisis estadísticos, que acabó siendo una grandísima compañera de trabajo y de excavaciones, y que siempre ha tenido sonrisas y buenas palabras para mí. Aitziber, que pese a su genio norteño es una de las personas más voluntariosas y amables que conozco. Ya puede estar pasándolas canutas, que siempre tiene tiempo para interesarse por cómo te va todo, o si puede ayudarte en algo. El gran fichaje del Atance, sin duda. Y las últimas incorporaciones, con quien no he tenido el gusto de compartir tantísimo tiempo, pero que aun así se han ganado el derecho de tener un huequito en este capítulo. Ane, mi compañera cocodrilera. Iba a ponerte lo mismo que a Páramo, pero como no es cuestión, creo que es mejor decir que esta tesis tampoco hubiera llegado a ser lo que es sin tu ayuda y todas las referencias que me has pasado. ¡Ánimo con esa base de datos! Andrea, siempre con una sonrisa en la cara, aunque la empujes ladera abajo. Una sonrisa que contagia a los demás su buen rollo, aunque hayan tenido un día horrible. Eloy, que en un bucle espacio-temporal es capaz de ser la fusión del Greg Paul de 1988, el Mauricio Antón del 2004, y el Míster Jägger del 2016, pero en el 2018 y con mucho más swag. Y Dani(lopithecus), con quien por desgracia no tuve demasiado trato durante la carrera, pero me ha demostrado ser un grandísimo compañero y amigo. ¡Por más canciones como las del EJIP de Portugal!

Y no podían faltar mis compañeros toxicólogos de la UNED. A mis compis de despacho, Irene, Marta y Ana, que han aguantado mi control sobre el aire acondicionado sin apenas quejas (a cambio de galletas, todo hay que decirlo). Y por los buenos ratos con Charo, Óscar, Lola y Mónica. ¡¡Vámos Amililllo, que ya no queda nada!!

Quiero también añadir a todos los compañeros que durante la carrera, el máster y el doctorado estuvieron ahí para ayudarme y hacerme mucho más interesante el camino hasta aquí. Eva, Javi, Ali, Lorena, Patri, Joak, Adri, Inés, Ana, Judith, Gloria, Alex, Candela, Sandra, Sofía, Ana, Beti, Ioannis, Álvaro, Hugo, Abel, David.

However, they aren't the only ones that put up me. During the three months I spent in Birmingham, I met a group of wonderful people that embraces me as one of them. Juan, Andy, Dan, Emma, Pedro, thank you very much. I will always remember you when I will make a joke to my workmates. And special acknowledgements to Stephan, who helps me more than I could imagine and always was there to take care of me.

Veo también esencial incluir también a una serie de personas sin las cuales esta tesis no habría llegado muy lejos, ya no por apoyo emocional, sino por medios. Al Dr. Josep Fortuny, del Institut Català de Paleontologia Miquel Crusafont, que amablemente me cedió los TACs de varios especímenes actuales, con los que pude empezar a trabajar hasta que conseguí, tras muchos y desesperantes intentos infructuosos, empezar a obtener resultados. También a Luis Carlos Vicente y el personal del Centro Médico de Diagnóstico, a Marina de la Fuente y el personal del Hospital Quirón Ruber, y al Céntro de Diagnóstico Cuenca, gracias a los cuales conseguí unas imágenes suficientemente nítidas como para poder trabajar con los ejemplares de Lo Hueco.

Entrando en lo personal, hay un montón de gente a la que quiero agradecer el apoyo en los momentos difíciles, el interés en como llevaba el trabajo y sobre todo su compañía.

A Gloria, Rubén, y Guille, con los que he compartido millones de buenos momentos. Os habéis convertido casi desde el principio en personas muy importantes para mí, que siempre están ahí. A David y María, mi hermanita, con quien no tenía suficiente contacto así que compartimos juntos esta forma de vida que es la biología, lo que me ha unido a ti incluso más. A mi grupito: Guti, Antonio, Deva, Almu y Lucía, por esas tardes de domingo que, pese a la pereza, no cambiaría por nada. Y en especial a mi gran amiga Mª Isabel, que tiene la capacidad de hacerme sentir mucho más grande de lo que yo creo que soy. A mis compañeros warhammeros, Rubén, Óscar, Vicente, Luisfer, Dani y Fer, con quien he pasado tardes memorables gracias a unas insignificantes tiradas de dados. También a mis compañeros del KDT, que han soportado mis batallitas de excavaciones y mis comentarios biológicos sin venir a cuento: Alfonso, Pablo, Marcos, Carro, Zamo, Teto, David, Alba Monty, María, Inma, Maya, Mila, Lucía, Alba S., Silvia, Elisa, y en especial a Diana, la otra doctora del grupo, que tanto

me ha ayudado, comprendido y animado para seguir en este duro sendero que es la investigación.

Voy a ir concluyendo con los pesos pesados. Muchas gracias, mamá, papá, por comprar a vuestro hijo todos esos muñecos, películas y documentales de dinosaurios y esas colecciones interminables de fascículos. Por apoyarme en mi decisión de dedicarme a lo que me gustaba. Por ayudarme, lo pidiera o no. Y básicamente, por estar ahí SIEMPRE. Y a Guille, que desde pequeño jugó conmigo a los "dinomonstruos", y con quien siempre puedo contar para echarme unas risas y evadirme de todo lo demás. A mis tíos y primos, que han aguantado mis historias en las excavaciones (eso os pasa por preguntar), y en especial a Mª Cruz, que ha llegado a secuestrarme en las reuniones familiares para que le contase más y más cosas acerca de la biología, evolución, paleontología, y demás cosas de las que se supone que sé algo. Y a mis abuelos, que tanto me han cuidado y se han interesado por mí, pese a no entender del todo "por qué me voy tan lejos si en el patio de casa también hay arena para excavar".

Y también muchas gracias a mi otra familia, Marta, Macu y José, por apoyarnos e interesaros constantemente en que tal iba todo, por esas deliciosas cenas entre semana (alitas mmmm), y por tratarme siempre como a un hijo.

Y finalmente, Mery. No hay palabras para agradecer todo lo que has hecho, por esta tesis y por mí en general. ¿Quién me iba a decir que al entrar en la primera clase de Biología no solo estaba iniciando mi carrera en el tema en el que quería trabajar desde pequeño, sino que también conocería a la persona con la que quiero compartir mi futuro? Por darme ánimos y hacerme reír cuando estoy de bajón. Por nuestras locuras. Por ser mi compi de chistes malos. Por empezar y terminar cada día con una sonrisa. Por cada aventura juntos, y por las que nos quedan. Por estar siempre detrás de mí solucionando mis muchos despistes, a mi lado para ayudarme a levantarme cuando me caigo, y delante para guiarme. Por esto y millones de cosas más, muchísimas gracias.

Esta investigación se llevó a cabo gracias a una Ayuda para la Formación de Personal Universitario FPU13/03362, del Ministerio de Educación, Cultura y Deporte, cofinanciada por la Universidad Nacional de Educación a Distancia, que además incluía una ayuda para realizar una estancia de tres meses en la Universidad de Birmingham (Reino Unido). Este trabajo fue financiado también por los proyectos de investigación CGL2015-68363-P, del Ministerio de Economía, Industria y Competitividad y DGCLM/140565, de la Junta de Comunidades de Castilla-La Mancha.

ÍNDICE

- 3º PARTE

PRIMERA PARTE

FIRST PART

CAPÍTULO 1: INTRODUCCIÓN

INTRODUCTION

Introducción a la sistemática de Crocodylomorpha

La historia evolutiva de Crocodylomorpha se remonta a hace algo más de 250 millones de años, tras la gran extinción de finales del Pérmico. Durante el Triásico tuvo lugar una de las radiaciones evolutivas más importantes dentro de los vertebrados, en la que se diferenciaron los dos linajes principales de reptiles arcosaurios. El primero de ellos, Avemetatarsalia, incluye a los pterosaurios, los dinosaurios y las aves; mientras que el segundo, dará lugar a Crurotarsi (Fig. 1.1), grupo en el que se incluyen los cocodrilos actuales.

Los crurotarsos basales están representados por formas muy diversas (Brusatte et al., 2010; Nesbitt, 2011; Ezcurra, 2016): los fitosaurios son un grupo de animales semiacuáticos y longirrostros del Triásico tardío de Centroeuropa, norte de África y Norteamérica. Sin embargo, su posición filogenética dentro de Crurotarsi es dudosa, apareciendo en algunos análisis como grupo hermano de Archosauria (Nesbitt, 2011), o como el grupo de crurotarsos más basal (Ezcurra, 2016). Dentro de crurotarsos también se incluyen grupos como los aetosaurios (herbívoros acorazados del Triásico tardío de América, África y Europa); los ornitosuquios (del Triásico tardío de Argentina y Escocia, cuya posición filogenética dentro de Crurotarsi es aún incierta; von Baczko y Desojo, 2016); los rauisuquios (de amplia distribución y morfologías muy variables); y, finalmente, los crocodilomorfos, el único de estos grupos que supera el límite Triásico-Jurásico.

El clado Crocodylomorpha está ya bien delimitado gracias a numerosas sinapomorfías (Walker, 1970; Benton and Clark, 1988; Walker et al., 2002; Sereno et al., 2005). Está compuesto por una serie de grupos tanto fósiles como actuales. El grupo más basal, los ‘esfenosuquios’, está formado por diversas formas circunscritas al Triásico tardío-Jurásico temprano, y caracterizadas por tener unas extremidades muy gráciles. El grupo de los ‘esfenosuquios’ está formado por ejemplares muy fragmentarios y con numerosos caracteres morfológicos conflictivos, por lo que su monofilia está en debate, formando (Nesbitt, 2011)(Nesbitt, 2011)(Nesbitt, 2011)una serie de taxones hermanos de Crocodyliformes según las hipótesis filogenéticas más recientes (Nesbitt, 2011; Irmis et al., 2013).

Dentro de Crocodyliformes, se incluyen una serie de formas conocidas tradicionalmente como ‘protosuquios’, que van desde el Triásico al Cretácico, y presentan una amplia diversidad y distribución geográfica. Estos crocodiliformes no forman un grupo monofilético, y quedan distribuidos como un conjunto de taxones hermanos sucesivos de Mesoeucrocodylia.

Los mesoeucrocodilios a su vez comprenden dos grandes linajes: Notosuchia y Neosuchia. Los notosuquios son formas terrestres con una gran variedad de morfologías y dentición heterodonta, cuyo rango temporal abarca desde el Jurásico medio hasta el Mioceno medio (Gasparini, 1971; Pol et al., 2014; Dal Sasso et al., 2017).

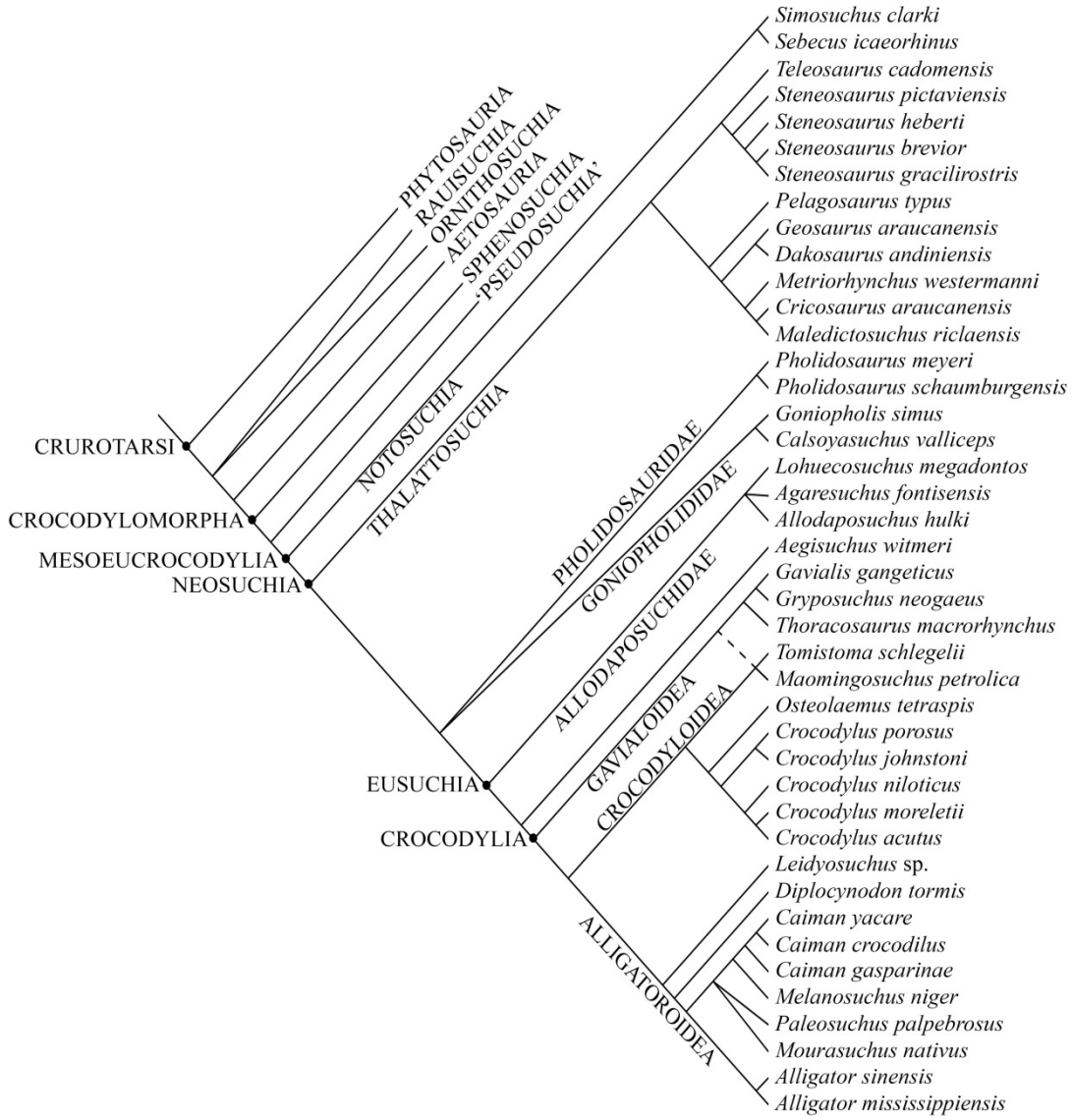

Fig. 1.1: Árbol filogenético de Crurotarsi, en el que se incluyen los taxones estudiados en la presente tesis doctoral (Modificado de Brochu, 2011; Brusatte et al., 2010; Fanti et al., 2016; Mueller-Töwe, 2005; Narváez et al., 2016).

Phylogeny of Crurotarsi, including all studied taxa in this PhD thesis (Modified from Brochu, 2011; Brusatte et al., 2010; Fanti et al., 2016; Mueller-Töwe, 2005; Narváez et al., 2016).

Por otro lado, los neosuquios incluyen, a su vez, una serie de formas longirrostras (Benton and Clark, 1988), entre las que destacan los talatosuquios, con una distribución temporal que va desde el Jurásico medio hasta el Cretácico temprano. Estos cocodrilos poseían adaptaciones a un modo de vida totalmente acuático, que en el caso de los metriorrínquidos, ya estaban completamente adaptados a una vida pelágica marina, con cuerpos alargados, cola con forma de aleta heterocerca para impulsarse, extremidades con forma de pala y unas glándulas de la sal hipertrofiadas (Fernández and Gasparini, 2008; Herrera et al., 2013a). Además, los neosuquios más derivados incluyen formas semiacuáticas como los goniofolídidos, del Jurásico-Cretácico o los 'folidosáuridos',

del Jurásico tardío-Cretácico, ambos con una amplia distribución geográfica (De Andrade et al., 2011; Bronzati et al., 2012).

El otro gran clado dentro de Neosuchia es el formado por los cocodrilos modernos o Eusuchia (Huxley, 1875), grupo monofilético definido por varias sinapomorfías como la presencia de una coana secundaria muy retrasada y formada por los pterigoides, y por la presencia de vértebras procélicas (Brochu, 1999; Salisbury et al., 2006).

Eusuchia incluye a una serie de grupos basales como Paralligatoridae, Hylaeochampsidae o Allodaposuchidae (Buscalioni et al., 2011; Turner, 2015; Narváez et al., 2016) que forman los sucesivos clados hermanos de Crocodylia, grupo que engloba a los representantes actuales del linaje.

Crocodylia integra nueve géneros y más de una veintena de especies actuales (Shirley et al., 2018) distribuidas en tres linajes: Gavialoidea, Crocodyloidea y Alligatoroidea. Sin embargo, en la actualidad, la diversidad mostrada por los cocodrilos es muy inferior a la observada a lo largo de su historia evolutiva, estando restringidos a hábitats semiacuáticos de distribución circumtropical. Los primeros registros de Crocodylia datan del Cretácico Superior de América del Norte (Mook, 1941; Erickson, 1972; Norell et al., 1994; Williamson, 1996; Wu et al., 1996), estimándose una divergencia entre los tres grandes linajes anterior al Campaniense (Brochu, 2003).

El estudio de formas de Eusuchia basales llevado a cabo durante la última década (Buscalioni et al., 2011; Bronzati et al., 2012; Blanco et al., 2014; Puértolas-Pascual et al., 2014; Turner, 2015; Narváez et al., 2016) ha proporcionado valiosa información para comprender esta radiación temprana de los cocodrilos modernos y para establecer una comparación morfológica entre estas formas cretácicas y los representantes actuales de Crocodylia. En este sentido, los ejemplares craneales recuperados en el yacimiento de Lo Hueco (Fuentes, Cuenca), resultan de especial importancia, ya que su óptima preservación permite no solo realizar detallados estudios descriptivos y cladísticos, sino también realizar análisis de tipo neuroanatómico.

Los primeros estudios neuroanatómicos en Crocodylomorpha

Hasta hace pocas décadas, los estudios neuroanatómicos eran poco frecuentes y estaban relacionados con los escasos hallazgos de moldes internos de sedimento, ejemplares fragmentados, la arriesgada fabricación de moldes de silicona, o directamente con disecciones de cráneos (Witmer et al., 2008). Los primeros estudios neuroanatómicos en crocodilomorfos fósiles se remontan al siglo XIX, cuando Richard Owen describió un molde interno natural del talatosuquio *Steneosaurus* sp., comparándolo con el encéfalo y las cavidades del seno faríngeo medio de disecciones realizadas a los cráneos de *Alligator lucius* (atribuido posteriormente a *Alligator mississippiensis)*, *Crocodylus acutus*, *Crocodylus biporcatus* (*Crocodylus porosus)* y *Gavialis gangeticus* (Fig. 1.2) (Owen, 1842, 1850).

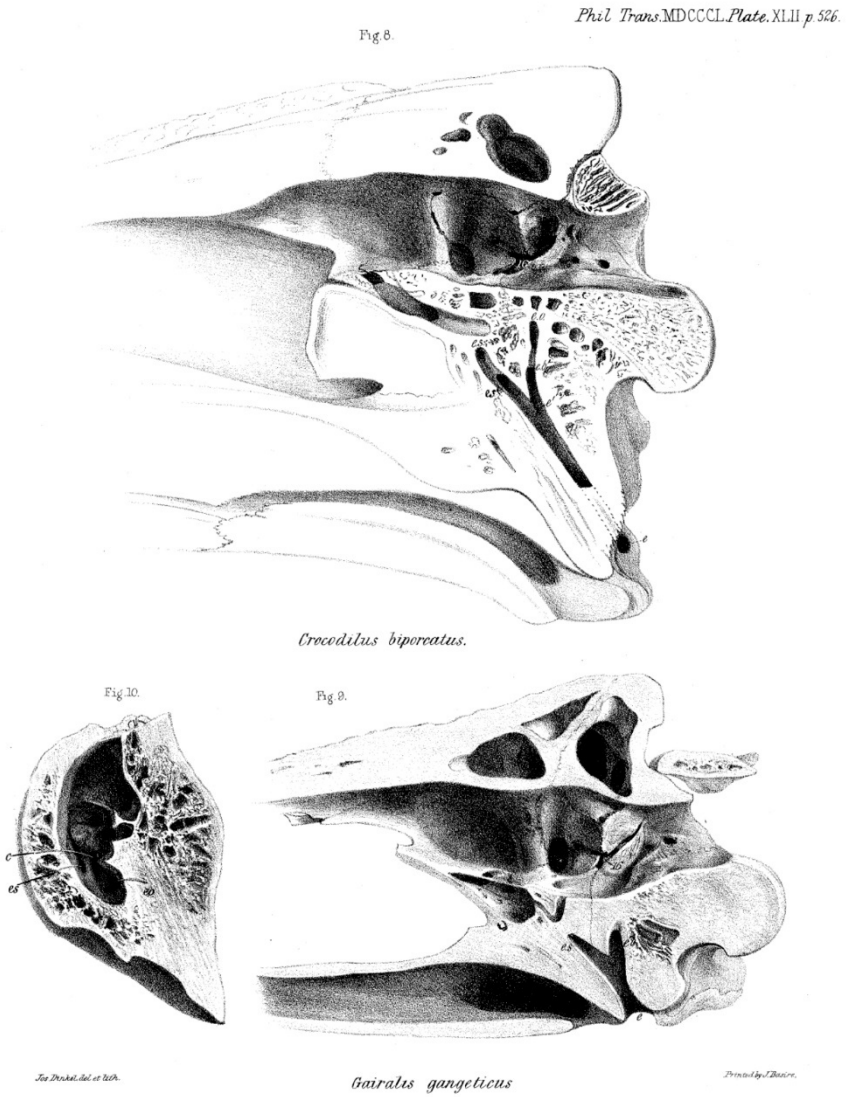

Fig. 1.2: Cortes sagitales de cráneos de *Crocodylus porosus* y de *Gavialis gangeticus*, modificado de Owen (1850):

Sagittal sections of the skulls of *Crocodylus porosus* and *Gavialis gangeticus*, modified from Owen (1850):

"*Plate XLII. Fig. 8. A vertical section of the cranium of the Crocodilus biporcatus, a little to the left of the median line, showing part of the left tympanic branches, es, eo, and the orifices, es', eo', of the right tympanic branches, of the primary divisions of the median canal, e' to e. Fig. 9. A vertical median section of the cranium of a Gavial, Gavialis gangeticus, showing the basioccipital division, eo, and the basisphenoid division, es, of the median Eustachian canal, e. Fig. 10. A vertical section of the tympanic cavity of the Crocodilus biporcatus, showing bristles inserted into the basioccipital branch, eo, and basispbenoid branch, es, of the Eustachian tube; c, the entry of the entocarotid canal.*"

Años más tarde, Eugène Eudes-Deslongchamps, (1864) compara la forma del interior del cráneo de los talatosuquios *Teleosaurus temporalis* (atribuido posteriormente a *Pelagosaurus typus*) y *Teleosaurus cadomensis*, y de diversos

ejemplares actuales, como *Caiman palpebrosus* (*Paleosuchus palpebrosus*) y *Crocodylus sp*., hallando similitudes en la composición, estructuras y forámenes del cráneo, pero también resaltando algunas ligeras variaciones, como un menor desarrollo de las rugosidades de las cavidades timpánicas y de la apófisis descendente de la región anterior del frontal en los ejemplares fósiles.

También dentro del grupo de los talatosuquios, Abel Morel de Glasville (1876) aprovechó la rotura transversal de un cráneo para describir y comparar en detalle las cavidades intracraneanas de *Steneosaurus heberti* y *T. cadomensis*, incluyendo medidas del encéfalo y de la estructura de los sistemas de senos faringotimpánicos y paranasales.

En 1880, Harry G. Seeley publicó el estudio de las dos secciones del neurocráneo del talatosuquio *Teleosaurus eucephalus* (posteriormente *Steneosaurus brevior*), describiendo en detalle la morfología del perfil del encéfalo, los nervios craneales y el seno faríngeo medio. Seeley también comparó las cavidades intracraneanas de *S. brevior* con las de los cocodrilos actuales (encontrando variaciones en la forma del cerebro, lóbulo óptico o del cerebelo) y otros reptiles como quelonios, plesiosaurios o dinosaurios.

Por su parte, Victor Lemoine recalcó la importancia del estudio de las estructuras blandas, y describió las similitudes morfológicas entre el encéfalo diseccionado de *Crocodylus lucius* (*Crocodylus niloticus*) y un molde natural del gavial de Mont-Aimé (*Gavialis macrorhynchus*, renombrado posteriormente como *Thoracosaurus macrorhynchus*), ya describiendo un menor desarrollo de los hemisferios cerebrales en el ejemplar fósil (Lemoine, 1884).

Ernst Koken también puso de manifiesto la gran similitud morfológica observada entre las cavidades intracraneanas del folidosaurio *Macrorhynchus meyeri* (redescrito como *Pholidosaurus meyeri*) y de los talatosuquios *T. cadomensis*, *P. typus*, *Teleosaurus eucephalus* (*S. brevior*) y *S. heberti* con las mostradas por miembros actuales de Crocodylia, observadas a partir de disecciones de *Alligator lucius* (*A. mississipiensis*), *Alligator palpebrosus* (*P. palpebrosus*), *Crocodylus vulgaris* (*C. niloticus*) y *G. gangeticus* (Koken, 1886, 1887, 1893).

Tilly Edinger es uno de los nombres clave de la paleoneuroanatomía. Enmarcó la paleoneuroanatomía en un contexto evolutivo, y analizó cada una de las estructuras que componen el sistema nervioso central (Edinger, 1929). En sus trabajos se encuentran descripciones neuroanatómicas de ejejmplares tanto fosiles como actuales de gran variedad de grupos, aunque centró sus estudios en la paleoneuroanatomía de mamíferos (Edinger, 1975). Dentro de Crocodylomorpha, Edinger describió los moldes internos naturales de los folidosaurios *P. meyeri* y *Pholidosaurus schaumburgensis* y del goniofolídido *Goniopholis pugnax* (*Goniopholis simus*), comparándolos con disecciones de *C. niloticus* y *A. mississippiensis*. De nuevo, remarcó la similitud entre las cavidades de estos animales, añadiendo, no obstante, que los ejemplares actuales parecen tener más desarrollado el cerebro (prosencéfalo) en comparación con el mesencéfalo (Edinger 1938).

Edwin Colbert fue pionero al aplicar la fabricación de moldes plásticos a partir de las cavidades intracraneanas previamente vaciadas, o de huesos craneales desarticulados, en crocodilomorfos. Este procedimiento consiste la aplicación de una capa fina de látex al interior de un cráneo previamente vaciado, que servirá de molde una vez extraído del fósil (Edinger, 1929; Radinsky, 1968). A partir del molde del encéfalo y del sistema de senos faringotimpánicos de *C. acutus*, Colbert (1946a) describió de forma completa la morfología del seno faríngeo medio de este taxón, que conecta el oído medio con la faringe. Además, comparó el molde de *C. acutus* con el del sebécido *Sebecus icaeorhinus* (Colbert, 1946b), hallando similitudes, pero también una serie de diferencias, como la morfología de los hemisferios cerebrales, el tamaño relativo del cerebro, la altura en la zona cerebelar y la forma de la hipófisis. También remarcó la similitud de los senos faríngeos medios en ambos taxones, proponiendo que el desarrollo del sistema eustaquiano de los cocodrilos actuales quedó ya establecido en formas más basales del grupo.

Yeh (1958) también describió varias diferencias en caracteres entre un molde de látex de *Alligator sinensis* y un molde natural del crocodiloideo tomistomino *Tomistoma petrolica* (reasignado como *Maomingosuchus petrolica*): la longitud relativa del cerebro, la forma general del encéfalo (más aplanada en *M. petrolica*) y la forma del cerebelo (menos marcada en *M. petrolica*).

En (Hopson, 1979), James Hopson publicó un tratado de paleoneurología donde realizó una extensa descripción de un molde de látex y un encéfalo diseccionado de *Caiman crocodilus*, comparándolo con una amplia muestra de reptiles, como tortugas, mosasaurios, notosaurios, placodontos, pterosaurios, dinosaurios y crurotarsos, incluyendo algunos ejemplares basales. En el mismo, también publicó la reinterpretación de las cavidades intracraneanas de *P. meyeri* y *S. icaeorhinus* realizadas, respectivamente, por Koken (1887) y Colbert (1946b). Además, propuso por primera vez los conceptos de la proporción entre las meninges y el encéfalo, y el cociente de encefalización en estos animals (Fig. 2.3), que cobraron especial relevancia en estudios posteriores, enfocados en analizar las capacidades neurosensoriales y cognitivas en función del tamaño y forma del órgano neurosensorial asociado.

Glenn Storrs, Spencer G. Lucas y Robert M. Schoch describieron en 1983 el molde natural de un aligatoroideo basal asignado al género *Leidyosuchus*, comparándolo con análisis previos sobre la neuroanatomía de especies actuales como *A. mississippiensis* y *C. crocodilus*. En dicho trabajo concluyeron que pueden observarse diferencias entre formas basales y actuales de aligatoroideos a pesar de los escasos cambios ocurridos en el encéfalo del linaje durante su historia evolutiva. Entre las citadas diferencias destacan un perfil lateral más recto en el espécimen basal, semejante al mostrado por los crocodiloideos, y unos hemisferios cerebrales de mayor tamaño en las formas actuales.

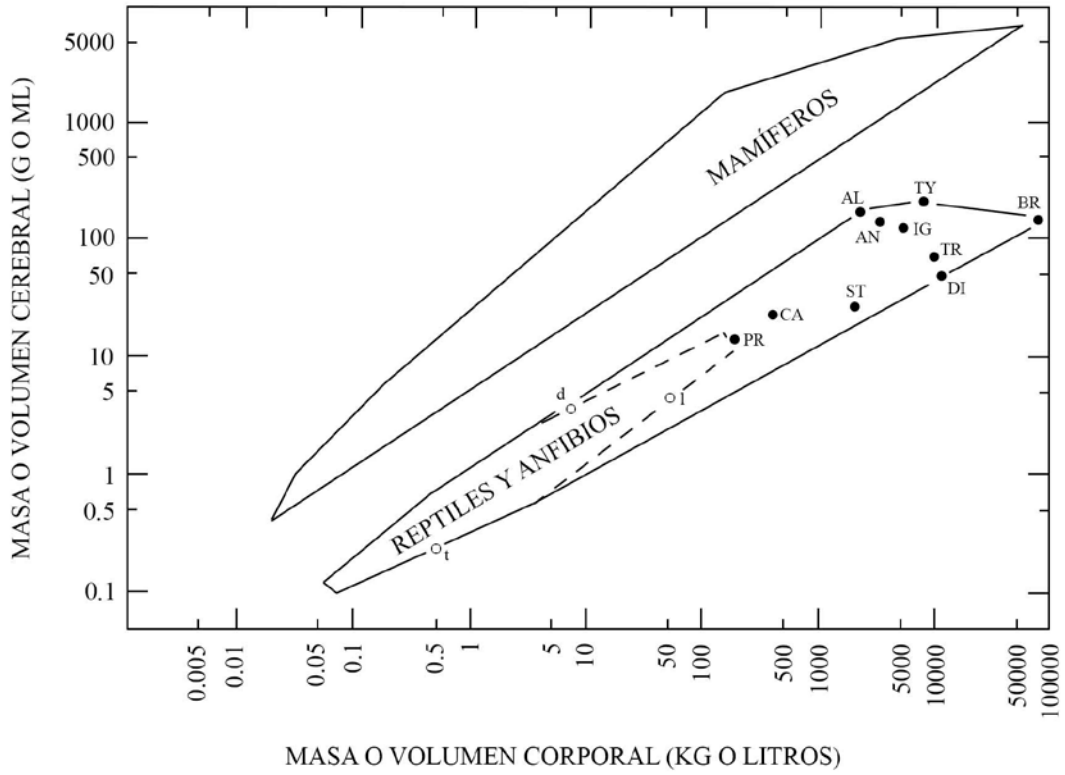

Fig. 1.3: Gráfico de dispersión que muestra la relación entre el volumen/masa cerebral y el peso/volumen corporal de diversos tetrápodos, modificada de Hopson (1979):
Dispersion plot that shows the relation between the cerebral volume/mass and the body volume/mass of different tetrapods, modified from Hopson (1979):
"Fig. 3. Brain to body size relations in fossil reptiles superimposed on minimum convex polygons for living species (modified from Jerison, 1973). Dinosaurs: AL, Allosaurus; AN, Anatosaurus; BR, Brachiosaurus; CA, Camptosaurus; DI, Diplodocus; IG, Iguanodon; PR, Protoceratops; ST, Stegosaurus; TR, Triceratops; TY, Tyrannosaurus Therapsids: d, Diademodon; l, Lystrosaurus; t, Thrinaxodon."

Más recientemente destacan los estudios de moldes naturales de varios metriorrínquidos de la Formación Vaca Muerta, del Jurásico Superior-Cretácico Inferior de Argentina. Así, se han descrito las cavidades internas de *Dakosaurus* cf. *andiniensis* (Herrera and Vennari, 2014), *Cricosaurus araucanensis* (Herrera, 2015) y *Geosaurus araucanensis* (Fernández and Gasparini, 2000, 2008), incidiendo especialmente en las glándulas de la sal, hipertrofiadas en estos animales.

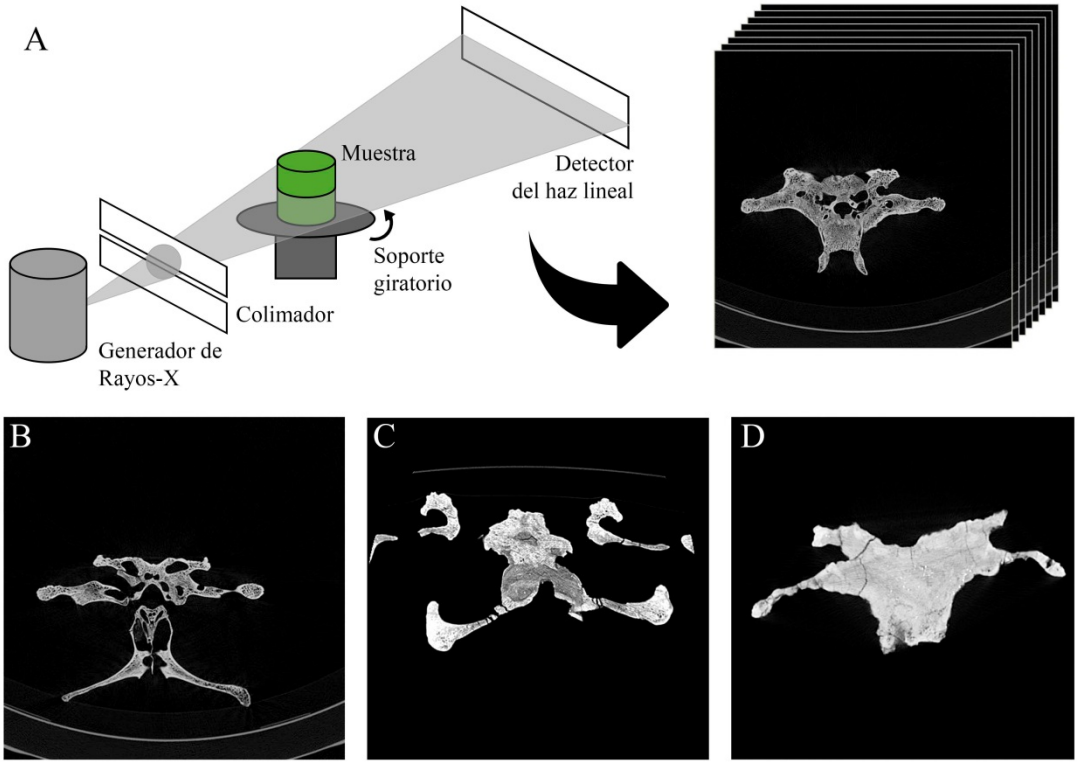

Fig. 1.4: Mecánica de un escáner de Tomografía Axial Computerizada, y ejemplos de los cortes obtenidos mediante esta metodología. **A**, diagrama de funcionamiento de un escáner de Tomografía Axial Computerizada. El haz colimado de rayos-X atraviesa el ejemplar durante una rotación de 360º. Esta secuencia es captada por el detector, y posteriormente interpretada mediante algoritmos para obtener cada corte. Este proceso se repite a lo largo del eje axial del ejemplar, con un interespaciado a determinar, para obtener un conjunto de cortes que pueden superponerse para generar una estructura digital tridimensional. **B**-**D**, cortes axiales en los que se observa la diferencia de densidades entre el hueso (más denso, y por tanto más claro en el TAC) y el relleno de las cavidades: **B**, *Alligator mississippiensis* actual. Las cavidades están rellenas de aire, y la diferencia de densidad entre ambos materiales es elevado. **C**, HUE-04498. La densidad del sedimento que rellena las cavidades intracraneanas es elevado, pero aún se perciben los límites entre el hueso mineralizado y el sedimento. **D**, HUE-02018. La densidad entre el sedimento y el hueso mineralizado es prácticamente la misma, no pudiéndose establecer los límites entre ambos.

How a CT scanner works, and examples of the slices obtained with this technique. **A**, Scheme of how CT scanning operates. The collimated X-ray beam goes through the sample during a 360º rotation. This sequence is received by the receptor and interpreted by several algorythms to obtain each of the slices. This process is repeated along the axial axis of the sample, with a determinate interslicing space, to obtain a set of slices that can be overlapped to generate a digital tridimensional structure. **B**-**D**, axial slices that show the difference of densities between the bones (denser and, therefore, lighter, in the slices) and the material that infills the cavities: **B**, extant *Alligator mississippiensis*. Cavities are filled by air, and the difference of density between bone and air is high. **C**, HUE-04498. The density of the sediment that infills the cavity is high, but the boundaries between the bone and the sediment of the cavities can still be distinguished. **D**, HUE-02018. The density of the sediment and that of the bone is almost the same, making impossible to distinguish the boundaries between both structures.

Aplicación de tecnologías no invasivas en paleoneuroanatomía

La aplicación de la Tomografía Axial Computerizada (TAC) sobre cráneos fósiles supuso un gran avance en el estudio de las cavidades intracraneanas de animales extintos. Esta tecnología permite obtener, mediante rayos X, una serie de imágenes de cortes axiales del ejemplar escaneado, en los que se puede apreciar la estructura interna, sin poner en riesgo alguno la integridad de la pieza estudiada. El escáner detecta las diferencias en la densidad del espécimen, y mediante una serie de algoritmos lo representa como un conjunto de imágenes en escala de grises del objeto (Goldman, 2007). De este modo, si la diferencia de densidad es suficiente, el escáner es capaz de discriminar entre el hueso fosilizado y la matriz que rellena las cavidades (Fig. 1.4).

Las primeras aplicaciones de la tecnología TAC en fósiles consistían en el análisis e interpretación bidimensional de las cavidades intracraneanas utilizando los cortes axiales y sagitales obtenidos en el escaneado (Conroy and Vannier, 1984). La primera aplicación de esta tecnología a un crocodilomorfo fósil fue para describir el sistema de senos paranasales del goniofolídido *Calsoyasuchus valliceps* (Tykoski et al., 2002).

Posteriormente, el desarrollo de programas informáticos capaces de superponer todos los cortes axiales para generar una estructura tridimensional supuso otro gran paso adelante en la paleoneuroanatomía. De esta forma, no solo se podía describir el contorno y realizar medidas lineales de las cavidades, sino también observar y manipular la propia estructura tridimensional, además de permitir la toma de medidas lineales y superficiales más allá de los planos ortogonales definidos por el escáner, y, por supuesto, volumétricas. No obstante, es necesario aclarar que la aplicación del 3D no es siempre necesaria, como demostraron Gold et al. (2014) en su detallado estudio acerca de la variación en el tamaño del seno faríngeo medio en Crocodylia, mediante morfometría geométrica. Además, a pesar de las ventajas de la tecnología TAC, su elevado coste y el hecho de que, en muchas ocasiones, estas máquinas suelen estar asociadas a centros médicos, ha hecho que sigan realizando moldes de látex de las cavidades intracraneanas, como los llevados a cabo en *G. gangeticus* y en el talatosuquio *Steneosaurus pictaviensis* (Wharton, 2000), o el realizado a *Caiman gasparinae* por Bona and Paulina Carabajal (2013), comparándolo con moldes de los actuales *Caiman yacaré* y un juvenil de *Caiman latirostris*.

La primera reconstrucción tridimensional de las cavidades intracraneanas de un crocodilomorfo se realizó en el ejemplar tipo del notosuquio *Simosuchus clarki* (Kley et al., 2010), en el que se describió la cavidad encefálica y parte del oído interno. Los talatosuquios continúan siendo el grupo de crocodilomorfos mejor representado en cuanto a estudios neuroanatómicos. A las numerosas descripciones de moldes naturales y cráneos vaciados mencionados en el apartado anterior hay que añadir las reconstrucciones digitales de las cavidades intracraneanas de *Steneosaurus* cf. g*racilirostris* (Brusatte et al., 2016), *Steneosaurus bollensis* (Herrera et al., 2018), *Pelagosaurus typus* (Pierce et al., 2017), *Metriorhynchus* cf. *westermanni* (Fernández et al., 2011), *Maledictosuchus riclaensis* (Parrilla-Bel et al., 2016), *Geosaurus*

araucanensis (Fernández and Herrera, 2009) y *Cricosaurus araucanensis* (Herrera et al., 2013b, 2018). Los estudios de las cavidades intracraneanas de este clado suelen enfocarse en el desarrollo de las glándulas de la sal, unas estructuras hipertrofiadas en este grupo, localizadas a ambos lados del lóbulo olfativo.

Por otro lado, Brusatte et al. (2016) y Pierce et al. (2017) no solo describieron la morfología de las cavidades intracraneanas de estos crocodilomorfos, sino que también realizaron diferentes análisis comparativos y métricos para estimar sus capacidades neurosensoriales, centrándose sobre todo en la capacidad auditiva y del equilibrio. Destaca también el análisis de caracteres filogenéticos relacionados con el endocráneo de este grupo de animales realizado por Herrera et al., (2018), en el que se comparan las cavidades intracraneanas de los talatosuquios descritos hasta el momento. En ese estudio se proponen y describen diez caracteres morfológicos relacionados con el basicráneo y las cavidades intracraneanas, y como varían sus respectivos estados a lo largo del clado Thalattosuchia.

La mayoría de los estudios neuroanatómicos en Eusuchia están centrados en representantes actuales del grupo. Sin embargo, la posibilidad de realizar estudios etológicos (ej: Vergne et al., 2009; Weldon and Ferguson, 1993; Wever, 1971), y de analizar los propios órganos en vez de centrarse solo en la cavidad contenedora (ej: Nagloo et al., 2016; Porter et al., 2016; Weldon et al., 1990), han relegado la aplicación de la tecnología TAC a un segundo plano. No obstante, destacan los trabajos de Dufeau and Witmer (2015), en el que se describieron los cambios sufridos en las cavidades intracraneanas de *Alligator mississippiensis* a lo largo de una serie ontogenética de trece especímenes; y el de Jirak and Janacek (2017) y Watanabe et al., (2018), donde se analizó la proporción entre el volumen del encéfalo y el de la propia cavidad en varios ejemplares de miembros de Crocodylia en distintos momentos ontogenéticos. Finalmente, son también reseñables las reconstrucciones tridimensionales de las cavidades intracraneanas de *A. mississippiensis* (Witmer and Ridgely, 2009), *Caiman crocodilus* (Brusatte et al., 2016), *Crocodylus moreletii* (Franzosa, 2004), *Crocodylus johnstoni* (Witmer et al., 2008) *Crocodylus siamensis* (Kawabe et al., 2009) y *Gavialis gangeticus* (Bona et al., 2017; Pierce et al., 2017), utilizadas como referencia de comparación en los estudios de ejemplares fósiles, y que son de gran ayuda para la construcción de una base de datos.

Por último, el conocimiento acerca de la neuroanatomía de eusuquios fósiles es, en comparación, muy escaso. En la actualidad, la información acerca de las cavidades intracraneanas en la base de Eusuchia está solo representada por las breves descripciones de las reconstrucciones tridimensionales de las cavidades intracraneanas de *Aegisuchus witmeri* (Holliday and Gardner, 2012) y *Allodaposuchus hulki* (Blanco et al., 2015). Y dentro de Crocodylia, encontramos solo información del gavialoideo *Gryposuchus neogaeus* (Bona et al., 2017), de cavidades faringotimpánicas de reducido tamaño y agudeza auditiva menos desarrollada que la del resto de sus parientes; y del caimanino *Mourasuchus nativus* (Bona et al., 2013).

Introduction to Crocodylomorpha systematic

The origin of Crocodylomorpha goes back to 250 million years ago, after the Permian mass extinction. During the Triassic takes place one of the most important evolutionary radiation among vertebrates, in which the two major lineages of archosaurs diverged. One, Avemetatarsalia, includes pterosaurs, nonavian dinosaurs and birds; and the second, Crurotarsi (Fig. 1.1), includes a huge diversity of extinct taxa as well as extant crocodiles.

Basal crurotarsals are represented by diverse groups (Brusatte et al., 2010; Nesbitt, 2011; Ezcurra, 2016): phytosaurians were semiaquatic and longirostrine animals from the Late Triassic of Central Europe, North Africa and North America. However, their precise phylogenetical position is under debate, some analyses recovering them as the sister-group of Archosauria (Nesbitt, 2011), or as the basalmost group of Crurotarsi (Ezcurra, 2016). Crurotarsi also included aetosaurians (armoured herbivores from the Triassic of America, Africa and Europe); ornithosuchids (a phylogenetically conflictive group from the Late Triassic of Argentina and Scotland; von Baczko and Desojo, 2016); rauisuchians (with wide geographical distribution and disparate morphologies); and, finally, crocodylomorphs, the only of these clades that overtook the Triassic-Jurassic transition.

Crocodylomorpha is a well-established clade with several synapomorphies supporting it (Walker, 1970; Benton and Clark, 1988; Walker et al., 2002; Sereno et al., 2005). It includes a series of extinct and extant groups: ‘Spehnosuchians’, the basalmost one, includes diverse forms with graceful limbs and were limited to the Late Triassic-Early Jurassic. ‘Sphenosuchians’ comprise very fragmentary specimens with a lot of conflictive characters, so its monophyly is under debate. The latest hypotheses (Nesbitt, 2011; Irmis et al., 2013) placed it as a series of sister-taxa of Crocodyliformes.

Crocodyliformes includes a series of basal forms known as ‘protosuchians’, dated from Triassic to Cretaceous, which were highly diverse and with a wide geographical distribution. These crocodyliforms are a paraphyletic group composed by successive sister-taxa of Mesoeucrocodylia.

Mesoeucrocodylia includes two major lineages: Notosuchia and Neosuchia. Notosuchians were terrestrial forms, with variable morphology and heterodont dentition, ranging from Middle Jurassic to Middle Miocene (Gasparini, 1971; Pol et al., 2014; Dal Sasso et al., 2017).

Neosuchians include a series of longirostral forms (Benton and Clark, 1988). One of them, Thalattosuchia, from Middle Jurassic to Early Cretaceous, had adaptations to an aquatic lifestyle, being metriorhynchids completely adapted to a marine pelagic lifestyle, with a long body, heterocercal fin-shape tail, shovel-shaped limbs and hypertrophied salt-glands (Fernández and Gasparini, 2008; Herrera et al., 2013a). Furthermore, more derived neosuchians include semiaquatic forms such as goniopholidids, from Jurassic-Cretaceous, or ‘pholidosaurids’, from Late Jurassic to

Cretaceous, both with a wide geographical distribution (De Andrade et al., 2011; Bronzati et al., 2012).

The other major lineage of Neosuchia includes modern crocodiles, or Eusuchia (Huxley, 1875), a monophyletic group diagnosed by several synapomorphies such as the presence of a caudally displaced secondary choana formed by the pterygoids, and procoelous vertebrae (Brochu, 1999; Salisbury et al., 2006).

Eusuchia includes a series of basal groups such as Paralligatoridae, Hylaeochampsidae or Allodaposuchidae (Buscalioni et al., 2011; Turner, 2015; Narváez et al., 2016), which form the successive sister-groups to Crocodylia, the clade that includes the extant representatives of the lineage.

Crocodylia consists of nine genera and more than twenty extant species (Shirley et al., 2018), from three lineages: Gavialoidea, Crocodyloidea and Alligatoroidea. The diversity of extant crocodylians is remarkably lower than that observed in their evolutionary history, since they are now restricted to circumtropical semiaquatic habitats. Earliest records of crocodylians date from the Upper Cretaceous of North America (Mook, 1941; Erickson, 1972; Norell et al., 1994; Williamson, 1996; Wu et al., 1996). The divergence between the three lineages with extant representatives has been estimated prior to the Campanian (Brochu, 2003).

The study of basal eusuchians in the last decade Buscalioni et al., 2011; Bronzati et al., 2012; Blanco et al., 2014; Puértolas-Pascual et al., 2014; Turner, 2015; Narváez et al., 2016) has yielded a great deal of information to understand the early radiation of modern crocodiles and to establish a morphological comparison framework between these Cretaceous forms and extant crocodylians. This way, the cranial samples retrieved from the Lo Hueco fossil site (Fuentes, Cuenca), are remarkably relevant due to their good preservation, which allows making detailed descriptive, cladistics and even neuroanatomical analyses.

Firsts neuroanatomical studies in Crocodylomorpha

Until a few decades ago, neuroanatomical studies were infrequent, being limited to the scarce findings of internal sediment casts, fractured specimens, the dangerous fabrication of latex endocasts, or actual skull dissections (Witmer et al., 2008). The first neuroanatomical studies applied to fossil crocodylomorphs were from the XIX century, when Richard Owen described a natural inner skull cast of the thalattosuchian *Steneosaurus* sp., and compared it with the brain and median pharyngeal sinus cavities from dissected skulls of *Alligator lucius* (posteriorly attributed to *Alligator mississippiensis)*, *Crocodylus acutus*, *Crocodylus biporcatus* (*Crocodylus porosus)* and *Gavialis gangeticus* (Fig. 1.2) (Owen, 1842, 1850).

Some years later, Eugène Eudes-Deslongchamps, (1864) compared the shape of the inner skull cavities of the thalattosuchians *Teleosaurus temporalis* (posteriorly

attributed to *Pelagosaurus typus*) and *Teleosaurus cadomensis*, with some extant species such as *Caiman palpebrosus* (*Paleosuchus palpebrosus*) and *Crocodylus sp*., finding similarities between them in the composition, structures and foramina location of the skull cavities. However, he also underlined some variations, such as a lesser development of the rugosities of both the tympanic cavities and descending apophysis of the anterior region of the frontal in the fossil samples.

Also focusing in thalattosuchians, Abel Morel de Glasville (1876) described and compared in detail, through a transversal fracture of the skull, the inner cavities of *Steneosaurus heberti* and *T. cadomensis*, including measurements of the brain and pharyngotympanic and paranasal cavities.

In 1880, Harry G. Seeley published a study of the two sections of the basicranium of the thalattosuchian *Teleosaurus eucephalus* (now *Steneosaurus brevior*), describing in detail the shape of the brain outline, the cranial nerves and the median pharyngeal sinus. Seeley also compared the cavities of *S. brevior* with those of other extant crocodiles (finding differences in the shape of the cerebrum, optic lobe and cerebellum) and other reptiles such as turtles, plesiosaurs or dinosaurs.

Victor Lemoine also remarked the importance of the study of soft-tissues and described the similarities in the shape of the dissected brain of *Crocodylus lucius* (*Crocodylus niloticus*) and a natural cast of the gharial from Mont-Aimé (*Gavialis macrorhynchus*, posteriorly renamed *Thoracosaurus macrorhynchus*), noticing a lesser development of the cerebral hemispheres of the fossil specimen (Lemoine, 1884).

Ernst Koken also emphasized the great shape similitude observed between the inner skull cavities of the pholidosaur *Macrorhynchus meyeri* (renamed as *Pholidosaurus meyeri*) and the thalattosuchians *T. cadomensis*, *P. typus*, *Teleosaurus eucephalus* (*S. brevior*) and *S. heberti* with dissections of extant crocodylian samples of *Alligator lucius* (*A. mississipiensis*), *Alligator palpebrosus* (*P. palpebrosus*), *Crocodylus vulgaris* (*C. niloticus*) and *G. gangeticus* (Koken, 1886, 1887, 1893).

Tilly Edinger is one of the key names in paleoneuroanatomy. She frame paleoneuroanatomy into an evolutionary context, and analyzed each of the structures that composed the central nervous system (Edinger, 1929). In her studies, there are neuroanatomical descriptions of extant and extinct specimens from a great diversity of groups, but she principally focused her studies in the paleoneurology of mammals (Edinger, 1975). Among Crocodylomorpha, Edinger described natural casts of the pholidosaurs *P. meyeri* and *Pholidosaurus schaumburgensis* and the goniopholidid *Goniopholis pugnax* (now *Goniopholis simus*), comparing them with dissections of *C. niloticus* and *A. mississippiensis*. She also emphasized the similarities among these animals, suggesting that extant specimens seemed to have a more developed cerebrum (prosencephalon) in comparison to the mesencephalon (Edinger 1938).

Edwin Colbert was among the first person to apply techniques to make plastic casts of inner skull cavities to crocodylomorphs. This process consists of the application

of a thin layer of latex to the inner surface of a braincase previously emptied, that will be used as the cast once extracted from the fossil (Edinger, 1929; Radinsky, 1968). Using a cast of the brain and the pharyngotympanic sinus system of *C. acutus*, Colbert (1946a) described the morphology of the median pharyngeal sinus, which joins the middle ear with the pharynx on this taxon. Furthermore, he compared the cast of *C. acutus* with that of the sebecid *Sebecus icaeorhinus* (Colbert, 1946b), finding similarities, but also several differences, such as the shape of the cerebral hemispheres, the relative size of the cerebrum, the height of the cerebellar region and the shape of the hypophysis. He also noticed similarities in the median pharyngeal sinus of both taxa, proposing that the development of the Eustachian system in extant crocodiles was already established in basal forms of Crocodylomorpha.

Yeh (1958) also described several morphological differences between a latex cast of *Alligator sinensis* and a natural cast of the tomistomine crocodyloid *Tomistoma petrolica* (renamed *Maomingosuchus petrolica*): the relative length of the cerebrum, the general shape of the brain (more flattened in *M. petrolica*) and the shape of the cerebellum (less marked in *M. petrolica*).

In 1979, James Hopson published a paleoneuroanatomy treatise making an extensive description of a latex cast and a dissected brain of *Caiman crocodilus*, comparing them with a large sample of reptiles such as turtles, mosasaurs, nothosaurs, placodonts, pterosaurs, dinosaurs and crurotarsals, including some basal species. In this treatise, he also reinterpreted the inner skull cavities of *P. meyeri* y *S. icaeorhinus* published by Koken (1887) and Colbert (1946b). He also proposed for the first time the concepts of the proportion between the dural envelope and the brain, and the encephalization quotient in these animals (Fig. 1.3), which will gain relevance in posterior studies, focused in analyzing the neurosensorial and cognitive capabilities in function of the size and shape of the associated neurosensorial organ.

Glenn Storrs, Spencer G. Lucas and Robert M. Schoch described in 1983 a natural cast of a basal alligatoroid assigned to the genus *Leidyosuchus*, comparing it to previous neuroanatomical analyses of the extant *A. mississippiensis* and *C. crocodilus*. In this study, they noticed that there were some differences between the basal alligatoroid and extant ones despite the expected conservativeness of the brain of these crocodylians, such as a lateral straight outline in the basalmost sample, similar to the crocodyloid condition, and larger cerebral hemispheres in the extant samples.

The latest studies in natural casts are focused in several metriorhynchids from the Upper Jurassic-Lower Cretaceous of the Vaca Muerta Formation, in Argentina. In those, the inner skull cavities of *Dakosaurus* cf. *andiniensis* (Herrera and Vennari, 2014), *Cricosaurus araucanensis* (Herrera, 2015) and *Geosaurus araucanensis* (Fernández and Gasparini, 2000, 2008) have been described, emphasizing the hypertrophied salt glands of these animals.

Application of non-invasive techniques in paleoneuroanatomy

The application of Computerized Tomography (CT) to fossil skulls signified great progress in the study of the inner skull cavities of fossil animals. This technology uses X-rays to obtain a series of axial slices of the scanned specimen, where the internal structure of the skull can be distinguished without endangering it. The scanner detects differences in the density of the sample and represents it as a set of greyscale images, by several algorithms (Goldman, 2007). In this way, if the difference of densities is high enough, the scanner allows to distinguish between the mineralized bone and the infilling sediment (Fig. 1.4).

The first applications of the CT technology to fossils lied in the bidimensional analyses and interpretations of the inner skull cavities by using some of the axial and sagittal slices (Conroy and Vannier, 1984). The first application of this technology to a fossil crocodylomorph was to describe the paranasal sinus system of the goniopholidid *Calsoyasuchus valliceps* (Tykoski et al., 2002).

Later, the development of several softwares that allow overlapping these axial slices to generate a tridimensional structure signified another big step for the paleoneuroanatomy. This way, the description of the outline and the linear measurements of the cavities can be done, but it is also possible also to observe and handle the tridimensional structure itself, and to make linear and surface measurements beyond the orthogonal axes defined by the scanner and, of course, to make volumetric measurements. However, it must be said that the application of 3D is not always necessary, as demonstrated Gold et al. (2014) in their detailed study about the variation in the size and shape of the median pharyngeal sinus in Crocodylia, using on bidimensional geometric morphometry. Furthermore, despite the advantages of CT technology, its high cost and the fact that these machines are usually associated with medical centres makes latex casts of inner skull cavities still employed, such as those of *G. gangeticus* and the thalattosuchian *Steneosaurus pictaviensis* (Wharton, 2000), or the comparison between that of *Caiman gasparinae* with those of the extant *Caiman yacaré* and a juvenile of *Caiman latirostris* done by Bona and Paulina Carabajal (2013).

The first tridimensional reconstruction of the inner skull cavities of a crocodylomorph was that of the notosuchian *Simosuchus clarki* (Kley et al., 2010), which described its brain cavity and part of the inner ear. Thalattosuchians are still the most represented group in these studies. Besides the numerous descriptions of natural and latex casts and emptied skulls aforementioned, the digital reconstructions of *Steneosaurus* cf. g*racilirostris* (Brusatte et al., 2016), *Steneosaurus bollensis* (Herrera et al., 2018), *Pelagosaurus typus* (Pierce et al., 2017), *Metriorhynchus* cf. *westermanni* (Fernández et al., 2011), *Maledictosuchus riclaensis* (Parrilla-Bel et al., 2016), *Geosaurus araucanensis* (Fernández and Herrera, 2009) and *Cricosaurus araucanensis*, Herrera et al., (2018) have been published. The studies on the inner skull cavities of this clade have been primarily focused in the development of the hypertrophied salt glands, located at both sides of the olfactory bulb of these animals.

Furthermore, Brusatte et al. (2016) and Pierce et al. (2017) not only described the shape of the inner skull cavities of these thalattosuchians, but also made different comparative and metric analyses to estimate the neurosensorial capabilities of these animals, focusing on the hearing and balance capabilities. It is also remarkable the analysis of phylogenetic characters related to the endocast of thalattosuchians done by Herrera et al., (2018), who compared the inner skull cavities of all the described thalattosuchians. In this study, ten morphological characters related to the basicranium and inner skull cavities were proposed, following their evolution along the thalattosuchian lineage.

Most eusuchian neuroanatomical studies have focused on extant representatives of the clade. However, the possibility of doing etological studies (e.g.: Vergne et al., 2009; Weldon and Ferguson, 1993; Wever, 1971), or analyzing the organs themselves instead of the skull cavities (e.g.: Nagloo et al., 2016; Porter et al., 2016; Weldon et al., 1990) in extant samples, have relegated the application of CT technology as secondary. However, it is the remarkable study of Dufeau and Witmer (2015), who described the changes of the inner skull cavities of *Alligator mississippiensis* during ontogeny; as well as those of Jirak and Janacek (2017) and Watanabe et al., (2018), who analyzed the proportion between the brain and the brain cavity volumes in several samples of Crocodylia in different ontogenetic states. Finally, the tridimensional reconstructions of the inner skull cavities of *A. mississippiensis* (Witmer and Ridgely, 2009), *Caiman crocodilus* (Brusatte et al., 2016), *Crocodylus moreletii* (Franzosa, 2004), *Crocodylus johnstoni* (Witmer et al., 2008) *Crocodylus siamensis* (Kawabe et al., 2009) and *Gavialis gangeticus* (Bona et al., 2017; Pierce et al., 2017), used as comparative reference in the study of fossil samples must be mentioned too, for their relevance in the generation of an extant inner skull cavities comparative database.

To summarize, the knowledge on the neuroanatomy of fossil eusuchians is, in comparison to all aforementioned studies, scarce. Nowadays, the information of the inner skull cavities of basal eusuchians is only represented by the brief descriptions of the inner skull cavities of *Aegisuchus witmeri* (Holliday and Gardner, 2012) and *Allodaposuchus hulki* (Blanco et al., 2015). Among Crocodylia, there is only information about the gavialoid *Gryposuchus neogaeus* (Bona et al., 2017), whose pharyngotympanic cavities are smaller, and its hearing acuity is less developed than its relatives, and about the caimanine *Mourasuchus nativus* (Bona et al., 2013).

CAPÍTULO 2: HIPÓTESIS Y OBJETIVOS

HYPOTHESES AND OBJECTIVES

HIPÓTESIS Y OBJETIVOS

El desarrollo de esta memoria de tesis pretende contrastar una hipótesis general acerca del origen y evolución de las estructuras intracraneanas en la radiación temprana de los cocodrilos modernos (Eusuchia), es decir, el grupo de crocodilomorfos que incluye al antecesor común y todo los descendientes del grupo corona Crocodylia, *Hylaeochampsa vectiana* y todos sus descendientes.

En el yacimiento de Lo Hueco (Fuentes, Cuenca) ha proporcionado una abundante colección de material atribuido al clado Allodaposuchidae, considerado como el grupo hermano de Crocodylia (Narváez et al., 2015). Entre el material de Lo Hueco se encuentran varios cráneos asignables a distintos morfotipos, que han sido atribuidos a dos especies: *Lohuecosuchus megadontos* y *Agaresuchus fontisensis*. Algunos ejemplares presentan morfología y proporciones que difieren de las descritas para los dos taxones mencionados y se han considerado aquí como miembros de un potencial tercer taxón de alodaposúquido.

Para poder establecer un contexto evolutivo, la información obtenida a partir de la reconstrucción digital de las cavidades intracraneanas de estos especímenes se ha comparado con las reconstrucciones intracraneanas de miembros tanto actuales como extintos de Crocodylia, incluyendo uno de los paratipos de *Diplocynodon tormis*, un aligatoroideo basal del Eoceno de la Cuenca del Duero.

La reconstrucción de las cavidades intracraneanas permite un estudio comparativo de estas estructuras y resulta informativa sobre las capacidades neurosensoriales y cognitivas de estos animales.

De este modo, las hipótesis y los correspondientes objetivos abordados en esta tesis doctoral son:

Hipótesis general: La morfología de las cavidades intracraneanas de los miembros de Crocodylia es plesiomórfica, pues está presente en los grupos basales de Eusuchia.

1.- Hipótesis específicas sobre la transformación de caracteres en la morfología de las cavidades intracraneanas a lo largo de la filogenia de Crocodylia

- Hipótesis 1.1: Existe una combinación de caracteres autopomórficos de las cavidades intracraneanas de Crocodylia, constituida por: un perfil sinusoidal del encéfalo en vista lateral, una pituitaria orientada caudoventralmente, un canal semicircular anterior dorsalmente elongado y un elevado desarrollo del sistema de senos faringotimpánicos.

- Hipótesis 1.2: Existen diferencias en la morfología de las cavidades intracraneanas que permiten diferencias los linajes mayores de Crocodylia, como la presencia de una convexidad en la superficie posterodorsal del cerebro de los aligatoroideos y un seno faríngeo medio largo en crocodiloideos.

-Hipótesis 1.3: Las capacidades neurosensoriales y cognitivas inferidas en Crocodylia están más relacionadas con el tamaño máximo de los ejemplares adultos que distruibuida de forma congruente con su relación filogenética.

2.- Hipótesis específicas sobre la morfología intracraneana del aligatroroideo basal *Diplocynodon tormis*

- Hipótesis 2.1: Las cavidades intracraneanas de *Diplocynodon tormis* presentan las novedades evolutivas reconocidas en los representantes actuales de Alligatoroidea.

- Hipótesis 2.2: Las capacidades neurosensoriales y cognitivas inferidas para *Diplocynodon tormis* corresponden a las de los Crocodylia de tamaño medio, como *Caiman crocodilus, Melanosuchus niger* u *Osteolaemus tetraspis.*

3.- Hipótesis específicas sobre la morfología intracraneana de *Lohuecosuchus megadontos.*

- Hipótesis 3.1: Las cavidades intracraneanas de *Lohuecosuchus megadontos* ya presentan la morfología y novedades evolutivas presentes en los miembros de Crocodylia.

- Hipótesis 3.2: Las capacidades neurosensoriales y cognitivas inferidas para *Lohuecosuchus megadontos* corresponden a las de los Crocodylia de gran tamaño, como *Alligator mississippiensis* o *Crocodylus niloticus.*

4.- Hipótesis específicas sobre la morfología intracraneana de *Agaresuchus fontisensis.*

- Hipótesis 4.1: Las cavidades intracraneanas de *Agaresuchus fontisensis* ya presentan la morfología y novedades evolutivas presentes en los miembros de Crocodylia.

- Hipótesis 4.2: Las capacidades neurosensoriales y cognitivas inferidas para *Agaresuchus fontisensis* corresponden a las de los Crocodylia de gran tamaño, como *Alligator mississippiensis* o *Crocodylus niloticus.*

5.- Hipótesis específicas sobre la morfología intracraneana del tercer morfotipo craneal de Lo Hueco.

- Hipótesis 5.1: Las cavidades intracraneanas de los representantes del tercer morfotipo craneal de Lo Hueco presentan una morfología similar a las de *Lohuecosuchus megadontos* y *Agaresuchus fontisensis*, debido a su proximidad filogenética y por lo tanto, semejante a la de los miembros de Crocodylia

- Hipótesis 5.2: Las capacidades neurosensoriales y cognitivas inferidas para los representantes del tercer morfotipo craneal de Lo Hueco coinciden con las de los Crocodylia de tamaño medio, como *Caiman crocodilus*, *Melanosuchus niger* u *Osteolaemus tetraspis.*

A partir de estas hipótesis, se plantean los siguientes objetivos:

- Objetivo 1: Reconstrucción y comparación de las cavidades internas y análisis de las capacidades neurosensoriales y cognitivas de ejemplares representativos de los distintos linajes y tamaños de cocodrilos actuales.

- Objetivo 2: Comparación de la reconstrucción de las cavidades internas y análisis de las capacidades neurosensoriales y cognitivas de *Diplocynodon tormis* con la colección de reconstrucciones tridimensionales de las cavidades craneales de ejemplares de cocodrilos actuales.

- Objetivo 3: Comparación de la reconstrucción de las cavidades internas y análisis de las capacidades neurosensoriales y cognitivas de *Lohuecosuchus megadontos* con la colección de reconstrucciones tridimensionales de las cavidades craneales de ejemplares de cocodrilos actuales.

- Objetivo 4: Comparación de la reconstrucción de las cavidades internas y análisis de las capacidades neurosensoriales y cognitivas de *Agaresuchus fontisensis* con la colección de reconstrucciones tridimensionales de las cavidades craneales de ejemplares de cocodrilos actuales.

- Objetivo 5: Comparación de la reconstrucción de las cavidades internas y análisis de las capacidades neurosensoriales y cognitivas de los ejemplares del tercer morfotipo craneal de Lo Hueco con la colección de reconstrucciones tridimensionales de las cavidades craneales de ejemplares de cocodrilos actuales y de las otras dos especies halladas en el yacimiento de Lo Hueco: *Lohuecosuchus megadontos* y *Agaresuchus fontisensis*.

HYPOTHESES AND OBJECTIVES

The aim of this PhD thesis is to test a general hypothesis about the origin and evolution of the inner skull cavities in the early radiation of Eusuchia (modern crocodiles), crocodylomorphs that include the common ancestor of crown-group Crocodylia, *Hylaeochampsa vectiana* and all its descendants.

The fossil site of Lo Hueco (Fuentes, Cuenca. Spain) has yielded a huge collection of remains assigned to Allodaposuchidae, the sister-group of Crocodylia (Narváez et al., 2015). Among these remains, there are several skulls referred to two new species: *Lohuecosuchus megadontos* and *Agaresuchus fontisensis*. Furthermore, some specimens show different size and morphology from the aforementioned species, and have been treated as a third potential allodaposuchid taxon.

To establish an evolutionary framework, the information obtained from digital reconstructions of the inner skull cavities of these specimens was compared to those from extant and extinct specimens of Crocodylia, including a paratype of *Diplocynodon tormis*, a basal alligatoroid from the Eocene of Salamanca, Spain.

The reconstruction of the inner skull cavities allows to make a comparative study of these structures, and also to estimate the neurosensorial and cognitive capabilities of these animals.

Therefore, the hypotheses and corresponding objectives of this PhD thesis are:

General hypothesis: The morphology of the inner skull cavities of Crocodylia is shared with basal Eusuchia, and therefore plesiomorphic.

1.- Specific hypotheses regarding the variability of morphological characters in the inner skull cavities of Crocodylia.

- Hypothesis 1.1: There is an autapomorphic character combination in the inner skull cavities of Crocodylia, such as a sigmoid brain outline in lateral view, a caudoventrally oriented pituitary, a dorsally elongated anterior semicircular canal and a very developed pharyngotympanic sinus system.

- Hypothesis 1.2: There are differences in the shape of the inner skull cavities of the major lineages of Crocodylia, such as the presence of a convexity in the posterodorsal surface of the brain in alligatoroids and a long median pharyngeal sinus in crocodyloids.

- Hypothesis 1.3: Inferred neurosensorial and cognitive capabilities of Crocodylia are related to the maximum size of the adult specimens rather than to phylogeny

2.- Specific hypotheses regarding the shape of the inner skull cavities of the basal alligatoroid *Diplocynodon tormis.*

- Hypothesis 2.1: The inner skull cavities of *Diplocynodon tormis* show the same morphology and evolutionary novelties than those of extant representatives of Alligatoroidea.

- Hypothesis 2.2: Inferred neurosensorial and cognitive capabilities of *Diplocynodon tormis* are similar to those of medium-sized crocodylians, such as *Caiman crocodilus, Melanosuchus niger* and *Osteolaemus tetraspis.*

3.- Specific hypotheses regarding the inner skull cavities of *Lohuecosuchus megadontos.*

- Hypothesis 3.1: The inner skull cavities of *Lohuecosuchus megadontos* show the same morphology and evolutionary novelties than those of extant representatives of Crocodylia.

- Hypothesis 3.2: Inferred neurosensorial and cognitive capabilities of *Lohuecosuchus megadontos* are similar to those of large-sized crocodylians, such as *Alligator mississippiensis* and *Crocodylus niloticus.*

4.- Specific hypotheses regarding the inner skull cavities of *Agaresuchus fontisensis*.

- Hypothesis 4.1: The inner skull cavities of *Agaresuchus fontisensis* show the same morphology and evolutionary novelties than those of extant representatives of Crocodylia.

- Hypothesis 4.2: Inferred neurosensorial and cognitive capabilities of *Agaresuchus fontisensis* are similar to those of large-sized crocodylians, such as *Alligator mississippiensis* and *Crocodylus niloticus.*

5.- Specific hypotheses regarding the inner skull cavities of the third skull morphotype from Lo Hueco.

- Hypothesis 5.1: The shape of the inner skull cavities of the third skull morphotype from Lo Hueco are similar to those of *Lohuecosuchus megadontos* and

Agaresuchus fontisensis, due to their phylogenetical proximity and therefore, similar to those of Crocodylia too.

- Hypothesis 5.2: Inferred neurosensorial and cognitive capabilities of the third skull morphotype from Lo Hueco are similar to those of medium-sized crocodylians, such as *Caiman crocodilus*, *Melanosuchus niger* and *Osteolaemus tetraspis.*

In order to test these hypotheses, the following objectives are proposed:

- Objective 1: To generate and compare between the reconstructions of inner skull cavities and analyses of neurosensorial and cognitive capabilities of several extant Alligatoroidea, Crocodyloidea and Gavialoidea specimens.

- Objective 2: To compare the reconstruction of inner skull cavities and analyses of neurosensorial and cogntive capabilities of *Diplocynodon tormis* with data from extant crocodiles obtained in O1.

- Objective 3: To compare the reconstructions of inner skull cavities and analysis of neurosensorial and cognitive capabilities of *Lohuecosuchus megadontos* with data from extant crocodiles obtained in O1..

- Objective 4: To compare the reconstructions of inner skull cavities and analyses of neurosensorial and cognitive capabilities of *Agaresuchus fontisensis* with data from extant crocodiles obtained in O1.

- Objective 5: To compare the reconstructions of inner skull cavities and analyses of neurosensorial and cognitive capabilities of the third skull morphotype from Lo Hueco with data from extant crocodiles obtained in O1 and the other two allodaposuchid species found in Lo Hueco.

CAPÍTULO 3: MATERIAL Y MÉTODOS

MATERIAL AND METHODS

Materiales

Los principales objetos de estudio de la presente tesis doctoral son una colección de cráneos de eusuquios procedentes del yacimiento del Cretácico Superior de Lo Hueco (Fuentes, Cuenca) y del yacimiento del Eoceno medio de Teso de la Flecha (Salamanca). Los cráneos analizados de Lo Hueco son los pertenecientes al holotipo de *Lohuecosuchus megadontos* (HUE-04498), el holotipo y uno de los paratipos de *Agaresuchus fontisensis* (HUE-02502 y 03713 respectivamente), y tres ejemplares inéditos de alodaposúquido indeterminado (HUE-02018, HUE-02815 y HUE-08881). En cuanto al material de Teso de la Flecha, se estudió un basicráneo asignado como uno de los paratipos de *Diplocynodon tormis* (STUS-344).

Para llevar a cabo comparaciones morfológicas, se han reconstruido también diversos ejemplares actuales, que abarcan la totalidad de los linajes que componen actualmente Crocodylia, así como la inclusión de ejemplares de distintos tamaños, siguiendo la subdivisión propuesta por Dufeau and Witmer (2015). La base de datos comparativa está compuesta por el aligatoroideo de gran tamaño *Alligator mississippiensis* (MZB 92-0231), el aligatoroideo de tamaño medio *Caiman crocodilus* (caiman_crocodilus_CRARC), los crocodiloideos de gran tamaño *Crocodylus niloticus* (MZB 2003-1423) y *Tomistoma schlegelii* (TMM M-6342), el crocodiloideo de tamaño medio *Osteolaemus tetraspis* (MZB 2006-0039), y el gavialoideo *Gavialis gangeticus* (UF118998). En los análisis más recientes, se ha podido añadir también el aligatoroideo *Melanosuchus niger* (RVC-JRH-FBC1), cuya longitud craneana coincide con el límite sugerido entre las dos subdivisiones, y el crocodiloideo de tamaño medio *Crocodylus moreletii* (RVC-JRH-FMC3).

Para la realización de los análisis de las capacidades neurosensoriales y cognitivas, se incluyeron también cinco taxones actuales a modo de grupos externos (Fig. 3.1): los saurópsidos no-arcosauromorfos están representados por la tortuga *Elseya dentata* (TMM M-9315), el lacértido *Varanus exanthematicus* (FMNH 58299) y la serpiente *Aspidites melanocephalus* (FMNH 97055). También se incluyeron las aves *Struthio camelus* (TMM M-4826) y *Coragyps atratus* (FMM, sin sigla).

Los TACs de *A. mississippiensis*, *C. crocodilus*, *C. niloticus* y *O. tetraspis* fueron amablemente cedidos por el Dr. Josep Fortuny (Institut Català de Paleontologia Miquel Crusafont, Sabadell). Los de *T. schlegelii*, al igual que *E. dentata*, *V. exanthematicus*, *A.*

melanocephalus, *S. camelus* y *C. atratus*, fueron obtenidos a través de la plataforma www.digimorph.com. El TAC de *G. gangeticus* fue obtenido a través de www.morphosource.org. Finalmente, los de *M. niger* y *C. moreletii* se obtuvieron gracias a la plataforma https://osf.io/.

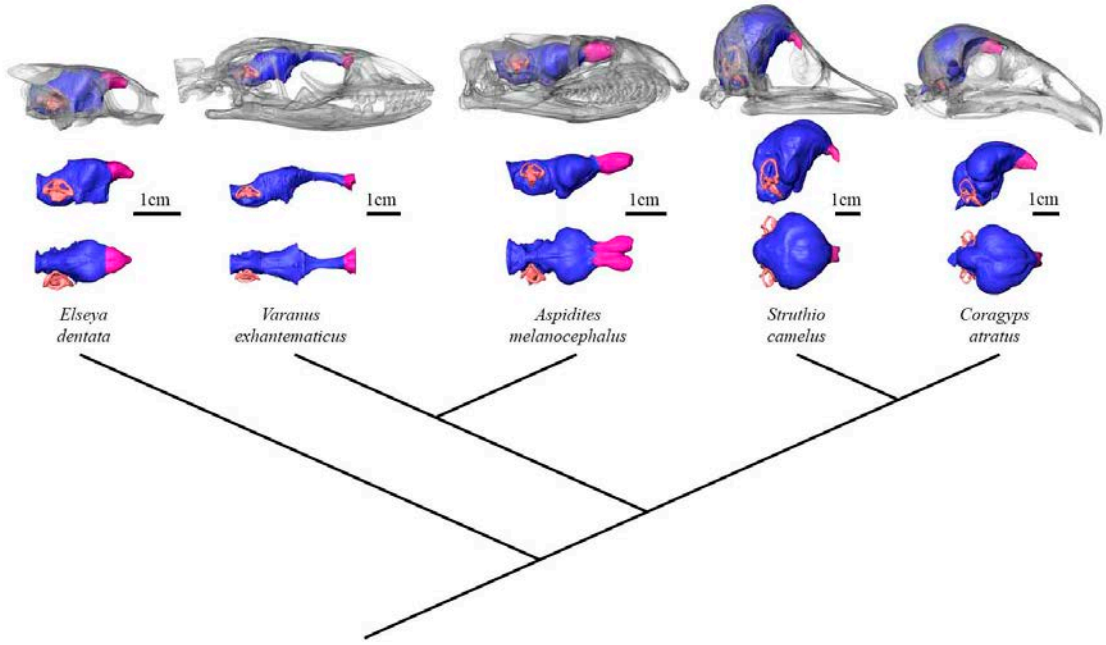

Fig. 3.1: Filogenia de Sauropsida que incluye los cinco taxones utilizados como grupos externos para el análisis de las capacidades neurosensoriales y cognitivas de los cocodrilos. Gris transparentado: huesos del cráneo. Azul: encéfalo. Amarillo: región olfativa. Rosa: oído interno.
Sauropsida phylogeny, including the five taxa used as outgroups in the analyses of neurosensorial and cognitive capabilities of crocodiles. Transparented grey: skull bones. Blue: brain. Yellow: olfactory region. Pink: inner ear.

Métodos

Para la realización de la presente tesis doctoral se han reconstruido de primera mano la totalidad de las cavidades intracraneanas de los diferentes ejemplares de cocodrilos eusuquios procedentes del yacimiento del Cretácico Superior de Lo Hueco y del yacimiento del Eoceno medio de Teso de la Flecha. Los cráneos fueron escaneados en diversas instituciones:

Los ejemplares de Lo Hueco HUE-02502, HUE-04498 y HUE-08881 se digitalizaron en un escáner Optima CT600, en la Clínica Quirón Juan Bravo (Madrid). Los ejemplares HUE-02502, HUE-02815 y HUE-04498 se escanearon en un Toshiba Asteion, en el Centro Médico de Diagnóstico Talavera (Talavera de la Reina). Los

ejemplares HUE-02018 y HUE-03713 se digitalizaron en un escáner Sinus 1.25 H80s, en el Centro de Diagnóstico de Cuenca (Cuenca). El ejemplar HUE-02815 se escaneó en un Yxlon Y.TU 450-D09, en el Institut Català de Paleontologia Miquel Crusafont (Sabadell). Algunos de los cráneos se escanearon en más de una ocasión, ya sea en el mismo centro o en un centro distinto, con el fin de optimizar los resultados obtenidos previamente, para mejorar la resolución de las pruebas previas y facilitar la discriminación de las cavidades intracraneanas, o para centrarse en una parte concreta del cráneo y obtener imágenes más detalladas de la misma.

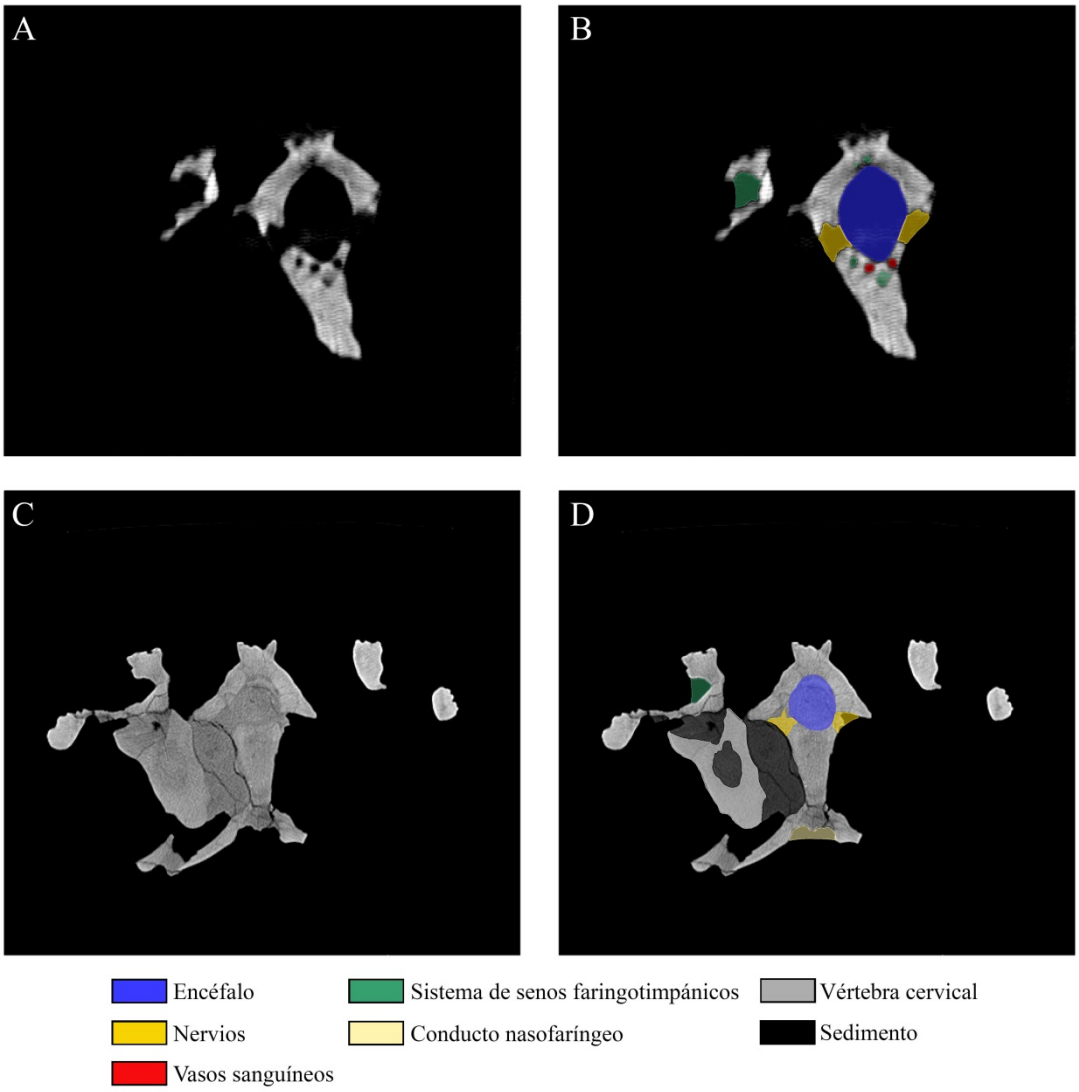

Fig. 3.2: Secciones craneales en plano axial obtenidos a partir de un escáner TAC de *Diplocynodon tormis* STUS-344 (**A**, **B**) y *Agaresuchus fontisensis* HUE-02502 (**C**, **D**), marcando las cavidades identificadas.

Cranial axial sections obtained from a CT-scan of *Diplocynodon tormis* STUS-344 (**A**, **B**) and *Agaresuchus fontisensis* HUE-02502 (**C**, **D**), remarking each identified cavity. Blue: brain. Yellow: nerves. Red: blood vessels. Green: pharyngotympanic sinus system. Light yellow: nassopharyngeal duct. Grey: cervical vertebra. Black: sediment.

El paratipo de *Diplocynodon tormis* (STUS-344) incluido en la base de datos de crocodilios fue también escaneado en el Institut Català de Paleontologia Miquel Crusafont.

Los cortes obtenidos a partir del escáner de Tomografía Computerizada (u obtenidos a través de las plataformas antes mencionadas) se importaron al software de segmentación Avizo 7.1 (VSG, Burlington, MA, USA). En este programa se analizaron cada una de las imágenes para identificar las cavidades intracraneanas, diferenciando entre estructuras óseas y cavidades (Fig. 3.2A y 3.2B), o entre estructuras óseas y sedimento contenido en la cavidad (Fig. 3.2C y 3.2D).

Como se mencionó anteriormente, la tecnología TAC detecta la diferencia de densidades entre los distintos materiales que componen la muestra (Goldman, 2007), por lo que si el sedimento que rellena la cavidad y el hueso mineralizado tienen una densidad similar, será complicado, en el mejor de los casos, discriminar los límites entre ambas estructuras (Fig 1.4). Una vez identificadas y señaladas las cavidades, Avizo permite combinar el conjunto de imágenes para generar una estructura tridimensional. Algunas de las cavidades, como la del encéfalo o el oído interno, son sencillas de identificar y delimitar en los propios cortes del TAC, debido a su posición en el basicráneo o su morfología. Sin embargo, en el caso de sistemas más complejos, compuestos por varias cavidades, como los del sistema de senos faringotimpánicos, o cada una de las regiones del encéfalo, se reconstruye primero toda la estructura y posteriormente se delimita cada una de las cavidades menores en la malla tridimensional (Fig. 3.3).

Algunos de los cráneos, como el holotipo de *L. megadontos* (HUE-04498) o el paratipo de *A. fontisensis* (HUE-03713) presentan una marcada compresión, ya sea dorsoventral en el primer caso o lateral en el segundo. Para tratar de compensar este efecto, estas reconstrucciones fueron retrodeformadas. Para ello, se analizaron las proporciones de ejemplares cercanamente emparentados y cuyas morfologías se asemejen a los especímes a retrodeformar: el holotipo de *A. fontisensis* en el caso de HUE-03717, y los cráneos de los ejemplares de *Allodaposuchus precedens* de Oarda de Jos, Rumanía (Delfino et al., 2008) y *Agaresuchus subjuniperus* de Beranuy, España (Puértolas-Pascual et al., 2014). Una vez establecida la proporción aproximada de los ejemplares deformados, se les aplicó un reescalado a los ejes correspondientes,

mediante la herramienta "transform editor" de Avizo. Debe tenerse en cuenta que estos procesos de retrodeformación solo permiten acercar el modelo deformado a la morfología original del animal, no obtener una réplica exacta del mismo (Tschopp et al., 2013; Lautenschlager and Butler, 2016; Lautenschlager et al., 2016; Vidal and Díez Díaz, 2017).

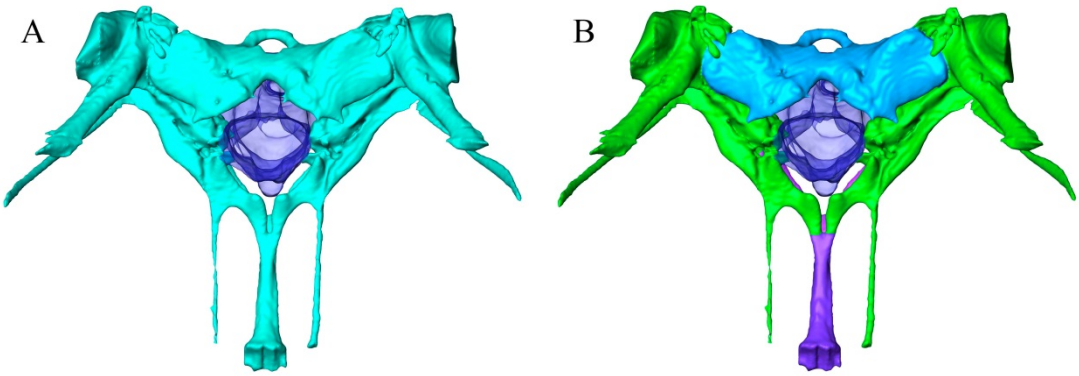

Fig. 3.3: Proceso de identificación de las cavidades que componen el sistema de senos faringotimpánicos en *Crocodylus niloticus*, con el encéfalo transparentado para una mejor visualización. **A**; malla tridimensional obtenida tras la segmentación en Avizo 7.1. **B**; malla tridimensional modificada en un editor de objetos 3D, en el que se han delimitado e individualizado las cavidades menores que componen el sistema.
Identification process of the cavities that form the pharyngotympanic sinus system of *Crocodylus niloticus*, with the brain rendered transparent for better visualization. **A**; tridimensional reconstruction obtained by segmentation in Avizo 7.1. **B**; tridimensional reconstruction modified in a tridimensional object editor. The small cavities that form the system were delimited and isolated.

También es necesario remarcar que, aunque en este tipo de estudios se denomine a las estructuras reconstruidas como cada uno de los distintos órganos contenidos en ellas, lo que realmente se reconstruye son las cavidades que albergan estos órganos. Así, siguiendo la propuesta de Witmer et al., (2008), se utiliza el término “oído interno” en vez de “cavidad que aloja el oído interno”. Por otro lado, estas reconstrucciones incluyen todas las estructuras asociadas a dicho órgano. Así, lo que en la presente tesis doctoral se denomina “encéfalo”, está realmente formado por el propio encéfalo además de sus estructuras anejas (Hopson, 1977; Witmer et al., 2008) como las meninges, que pueden llegar a ocupar hasta el 70% del volumen de la cavidad encefálica (Jirak and Janacek, 2017).

Las descripciones y representaciones de las cavidades intracraneanas se basan en la terminología y la paleta de colores utilizados en diversos estudios previos. De esta forma, la terminología y la gama de colores utilizada para el encéfalo se corresponden con la sugerida por Witmer et al., (2008). Para el sistema de senos faringotimpánicos se ha empleado la terminología utilizada en el estudio embrionario centrado en dichas cavidades de Dufeau y Witmer, (2015). Finalmente, el sistema de senos paranasales se basó en la terminología y colores empleados por Witmer y Ridgely, (2008).

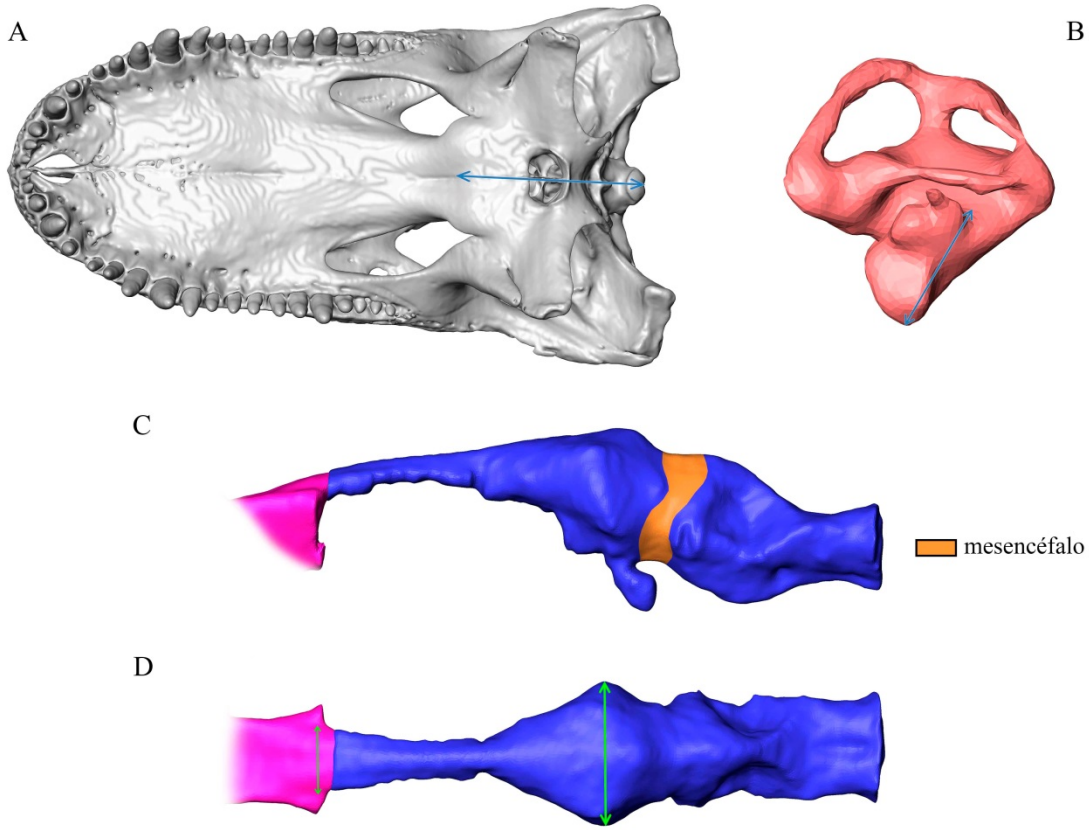

Fig. 3.4: Medidas realizadas a la reconstrucción de *Alligator mississippiensis* para los distintos análisis neurosensoriales y cognitivos. **A**; reconstrucción del cráneo de *A. mississippiensis* en vista ventral, señalando la longitud basicraneal necesaria para estimar la agudeza acústica. **B**; reconstrucción del oído interno izquierdo, en vista lateral izquierda, señalando la longitud de la cóclea, necesaria para estimar la agudeza acústica. **C**; reconstrucción del encéfalo en vista lateral izquierda, destacando la región del mesencéfalo, utilizado para estimar la agudeza visual. **D**; reconstrucción del encéfalo en vista dorsal, señalando la máxima longitud del lóbulo olfativo y de los hemisferios cerebrales, necesarios para estimar la agudeza olfativa.

Measurements for the different neurosensorial and cognitive analyses in the reconstruction of *Alligator mississippiensis*. **A**; reconstruction of the skull in ventral view, marking basicranial length, necessary for the hearing capability analysis. **B**; reconstruction of the inner ear, in left lateral view, marking the cochlear length, necessary for the hearing capability analysis. **C**; reconstruction of the brain in left lateral view, marking the mesencephalic region, necessary for the visual capability analysis. **D**; reconstruction of the brain in dorsal view, marking the maximum length of the olfactory bulb and the cerebral hemispheres, necessary for the hearing capability analysis. Orange region: mesencephalon.

Para el análisis de las capacidades neurosensoriales y cognitivas, se realizaron una serie de medidas lineales y volumétricas en regiones concretas de las cavidades aquí reconstruidas. Dichas mediciones se realizaron a través del software Avizo 7.1, en el modo "vista ortogonal", de forma que el plano de proyección sea el mismo independientemente del ángulo y la proximidad con que se vea la reconstrucción.

Para estimar la agudeza olfativa, Zelenitsky et al., (2009, 2011) compara la longitud linear mayor del lóbulo olfativo y de los hemisferios cerebrales (Fig. 3.4D, medidas en verde), y posteriormente los transforma logarítmicamente. Con el fin de calcular la agudeza auditiva, Walsh et al., (2009) establece una relación entre la longitud de la cóclea y la longitud basicraneal (longitud entre el punto más caudal del cóndilo basioccipital y el punto más medial de la sutura entre pterigoides y palatino) (Fig. 3.4A y B, medidas en azul), también transformada logarítmicamente. Para inferir la agudeza visual, a falta de estudios que relacionen el tamaño de la órbita con el del globo ocular, se ha comparado el volumen del mesencéfalo (Fig. 3.4C) con el volumen total del encéfalo. Finalmente, para calcular el cociente de encefalización, se ha aplicado la fórmula de Hurlburt, (1996) específica para "reptiles":

$$REQ = \frac{masa\ encéfalo\ (g)}{0.0155 \times masa\ corporal^{0.533}}$$

Para estimar qué volumen del total de la cavidad encefálica está ocupado por el encéfalo y cual por las meninges, se realizó un gráfico de dispersión que incluía el volumen de la cavidad encefálica frente al volumen relativo del encéfalo de cocodrilos actuales en distinto estadío ontogenético, a partir de los datos de Jirak y Janacek, (2017) primero (Fig. 4.5A), y posteriormente añadiendo los de Watanabe et al., (2018) (Fig. 3.5B), y se calculó una curva de regresión en el software SPSS 24.0 (IBM, Armonk, New York). La curva calculada, con un R^2=0.824, representa la ecuación potencial:

$$y = 624.293x^{-0.286}$$

Dónde "y" es el volumen relativo del encéfalo (en porcentaje), y "x" es el volumen de la cavidad encefálica. Una vez calculado el volumen del encéfalo, se calculó su masa aplicando una densidad de 1g/cm3 (Franzosa, 2004). Finalmente, la masa corporal se ha obtenido aplicando las fórmulas de Dodson, (1975), Webb y Messel, (1978) y Platt et al., (2011), en función del tamaño y grupo filogenético de las muestras, que relacionan la longitud craneal de estos animales con su masa corporal.

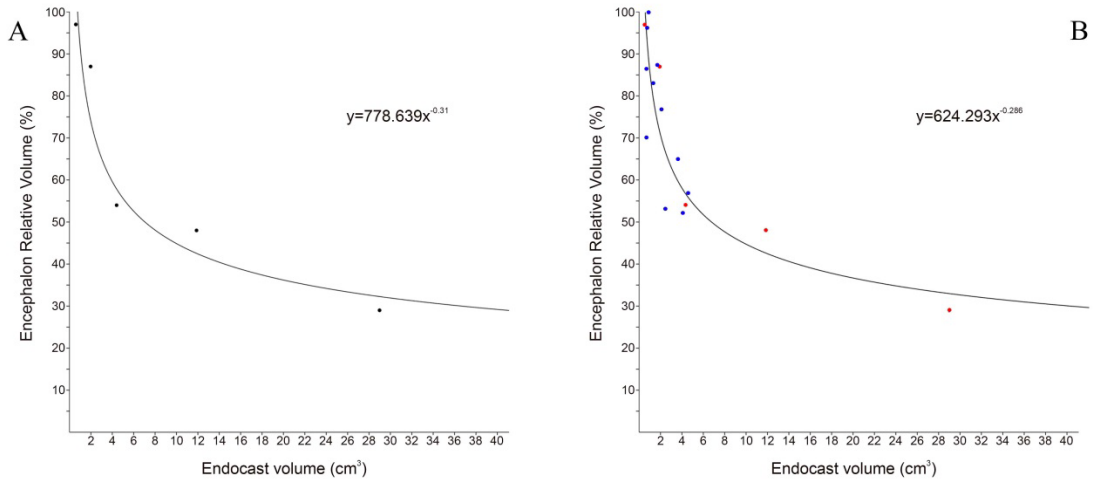

Fig. 3.5: Gráfica de dispersión y curva de regresión que enfrenta el volumen relativo del cerebro frente al volumen total de la cavidad encefálica a lo largo de la ontogenia en cocodrilos, basado en: **A**, los datos obtenidos de Jirak y Janacek, (2017). **B**, los datos obtenidos de Jirak y Janacek, (2017), marcados en color rojo, y Watanabe *et al.* (2018), marcados como puntos azules.
Plot and regression of the relative volume of the encephalon versus the endocast total volume during the ontogeny of crocodiles, basing on: **A**, the data of Jirak and Janacek, (2017). **B**, the data of Jirak and Janacek, (2017), plotted as red dots, and Watanabe *et al.* (2018), plotted as blue dots.

Material

The main research specimens of this PhD dissertation are several eusuchian skulls found in the Late Cretaceous fossil site of Lo Hueco (Fuentes, Cuenca, Spain) and in the Middle Eocene fossil site of Teso de la Flecha (Salamanca, Spain). The skulls are those of the holotype of *Lohuecosuchus megadontos* (HUE-04498), the holotype and one of the paratypes of *Agaresuchus fontisensis* (HUE-02502 and HUE-03713 respectively), and three unpublished specimens of an indeterminate allodaposuchid (HUE-02018, HUE-02815 and HUE-08881). The sample from Teso de la Flecha is a basicranium of one of the paratypes of the basal alligatoroid *Diplocynodon tormis* (STUS-344).

To carry on morphological comparisons, several extant crocodylians have been reconstructed as comparative framework, including specimens of the major crocodylian lineages of different sizes following the division proposed by Dufeau and Witmer (2015). The sample is composed by the large-sized alligatoroid *Alligator mississippiensis* (MZB 92-0231), the medium-sized alligatoroid *Caiman crocodilus* (caiman_crocodilus_CRARC), the large-sized crocodyloids *Crocodylus niloticus* (MZB 2003-1423) and *Tomistoma schlegelii* (TMM M-6342), the medium-sized crocodyloid *Osteolaemus tetraspis* (MZB 2006-0039), and the gavialoid *Gavialis gangeticus* (UF118998). The alligatoroid *Melanosuchus niger* (RVC-JRH-FBC1), whose cranial length coincides with the limit between both categories suggested by Dufeau and Witmer (2015), and the medium-sized crocodyloid *Crocodylus moreletii* (RVC-JRH-FMC3) were added to at the final research stages.

For the neurosensorial and cognitive analyses, five more taxa were included as outgroups (Fig. 3.1): non-archosauromorph sauropsids are represented by the testudine *Elseya dentata* (TMM M-9315), the lacertid *Varanus exanthematicus* (FMNH 58299) and the serpente *Aspidites melanocephalus* (FMNH 97055). The birds *Struthio camelus* (TMM M-4826) and *Coragyps atratus* (FMM, uncatalogued) were also included in the sample.

CT-scans of *A. mississippiensis*, *C. crocodilus*, *C. niloticus* and *O. tetraspis* were kindly provided by Dr Josep Fortuny (Institut Català de Paleontologia Miquel Crusafont, Sabadell, Spain). Those of *T. schlegelii*, as those of *E. dentata*, *V. exanthematicus*, *A. melanocephalus*, *S. camelus* and *C. atratus*, were obtained from the online digital repository www.digimorph.com. CT-scan of *G. gangeticus* was obtained

from the online digital repository www.morphosource.org. Finally, those of *M. niger* and *C. moreletii* were obtained from the online digital repository https://osf.io/.

Methods

In order to test the hypotheses proposed for this PhD thesis, all the inner skull cavities of the eusuchian from the Upper Cretaceous fossil site of Lo Hueco and from the Middle Eocene fossil site of Teso de la Flecha were digitally reconstructed with CT-scanning. The skulls were CT-scanned at different institutions.

HUE-08881, HUE-02502 and HUE-04498 were scanned in an Optima CT600, at the Clínica Quirón Juan Bravo (Madrid, Spain). HUE-02815, HUE-02502 and HUE-04498 were scanned in a Toshiba Asteion, at the Centro Médico de Diagnóstico Talavera (Talavera de la Reina, Spain). HUE-02018 and HUE-03713 were scanned in a Sinus 1.25 H80s, at the Centro de Diagnóstico de Cuenca (Cuenca, Spain). HUE-02815 was scanned at an Yxlon Y.TU 450-D09, in the Institut Català de Paleontologia Miquel Crusafont (Sabadell, Spain). Some skulls were scanned more than once, at the same centre on a different one. This was done to optimize previously obtained results, improving the contrast and to aid in the discrimination of the inner skull cavities, or to focus on a specific part of the skull and obtaining more detailed images of it.

The included paratype of *Diplocynodon tormis* (STUS-344) was also scanned at the Institut Català de Paleontologia Miquel Crusafont.

Slices obtained from the CT-scanner were imported to the segmentation software Avizo 7.1 (VSG, Burlington, MA, USA). In this software, all images were analyzed to identify each of the inner skull cavities, distinguishing between bony structures and cavities (Fig. 3.2A and 3.2B), or between the bone and the sediment that fills the cavity (Fig. 3.2C and 3.2D).

As mentioned, CT technology detects and discriminates the difference of densities of the specimen (Goldman, 2007). Therefore, if the infilling sediment and the mineralized bone has a similar density, it will be difficult (in the best case) to determine the boundaries between both structures (Fig 1.4). Once identified and delimited the cavities, Avizo allows overlapping the images to generate a three dimensional polygon mesh.

Some cavities, such as the brain or inner ear, are easy to identify and to delimit in the individual CT slices, due to their location in the braincase or their particular morphology. However, to reconstruct more complex structures, such as the pharyngotympanic sinus system or each of the brain regions, the whole cavity is reconstructed first, and then every single part is delimited in the three-dimensional model (Fig. 3.3).

Some skulls, such as the holotype of *L. megadontos* (HUE-04498) or the paratype of *A. fontisensis* (HUE-03713) show remarkable taphonomical compression, dorsoventrally in the former and lateral in the latter. To try to diminish this effect, these reconstructions were retrodeformed. To do this, proportions of closely related specimens and/or species with similar morphology were analyzed: the holotype of *A. fontisensis* for HUE-03713, and the skulls of the *Allodaposuchus precedens* from Oarda de Jos, Rumanía (Delfino et al., 2008) and *Agaresuchus subjuniperus* from Beranuy, España (Puértolas-Pascual et al., 2014) for HUE-04498. Once the expected proportions were obtained, each sample was scaled in the corresponding axis using the "transform editor" in Avizo. It must be taken into account that these retrodeformation processes just allow making a hypothetical approach to the original skull morphology, not recovering their original shape (Tschopp et al., 2013; Lautenschlager and Butler, 2016; Lautenschlager et al., 2016; Vidal and Díez Díaz, 2017).

It must be said that the structures here reconstructed are the cavities that housed soft-tissues, not the soft-tissues themselves. To ease the description, and following the suggestion of Witmer et al., (2008), these cavities are named as the organs contained in them. In this way, we use “inner ear” instead “recess that housed the inner ear”. Furthermore, the reconstructed structures include the organ and all associated tissues: the here named “brain” is composed of the brain itself and its annexed organs, such as the dural envelope (Hopson, 1977; Witmer et al., 2008), which may fill up to the 70% of the total volume of the brain cavity (Jirak and Janacek, 2017).

Descriptions and figures of the inner skull cavities are based in the terminology and colour map used in different studies: the terminology and colour map used for the brain are those used by Witmer et al., (2008). Names and colours of the pharyngotympanic sinus system are those used by Dufeau y Witmer, (2015). Finally,

the paranasal sinus system is based on the terminology and colour map proposed by Witmer and Ridgely, (2008).

For the analyses of the neurosensorial and cognitive capabilities, several linear and volumetric measurements of the inner skull cavities were required. These measurements were made with Avizo 7.1, in the "orthogonal view" mode, so that the projection plane is the same regardless of the angle or proximity of the reconstruction. For the olfactory acuity estimations, Zelenitsky et al., (2009, 2011) compared the longest longitude of the olfactory bulb and cerebral hemispheres (Fig. 3.4D, green measurements), and log-transformed them. For the auditory capability, Walsh et al., (2009) related the cochlear length and the basicranial length (the length between the caudalmost point of the basioccipital condyle and the medialmost point of the pterygoid-palatine suture) (Fig. 3.4A and B, blue measurements), log-transforming it too. For the visual acuity analysis, in the absence of studies that relate the size of the eyeball and the orbit, telencephalic volume was compared to the total brain volume (Fig. 3.4C). Finally, to calculate the encephalization quotient, the specific formula for reptiles proposed by Hurlburt, (1996) was applied:

$$REQ = \frac{brain\ mass\ (g)}{0.0155 \times body\ mass^{0.533}}$$

To estimate how much volume of the brain cavity is filled by the brain itself and how much is occupied by the dural envelope, a dispersion plot which relates the volume of the brain cavity with the relative volume of the brain in extant crocodiles with a different ontogenetic state, was generated basing first on the data of Jirak and Janacek, (2017) (Fig. 3.5A), and posteriorly adding the data of Watanabe et al., (2018) (Fig. 4.5B), and a regression curve was calculated in the software SPSS 24.0 (IBM, Armonk, New York). The potential equation obtained has R^2=0.824.

$$y = 624.293x^{-0.286}$$

Where "y" is the relative volume of the brain (in percentage), and "x" is the volume of the brain cavity. Once the volume of the brain was estimated, its mass was calculated applying a density of 1g/cm3 (Franzosa, 2004). Finally, body mass was obtained using the formulas proposed by Dodson, (1975), Webb and Messel, (1978) and Platt et al., (2011), depending on the size and phylogenetic position of each specimen, which relates the body mass with the skull length of these animals.

SEGUNDA PARTE

SECOND PART

CAPÍTULO 4: INNER SKULL CAVITIES OF CROCODYLIA

4.1 GENERAL SIGHT TO THE INNER CAVITIES OF EXTANT CROCODYLIANS

Crocodylian neuroanatomy is relatively well known, basing on necropsies (e.g. Vergne et al., 2009; Weldon and Ferguson, 1993; Wever, 1971) and etological studies (e.g. Nagloo et al., 2016; Porter et al., 2016; Weldon et al., 1990). However, only a few works describe thoroughly the crocodylian brain cavity structure. Interpretation of skull sections, latex endocasts and application of CT technology allow knowing the general shape of the crocodylian inner skull cavities.

All mesoeucrocodylian inner skull cavities show a similar morphological pattern, due to the conservativeness of these structures (Witmer and Ridgely, 2009; Kley et al., 2010; Knoll et al., 2012; Jirak and Janacek, 2017; Paulina-Carabajal et al., 2017). In this way, extant crocodylian brain is usually elongated, with long olfactory tracts and sigmoid morphology in lateral view. Cerebral hemispheres are clearly visible in dorsal view as two convex structures. The optic lobe is located just caudally from the cerebrum. It is easily distinguishable as a narrowing between the cerebrum and the hindbrain (Jirak and Janacek, 2017). Hindbrain has two dorsolateral concavities formed by the otic capsules, so the dorsal region of the hindbrain, which houses the dorsal longitudinal sinus, is narrower than the ventral part. Ventral longitudinal sinus is clearly visible as a longitudinal ridge in the ventral surface of the hindbrain. Hypophyseal fossa emerges from the caudoventralmost surface of the cerebrum. It extends caudoventrally and, from its tip, emerge two cerebral carotid arteries. These arteries course caudally, turn dorsally to pass through the pharyngotympanic sinus system and finally turn caudoventrally to open by the *foramen caroticum*, on the otoccipital.

Twelve pairs of cranial nerves emerge from the brain. The first pair forms the olfactory tracts. Optic (II), oculomotor (III) and trochlear (IV) nerves emerge laterally from the cerebrum. Trigeminal nerve (V) is the largest one, and it is located in the rostralmost part of the hindbrain. Abducens nerves (VI) are the thinnest, and emerge from the ventral surface of the hindbrain. Facial nerve is located just rostral to the inner ear, and vestibulocochlear nerves (VIII) connect the brain with the inner ear. Glossopharyngeal (IX), vagus (X) and accessory (XI) nerves share a common posterolaterally oriented canal. On the other hand, hypoglossal nerves (XII), the caudalmost of the cranial nerves, are divided into paired canals.

Inner ear is divided into two regions. The dorsal one is the vestibular apparatus, responsible for the spatial proprioception and locomotor behaviour. It is formed by the semicircular canals and sacculus. The anterior semicircular canal is always the largest one in extant crocodiles. Ventrally, the rostrally elongated cochlear duct (or lagena) is in charge of the auditory sensibility.

Crocodiles have a large complex of pneumatic sinuses around the hindbrain that connect the inner ear with the external auditory meatus and the pharynx. Paratympanic sinus system is embryologically divided into two major systems: pharyngotympanic system and median pharyngeal system (Dufeau and Witmer, 2015). Pharyngotympanic system is composed of the pharyngotympanic sinus and its diverticula. Pharyngotympanic sinuses are large lateral cavities between the inner ear and the external auditory meatus. These cavities converge dorsal to the hindbrain by the intertympanic diverticula. This recess is pierced by the parietal pillars, and could extend rostrally in the parietal diverticulum. Ventrally, pharyngotympanic sinuses communicate with the pharynx via the pharyngotympanic tubes. Median pharyngeal system includes the median pharyngeal sinus, a medial canal that joins the pharynx, located ventrally from the hindbrain and between the aforementioned pharyngotympanic tubes. It has a caudorostal bifurcation in its dorsal region. Rostral canal forms the basisphenoid diverticula, which extends dorsally to join the pharyngotympanic sinus. Caudal canal connects with pharyngotympanic system, close to the pharyngotympanic tubes.

Nasal cavities cross the crocodylian skull, extending from the external nares, at the tip of the snout, to the internal choana, in the ventral surface of the basicranium. Nasal passageway is a wide canal that extends horizontally from the nares to the level of the lacrimo-prefrontal area, where it divides into two recesses. The dorsal one is the olfactory region of the nasal cavity, a large recess that continues caudally with the olfactory bulb, olfactory tracts and the brain. Ventrally, the nasal passageway divides into the paired nasopharyngeal ducts. They finally turn ventrally in a right angle to open to the pharynx.

Paranasal sinus system is located in variable-shape cavities at both lateral sides of the nasal passageway. In crocodylians, it is formed by antorbital and postvestibular sinuses and nasolacrimal duct.

Dorsal alveolar canal is a neurovascular structure that crosses rostrodorsally the snout. It houses the maxillary veins and arteries, and the maxillary branches of the trigeminal nerve. At the level of the maxillary-premaxillary suture, it forms a widening, the paravestibular vascular bundle, from where emerge two canals: medial subnarial anastomosis, which connects medially with the nasal passageway, and a ventrally oriented canal that opens onto the palate.

The opportunity of studying the cavities and its content in extant crocodiles is a good starting point to understand the structures showed by their fossil relatives. In this way, a database of eight extant crocodylian specimens was created: the alligatorids *Alligator mississippiensis*, *Caiman crocodilus* and *Melanosuchus niger*; the crocodyloids *Crocodylus niloticus*, *Crocodylus moreletii*, *Osteolaemus tetraspis* and *Tomistoma schlegelii*; and the gavialoid *Gavialis gangeticus*.

Anatomical abbreviations: **aos**: antorbital sinus. **bsd**: basisphenoid diverticula. **car**: cerebral carotid artery. **cer**: cerebral hemispheres. **cq**: cranioquadrate sinus. **dac**: dorsal alveolar canal. **en**: external naris. **ic**: internal choana. **ie**: inner ear. **itd**: intertympanic diverticula. **mps**: medial pharyngeal sinus. **nld**: nasolacrimal duct. **np**: nasal passageway. **npd**: nasopharyngeal duct. **ob**: olfactory bulb. **ol**: optic lobe. **ornc**: olfactory region of the nasal cavity. **ot**: olfactory tract. **pd**: parietal diverticulum. **pfo**: pituitary (hypophyseal) fossa. **pts**: pharyngotympanic sinus. **ptt**: pharyngotympanic tube. **pvs**: postvestibular sinus. **pvvb**: paravestibular vascular bundle. **s**: siphonial tube. **II**: optic nerve canal. **III**: oculomotor nerve canal. **IV**: trochlear nerve canal. **V**: trigeminal nerve canal. **VI**: abducens nerve canal. **VII**: facial nerve canal. **IX-XI**: shared canal for glossopharyngeal, vagus and accessory nerves. $\mathbf{X_{tymp}}$: canal for tympanic branch of vagus nerve. **XII**: hypoglossal nerve paired canals.

Alligator mississippiensis (Fig. 4.1.1)

American alligator is one of the largest alligatoroids. It is from freshwater wetlands of the southeastern of North America. Adult males can measure between 3.5 and 4.5m and weigh up to 450kg.

The specimen MZB 92-0231 was CT-scanned in Hospital Mutua de Terrassa (Terrassa, Spain), in a Siemens Sensation 16, with a voltage of 120kV, a currency of 50mA and an interslicing of 0.5mm. The CT-data was given up by Dr. Josep Fortuny, from the Institut Català de Paleontologia Miquel Crusafont (Sabadell, Spain).

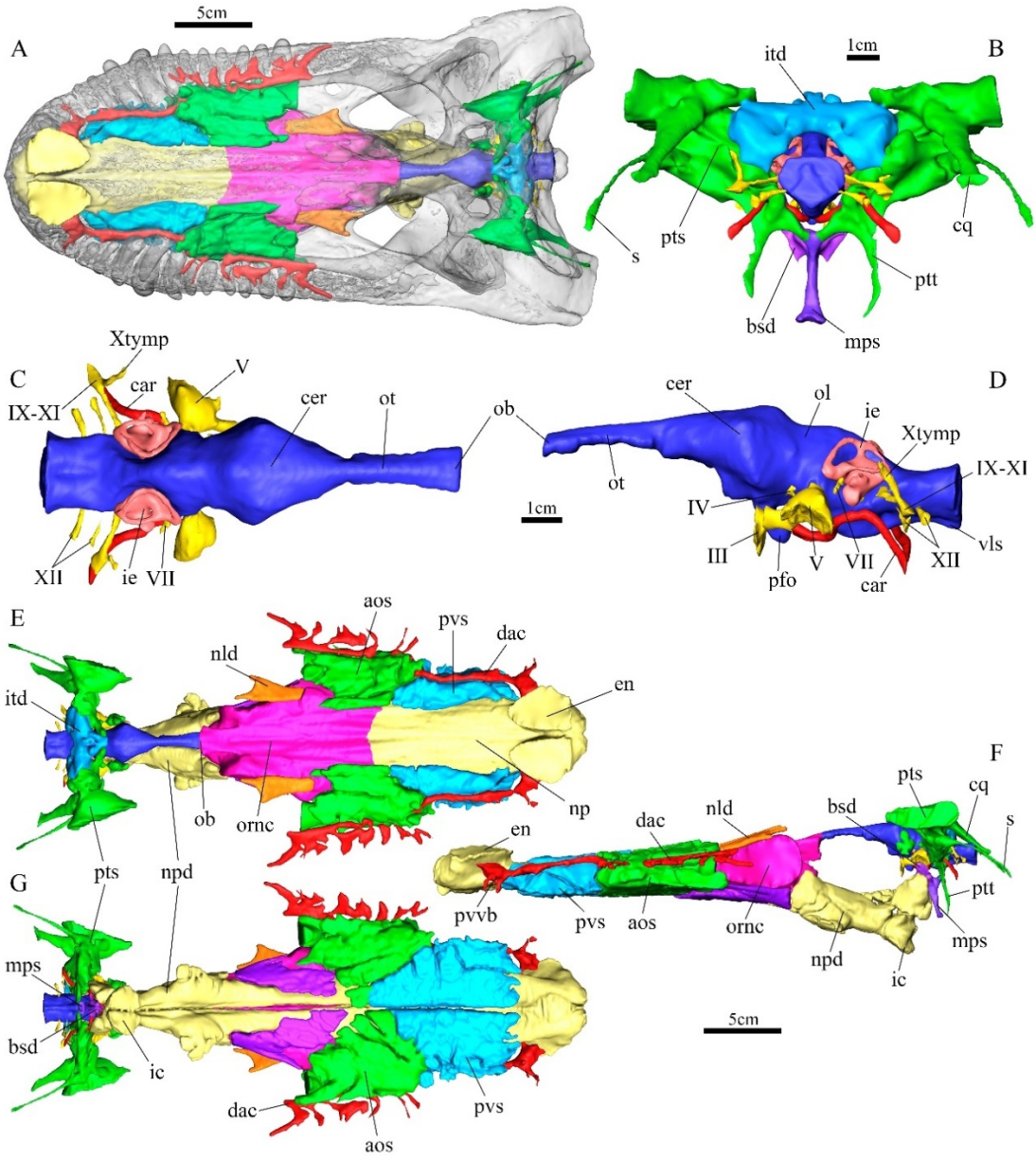

Fig. 4.1.1: Three-dimensional reconstruction of the inner skull cavities of *Alligator mississippiensis*. **A**: in-situ position of the inner skull cavities with the skull rendered semi-transparent, in dorsal view. Scale bar equals 5cm. **B**: *A. mississippiensis* brain, nerves, endosseous labyrinth, arteries and pharyngotympanic sinus system in caudal view. Scale bar equals 1cm. **C**-**D**: *A. mississippiensis* brain, nerves, endosseous labyrinth and arteries in **C**, dorsal and **D**, left lateral views. Scale bar equals 1cm. **E**-**G**: *A. mississippiensis* brain, nerves, endosseous labyrinth, arteries and pharyngotympanic and paranasal sinus systems in **E**, dorsal; **F**, left lateral and **G**, ventral views. Scale bar equals 5cm.

The cerebral hemispheres of *A. mississippiensis* (Fig. 5.1) are easy to distinguish in lateral and dorsal views, as an inflated structure, looking conical in dorsal view. The caudal part of the dorsal brain surface has a marked convexity just before the boundary with a depression formed by the optic lobe. The hindbrain has a marked ventral longitudinal sinus in its ventral surface.

The pharyngotympanic sinus system is large. The central region of the intertympanic diverticula is larger than the lateral ones, and two narrow prefrontal pillar drillings in the boundaries of these two regions. The median pharyngeal sinus is long, although the part ventral to the basisphenoid diverticula is only slightly longer than the dorsal part.

Caiman crocodilus (Fig. 4.1.2)

Common caiman is a small to medium-sized alligatoroid, from wetlands and rivers of Central and South América. Average adults can reach 2m length and 40kg weight.

The specimen caiman_crocodrylus_CRARC was CT-scanned in a Yxlon Y.TU 450-D09, in the Institut Català de Paleontologia Miquel Crusafont (Sabadell, Spain), with a voltage of 400kV, a currency of 1.75mA and an interslicing of 0.25mm. The CT-data was given up by Dr. Josep Fortuny.

Brain endocast of *C. crocodilus* is caudorostrally compressed, having a strongly-marked sigmoid-shape in lateral view. Cerebral hemispheres are round in dorsal view, and its caudodorsal region forms a slight convexity. Hypophyseal fossa has a triangular cross-section.

The central region of the intertympanic diverticula is larger than the lateral parts. Prefrontal pillar drillings are wide. Median pharyngeal sinus is short, being also the region ventral to the basisphenoid diverticula shorter than the dorsal one.

Nasal passageway and nasopharyngeal ducts are aligned, having two 90º turns: just caudal to the external nares, and just rostral to the internal choana. Dorsal alveolar canal opens into the olfactory region of the nasal cavity. Antorbital sinus is very reduced.

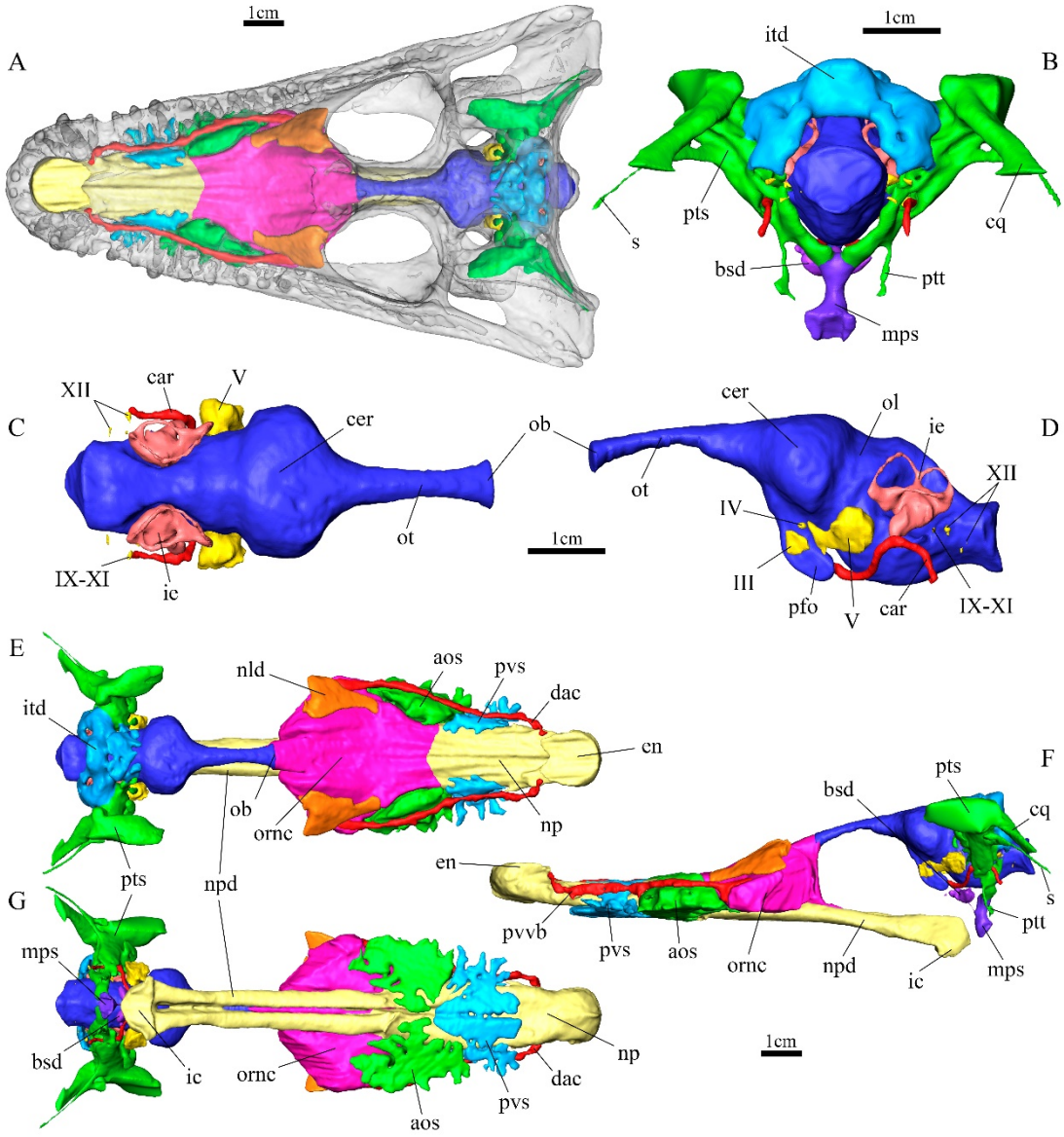

Fig. 4.1.2: Three-dimensional reconstruction of the inner skull cavities of *Caiman crocodilus*. **A**: in-situ position of the inner skull cavities with the skull rendered semi-transparent, in dorsal view. Scale bar equals 1cm. **B**: *C. crocodilus* brain, nerves, endosseous labyrinth, arteries and pharyngotympanic sinus system in caudal view. Scale bar equals 1cm. **C**-**D**: *C. crocodilus* brain, nerves, endosseous labyrinth and arteries in **C**, dorsal and **D**, left lateral views. Scale bar equals 1cm. **E**-**G**: *C. crocodilus* brain, nerves, endosseous labyrinth, arteries and pharyngotympanic and paranasal sinus systems in **E**, dorsal; **F**, left lateral and **G**, ventral views. Scale bar equals 1cm.

Melanosuchus niger (Fig. 4.1.3)

Black caiman is the largest extant alligatoroid. It lives in fresh water environments from South América. It can grow to 5m length and weight more than 400kg.

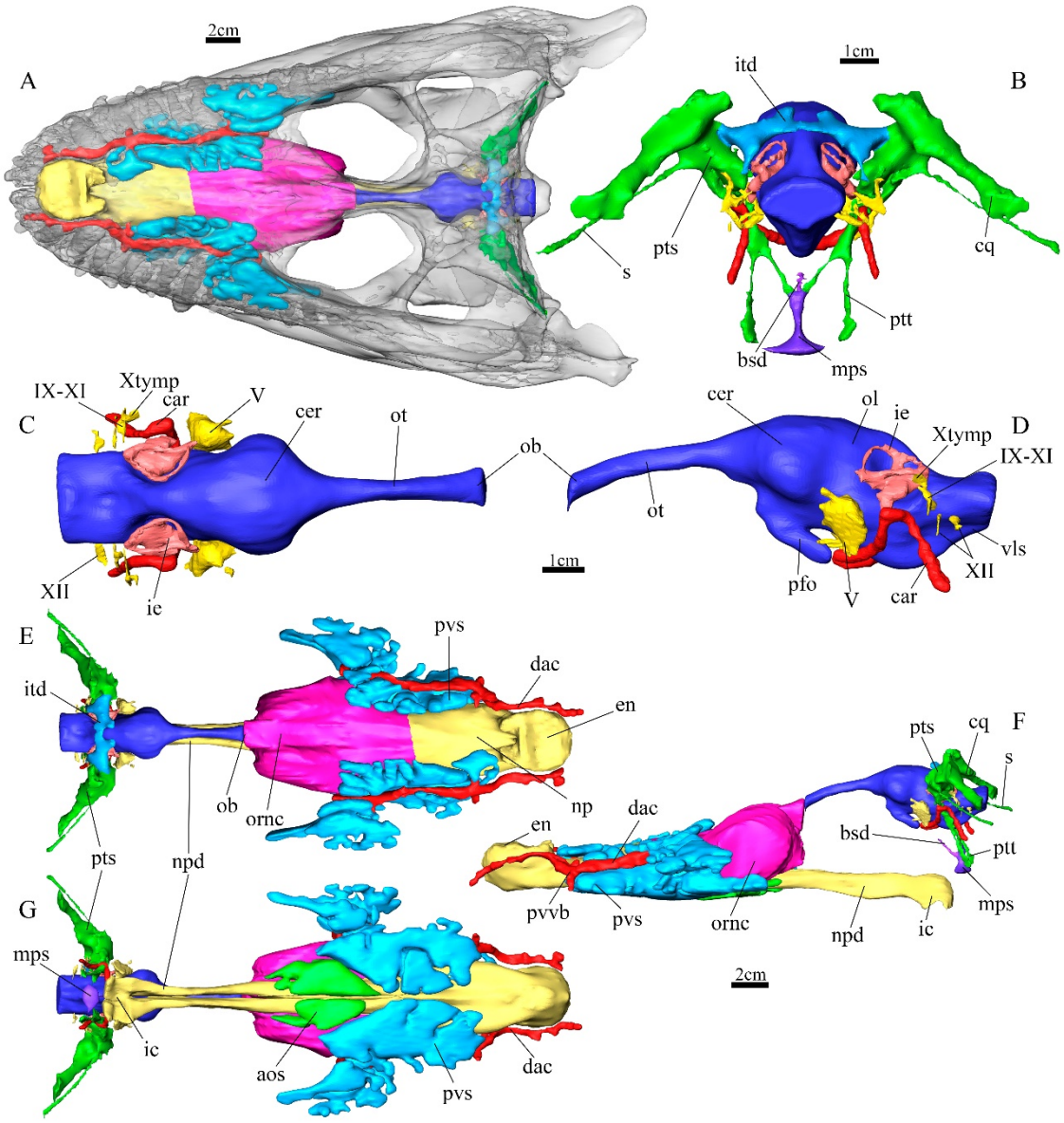

Fig. 4.1.3: Three-dimensional reconstruction of the inner skull cavities of *Melanosuchus niger*. **A**: in-situ position of the inner skull cavities with the skull rendered semi-transparent, in dorsal view. Scale bar equals 2cm. **B**: *M. niger* brain, nerves, endosseous labyrinth, arteries and pharyngotympanic sinus system in caudal view. Scale bar equals 1cm. **C**-**D**: *M. niger* brain, nerves, endosseous labyrinth and arteries in **C**, dorsal and **D**, left lateral views. Scale bar equals 1cm. **E**-**G**: *M. niger* brain, nerves, endosseous labyrinth, arteries and pharyngotympanic and paranasal sinus systems in **E**, dorsal; **F**, left lateral and **G**, ventral views. Scale bar equals 2cm.

The specimen RVC--JRH-FBC1 was CT-scanned in a Philips Mx8000 IDT 16, in the Royal Veterinary College (North Mymms, UK) with a voltage of 120kV, a currency of 133mA and an interslicing of 1.5mm. The CT-data was facilitated by Dr. John Hutchinson and obtained from www.osf.io.

Cerebral hemispheres of *M. niger* are round in dorsal view, with a slight lump in its caudodorsalmost surface. Ventral longitudinal sinus is clearly visible in the ventral surface of the hindbrain.

Its intertympanic diverticula are not as large as in other alligatoroids, but the central region is larger than the lateral ones, as its relatives. Median pharyngeal sinus is short, and basisphenoid diverticula are reduced to a narrow rostrodorsally oriented canal.

Nasal passageway, as the nasopharyngeal ducts, is horizontally oriented. Dorsal alveolar canal opens close to the olfactory region of the nasal cavity.

Crocodylus niloticus (Fig. 4.1.4)

Nile crocodile is the second largest crocodile, only behind *Crocodylus porosus*. It inhabits in lakes and rivers from sub-Saharian Africa. Average Nile crocodiles are between 4.5 and 5.5m length and weight up to 1000kg.

The specimen MZB 2003-1423 was CT-scanned in a Yxlon Y.TU 450-D09, in the Institut Català de Paleontologia Miquel Crusafont (Sabadell, Spain), with a voltage of 400kV, a currency of 3.75mA and an interslicing of 0.5mm. The CT-data was given up by Dr. Josep Fortuny.

Cerebral hemispheres of *C. niloticus* are conical in dorsal view. Hindbrain is rostrocaudally elongated, but keeping the sigmoid morphology.

Pharyngotympanic sinus system is large. Lateral regions of the intertympanic diverticula are laterally expanded. Parietal pillar drillings are barely visible. The ring-shaped parietal diverticulum is located in the dorsorostral surface of the intertympanic diverticula. Median pharyngeal sinus is long, being the ventral part more than four times the length of the dorsal one.

Nasopharyngeal ducts are caudally oriented, but they slightly turn ventrally before recover the horizontality, and finally do a 90º turn to open by the internal choana.

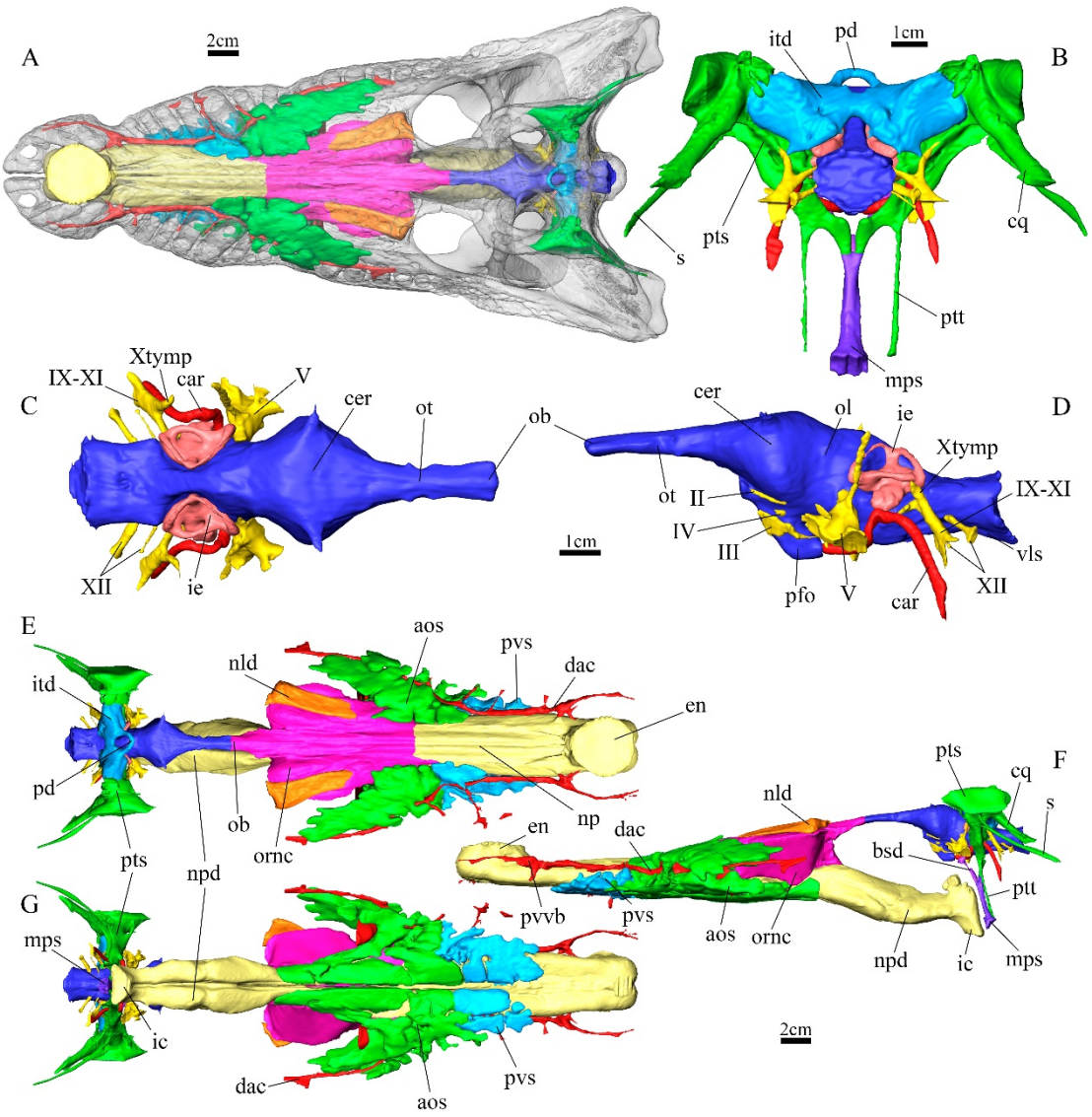

Fig. 4.1.4: Three-dimensional reconstruction of the inner skull cavities of *Crocodylus niloticus*. **A**: in-situ position of the inner skull cavities with the skull rendered semi-transparent, in dorsal view. Scale bar equals 2cm. **B**: *C. niloticus* brain, nerves, endosseous labyrinth, arteries and pharyngotympanic sinus system in caudal view. Scale bar equals 1cm. **C**-**D**: *C. niloticus* brain, nerves, endosseous labyrinth and arteries in **C**, dorsal and **D**, left lateral views. Scale bar equals 1cm. **E**-**G**: *C. niloticus* brain, nerves, endosseous labyrinth, arteries and pharyngotympanic and paranasal sinus systems in **E**, dorsal; **F**, left lateral and **G**, ventral views. Scale bar equals 2cm.

Crocodylus moreletii (Fig. 4.1.5)

Morelet's crocodile or Mexican crocodile is a fresh water medium size crocodile from Central America. It grows more than 2.5m length in average and can weigh between 40 to 60kg.

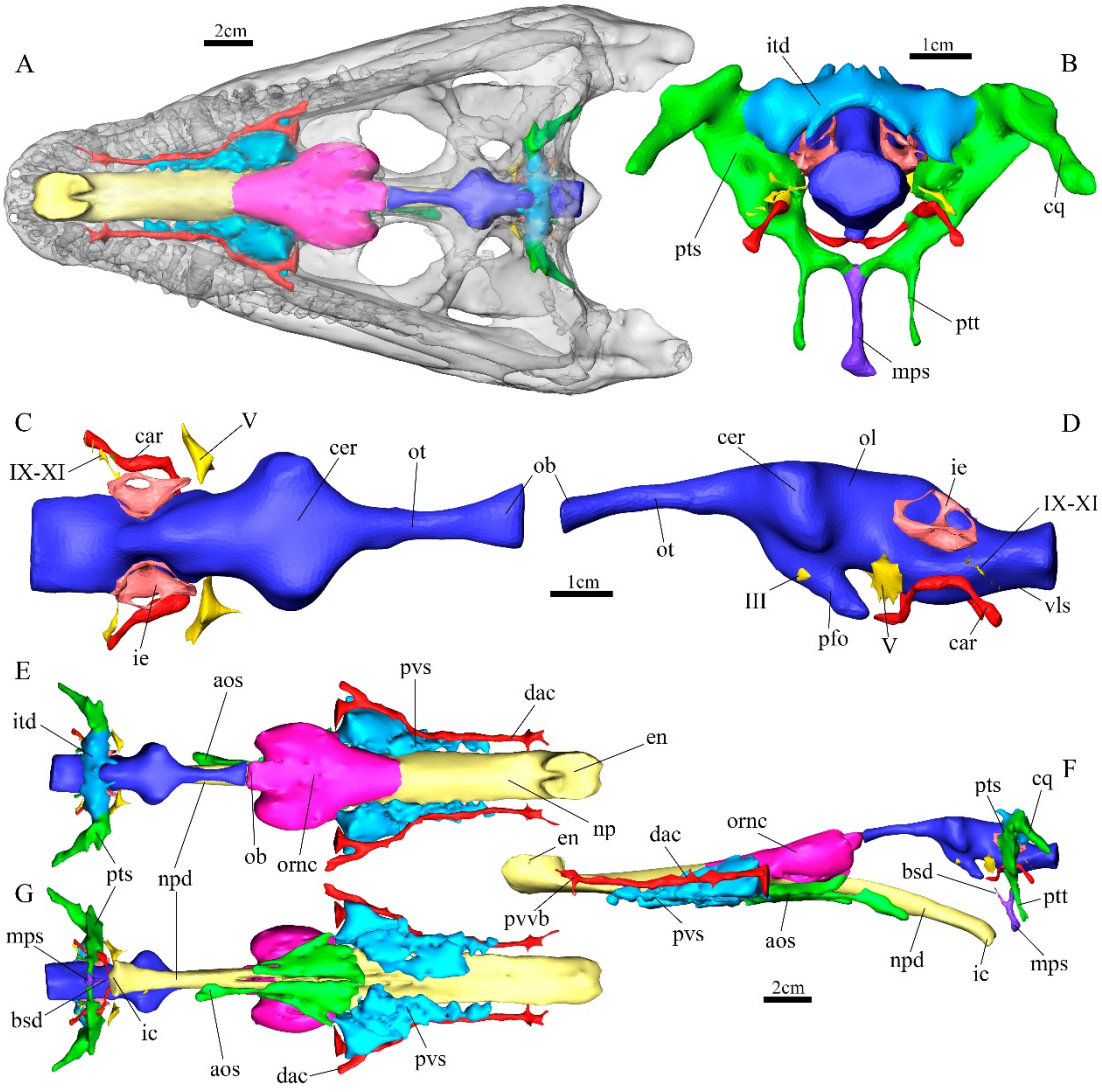

Fig. 4.1.5: Three-dimensional reconstruction of the inner skull cavities of *Crocodylus moreletii*. **A**: in-situ position of the inner skull cavities with the skull rendered semi-transparent, in dorsal view. Scale bar equals 2cm. **B**: *C. moreletii* brain, nerves, endosseous labyrinth, arteries and pharyngotympanic sinus system in caudal view. Scale bar equals 1cm. **C**-**D**: *C. moreletii* brain, nerves, endosseous labyrinth and arteries in **C**, dorsal and **D**, left lateral views. Scale bar equals 1cm. **E**-**G**: *C. moreletii* brain, nerves, endosseous labyrinth, arteries and pharyngotympanic and paranasal sinus systems in **E**, dorsal; **F**, left lateral and **G**, ventral views. Scale bar equals 2cm.

The specimen RVC-JRH-FMC3 was CT-scanned in X, in a CT-Lightspeed Ultra, in the Royal Veterinary College (North Mymms, UK) with a voltage of 120kV, a

currency of 100mA and an interslicing of 1.25mm. The CT-data was facilitated by Dr. John Hutchinson and obtained from www.osf.io.

Brain of *C. moreletii*, principally the hindbrain, is rostrocaudally stretched. The cerebral hemispheres are clearly visible in dorsal view. The caudodorsal surface of the cerebrum is flat.

Pharyngotympanic sinus system is rostrocaudally flattened. The lateral parts of the intertympanic diverticula are larger than the central one. Parietal pillar drillings are not laterally closed. Parietal diverticula emerge from the rostral surface of the intertympanic diverticula as two rostromedially oriented canals, but they do not reach to join between them. The region of the median pharyngeal sinus ventral to the basisphenoid recess is subequal to the dorsal one.

Nasal passageway is caudally oriented, but nasopharyngeal ducts slightly turn ventrally before open by the internal choana.

Osteolaemus tetraspis (Fig. 4.1.6)

Dwarf crocodile is a small-sized crocodyloid from West and Central Africa. The average length in adults is about 1.5m, and weight between 18 and 32kg.

The specimen MZB 2006-0039 was CT-scanned in Hospital Mutua de Terrassa (Terrassa, Spain), in a Siemens Sensation 16, with a voltage of 120kV, a currency of 50mA and an interslicing of 0.3mm. The CT-data was given up by Dr. Josep Fortuny.

Brain of *O. tetraspis* has marked sigmoid shape in lateral view. Cerebral hemispheres are rounded in dorsal view. The caudodorsal surface of the cerebrum is flat. Hypophyseal fossa is elongated. Ventral longitudinal sinus is clearly visible in the ventral surface of the hindbrain.

Central part of the intertympanic diverticula is less developed than the lateral ones. Parietal pillar drillings are wide. Median pharyngeal sinus is long, being the ventral part to basisphenoid diverticula three times the length of the dorsal part.

Nasopharyngeal ducts of *O. tetraspis* are the most complex of the crocodylians studied. They start coursing caudally, and then slightly turn dorsally to form two

bilateral large chambers. The ducts emerge again from the caudal surface of each chamber, course caudodorsally and finally turns ventrocaudally before open to the pharynx.

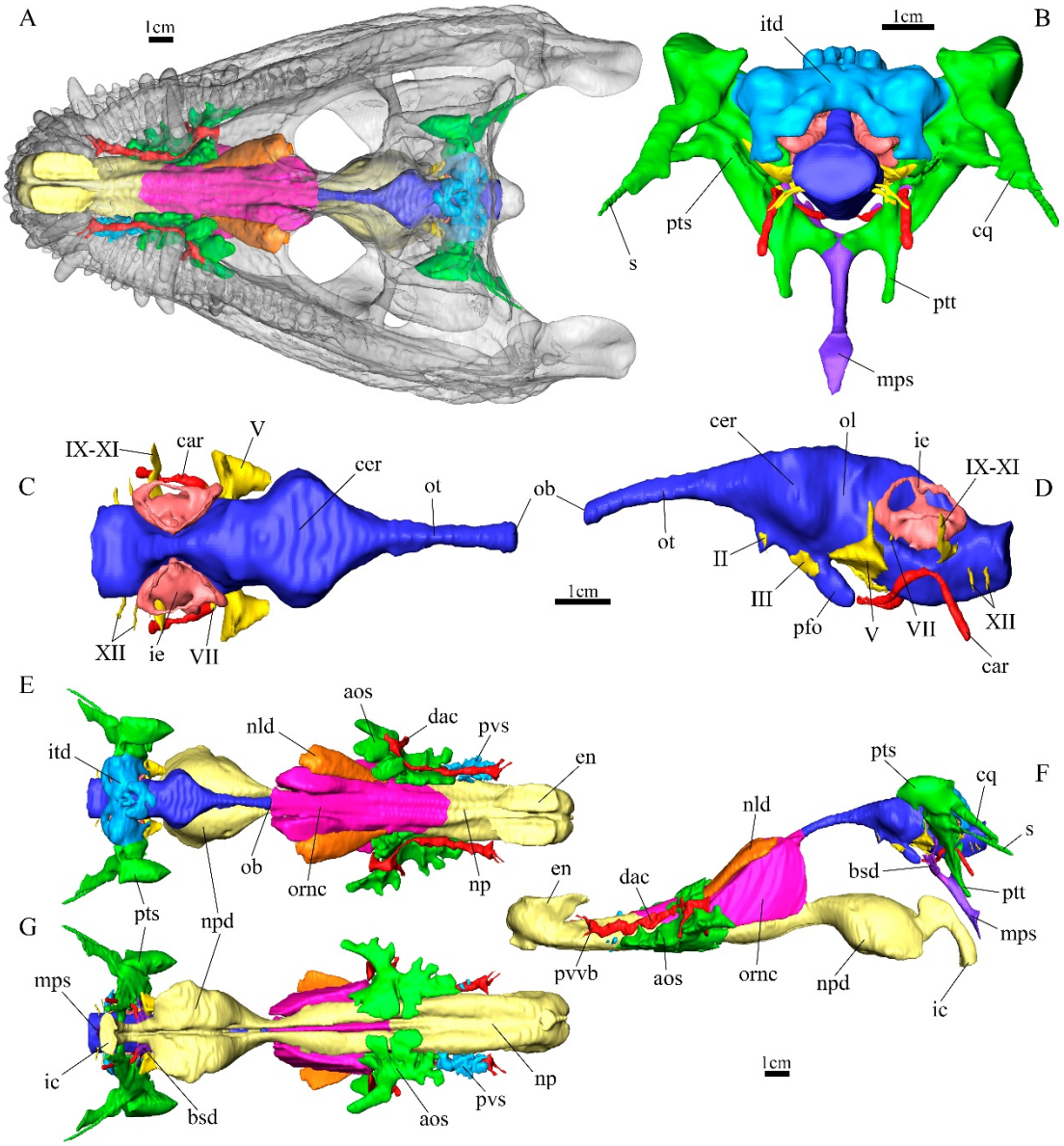

Fig. 4.1.6: Three-dimensional reconstruction of the inner skull cavities of *Osteolaemus tetraspis*. **A**: in-situ position of the inner skull cavities with the skull rendered semi-transparent, in dorsal view. Scale bar equals 1cm. **B**: *O. tetraspis* brain, nerves, endosseous labyrinth, arteries and pharyngotympanic sinus system in caudal view. Scale bar equals 1cm. **C**-**D**: *O. tetraspis* brain, nerves, endosseous labyrinth and arteries in **C**, dorsal and **D**, left lateral views. Scale bar equals 1cm. **E**-**G**: *O. tetraspis* brain, nerves, endosseous labyrinth, arteries and pharyngotympanic and paranasal sinus systems in **E**, dorsal; **F**, left lateral and **G**, ventral views. Scale bar equals 1cm.

Tomistoma schlegelii (Fig. 4.1.7)

False gharial is a large crocodyloid from freshwaters of South-East Asia. Its average length is between 3.6 and 3.9m and can weight up to 210kg. Its phylogenetical position is discussed. Morphological based cladograms assign it as a crocodyloid (Brochu, 1999, 2011), while morphological and molecular based analyses include it as a gavialoid (Densmore and Owen, 1989; Meganathan et al., 2010).

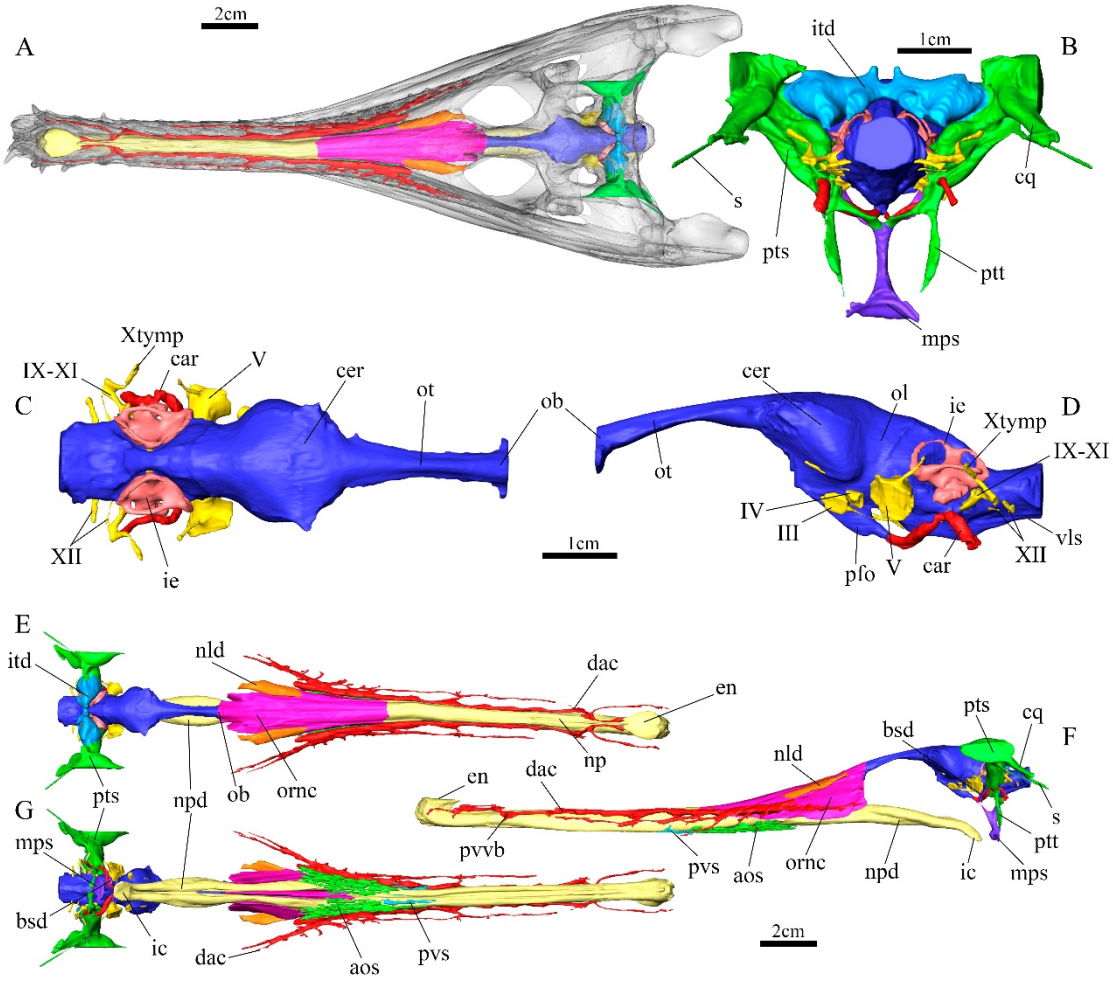

Fig. 4.1.7: Three-dimensional reconstruction of the inner skull cavities of *Tomistoma schlegelii*. **A**: in-situ position of the inner skull cavities with the skull rendered semi-transparent, in dorsal view. Scale bar equals 2cm. **B**: *T. schlegelii* brain, nerves, endosseous labyrinth, arteries and pharyngotympanic sinus system in caudal view. Scale bar equals 1cm. **C**-**D**: *T. schlegelii* brain, nerves, endosseous labyrinth and arteries in **C**, dorsal and **D**, left lateral views. Scale bar equals 1cm. **E**-**G**: *T. schlegelii* brain, nerves, endosseous labyrinth, arteries and pharyngotympanic and paranasal sinus systems in **E**, dorsal; **F**, left lateral and **G**, ventral views. Scale bar equals 2cm.

The specimen TMM M-6342 was CT-scanned in the University of Texas (USA), in a High-Resolution X-ray CT, with an interslicing of 0.46mm. The CT-data was facilitated by Dr. Chris Brochu (University of Iowa, Texas, USA), and obtained from www.digimorph.org.

Brain of *T. schlegelii* seems to have the more marked sigmoid shape of all the sample, probably due to the inclination of the olfactory tract. Ventral longitudinal sinus is clearly distinguishable in the ventral surface of the hindbrain.

The lateral regions of the intertympanic diverticula are more developed than the central region. Prefrontal pillar drillings are wide, having the left one its caudal boundary lost. Median pharyngeal sinus is short, being the regions dorsal and the ventral from the basisphenoid diverticula subequal.

Nasal passageway and nasopharyngeal ducts are caudally oriented until the caudalmost part, which slightly turns ventrally to open by the internal choana.

Gavialis gangeticus (Fig. 4.1.8)

Gharial is the only extant representative of Gavialoidea. It inhabits rivers from North India. Largest specimens can reach more than 6m length, and weight more than 950kg. Gharial is the only extant crocodile that shows sexual dimorphism: a nasal growth at the tip of the snout in males, whose function is not well understood yet.

The specimen UF118998 was scanned in the CT-scan of the Florida Museum of Natural History's Herpetology with a voltage of 120kV, a currency of 0,2mA and an interslicing of 0.15mm. The CT-data was obtained from www.morphosource.org.

The brain shape of *G. gangeticus* is cylindrical rather than sigmoidal, being the hindbrain at the same level than the forebrain. Cerebral hemispheres are rounded in dorsal view.

Intertympanic diverticula form a large part of the pharyngotympanic sinus system. Its lateral expansions are larger than the central region. Parietal diverticula project from the rostromedial area of the intertympanic diverticula as two rostrodorsal structures.

Median pharyngeal sinus is short but rostrocaudally elongated. Its ventral region to the basisphenoid diverticula is subequal than the dorsal one.

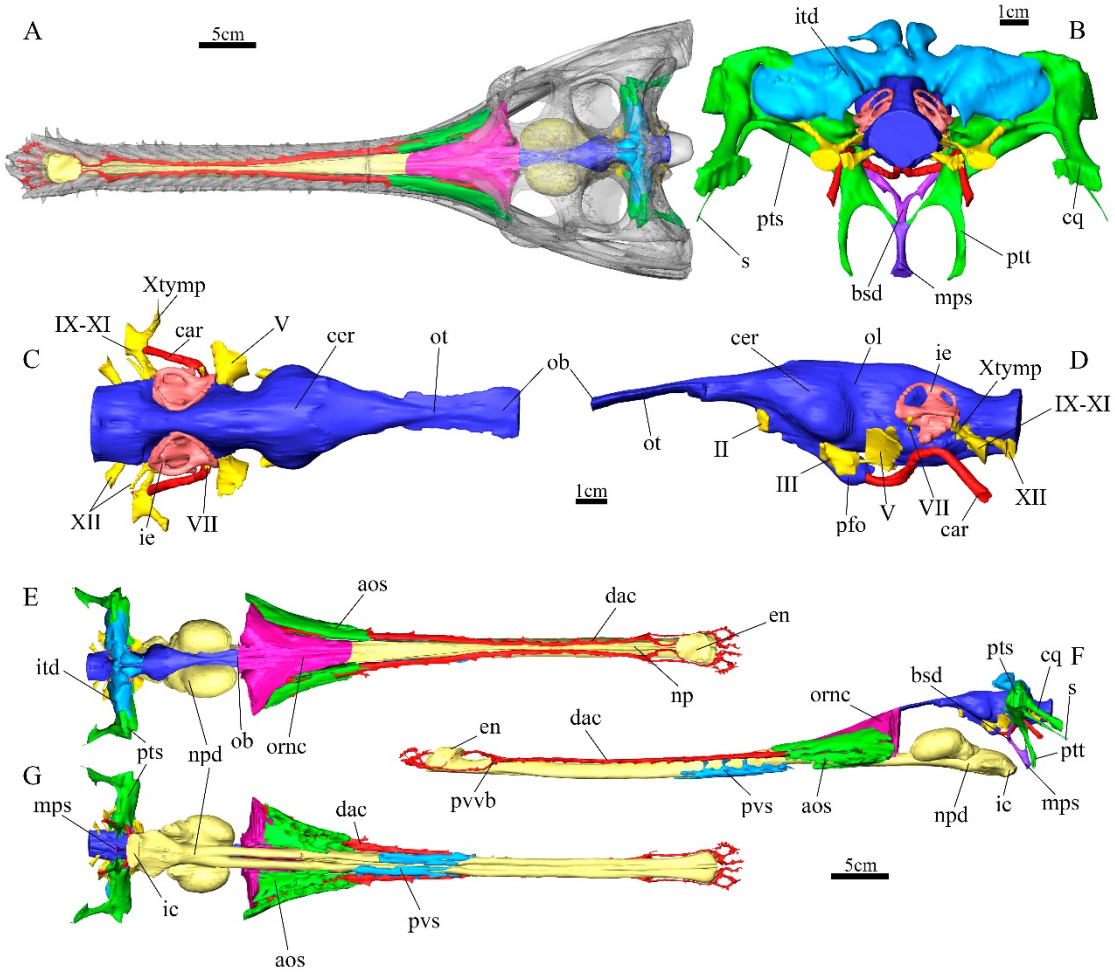

Fig. 4.1.8: Three-dimensional reconstruction of the inner skull cavities of *Gavialis gangeticus*. **A**: in-situ position of the inner skull cavities with the skull rendered semi-transparent, in dorsal view. Scale bar equals 5cm. **B**: *G. gangeticus* brain, nerves, endosseous labyrinth, arteries and pharyngotympanic sinus system in caudal view. Scale bar equals 1cm. **C-D**: *G. gangeticus* brain, nerves, endosseous labyrinth and arteries in **C**, dorsal and **D**, left lateral views. Scale bar equals 1cm. **E-G**: *G. gangeticus* brain, nerves, endosseous labyrinth, arteries and pharyngotympanic and paranasal sinus systems in **E**, dorsal; **F**, left lateral and **G**, ventral views. Scale bar equals 5cm.

4.2 *DIPLOCYNODON TORMIS*

4.2.1 INNER SKULL CAVITIES OF THE EXTINCT SPECIMEN *DIPLOCYNODON TORMIS*

Reference: Alejandro Serrano-Martínez; Fabien Knoll; Iván Narváez; Francisco Ortega. In press. Brain and pneumatic cavities of the braincase of the basal alligatoroid *Diplocynodon tormis* (Eocene, Spain). Journal of Vertebrate Paleontology (in press).

Brain and pneumatic cavities of the braincase of the basal alligatoroid *diplocynodon tormis* (eocene, spain)

Alejandro Serrano-Martínez[1*]; Fabien Knoll[2,3;] Iván Narváez[1]; Francisco Ortega[1]

[1]: Grupo de Biología Evolutiva. Facultad de Ciencias. Universidad Nacional de Educación a Distancia. Paseo Senda del Rey 9. 28040, Madrid

[2]: ARAID-Fundación Conjunto Paleontológico Teruel-Dinópolis. Avda. Sagunto, S/N, 44002, Teruel. Spain

[3]: School of Earth & Environmental Sciences, University of Manchester, Oxford Rd, M13 9PL, Manchester, United Kingdom.

* Corresponding author

Abstract

A well-preserved braincase of the basal alligatoroid *Diplocynodon tormis* was found in the Middle Eocene site of "Teso de la Flecha", Salamanca, Spain. The specimen was CT scanned and its inner cavities were digitally rendered in 3D. Most bones of the left side are missing, so the reconstruction was based mainly on the right half of the braincase. The endocast of the brain cavity, nerves, part of the inner ear and blood vessel canals were reconstructed, as well as a complex network of air-filled cavities around the hindbrain formed by the median pharyngeal sinus and pharyngotympanic sinus systems.

Inner cavities of the skull are considered to be conservative structures. The comparison of this specimen with several extant crocodilians (Alligatoroidea, Crocodyloidea and Gavialoidea) allows us to identify a neuroanatomical evolutionary pattern that matches current phylogenetic hypotheses. All internal cavities of the braincase of *Diplocynodon* are similar to those of other studied eusuchians, with some noteworthy differences in shape and size, particularly regarding the cerebrum or the paratympanic sinus system. Diplocynodon tormis shows a combination of alligatoroid synapomorphies and crocodylian symplesiomorphies in its internal cavities, consistent with its phylogenetical placement as a basal alligatoroid.

Institutional Abbreviations—**CRARC**: Centre de Recuperació d'Amfibis I Rèptils de Catalunya (Barcelona, Spain). **FMNH**: Field Museum of Natural History (Chicago, Illinois). **MCD**: Museu de la Conca Dellà (Lleida, Spain). **MLP**: Museo de La Plata (Buenos Aires, Argentina). **MZB**: Museu Zoològic de Barcelona (Barcelona, Spain). **OUVC**: Ohio University Vertebrate Collections (Athens, Ohio). **STUS**: Sala de las Tortugas "Emiliano Jiménez" de la Universidad de Salamanca (Salamanca, Spain). **TMM**: Texas Memorial Museum (Austin, Texas). **UF**: University of Florida (Gainesville, Florida). **UMZC**: University Museum of Zoology, Cambridge (Cambridge, UK).

Anatomical Abbreviations—**am**: auditory meatus. **BO**: basioccipital. **BS**: basisphenoid. **bsd**: basisphenoid diverticula. **car**: cerebral carotid artery. **carf**: cerebral carotid artery foramen. **cer**: cerebral hemisphere. **cq**: cranioquadrate sinus. **cqf**: cranioquadrate sinus foramen. **F**: frontal. **fa**: foramen aereum. **ie**: inner ear. **itd**: intertympanic diverticula. **lag**: lagena. **LS**: laterosphenoid. **mps**: medial pharyngeal sinus. **ob**: olfactory bulb. **OO**: otoccipital. **ot**: olfactory tract. **PF**: prefrontal. **pfo**: pituitary (hypophyseal) fossa. **PO**: postorbital. **POT**: prootic. **PT**: pterygoid. **pts**: pharyngotympanic sinus. **ptt**: pharyngotympanic tube. **Q**: quadrate. **s**: siphonial tube. **SO**: supraoccipital. **vls**: ventral longitudinal sinus. **II**: optic nerve canal. **III**: oculomotor nerve canal. **IV**: trochlear nerve canal. **V**: trigeminal nerve canal. **V_2**: maxillary nerve canal. **V_3**: mandibular nerve canal. **Vtymp**: tympanic branch of trigeminal nerve canal. **VI**: abducens nerve canal. **VII**: facial nerve canal. **IX-XI**: shared canal for glossopharyngeal, vagus and accessory nerves. **Xtymp**: canal for tympanic branch of vagus nerves. **XII**: hypoglossal nerve canal.

Introduction

Diplocynodon is one of the best known crocodiles in the European Cenozoic fossil record. This genus spans from the late Paleocene to the middle Miocene (Martin and Gross, 2011; Delfino and Smith, 2012). There are nine presently recognised *Diplocynodon* species, all of them from Europe (Brochu, 1999; Piras and Buscalioni, 2006; Martin, 2010; Delfino and Smith, 2012; Martin et al., 2014; Díaz Aráez et al., 2016). Three of those species appear in the Spanish record: *D. muelleri* (Piras and Buscalioni, 2006), *D. ratelii* (Díaz Aráez et al., 2016) and *D. tormis* (Buscalioni et al., 1992). *Diplocynodon* is phylogenetically positioned at the base of Alligatoroidea (Brochu, 1999; Delfino and Smith, 2012; Martin et al., 2014). This basal placement makes this taxon especially relevant to our understanding of the divergence between Alligatoroidea and Crocodyloidea as members of Brevirostres.

The Duero Basin, located in Salamanca, Zamora, and Soria Provinces (Spain), has yielded abundant crocodyliform remains. *Diplocynodon* is the most abundant genus, but

there are also remains of the crocodylomorphs *Iberosuchus*, *Asiatosuchus* and *Duerosuchus* (Ortega and Buscalioni, 1983; Jiménez Fuentes et al., 1989; Buscalioni et al., 1992; Luis-Alonso and Luis-Alonso, 2009; Fernández Díaz et al., 2013). Buscalioni et al. (1992) described the species *Diplocynodon tormis* Buscalioni, Sanz, Casanovas, 1992 based on specimens from the Areniscas de Cabrerizos Fm at Salamanca. The specimen studied below, STUS-344, was found at the "Teso de la Flecha" site (Cabrerizos. Salamanca) , which is, which is Middle Eocene in age (Jiménez Fuentes, 1983; Fernández Díaz et al., 2013). STUS-344 is a well-preserved braincase described previously by Jimenez-Fuentes (1983), who assigned it to *Diplocynodon* aff. *gracilis*. Later, Buscalioni et al. (1992) considered the specimen a paratype of *Diplocynodon tormis*. STUS-344 is remarkable for the excellent preservation of its endocranial cavities.

The first published CT-scan from a fossil crocodyliform is attributed to Tykoski et al., (2002). Only a few fossil crocodylians have been studied with those techniques. Among eusuchians, digital reconstructions of the endocranial cavities are available for *Gavialis gangeticus* (Bona et al., 2017; Pierce et al., 2017), *Crocodylus johnstoni* (Witmer et al., 2008), *Crocodylus moreletti* (Franzosa, 2004), *Alligator mississippiensis* (Witmer and Ridgely, 2008; Dufeau and Witmer, 2015) and *Caiman crocodilus* (Hopson, 1979), all of which are extant. As for extinct taxa, digital reconstructions of the basal eusuchian *Aegisuchus witmeri* from the Cenomanian of Morocco (Holliday and Gardner, 2012), the gavialoid *Gryposuchus neogaeus* (Bona et al., 2017) and the caimanine *Mourasuchus nativus* (Bona et al., 2013), both from the Miocene of Argentina have been carried out.

The aim of this study is to compare via CT imaging the internal cavities of STUS-344 with those of other members of Crocodylia, in order to understand the neuroanatomical evolution of the group and to identify possible phylogenetic signals in neuroanatomical and pneumatic features.

Material and methods

The specimen studied, STUS-344, is a partial braincase referred to Diplocynodon tormis (Buscalioni et al., 1992) (Fig. 4.2.1.1) housed in the collection of the STUS at the Universidad de Salamanca (Spain).

In order to reconstruct the encephalic, tympanic and pharyngotympanic endocasts, the specimen was scanned in the Institut Català de Paleontologia Miquel Crusafont, with a Yxlon Y.TU 450-D09 CT-scanner, with a voltage of 450kV and a current of 3.3 mA. 900 projections were made, with 50ms/projection. The inter-slice spacing was 0.33 mm. The scan data were imported into ImageJ 1.49b (National Institutes of Health,

USA) for artefact removal and to enhance the contrast. The data were finally segmented, rendered and analysed in Avizo 7.1.0 (VSG, Burlington, MA, USA) in order to build 3D models and conduct metrical and morphological analyses.

Interactive 3D PDFs of the skull bones and the inner skull cavities reconstructions are provided in Supplemental Data.

Results

Osteology

For a description of the external anatomy of the specimen and diagnosis of *Diplocynodon tormis*, see Jimenez-Fuentes (1983) and Buscalioni et al. (1992). STUS-344 is a partial braincase composed by most of the median and right side bones, and also part of the left prefrontal and laterosphenoid (Fig. 4.2.1.1 and 4.2.1.2).

The prefrontals only preserve their posterodorsalmost portions, which delimit anteromedially the orbits. They compose the lateral walls of the posterior part of the olfactory bulbs.

The frontal has a narrow anterior process with its anteriormost part broken. The dorsal surface of the frontal is flat, lacking any elevation along the outline of the orbits. The frontal and prefrontal table shows a profuse alveolar ornamentation but also three short longitudinal grooves. The frontal groove is sagittal, while the prefrontal groove are parallel to the orbit outline, coursing anterolaterally. In ventral view, the frontal constitutes the roof of the incipient olfactory bulbs, the walls and roof of the olfactory passage, and the roof of the brain cavity (Fig. 4.2.1.1F and 4.2.1.2F). Dorsally, the frontal forms the posteromedial edge of the orbits, and slightly contacts the anteromedial rim of the supratemporal fenestrae, separating the postorbital and the parietal.

The parietal, like the frontal and prefrontal, is flat with alveolar ornamentation on the dorsal surface. It forms the medial edge of the supratemporal fenestrae. The interfenestral bar is narrower than the interorbital bar across the frontal. The frontoparietal suture is an indented line with an anterolateral projection of the parietals, but it does not contact the postorbital. The suture with the squamosal is clearly visible as a parasagittal straight line. The ventral surface of the parietal forms the roof of the posterior part of the cerebrum cavity and the anterior part of the hindbrain cavity (Fig. 4.2.1.1B, 4.2.1.1F, 4.2.2B and 4.2.1.2F). The parietal also constitutes the roof of the paratympanic recesses (Fig. 4.2.1.1B and 4.2.1.2B). The orbitotemporal foramen is

located in the posterior part of the lateral margin of the parietal, opening into the paratympanic recesses.

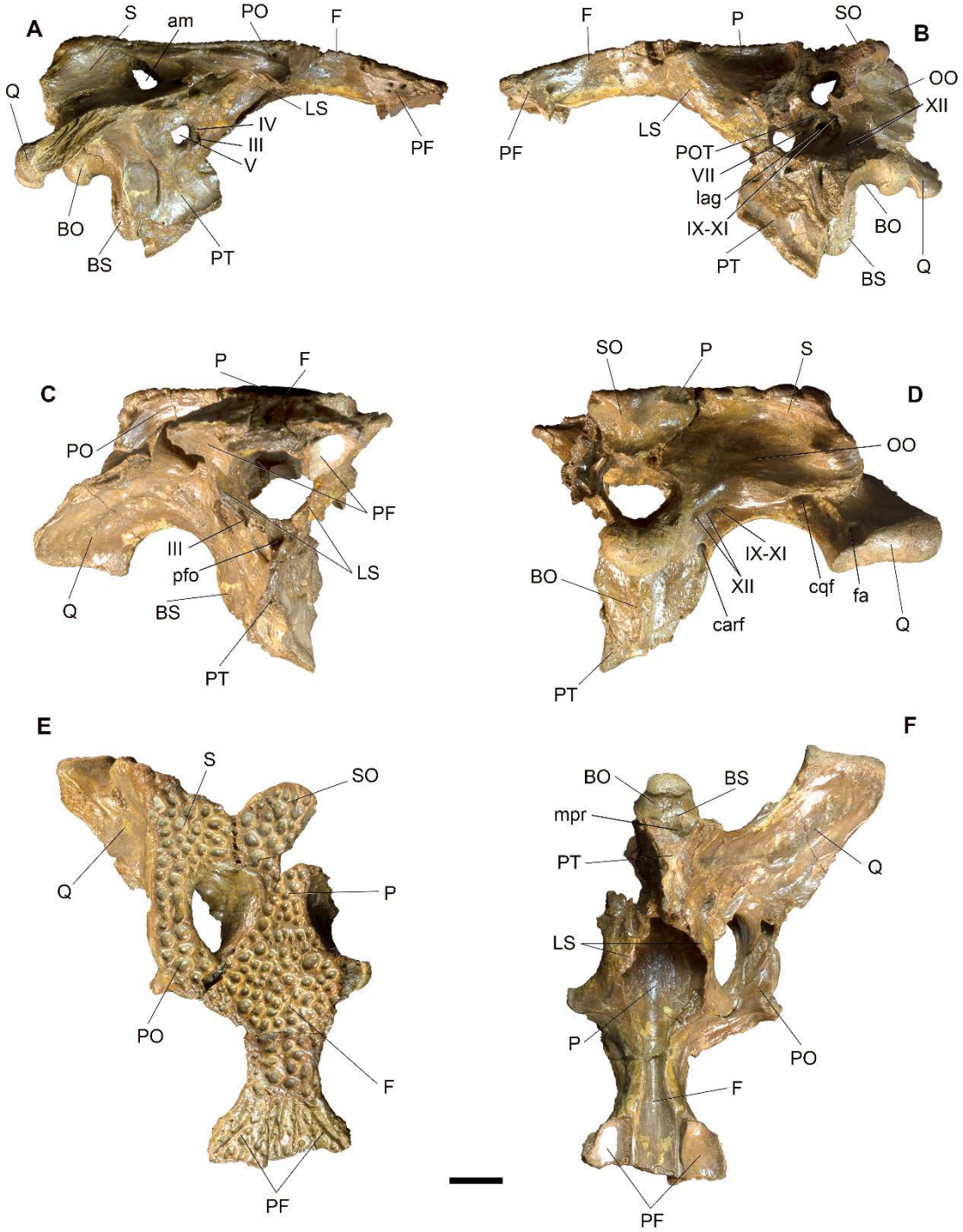

Fig. 4.2.1.1: *Diplocynodon tormis* braincase STUS-344. **A**, right lateral; **B**, left lateral; **C**, rostral; **D**, caudal; **E,** dorsal; **F**, ventral views. Scale bar equals 1cm.

The postorbital forms the posterior margin of the orbit and the anterolateral corner of the supratemporal fenestra. It is laterally oriented and longer than wide. As other bones of the skull table, its dorsal surface is flat with alveolar ornamentation. The postorbital bar is only partially preserved, but its subtriangular cross-section is clearly visible. The bar is laterally oriented, visible in dorsal view.

The squamosal constitutes the posterolateral margin of the supratemporal fenestra. Its dorsal surface is also flat with alveolar ornamentation. Posteriorly, the squamosal extends ventrally without reaching the lateral tip of the paraoccipital process. In lateral view, the paraoccipital process has a right-angle outline. Laterally, it forms the roof of the auditory meatus (Fig. 4.2.1.1A and 4.2.1.2A), and covers dorsally the lateralmost part of the paratympanic recesses.

The laterosphenoids are paired bones that form the lateral wall of the braincase at the level of the cerebrum and the optic lobe (Fig. 4.2.1.1C, 4.2.1.1F, 4.2.1.2C and 4.2.1.2F). The laterosphenoids also enclose the passages for the oculomotor and trochlear nerves, and form the anterior part of the trigeminal foramen (Fig. 4.2.1.1A and 4.2.1.2A). The anteriormost parts of both laterosphenoids are broken.

The quadrate is a smooth bone that does not extend posteriorly much further than the skull table level (Fig. 4.2.1.1E and 4.2.1.2E). The medial hemicondyle is smaller than the lateral hemicondyle. The quadrate constitutes the posterolateral part of the passage for the trigeminal nerve (Fig. 4.2.1.1A and 4.2.1.2A), the passage for the facial nerve and the ventral surface of the auditory meatus. It delimits posteroventrally the pharyngotympanic sinus (Fig. 4.2.1.1A, 4.2.1.1B, 4.2.1.2A and 4.2.1.2B), including the siphonial tube, which opens at the foramen aereum, and the anterior part of the cranioquadrate passage. The foramen aereum is located on the dorsal surface of the articular condyle, near the posteromedial margin of the quadrate (Fig. 4.2.1D). Although the quadratojugal is missing, the suture of the quadrate with this element is well preserved (Fig. 4.2.1.1A and 4.2.1.1E).

The basisphenoid is ventral with respect to the quadrate. It forms the anterior part of the floor of the brain cavity. In fact, the basisphenoid forms most of the ventral braincase structure, housing the cavity of the hypophysis, the passages for the cerebral carotid arteries, the passages for the abducens nerves and the median pharyngeal sinus system and the ventral cavities of the pharyngotympanic sinus system (Fig. 4.2.1.1B, 4.2.1.1C, 4.2.1.2B and 4.2.1.2C). Those paratympanic sinuses open at the medial Eustachian foramen, which is clearly visible to the naked eye.

Only the posterior part of the pterygoids is preserved, with some important structures, such as the choanae and the pterygoid wings missing. The pterygoids cover anterolaterally the basisphenoid, forming the anteroventral part of the passage for the trigeminal nerve (Fig. 4.2.1.1A and 4.2.1.2A).

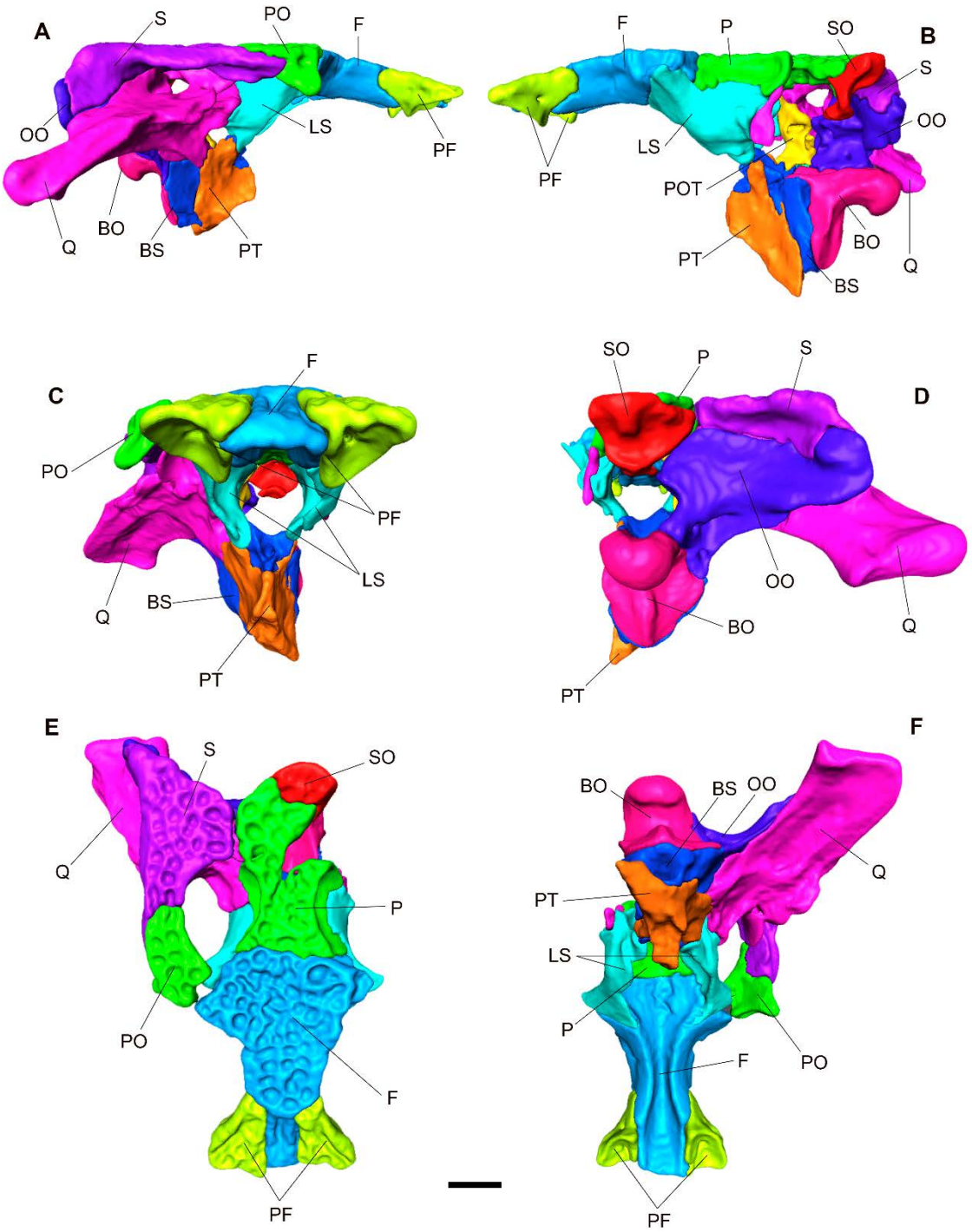

Fig. 4.2.1.2: Three dimensional volume rendering of the basicranium of *Diplocynodon tormis* STUS-344, differentiating the bones that compose it. **A**, right lateral; **B**, left lateral; **C**, rostral; **D**, caudal; **E,** dorsal; **F**, ventral views. Scale bar equals 1cm.

The prootic is partially hidden by the quadrate in lateral view. It forms the anterior part of the hindbrain region and the paratympanic recesses, and the posterior part of the trigeminal canal (Fig. 4.2.1.1B and 4.2.1.2B). Because the otic capsule is broken the dorsal part of the inner ear undistinguishable.

The dorsal surface of the supraoccipital is slightly concave with alveolar ornamentation, forming the posterior extremity of the skull table. It extends posteriorly, almost reaching the posteriormost end of the squamosal, covering the occipital condyle in dorsal view (Fig. 4.2.1.1E and 4.2.1.2E). In posterior view, the supraoccipital is wider than tall, extending laterally to contact the squamosal (Fig. 4.2.1.1D and 4.2.1.2D). It is partially broken internally, but still preserves part of the roof of the hindbrain region and the posterior walls of the paratympanic recesses (Fig. 4.2.1.1B and 4.2.1.2B).

As in most archosaurs, the opisthotic is totally fused to the exoccipital, forming the otoccipital. The otoccipitals constitute most of the occiput in posterior view (Fig. 4.2.1.1D and 4.2.1.2D). It forms the lateral margin of the foramen magnum. The paroccipital process extends laterally to contact the quadrate. It does not reach the level of the occipital condyle ventrally. The otoccipital contains the common passage of the glossopharyngeal, vagus and accessory nerves and, a bit posteromedially, the passages of the paired hypoglossal nerves (Fig. 4.2.1.1B, 4.2.1.1D, 4.2.1.2B and 4.2.1.2D). These passages open ventral to the crista tuberalis, a transversal ridge that starts dorsal to the cranioquadrate passage, and reaches the foramen magnum. The foramen caroticum is ventral to this group of nerve foramina, at the ventral level of the condyle. The otoccipital also forms the posterior walls of the pharyngotympanic sinus system (Fig. 4.2.1.1B and 4.2.1.2B), and delimits dorsally the distal section of the cranioquadrate passage.

The basioccipital forms the occipital condyle and the basioccipital plate. The basioccipital plate is hexagonal and bears a sagittal ridge with a dorsal tubercle (Fig. 4.2.1.1D and 4.2.1.2D). The internal part of the basioccipital extends anteriorly to contact the basisphenoid, forming the posteriormost brain cavity floor (Fig. 4.2.1.1B and 4.2.1.2B). The lateral margin of the basioccipital plate shares a notch with the basisphenoid where the pharyngotympanic tubes open.

Neuroanatomy

As most of the left bones are missing, the reconstruction was based on the right half of the endocast (Fig. 4.2.1.3 and 4.2.1.4). Since the anteroventral part of the endocast is missing (the anterior region of neither the basisphenoid nor the laterosphenoids are preserved), the anterior shape of the pituitary and the passage for the optic nerve cannot be reconstructed. As the otic capsule formed by the prootic and the otoccipital is not preserved, the dorsal limit of the cerebellar region must be also estimated. The semicircular canals of the inner ear and the vestibulocochlear nerve (VIII) cannot be observed. The posteroventral part of the supraoccipital and otoccipital are only partially

preserved, so the caudodorsal region of the endocast could not be reconstructed with accuracy (light blue areas in Fig. 4.2.1.3).

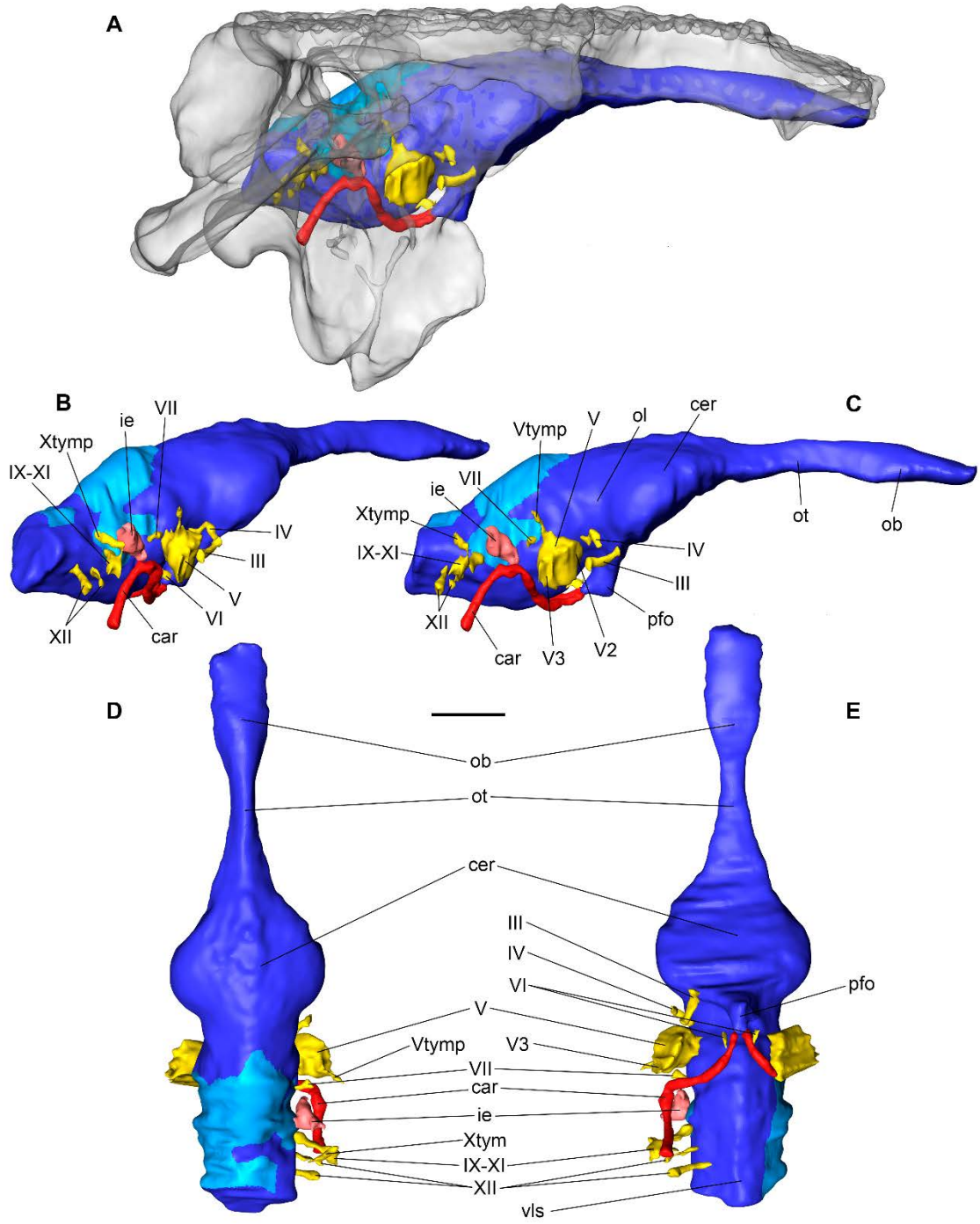

Fig. 4.2.1.3: Three dimensional reconstruction of the endocranial cavities of *Diplocynodon tormis* STUS-344. **A**, position of the cavities in the braincase rendered transparent, in right lateral view. **B**-**E**, STUS-344 brain, nerves, inner ear and arteries in **B**, right caudolateral; **C**, right lateral; **D**, dorsal and **E,** ventral views. The light blue represents the areas that had to be restored due to the breakage of the braincase internal surface. Scale bar equals 1cm.

We refer to the reconstructed digital casts of bone-bounded spaces that houses soft-tissue structures as if they were the structures themselves (e.g., “facial nerve” instead of “endocast of facial nerve canal”).

Brain: The endocast is formed by the brain itself but also its dural envelope, which takes up 40% of the braincase volume, and obscuring many parts of the brain (Hopson, 1977; Witmer et al., 2008; Jirak and Janacek, 2017). The endocast of *Diplocynodon tormis* has a sigmoid profile in lateral view (Fig. 4.2.1.3C). STUS-344 only preserves the posteriormost part of the olfactory bulbs, which connect to the brain by long olfactory tracts. Only the dorsal and lateral aspects of the olfactory tracts and bulbs could be reconstructed as no bone limits this structure ventrally (Witmer et al., 2008; Bona et al., 2013, 2017). The cerebral hemispheres are clearly visible as large rounded lumps in dorsal view (Fig. 4.2.1.3D). The cerebral region is separated from the hindbrain by a slightly dorsal narrowing, where the optic lobes are located (Fig. 4.2.1.3C and 4.2.1.3D). The hindbrain portions (metencephalon and myelencephalon) cannot be distinguished due to the breakage of the prootic and the otoccipital. However, the ventral longitudinal sinus is easily recognised as an elongated ridge in the ventral surface of the hindbrain (Fig. 4.2.1.3E). The pituitary emerges from the posteroventral side of the cerebrum and is posteroventrally oriented (Fig. 4.2.1.3C and 4.2.1.3E). The paired cerebral carotid arteries penetrate the posteriormost margin of the pituitary (Fig. 4.2.1.3E). They enter the skull by penetrating the caudal surface of the otoccipital, run dorsally to go through the pharyngotympanic sinus, curve abruptly ventromedially, and then deviate to be closer to parallel with one another before reaching the pituitary (Fig. 4.2.1.3C).

Cranial nerves: the nerves III, IV, V, VI, VII, IX-XI and XII of the right side have been recognized and reconstructed, but only the VI and the anterior part of the V are visible on the left side (Fig. 4.2.1.3C and 4.2.1.3E).

The oculomotor nerve (III) is dorsal to the pituitary. Its base is broken, but the middle and distal sections are still visible in the preserved part of the laterosphenoid. It is posterodistally oriented, and emerges anteriorly to the large trigeminal foramen.

The trochlear nerve (IV) is located in the lateroventral region of the optic lobe. It courses anterodorsally, but turns anteroventrally before emerging from the laterosphenoid, anterodorsally to the oculomotor foramen.

The trigeminal nerve (V) is, as usual, the largest of the cranial nerves. It broadens distally and divides into four branches, three of them are distinguishable in this specimen. The ophthalmic nerve (V_1) is not distinguishable. The trigeminal nerve divides distally into the maxillary (V_2) nerve, which is anteriorly oriented, and the mandibular nerve (V_3), which goes laterally. The thin tympanic branch (Vtymp) starts at the top of the main trigeminal trunk. It is posterodorsally oriented.

Both abducens nerves (VI) emerge from the ventral surface of the hindbrain, ventral to the trigeminal nerve and posterior to the pituitary. They are thin nerves that course anteroventrally.

The facial nerve (VII) is located posteriorly at the same dorsoventral level as the trochlear nerve. It courses dorsolaterally.

The glossopharyngeal (IX), vagus (X) and accessory (XI) nerves share the posterolaterally oriented metotic canal that opens at the posterior side of the otoccipital, dorsally to the foramen caroticum. The tympanic branch of the vagus nerve (Xtymp) splits from the rest of the metotic canal at midpoint and courses dorsally.

The caudal-most nerves are the paired canals of the hypoglossal nerve (XII). Both are short nerves that exit posteriorly to the metotic foramen, on the otoccipital.

Inner ear, and paratympanic sinus system: Only a portion of the cochlear duct has been preserved (Fig. 4.2.1B). It is fairly in between the metencephalon and myelencephalon region (Fig. 4.2.1.3C). The lagena is anteroventrally oriented.

The paratympanic sinus system is packed in bony recesses around the mid/hindbrain (Fig. 4.2.1.4A and 4.2.1.4B). We follow the embryological origin nomenclature proposed by (Dufeau and Witmer, 2015). The pharyngotympanic system is the principal pneumatic complex of the paratympanic sinus system, and joins the external auditory meatus with the inner ear and the pharynx by the lateral Eustachian tubes. These recesses are large in this specimen. The intertympanic diverticula are cavities dorsal to the neural endocast. The breakage of the prootic hinders tracing the ventral boundary of the intertympanic diverticula, but the dorsal region (formed by the parietal) is well delimited. In extant specimens, these diverticula are pierced by a pair of bony bridges that join the parietal and each prootic. However, only the dorsal part of the right bridge is preserved in STUS-344, and shows only a wide concavity in the dorsal surface of these diverticula. In posterior view, at the level of these parietal pillars (Fig. 4.2.4C), the intertympanic diverticula can be divided into three sections: a large central core and two smaller lateral expansions.

The intertympanic diverticula continue laterally with the pharyngotympanic sinus (Fig. 4.2.1.4C). The limit between these two structures is established by the supraoccipital-otoccipital suture (Dufeau and Witmer, 2015). Laterally, this recess opens broadly at the external auditory meatus (Fig. 4.2.1.4D). The pharyngotympanic sinus also extends into two posterolateral passages (Fig. 4.2.1.4D). Dorsally, the cranioquadrate passage is wide and opens between the quadrate and the otoccipital. The siphonium is long and slender, and opens at the *foramen aereum*, in the quadrate. Ventrally, the pharyngotympanic sinus extends in a narrow cavity that surrounds the carotid artery. The pharyngotympanic sinus connects with the pharynx by the

pharyngotympanic tubes, a pair of flat, ventrally oriented, canals that open between the basisphenoid and the basioccipital. However, only the right canal has been preserved (Fig. 4.2.1.4C and 4.2.1.4D). The left and right pharyngotympanic sinuses merge posteromedially at the level of the basioccipital diverticula, bordering ventrally the hindbrain.

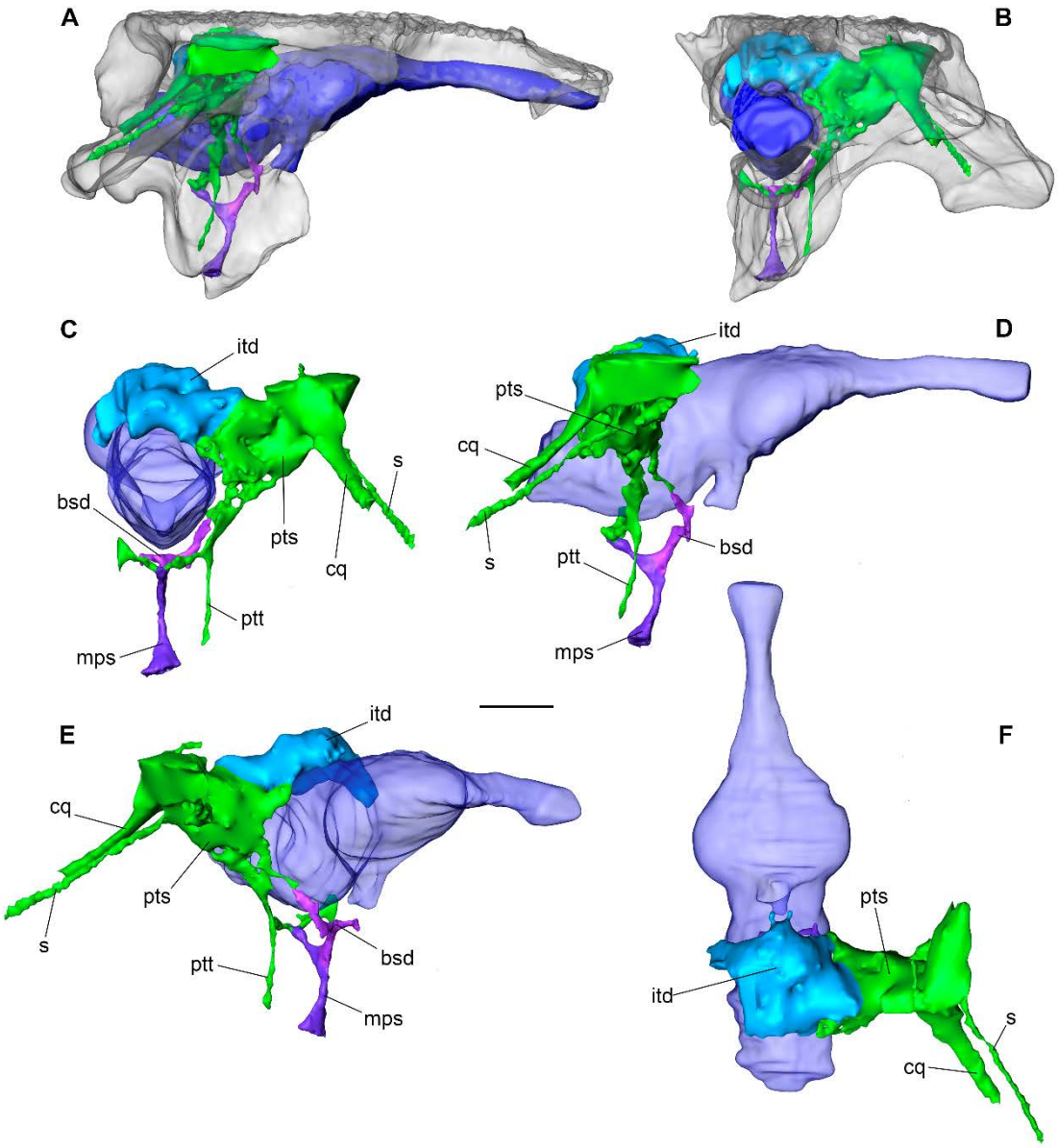

Fig. 4.2.1.4: Three dimensional reconstruction of the pharyngotympanic structures within the braincase of *Diplocynodon tormis* STUS-344. **A**, **B**: position of the cavities in the specimen rendered transparent, in **A**, right lateral; **B**, posterior views. **C**-**F**: STUS-344 the paratympanic sinus system with the brain rendered transparent, in **C**, caudal; **D**, right lateral; **E**, rostrolateral; **F,** dorsal views. Scale bar equals 1cm.

The median pharyngeal sinus system is located ventrally to the pharyngotympanic sinus. The median pharyngeal sinus courses anteroventrally to join the basisphenoid diverticulum, and then goes posteroventrally to finally open between the basisphenoid and the basioccipital, just posterior to the nasopharyngeal duct. The basisphenoid diverticulum are connected to the middle part of the median pharyngeal sinus, and course dorsolaterally to open in the pharyngtympanic sinuses (Fig. 4.2.1.4D and 4.2.1.4E).

Comparisons with other eusuchians

Our knowledge of the paleoneuroanatomy of eusuchians rests principally on the extant members of the group, represented in our comparative analyses by the alligatorine *Alligator mississippiensis* (our reconstruction based on MZB 92-0231; OUVC 9761, Witmer and Ridgely, 2008; a list of another 13 specimens from Dufeau and Witmer, 2015), the caimanine *Caiman crocodilus* (our reconstruction based on caiman_crocodilus_CRARC; FMNH 73711, Brusatte et al., 2016), the crocodyloids *Crocodylus niloticus* (our reconstruction based on MZB 2003-1423), *Crocodylus johnstoni* (OUVC 10425, Witmer et al., 2008), *Osteolaemus tetraspis* (our reconstruction based on MZB 2006-0039) and *Tomistoma schlegelii* (our reconstruction based on TMM M-6342, digimorph.org) as well as the gavialoid *Gavialis gangeticus* (our reconstruction based on UF118998, morphosource.org; MLP 602, Bona et al., 2017; UMZC R 5792, Pierce et al., 2017). However, in recent years, paleoneuroanatomical data from fossil eusuchians, such as the caimanine *Mourasuchus nativus* (MLP 73-IV-15-9, Bona et al., 2013), the gavialoid *Gryposuchus neogaeus* (MLP 73-IV-15-9, Bona et al., 2017) and *Allodaposuchus hulki* (MCD-5139, Blanco et al., 2015), have been published. The reconstruction of '*A. hulki'* was not included in all the analyses because the brain and pharyngotympanic regions are poorly preserved.

The neuroanatomical reconstruction of *Diplocynodon tormis* is quite similar to those of other eusuchians (Fig. 4.2.1.5). The cerebrum is connected to the olfactory bulbs by long olfactory tracts as in other members of the clade. The zone of transition between the olfactory tracts and the brain is abrupt in *D. tormis*, as in *C. crocodilus*, *T. schlegelii* and *O. tetraspis* (Fig. 4.2.1.3D and 4.2.1.5). In contrast, in *A. mississippiensis*, *C. niloticus*, *C. johnstoni* and *G. gangeticus*, the transition between the olfactory tracts and the cerebrum is more progressive (in *M. nativus* and *G. neogaeus* the anteriormost part of the brain could not be reconstructed).

All the eusuchians studied thus far have well-distinguishable cerebral hemispheres. In dorsal view, these hemispheres show a rounded morphology in *D. tormis*, *C. crocodilus*, *C. johnstoni*, *T. schlegelii* and *O. tetraspis*, while the other specimens present conical cerebral hemispheres (Fig. 4.2.1.5). In lateral view, *D. tormis* has a flat

posterodorsal outline of the cerebrum, just anterior to the optic lobe region (Fig. 4.2.1.3C). This is not the case in the rest of the alligatoroids studied, in which the outline of the brain has a well marked lump rostral to the connection with the optic lobe (Fig. 4.2.1.5). This convexity is more pronounced in *A. mississippiensis*, which shows even a rounded lump in this area. The physical endocast of *Leidyosuchus* (Storrs et al., 1983), a basal alligatoroid close to *Diplocynodon*, neither has this convexity in its posterodorsal cerebrum surface either. Furthermore, the studied crocodyloids and gavialoids also have a flat posterodorsal region of the cerebrum.

The paratympanic sinus system is very complex in eusuchian crocodiles (Witmer et al., 2008; Witmer and Ridgely, 2009; Bona et al., 2013; Dufeau and Witmer, 2015). The intertympanic diverticula present two variable features: i) In posterior view, at the level of the parietal pillars, the intertympanic diverticula could be divided in a central portion or core and two lateral expansions (Fig. 4.2.1.4C and 4.2.1.5). In alligatoroids, including *D. tormis*, the core is more developed, while crocodyloids and gavialoids have much larger lateral expansions. ii) In posterodorsal view (Fig. 4.2.1.4F), the cavity lead by the parietal pillars is wide in *D. tormis*, *C. crocodilus*, *T. schlegelii*, *O. tetraspis* and both gavialoids, whereas it is only a narrow cavity in *A. mississippiensis*, *M. nativus*, *C. johnstoni* and *C. niloticus*.

The median pharyngeal sinus is a structure of poorly understood origin and function (Witmer and Ridgely, 2009; Dufeau and Witmer, 2015). Tarsitano, (1985); Brochu, (2004); and Gold et al., (2014) suggested that this area is highly variability in Crocodylia, showing horizontal canals in early-stage specimens. These median pharyngeal sinuses become more vertical in larger specimens. In alligatoroids (including *D. tormis*, Fig. 4.2.1.4D and 4.2.1.5), the cross section of the median pharyngeal sinus is circular, while in crocodyloids the cross-section is D-shaped, with the flat side anterior. Furthermore, the ventral part of the alligatoroid median pharyngeal sinus, ventral to the junction with the basisphenoid diverticulum, is subequal or at least less than twice than the length of the dorsal section, dorsal to the junction with the basisphenoid diverticulum. In crocodyloids, the ventral part of the median pharyngeal sinus is more than twice the length of the dorsal part. However, *T. schlegelii* shows the alligatoroid condition, with the ventral section slightly longer (33% longer) than the dorsal part. *G. gangeticus* also has a short medial pharyngeal sinus with a flat anterior surface.

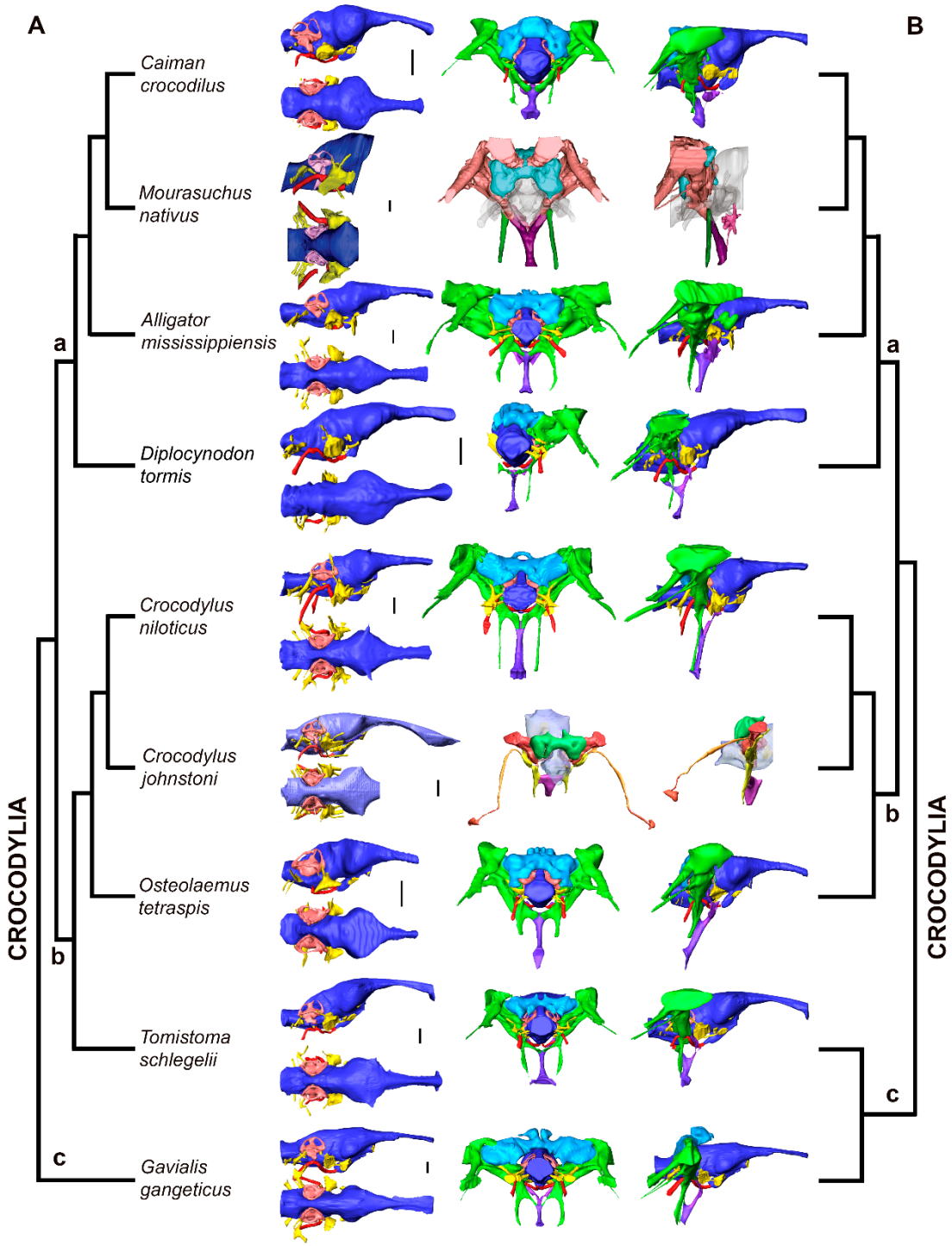

Fig. 4.2.1.5: Three Evolutionary pattern of the crocodylian brain. **A**, Phylogeny of Crocodylia based on morphological characters, modified from Brochu, (1999, 2011). **B**, Phylogeny of Crocodylia based on morphological and molecular characters, modified from Densmore and Owen, (1989) and Meganathan et al., (2010). It includes STUS-344, *M. nativus* (Bona et al., 2013) and *C. johnstoni* (Witmer et al., 2008), and the reconstructed specimens that complement the database. **a**, Crocodyloidea; **b**, Alligatoroidea; **c**, Gavialoidea. The images correspond to lateral (up and left) and dorsal (down and left) views of the encephalon with cranial nerves, blood vessels and inner ear; and posterior (middle) and lateral (right) views of the encephalon with the paratympanic sinus system.

Discussion and Conclusions

The studied specimen was identified as *Diplocynodon* aff. *gracilis* by Jiménez-Fuentes (1983), and later designated by Buscalioni et al. (1992) as a paratype of *D. tormis*. STUS-344 shares several synapomorphies of *Diplocynodon*, like the particular prefrontal and frontal ornamentation composed by three canals, the linear suture between the parietal and frontal, or the subtriangular section of the postorbital bar (Buscalioni et al., 1992; Brochu and Storrs, 2012; Narváez et al., 2015). STUS-344 shares specifically with *D. tormis* a projection of the posterior edge of the cranial roof, composed by the parietal and supraoccipital, which hides the occipital condyle in dorsal view (Buscalioni et al., 1992; Brochu and Storrs, 2012; Narváez et al., 2015).

Our knowledge of the anatomy and evolution of the structures within the skulls of archosaurs, particularly crocodiles, has improved dramatically over the last decade (Bona et al., 2013, 2017; Blanco et al., 2015; Dufeau and Witmer, 2015; Klein, 2016; Lautenschlager and Butler, 2016). Braincases are usually considered very conservative structures (Witmer and Ridgely, 2009; Holloway, 2011; Knoll et al., 2012), so the differences found among them may be useful in phylogenetical inference at a higher level. However, some studies have questioned the conservativeness of the braincase (at least in theropods: Rauhut, 2007), and some authors have shown how much the endocast shape can change depending on size or ontogeny (Dufeau and Witmer, 2015; Jirak and Janacek, 2017). Furthermore, the growth rate of wild and captive animals shows differences (Erickson et al., 2004 and references therein). The samples analysed below are principally from zoological institutions. Thus, any neuroanatomical differences in eusuchians must be taken with caution.

In order to overcome this caveat, the comparative studies sample includes skulls of different sizes in each phylogenetical group, based on the ontogeny of *A. mississippiensis* (Dufeau and Witmer, 2015). Two categories have been established: medium-sized specimens, with a length of 100-300 mm from the posterior edge of the supraoccipital to the anteriormost tip of the premaxilla (*C. crocodilus*, *O. tetraspis* and *D. tormis*), and large-sized specimens, longer than 300 mm in the same measurement (*A. mississippiensis*, *M. nativus*, *C. niloticus*, *C. johnstoni*, *T. schlegelii*, *G. gangeticus* and *G. neogaeus*). It must be stressed, though, that the comparative sample is limited.

Some characters may vary with the size and the ontogeny of the animal. For example, the large individuals have a slightly marked transition between the olfactory tract and the cerebrum, conical cerebral hemispheres, and narrow parietal pillars between the parietal and the prootics. On the other hand, the medium-sized individuals, including a subadult of *A. mississippiensis* (Dufeau and Witmer, 2015) and STUS-344, have an abrupt transition between the olfactory tract and the cerebrum, rounded hemispheres and relatively wide parietal pillars. *T. schlegelii* is grouped among the large size sample, but it shows the same features than the medium-sized samples. This

maybe due to the fact that its length is only a few centimetres over the limit suggested by Dufeau and Witmer (2015) or, alternatively, to the particular morphology presented by this animal, with a very elongated snout in relation with the braincase.

On the other hand, there is a set of highly phylogenetically informative endocast characters (Brochu and Storrs, 2012; Martin et al., 2014). Eusuchians usually have a flat posteriormost top of the cerebrum. However, derived members of Alligatoroidea develop a dorsal convexity of variable size (Fig. 4.2.1.5). The appearance of this dorsal convexity is therefore expected to occur in alligatoroids more derived than *D. tormis*, as no concavity appears in STUS-344.

The relative development of the different regions of the intertympanic diverticula seems also to have phylogenetic significance. In crocodyloids and gavialoids, the lateral expansions are more developed than the central region. In alligatoroids (including STUS-344) this central portion is subequal or larger than the lateral expansions. Therefore, the relative development of the central region might be considered as a synapomorphy of Alligatoroidea.

In alligatoroids, the ventral part of the median pharyngeal sinus is short and has circular cross-section, while it is long and has D-shape cross-section in crocodyloids (except *T. schlegelii*). The gavialoids, the basalmost members studied, have a short median pharyngeal sinus (as alligatoroids), with a flat anterior surface (as in crocodyloids). The studies of Brochu (2004) and Gold et al. (2014) show a "verticalization pattern" and elongation of the median pharyngeal sinus in large specimens of both clades. The larger alligatoroid studied, A. mississippiensis, has a long ventral section of the median pharyngeal sinus (75% longer than the dorsal part). However, O. tetraspis, the smaller crocodyloid studied, has a ventral part of the median pharyngeal sinus three times longer than the dorsal part.

Thus, the presence of a circular cross-section in this recess would be a synapomorphy of Alligatoroidea, whereas the lengthening of the median pharyngeal sinus would be a synapomorphy of Crocodyloidea. The differences between T. schlegelii and the rest of the crocodyloid samples, and its similarities with G. gangeticus may be due to the possible close relationships between both species (Densmore and Owen, 1989; Meganathan et al., 2010).

The neuroanatomical morphology of Diplocynodon tormis is consistent with that of a basal alligatoroid. Its internal cavities have both alligatoroid synapomorphies, such as the development of the central core of the intertympanic diverticula and a short median pharyngeal sinus; and purported crocodilian symplesiomorphies, such as a flat posterior outline of the cerebrum in lateral view (lost in more derived alligatoroids) and a convex anterior region of the median pharyngeal sinus.

ACKNOWLEDGMENTS

The authors acknowledge J. Fortuny (Institut Català de Paleontologia Miquel Crusafont, Sabadell) and Transmitting Science, for sharing the CT scans of the extant specimens here studied. We also acknowledge D. Vidal, for his useful comments which improved this article. We also acknowledge the valuable suggestions of D. Dufeau (Marian University, Indianapolis) and C. Brochu (University of Iowa, Iowa City).

This is a contribution to the research project DGCLM/140565, from the Junta de Comunidades de Castilla-La Mancha (Spain) and CGL2017-89123-P, from the Ministerio de Economía, Industria y Competitividad (Spain). ASM is an FPU grantee (FPU13/03362) of the Spanish Ministry of Education, Culture and Sport. FK is an ARAID researcher.

4.2.2 SENSORIAL AND COGNITIVE CAPABILITIES OF *DIPLOCYNODON TORMIS*

Three-dimensional reconstructions of the inner skull cavities allow their morphological description, but also the neurosensorial and cognitive skills by studying the structures that housed these sensorial organs.

Olfactory acuity depends on the number and size of mitral cells and the number of smell receptors and olfactory receptor genes, and these factors are related to the relative size of the olfactory bulb (Zelenitsky et al., 2011, 2009 and references therein). Olfactory ratio was obtained by comparing the largest diameter of the olfactory bulb and the maximum diameter of the cerebral hemispheres, and then normalizing it with a log-transformation. Zelenitsky et al. (2009) obtained that crocodylians have a high olfactory ratio which agrees with their acute olfactory sense (Weldon et al., 1990; Weldon and Ferguson, 1993). Our results coincide with them, being the olfactory ratio of *Alligator mississippiensis* (1.76) close the range assigned for this taxon (1.70-1.74) by Zelenitsky et al. (2009). The rest of the sample (168-1.82) is also close to the *A. mississippiensis* range, having crocodyloids (1.79-1.82) higher olfactory ratios than alligatoroids (1.68-1.76), independently of their size (Table 4.2.2.1). The basal alligatoroid *D. tormis* has an olfactory ratio of 1.75, within the range calculated for the alligatoroids.

taxon	Olfactory bulb diameter (mm)	Cerebral hemispheres diameter (mm)	Olfactory ratio	Log-transformed olfactory ratio
A. mississippiensis	17.3	29.8	58.05	1.76
M. niger	13.95	28.73	48.56	1.69
C. crocodilus	10.92	19.62	55.66	1.75
C. niloticus	20.37	30.5	66.79	1.82
O. tetraspis	15.43	24.9	61.97	1.79
T. schlegelii	19.13	28.89	66.22	1.82
G. gangeticus	16.65	33.29	50.02	1.70
D. tormis	12.14	21.3	57.00	1.76

Table 4.2.2.1: Measurements for the olfactory capability calculations, based on Zelenitsky et al. (2011, 2009).

Visual acuity is related to the size of the eyeball in vertebrates (Hall and Ross, 2007; Schmitz, 2009). There are studies relating the size of the eyeball and the ocular orbit, a measurable structure in fossil specimens in birds (Hall, 2008) and lepidosaurs (Hall, 2009), but not in crocodiles. However, crocodylians have an easily recognizable optic lobe (Jirak and Janacek, 2017), and its relative volume can be used as a proxy for optic capabilities. The relative volume of the optic lobe with respect to the brain is between 10 and 15% in the large-sized samples described in Chapter 4.2.1; and between 19 and 22% in the medium-sized ones (Table 4.2.2.2). *D. tormis* has a relative volume of the optic lobe of 16%, higher than those of the large-sized sample, but not reaching the medium-sized specimens.

taxon	Brain volume (mm^3)	Optic lobe volume (mm^3)	Ratio
A. mississippiensis	18719.90	2467.94	0.13
M. niger	24001,20	4447,06	0,19
C. crocodilus	4941.74	936.482	0.19
C. niloticus	24764.82	3789.03	0.15
O. tetraspis	11593.14	2577.36	0.22
T. schlegelii	19390.50	2105.72	0.11
G. gangeticus	38309.91	6996.52	0.18
D. tormis	7000.33	1149	0.16

Table 4.2.2.2: Measurements for the optic capability calculations.

Reptile Encephalization Quotient (REQ) is an equation adjusted to the reptilian brain proportions estimate cognitive capabilities basing on the volume of the brain endocast (Hurlburt, 1999). Body mass was estimated based on skull measurements (Dodson, 1975b; Webb and Messel, 1978; Platt et al., 2011). Endocast volume was obtained using the measurement tool of AVIZO. It is known that the endocast contains the brain itself and the dural envelope, a connective tissue that protects the brain. Brain/envelope proportion was described for a crocodylian ontogenetic series by Jirak and Janacek (2017) and Watanabe et al. (2018). These data were added into a regression formula that compares the endocast volume and the relative volume of the brain (Fig. 4.2.2.1). Once the brain volume was estimated, brain mass was calculated assuming a density of $1g/cm^3$ (Franzosa, 2004). In this way, crocodylian REQ is between 0.96 and 1.71 in our specimens (Table 4.2.2.3). *Osteolaemus tetraspis* and *Caiman crocodilus* have the highest REQs calculated, while the range of large-sized samples is between 0.9 and 1.2

(except for *Melanosuchus niger*, although it does not reach the REQs of the medium-sized samples). The REQ of *D. tormis* is 1.13, within the obtained crocodylian range, but low compared with the other medium-sized samples. This may be due to the breakage of some structures such as the otic capsules and the rostroventral part of the laterosphenoids, which impede the complete reconstruction of the brain.

taxon	Vol cereb (mm3)	Brain/envelope proportion*	Brain mass (gr)	Body mass (gr)	REQ
A. mississippiensis	18719.9	37,45	6.91	104328.28[1]	0,96
M. niger	24001	34,89	8.20	59108.00[1]	1,55
C. crocodilus	4941.74	54,82	2.75	5887.67[1]	1,71
C. niloticus	24764.8	34,57	8.38	151389.30[2]	0,96
O. tetraspis	11593.1	42,96	4.96	20228.39[2]	1,63
T. schlegelii	19390.5	37,08	7.08	93619.60[3]	1,04
G. gangeticus	38309.9	30,58	11.32	170000.00**	1,23
D. tormis	7000.33	49,62	3.50	20885.51[1]	1,12

Table 4.2.2.3: Measurements for the Reptile Encephalization Quotient calculations, based on Hurlburt et al. (2003). *The brain/envelope proportion was estimated introducing the data of Jirak and Janacek, (2017) and Watanabe *et al.* (2018) in a regression plot (Fig. 4.2.2.1). The body mass was estimated using skull measurements, basing in [1]Dodson, (1975); [2]Webb and Messel, (1978); [3]Platt et al. (2011) and **average species body mass.

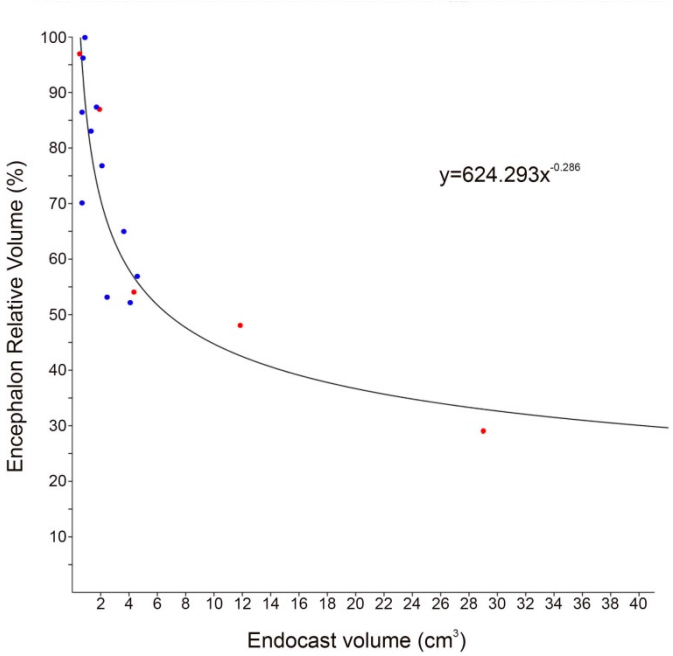

Fig. 4.2.2.1: Plot and regression of the relative volume of the encephalon versus the endocast total volume during the ontogeny of crocodiles, basing on the data of Jirak and Janacek, (2017), plotted as red dots, and Watanabe *et al.* (2018), plotted as blue dots.

CAPÍTULO 5: INNER SKULL CAVITIES OF THE SPECIMENS FROM LO HUECO

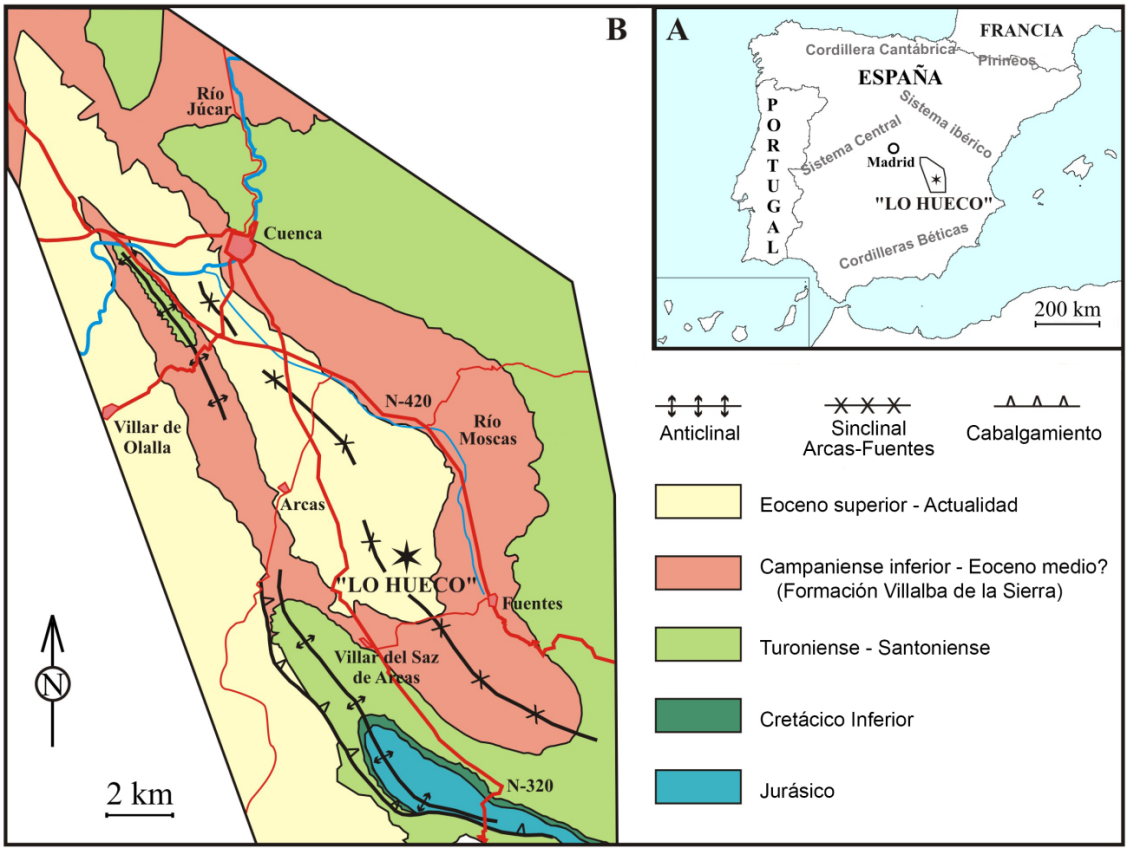

Fig. 5.1: Geographical and geological location of the Lo Hueco fossil site (Cuenca, Castilla - La Mancha, España).

The fossil site of Lo Hueco was found in 2007, in Fuentes (Cuenca, Spain, Fig. 5.1). This site is Upper Campanian-Lower Maastrichtian in age, attending to its stratigraphic position, in the upper part of the "Margas, Arcillas y Yesos de Villalba de la Sierra" Formation; and its paleontological remains (Ortega, 2008; Barroso-Barcenilla et al., 2009; Ortega et al., 2015). Lo Hueco fossil site (Upper Cretaceous. Cuenca, Spain) has yielded a large collection of vertebrate remains, including teleost fishes, amphibians, turtles, squamates and dinosaurs, besides a large amount of crocodile remains (Ortega et al., 2015 and references therein). Several postcranial remains, such as pelvic and femoral bones, were described and analyzed using traditional morphometric methods (de Celis et al., 2018). This work suggests the presence of two different morphotypes of allodaposuchids in this fossil site. Focusing in cranial remains,

two new species have been confirmed basing on four complete skulls, a fragmentary palate and four lower jaws: *Lohuecosuchus megadontos*, with a broad rostrum and hypertrophied teeth, a pair of parasagittal foramina located in the palatal surface of the maxilla, a jugal-quadratojugal suture located in the posterior angle of the infratemporal fenestra, and a posteroventrally oriented choana (Narváez et al., 2015), and *Agaresuchus fontisensis*, with a more elongated and narrower snout and a dorsally extended naris (Narváez et al., 2016).

5.1 *LOHUECOSUCHUS MEGADONTOS*

Reference: Alejandro Serrano-Martínez; Fabien Knoll; Iván Narváez; Stephan Lautenschlager; Francisco Ortega. 2018. Inner skull cavities of the basal eusuchian *Lohuecosuchus megadontos* (Upper Cretaceous, Spain) and neurosensorial implications. Cretaceous Research 93: 66-77. doi: 10.1016/j.cretres.2018.08.016

Inner skull cavities of the basal eusuchian *Lohuecosuchus megadontos* (Upper Cretaceous, Spain) and neurosensorial implications

Alejandro Serrano-Martínez[1*]; Fabien Knoll[2]; Iván Narváez[1]; Stephan Lautenschlager[3]; Francisco Ortega[1]

[1]Grupo de Biología Evolutiva, Universidad Nacional de Educación a Distancia, pº Senda del Rey 9, 28040, Madrid, Spain, a.serrano@ccia.uned.es, inarvaez@ccia.uned.es, fortega@ccia.uned.es;

[2]ARAID—Fundación Conjunto Paleontológico de Teruel-Dinópolis, Av. Sagunto, 44001, Teruel, Spain, knoll@fundaciondinopolis.org

[3] School of Geography, Earth and Environmental Sciences. University of Birmingham. B15 2TT, Birmingham. United Kingdom, s.lautenschlager@bham.ac.uk

[*] Corresponding author

Abstract

The Late Cretaceous fossil site of Lo Hueco (Cuenca, Spain) has yielded a large collection of tetrapod remains, in which crocodyliforms are one of the best represented groups. The crocodyliforms from Lo Hueco helped establish Allodaposuchidae as one of the sister-groups of Crocodylia. A complete skull of the holotype of the allodaposuchid *Lohuecosuchus megadontos* was CT scanned, and all its inner cavities, including those of the brain, nerves, inner ear and blood vessels, as well as the paratympanic sinus system and the paranasal sinuses, were three-dimensionally reconstructed and compared to those of several extant and extinct crocodylians. The endocranial anatomy of *Lohuecosuchus megadontos* is congruent with its phylogenetic position as a basal eusuchian. Our work suggests that some of the neurosensorial capabilities found in the crown-group Crocodylia such as an acute sense of olfaction and a low frequencies hearing are already present at the base of Eusuchia.

Institutional Abbreviations—**CRARC**: Centre de Recuperació d'Amfibis I Rèptils de Catalunya (Barcelona, Spain). **FMNH**: Field Museum of Natural History (Chicago, Illinois). **MCD:** Museu de la Conca Dellà (Lleida, Spain). **MLP**: Museo de La Plata (Buenos Aires, Argentina). **MZB:** Museu Zoològic de Barcelona (Barcelona, Spain). **OUVC**: Ohio University Vertebrate Collections (Athens, Ohio). **STUS:** Sala de las Tortugas "Emiliano Jiménez" de la Universidad de Salamanca (Salamanca, Spain). **TMM**: Texas Memorial Museum (Austin, Texas). **UA**: Université d'Antananarivo (Antananarivo, Madagascar). **UF**: University of Florida (Gainesville, Florida). **UMZC**: University Museum of Zoology, Cambridge (Cambridge, UK).

Anatomical Abbreviations—**am**: auditory meatus. **ant**: anterior semicircular canal**. bsd**: basisphenoid diverticula. **car**: cerebral carotid artery. **cer**: cerebral hemispheres. **co**: cochlear duct. dac: dorsal alveolar canal. **ef**: Eustachian foramen. **en**: external naris. **fm**: *foramen magnum*. **ic**: internal choana. **ie**: inner ear. **itd**: intertympanic diverticula. **lat**: lateral semicircular canal. **mes**: mesencephalon. **mps**: medial pharyngeal sinus. **np**: nasal passageway. **npd**: nasopharyngeal duct. **ob**: olfactory bulb. **ol**: optic lobe. **ornc**: olfactory region of the nasal cavity. **ot**: olfactory tract. **pd**: parietal diverticulum. **pfo**: pituitary (hypophyseal) fossa. **pmmf**: premaxillary-maxillary foramen. **post**: posterior semicircular canal. **pros**: prosencephalon. **pss**: paranasal sinus system. **pts**: pharyngotympanic sinus. **pvvb**: paravestibular vascular bundle. **qs**: quadrate sinus. **rhomb**: rhombencephalon. **II**: optic nerve canal. **III**: oculomotor nerve canal. **IV**: trochlear nerve canal. **V**: trigeminal nerve canal. **IX-XI**: shared canal for glossopharyngeal, vagus and accessory nerves. $\mathbf{X_{tymp}}$: canal for tympanic branch of vagus nerve. **XII**: hypoglossal nerve paired canals.

Introduction

Extant crocodiles represent only a small fraction of Crocodylomorpha, whose evolutionary origins date back more than 230 million years. Crocodyliform remains, including cranial elements, are very common in Mesozoic and Cenozoic fossil sites. They show a great diversity and abundance of this group in many past ecosystems. Despite the existence of a large number of complete and well-preserved skulls of fossil crocodiles, only a few have been studied using tomographic techniques. This is

particularly unfortunate as these methods allow non-invasive observation of the internal anatomy of the inner skull, including cavities housing soft-tissue structures.

The first published CT-scan of a crocodyliform skull was that of the goniopholid *Calsoyasuchus valliceps* from the Early Jurassic of the USA (Tykoski et al., 2002). Digital explorations of fossil crocodilian cranial anatomy have significantly increased over the past few years. This holds true for both eusuchians *Aegisuchus witmeri* (Holliday and Gardner, 2012), *Mourasuchus nativus* (Bona et al., 2013), '*Allodaposuchus hulki'* (Blanco et al., 2015), *Gryposuchus neogaeus* (Bona et al., 2017), *Diplocynodon tormis* (Serrano-Martínez et al., in press) and more stemward forms (Kley et al., 2010; Fernández et al., 2011; Herrera et al., 2013b; Brusatte et al., 2016; Pierce et al., 2017). This has gone hand in hand with a similar improvement of the knowledge of the cavities in extant crocodiles (Witmer and Ridgely, 2008; Witmer et al., 2008; Gold et al., 2014; Dufeau and Witmer, 2015; Brusatte et al., 2016; Bona et al., 2017; Pierce et al., 2017). The analysis of neuroanatomical structures in the Late Cretaceous taxa takes on particular interest for the study of early evolution of Eusuchia. The radiation of eusuchians started sometime near the beginning of the Cretaceous (Buscalioni et al., 2011; Brochu, 2013; Turner, 2015; Narváez et al., 2016). The Late Cretaceous fossil record contains representatives of non-crocodylian Eusuchia which may provide valuable information about the transition and development of brain structures at this stage. By the early Cenozoic, the three main lineages of Crocodylia were already geographically widespread.

Over the last years, several taxa have been described from the Campanian-Maastrichtian of Europe (Blanco et al., 2015, 2014; Buscalioni et al., 2001; Delfino and Smith, 2012; Martin, 2010; Martin and Buffetaut, 2008, 2005; Narváez et al., 2017, 2016, 2015; Puértolas-Pascual et al., 2014, 2011). Some of these taxa have been included in a recently defined clade named Allodaposuchidae and considered as one of the closest outgroups to Crocodylia (Narváez et al., 2016). Within Allodaposuchidae, the specimens described from the late Cretaceous site of Lo Hueco (Cuenca, Spain. Fig. 5.1.1) are noteworthy due to their completeness and are thus particularly interesting for the analysis of the brain and pneumatic structures.

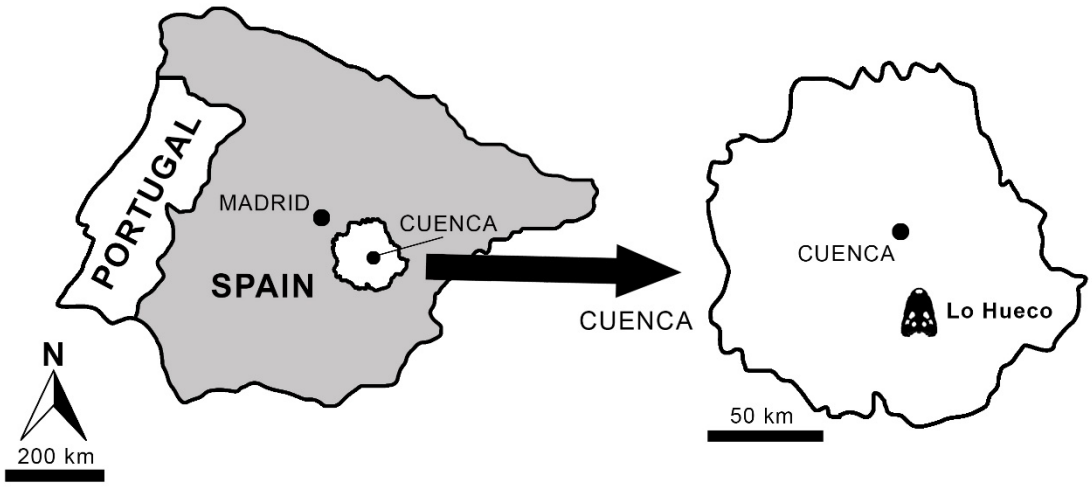

Fig. 5.1.1: Geographic location of the Spanish fossil site of Lo Hueco (Cuenca, Spain). Modified from Narváez et al. (2015).

Among the crocodiles from Lo Hueco, *Lohuecosuchus megadontos* was a medium size allodaposuchid with a broad and short rostrum and extremely hypertrophied teeth, larger than those of any other related taxon (Narváez et al., 2015). The well-preserved holotype specimen of *Lohuecosuchus megadontos* represents an unparalleled opportunity to provide a detailed description of the complete inner skull cavities in basal Eusuchia, an aspect of their anatomy on which information is scarcely available. These cavities are further compared to those of the other described Crocodyliformes to identify possible differences and similarities in order to contribute to the development of a neurosensorial evolutionary framework for this group of crocodiles.

Material and methods

The specimen studied herein, HUE-04498 (Fig. 5.1.2), is a complete and fully articulated skull, part of the holotype of *Lohuecosuchus megadontos* Narvaez et al. (2015), housed in the collection of the Museo de Paleontología de Castilla-La Mancha (MuPaCLM, Cuenca, Spain). The skull is well preserved, although it has suffered plastic deformation in dorsoventral direction, and a shear deformation along its sagittal plane (~10-15º clockwise, in caudal view). It is also partially covered in a ferrous coating, which cannot be removed without damaging the fossil. For a detailed osteological description of the specimen, see Narváez et al. (2015).

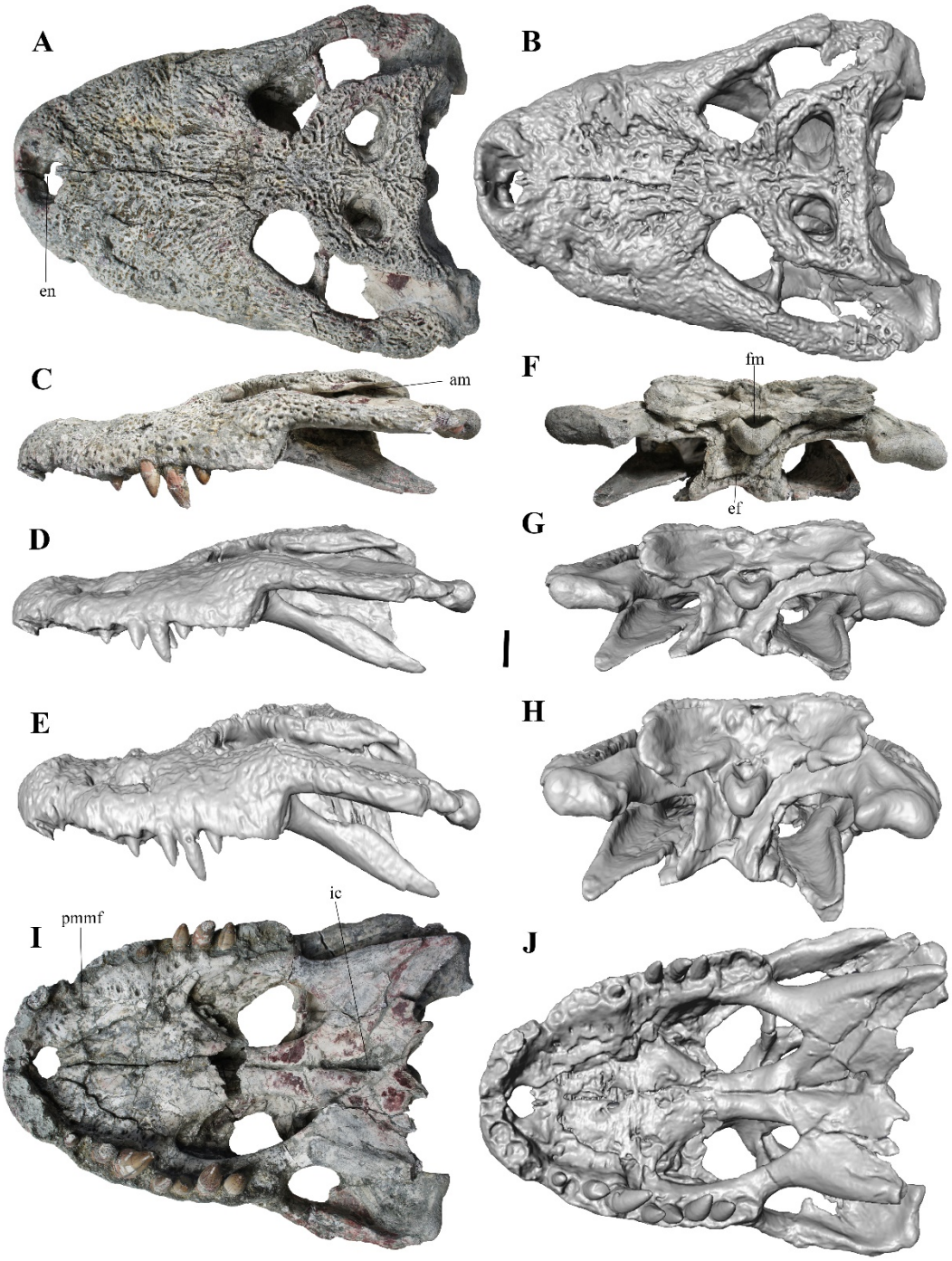

Fig. 5.1.2: Skull of *Lohuecosuchus megadontos* (HUE-04498). **A**: dorsal view of the skull. **B**: dorsal view of the unmodified digital model. **C**: left view of the skull. **D**: left view of the unmodified digital model. **E**: left view of the retrodeformed digital model. **F**: caudal view of the skull. **G**: caudal view of the unmodified digital model. **H**: caudal view of the retrodeformed digital model. **I**: ventral view of the skull. **J**: ventral view of the unmodified digital model. Scale bar equals 5cm.

In order to reconstruct digitally the endocast of the brain and the paratympanic and paranasal cavities, the specimen was scanned with a Toshiba Asteion Super 4 CT-scanner and with an Optima CT600, with a voltage of 135kV and a current of 75 mA. The inter-slice spacing was 0.33mm. The scan data were imported to ImageJ 1.49b (National Institutes of Health, USA) for artefact removal and optimizing the contrast and then into Avizo 7.1.0 (VSG, Burlington, MA, USA) for segmentation, visualization and analysis.

The resulting reconstruction was retrodeformed to compensate for the compression suffered by the fossil. With this end in view, the model was scaled in dorsoventral direction using the "transform editor" in Avizo. Based on specimens of related and morphologically similar taxa, such as *Allodaposuchus precedens* from Oarda de Jos, Romania (Delfino et al., 2008) and *Agaresuchus subjuniperus* from Beranuy, Spain (Puértolas-Pascual et al., 2014), a scaling factor of 140% was applied to the Z-axis (Fig. 5.1.2C-E and 5.1.2F-H). Although the original condition is unknown, the applied retrodefromation method provides a “best-approach” hypothesis, approximating the alleged original skull morphology (Tschopp et al., 2013; Lautenschlager, 2016; Vidal and Díez Díaz, 2017).

The inner skull cavities of HUE-04498 were compared to those of all mesoeucrocodylians for which descriptions of the cranial cavities are currently available. The basalmost specimens are represented by the notosuchian *Simosuchus clarki* (UA-8679, Kley et al., 2010) and the partially preserved allodaposuchid '*Allodaposuchus hulki'* (MCD-5139, Blanco et al., 2015). Within Crocodylia, Alligatoroidea is represented by the basal alligatoroid *Diplocynodon tormis* (STUS-344, Serrano-Martínez in press), the alligatorine *Alligator mississippiensis* (MZB 92-0231, pers. obs.; OUVC-9761, Witmer and Ridgely, 2008; Dufeau and Witmer, 2015) and the caimanines *Caiman crocodilus* (caiman_crocodilus_CRARC, pers. obs.; FMNH 73711, Brusatte et al., 2016) and *Mourasuchus nativus* (MLP73-IV-15-9, Bona et al., 2013). The crocodyloid sample comprises *Crocodylus johnstoni* (OUVC 10425, Witmer et al., 2008), *Crocodylus niloticus* (MZB 2003-1423, pers. obs.), *Osteolaemus tetraspis* (MZB 2006-0039, pers. obs.) and *Tomistoma schlegelii* (TMM M-6342, www.digimorph.org, pers. obs.). Digital reconstruction of the gavialoids *Gavialis gangeticus* (UF118998, www.morphosource.org, pers. obs.; MLP 602, Bona et al., 2017; UMZC R 5792, Pierce et al., 2017) and *Gryposuchus neogaeus* (MLP 68-IX-V-1, Bona et al., 2017) complete

the comparative sample. This taxon sample was divided into two size-based groups corresponding to the “yearling to subadult” and “adult” categories based on the ontogeny of *A. mississippiensis* (Dufeau and Witmer, 2015). Medium-sized specimens of *S. clarki*, *C. crocodilus*, *O. tetraspis* and *D. tormis* have a skull length (from the posterior edge of the supraoccipital to the anteriormost tip of the premaxilla) between 100 and 300 mm. The large-sized sample includes *A. mississippiensis*, *M. nativus*, *C. niloticus*, *C. johnstoni*, *T. schlegelii*, *G. neogaeus*, *G. gangeticus*, *'A. hulki'* and *L. megadontos*, with a skull length over than 300 mm.

For the neurosensorial analyses, only the generated reconstructions of *D. tormis*, *A. mississippiensis*, *C. crocodilus*, *C. niloticus*, *O. tetraspis*, *T. schlegelii*, *G. gangeticus* and HUE-04498 were taken into account. Further reconstructions of members of the outgroup were also included in the neurosensorial analyses: “Non archosauromorph Sauropsida” is represented by the savannah monitor (Varanidae, *Varanus exanthematicus* FMNH 58299, Gauthier et al., 2012), the black-headed python (Serpentes, *Aspidites melanocephalus* FMNH 97055, Gauthier et al., 2012) and the northern snapping turtle (Testudines, *Elseya dentata* TMM M-9315). We decided to add information from two extant birds as derived archosaurs: the ostrich (*Struthio camelus* TMM M-4826) and the black vulture (*Coragyps atratus* FMM uncatalogued). We reconstructed all these specimens by CT slices obtained from the database of www.digimorph.org.

We refer to the reconstructed bone-bounded spaces that house soft-tissue structures as if they were the structures themselves (e.g., "facial nerve" instead of "endocast of facial nerve canal").

Results

Neuroanatomy

The three-dimensional reconstruction obtained from the CT data provides a rendering of the inner skull cavities, including the brain cavity endocast, with the bases of the cranial nerves and the inner ear (Fig. 5.1.3), as well as the paratympanic sinus system and paranasal sinuses (Fig. 5.1.4). However, the cavity boundaries are difficult to recognise in several regions, such as the hindbrain and the structures located around

it, due to the similar density of the sediment filling the cavities and the mineralised bone.

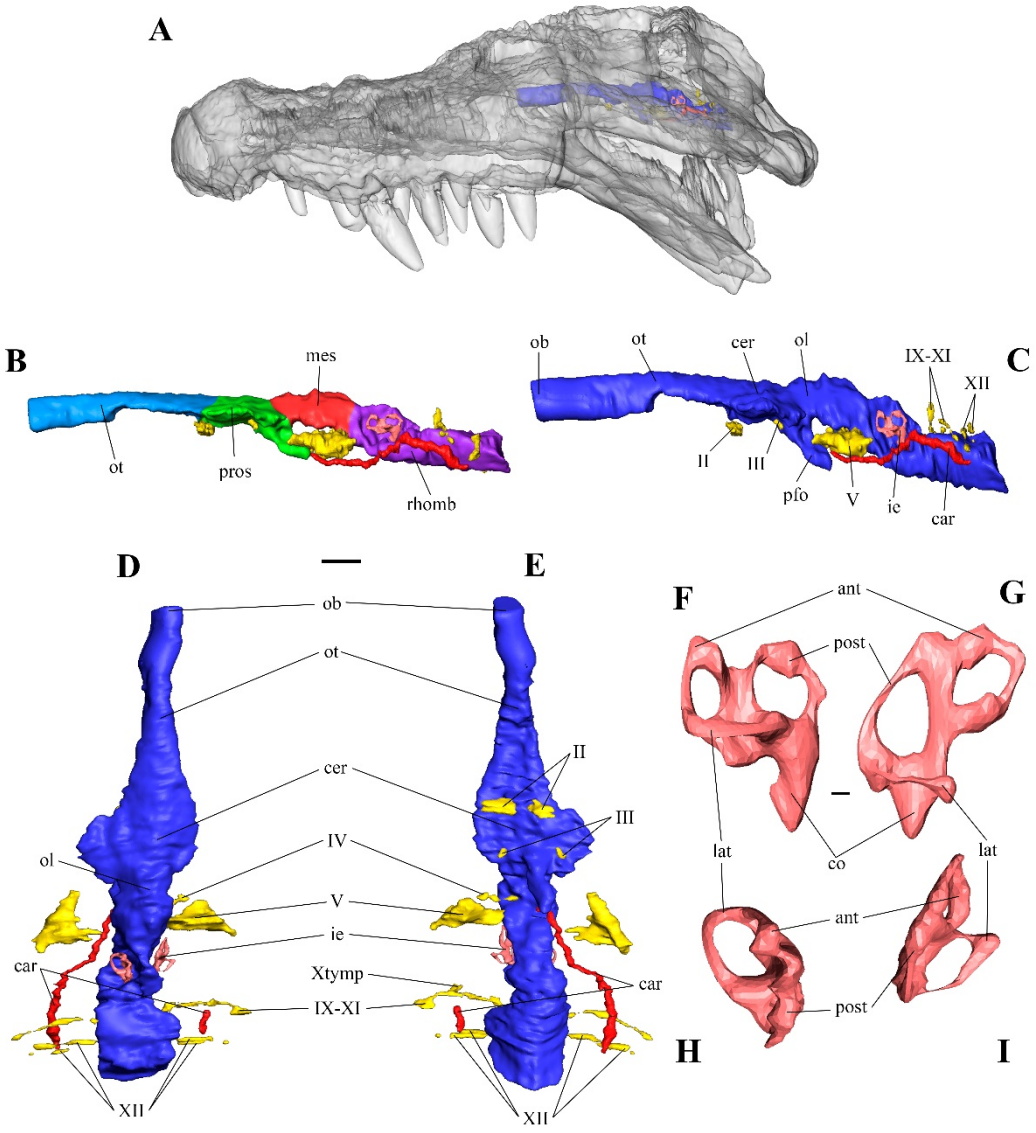

Fig. 5.1.3: Three-dimensional reconstruction of the endocranial components of *Lohuecosuchus megadontos* (HUE-04498). **A**: in-situ position of the brain endocast with the skull rendered semi-transparent, in left lateral view. **B**-**E**: HUE-04498 brain, nerves, endosseous labyrinth and arteries in **B**, unmodified, in left lateral view; **C**, left lateral view after retrodeformation; **D**, dorsal and **E**, ventral views. Scale bar equal to 1cm. **F**-**I**: HUE-04498 endosseous labyrinths in: **F**, left endosseous labyrinthin left lateral view; **G**, right endosseous labyrinth in right lateral view; **H**, left endosseous labyrinth in dorsal view and **I**, right endosseous labyrinth in dorsal view. Scale bar equals 1mm.

Brain: The brain is the structure that has been affected the most by the taphonomic dorsoventral compression. Despite the applied retrodeformation correction, the reconstructed anatomy does not fully represent the original morphology (Fig. 5.1.3B and 5.1.3C). However, the sigmoid morphology of the brain in a lateral view shown by all mesoeucrocodylians (Kley et al., 2010; Bona et al., 2013, 2017) is still distinguishable. The inner cavities also suffer from a slight shear deformation along the sagittal plane. The frontal forms the roof and lateral walls of the long olfactory tract. The cerebral hemispheres are flattened, but can still be delimited rostrally by the position of the optic nerves and caudally by the pituitary fossa (Fig. 5.1.3B). The forebrain is covered dorsally by the frontal and the parietal, laterally by the laterosphenoids, and ventrally by the basisphenoid.

The mesencephalon is an elongated region (Fig. 5.1.3B), delimited rostrally by the pituitary fossa, and caudally by the concavities resulting from the otic capsules (Fig. 5.1.3C). The hindbrain is limited dorsally by the parietal, dorsodistally by the otoccipital, distally by the prootics and ventrally by the basioccipital. The hindbrain portion has two lateral concavities that made room for the otic capsules in life. The shear deformation of the region resulted in the left concavity being larger than the right one (Fig. 5.1.3D). The caudal region of the hindbrain, rostral to the *foramen magnum*, has also been compressed, but to a lesser degree than the telencephalon. The pituitary extends from the ventral surface of the brain, in the caudalmost area of the cerebral hemispheres. It is caudoventrally oriented and appears to be somewhat displaced due to the shear deformation. The cerebral carotid arteries emerge from the caudalmost part of the pituitary. The left artery could be completely reconstructed, but the right one seemed to be only partially preserved (Fig. 3B and 3E). The arteries enter the *foramen caroticum*, on the otoccipital, then course rostrally until reaching the pituitary space, in the basisphenoid.

Cranial nerves: Right and left canals of the optic (II), oculomotor (III), trigeminal (V), glossopharyngeal (IX), vagus (X), accessory (XI) and hypoglossal (XII) nerves, and the right canal of the trochlear (IV) nerve are preserved (Fig. 3E). The abducens nerves (VI) are usually very thin in eusuchian crocodiles and could not be recognized with the resolution of the CT data. The region surrounding the anterior part of the hindbrain is obscured due to the density of the matrix being very similar to that of the

bone, precluding the reconstruction of the facial (VII) and vestibulocochlear (VIII) nerves.

The optic nerves are located ventrally, close to the sagittal plane, in the rostralmost part of the telencephalon. They are short but large nerves that exit the braincase rostrally between the laterosphenoids and the basisphenoid. The oculomotor nerves are located ventral to the flattened hemispheres, close to the rostral edge of the pituitary. They are caudodistally oriented. Their foramina are located on the laterosphenoids, although they are not visible on the fossil as they are covered by the iron coating. The right trochlear nerve is slender and long. It emerges from the mesencephalon and exits the braincase ventrodistally through the laterosphenoid, rostral to the trigeminal foramen. The trigeminal nerves are the largest, as in other archosaurs. They project laterally, being wider at their distal end than at their proximal base. Their distal branches cannot be distinguished. The glossopharyngeal, vagus and accessory nerves share a common caudodistally oriented passage through the otoccipital, dorsolaterally from the *foramen caroticum*. The right nerve also preserves the tympanic branch of the vagus nerve (Xtymp), which splits dorsally, close to the IX-XI foramen. The hypoglossal nerves find their way out the neurocranium via paired canals on each side. The rostral canals were fully recognized and reconstructed, but the caudal canals were only partially distinguishable, allowing only the reconstruction of the middle and distal parts. The rostral pair direct laterally over its entire length. The caudal hypoglossal branches emerge from the hindbrain slightly more dorsally than the rostral ones and course dorsolaterally before deviating ventrally and exiting the braincase through the otoccipital, close to the *foramen magnum*.

Endosseous labyrinth and paratympanic sinus system: The endosseous labyrinths are located in the otic capsules, formed by the prootics and the otoccipitals. Both labyrinths are preserved in the specimen, but their morphology appears to have been altered by the aforementioned shear deformation of the skull. In fact, the angle between the planes of the rostral and caudal semicircular canals is 120º in the left labyrinth (Fig. 5.1.3H) but in the right one it is spread almost 180º (Fig. 5.1.3I). The semicircular canals of HUE-04498 do not reach the size expected in comparison to other crocodylians. Furthermore, the rostral canal is the smallest (Fig. 5.1.3F and 5.1.3G), whereas it uses to be the most developed one in archosaurs (Sobral and Müller, 2016). Whereas the left lateral semicircular canal is circumscribed at the ventral extremity of

the rostral and caudal canals, the right lateral canal lies almost entirely rostral to the *crus commune*. The left cochlear duct projects ventrally, although its tip is slightly curved rostrally. The right cochlea only preserves the dorsalmost part, which is ventrally oriented.

The paratympanic and median pharyngeal sinus systems are housed in bony recesses around the mid/hindbrain (Fig. 5.1.4). The effects of the shear deformation are clearly visible, resulting in these cavities having rotated clockwise (Fig. 5.1.4E) in caudal view of the skull. In this region of the braincase, the similar density between the matrix and the bone made the distinction of these cavities difficult.

The intertympanic diverticula are located dorsally to the endocast, housed by the parietal, supraoccipital and both prootics. The lateral regions are wider (more prominently on the right side) than the central part (Fig. 5.1.4C), which appears reduced to a transverse narrow canal in dorsal view. The parietal diverticulum forms a ring-shaped structure, rostrally oriented, which emerges from both lateral regions of the intertympanic diverticula and converge rostromedially.

The pharyngotympanic sinus connects the intertympanic diverticula and the inner ear with the external auditory meatus, which opens distally between the quadrate and the squamosal. The other two passages of the pharyngotympanic sinus, the cranioquadrate canal and the siphonial tube were not recognizable in this specimen, and could not be reconstructed. Ventrally, the pharyngotympanic sinuses are reduced to two relatively short and narrow canals that course obliquely in caudal view (Fig. 5.1.4E). In eusuchians, the pharyngotympanic sinuses connect with the pharynx by two narrow canals, but these could not be distinguished in this specimen.

The median pharyngeal sinus system is located ventral to the pharyngotympanic sinuses, in bony recesses excavated in the basisphenoid.

Both pharyngotympanic sinuses merge in the median pharyngeal sinus. From there, a long single canal passes caudoventrally to finally open between the basisphenoid and the basioccipital (Fig. 5.1.4D). The basisphenoid diverticula only preserve the ventral connection with the median pharyngeal sinus, close to the merging point of the two ventral branches of the pharyngotympanic sinuses (Fig. 5.1.4D). The basisphenoid diverticula form a single canal, rostrodorsally oriented.

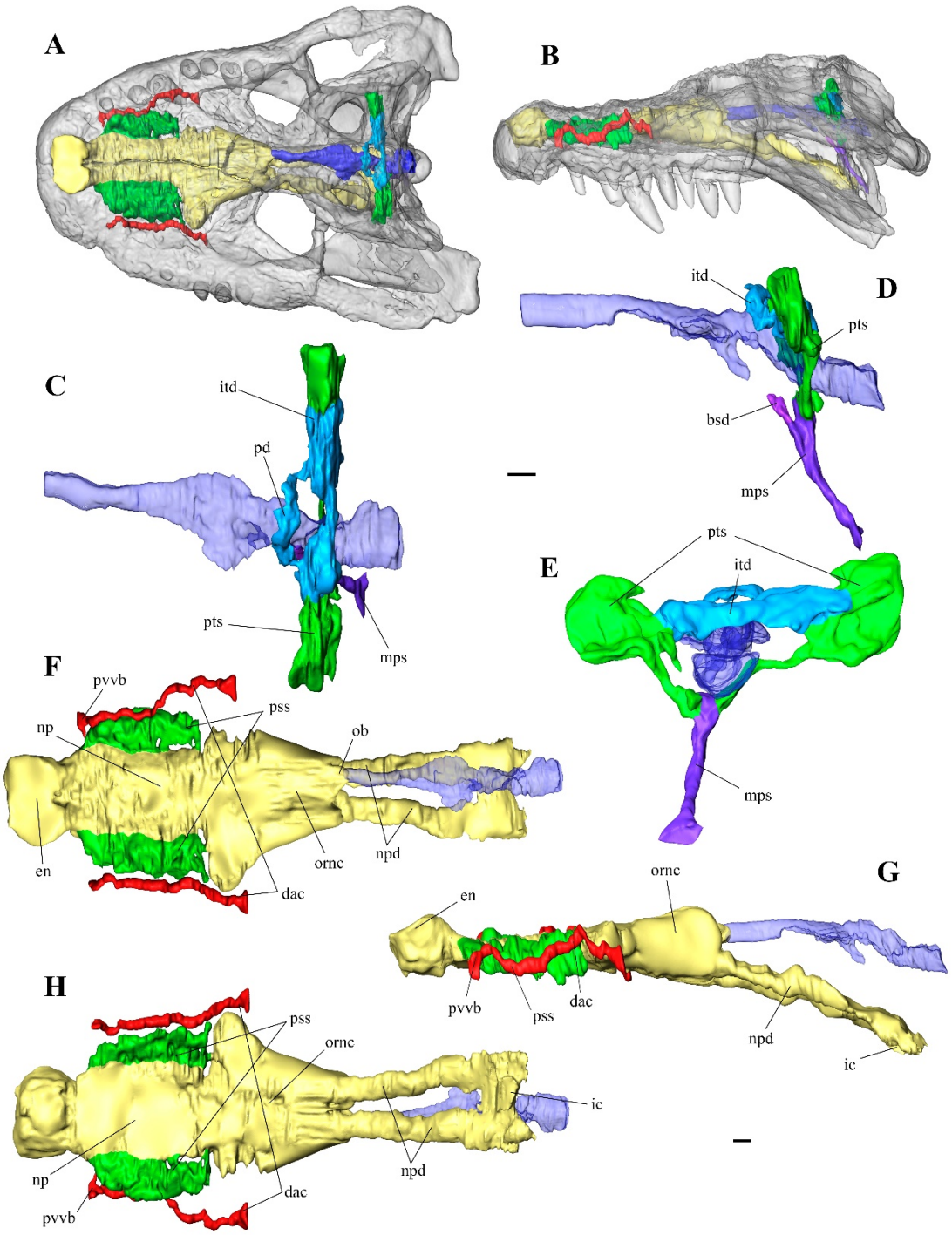

Fig. 4: Three-dimensional reconstruction of the paratympanicsinus system and paranasal structures within the braincase of *Lohuecosuchus megadontos* (HUE-04498). **A**, **B**: in-situ position of the paratympanic sinus system and paranasal structures with the skull rendered semi-transparent, in **A**, dorsal; **B**, left lateral views. **C**-**E**: HUE-04498 the median pharyngeal and pharyngotympanic sinus systems with the brain rendered transparent, in **C**, dorsal; **D**, left lateral; **E**, caudal views. **F**-**H**: HUE-04498 the paranasal system with the brain rendered transparent, in **F**, dorsal; **G**, left lateral; **H**, ventral views. Scale bar equals 1cm.

Nasal cavity and associated structures: Archosaurs have a large system of nasal inner cavities, and those of *Lohuecosuchus megadontos* extend from the external nares, at the tip of the snout, to the internal choana, in the caudoventral region of the basicranium. Insufficient resolution of the CT data makes it difficult to distinguish the limits of these structures. The external nares, formed by the premaxillae, are slightly wider than long (Fig. 5.1.4F). The nasal passageway proceeds from them ventrally, over a short distance before turning at an almost right angle to extend caudally. It is ventrally and laterally delimited by the maxillae, and dorsally by the nasals. Fairly ventrally to the lacrimo-prefrontal area, the nasal passageway divides into two structures. Dorsally, the canal widens, forming the olfactory region of the nasal cavity. Its rendering looks like a large, bilaterally symmetrical bulb, with a sagittal groove on its dorsal surface (Fig. 5.1.4F). This chamber, caudally delimited by the prefrontal pillars and dorsally by the frontals, continues caudally to the olfactory bulbs, which are connected with the brain by long olfactory tract. On the ventral side of the olfactory region of the nasal cavity, the nasal passageway continues caudally in the form of paired nasopharyngeal ducts. These canals pass firstly through the palatine, and then caudally through the pterygoid. Their dorsal boundaries with the olfactory region are damaged (Fig. 5.1.4G), but the remains of the septum between the nasopharyngeal ducts is still discernible as a sagittal groove on their ventral surface (Fig. 5.1.4H). Both ducts course ventrocaudally before merging in a single canal. Finally, the fused nasopharyngeal ducts open at the caudoventral end of the cranium by the internal choanae, in the pterygoids (Fig. 5.1.4G).

The paranasal sinus system is housed in the maxillae on both sides of the nasal passageway (Fig. 5.1.4F and 5.1.4H). Although the cavities are recognizable, the boundaries with the nasal passageway were hardly distinguishable. The paranasal sinus system is dorsoventrally compressed and has distally expanded projections. This system is composed of different cavities such as the antorbital sinus and the postvestibular sinus (Witmer and Ridgely, 2008; Pierce et al., 2017), but their limits cannot be distinguished in this specimen.

On each side, the dorsal alveolar canal extends lateral to the paranasal sinus systems. It housed the maxillary branches of the trigeminal nerve and the maxillary veins and arteries. The neurovascular canals pass rostrodorsally through the maxillae and premaxillae. The dorsal alveolar canal expands in the rostral part of the course

forming the paravestibular vascular bundle. From it emerge a canal oriented medially that connects with the nasal passageway, forming the medial subnarial anastomosis (Fig. 5.1.4F and 5.1.4H). From this bundle also emerges a ventrally oriented canal that opens onto the palate, by the premaxillary-maxillary foramen, located on the palatal premaxillary-maxillary suture (Fig. 5.1.4G). Caudally, the dorsal alveolar canal extends forming a large cavity before opening into the olfactory region of the nasal cavity.

Estimation of neurosensorial capabilities

Although we are conscious that assessing neurosensorial capabilities in a fossil taxon such as *Lohuecosuchus megadontos* is fraught with difficulties, we seized the opportunity offered by our digital reconstruction of the inner cranial cavities to attempt to provide a general picture of the sensorial and cognitive acuities of this taxon. Indeed, the endocranial components described above allow calculating linear and volumetric measurements that have bearing on the sensory abilities and cognitive capabilities of *L. megadontos*.

Olfactory acuity depends on the number and size of mitral cells and the number of smell receptors and olfactory receptor genes, and these factors seem to be related to the absolute and relative size of the olfactory bulb (Zelenitsky et al., 2011, 2009 and references therein). The olfactory ratio was calculated by comparing the largest diameter of the olfactory bulb to that of the cerebral hemispheres for each taxon. The results were subsequently log transformed. The obtained results agree with those reported by Zelenitsky et al. (2009): In this study, the olfactory ratio of *A. mississippiensis* (1.76) was found close the range assigned to this taxon (1,70 - 1,74) by Zelenitsky et al. (2009). The other crocodylians of the sample were also recovered close to the *Alligator* range proposed by Zelenitsky et al. (2009). The olfactory ratios of the extant taxa range between 1.70 and 1.82. The olfactory ratio of *L. megadontos* falls within this range at 1.79 (Table 5.1.1).

Taxon	Olfactory bulb (mm)	Cerebral hemispheres (mm)	**Log olfactory ratio**
A. mississippiensis	17,3	29,8	**1,76**
C. crocodilus	10,92	19,62	**1,75**
C. niloticus	20,37	30,5	**1,82**
O. tetraspis	15,43	24,9	**1,79**
T. schlegelii	19,13	28,89	**1,82**
G. gangeticus	16,65	33,29	**1,70**
L. megadontos	20,8	33,52	**1,79**
E. dentata	4,56	9,26	**1,69**
A. melanocephalus	6,6	10,71	**1,79**
V. exanthematicus	7,21	15,56	**1,67**

Table 5.1.1: Measurements for the olfactory capability calculations, based on Zelenitsky et al. (2011, 2009).

The bony labyrinth houses the neurosensory organs related to the hearing and balance. The cochlear region (Endosseous Cochlear Duct or ECD sensu Witmer et al., 2008), in the ventral part of the inner ear, houses the hearing organs. The hearing acuity in reptiles and birds seems to be related to the size of the ECD (Walsh et al., 2009). The ECD of the specimens were measured, scaled to the basicranium length and log transformed (Table 5.1.2). The extant crocodyliformes of the study have a scaled ECD that range between -0.73 and -1.09, close to the values given by Walsh et al. (2009) (range between -0.62 and -1). *L. megadontos* has a scaled ECD of -1.13, lower, but similar to those of *A.mississippiensis* and *C. niloticus*.

Taxon	ECD length (mm)	Basicranial axis (mm)	Scaled ECD length	**Scaled/transformed ECD length**
A. mississippiensis	7,6	92,38	0,08	**-1,08**
C. crocodilus	6,6	35,28	0,19	**-0,73**
C. niloticus	8,55	104,33	0,08	**-1,09**
O. tetraspis	8	70,77	0,11	**-0,95**
T. schlegelii	8,21	73,88	0,11	**-0,95**
G. gangeticus	8,8	86,33	0,10	**-0,99**
L. megadontos	6,55	87,76	0,07	**-1,13**

Table 5.1.2: Measurements for the auditory capability calculations, based on Walsh et al. (2009). **Abbreviations**: **ECD**, endosseous cochlear duct.

The visual acuity in vertebrates is often related to the size of the eyeball (Hall and Ross, 2007; Schmitz, 2009). The relationship between the size of the eyeball and the ocular orbit has been studied in lepidosaurs (Hall, 2009) and birds (Hall, 2008), but no such work is available for crocodiles. However, crocodilian endocasts have an easily distinguishable optic lobe (Fig. 5.1.3B; Jirak and Janacek, 2017), which can be used as a proxy for optic capabilities. The relative volume of the mesencephalon with respect to the whole brain in the extant specimens of our sample ranges between 10 and 15% in the large-sized specimens, and between 19 and 22% in the medium-sized ones. The mesencephalon of HUE-04498 has a relative size of 13%, similar to those of other large-sized specimens.

The volume of the endocast of the brain can be used to estimate cognitive capabilities using an equation adjusted to accommodate reptilian brain relative proportion, the Reptile Encephalization Quotient (REQ: Hurlburt, 1999). Volume measurements of the brain endocast were obtained using the measurement tool of AVIZO and converted into the mass assuming a density of $1g/cm^3$ (Franzosa, 2004). The body mass was estimated based on skull measurements (Dodson, 1975b; Webb and Messel, 1978; Platt et al., 2011). The endocast volume of *L. megadontos* is 13.6 cm^3 and its body mass was estimated to be around 89 kg (Webb and Messel, 1978). The actual brain volume of *L. megadontos* was calculated using Jirak and Janacek's (2017) data on extant crocodiles, using a regression formula that compares the endocast volume with the relative volume of the brain (Fig. 4.2.2.1). As a result of this adjustment, the REQs were reduced to 0.9-1.2 in the large-sized specimens and about 1.7 in the medium-sized ones. The REQ of *L. megadontos* is 0.82, a bit low compared with those of the large-sized specimens. This is probably due the crushing suffered by the brain cavity.

Discussion

Morphological implications

Braincases are usually considered conservative structures (Witmer and Ridgely, 2009; Holloway, 2011; Jirak and Janacek, 2017; Paulina-Carabajal and Filippi, 2017), and the differences found in these structures are potentially useful in phylogenetic analyses (Knoll et al., 2012; Paulina-Carabajal et al., 2017). The compression and shear

forces suffered by the specimen have substantially modified the shape of the inner skull cavities of *Lohuecosuchus megadontos*. However, the different regions that compose the brain and pneumatic cavities can still be distinguished. The reconstructed endocranial components of *L. megadontos* were compared to those of all mesoeucrocodylians previously described.

Although the morphology of the inner cavities is similar to the rest of the sample overall (Fig. 5.1.5), *L. megadontos* shows particular character states that are consistent with its phylogenetic position as a basal eusuchian (Narváez et al., 2015), shows distinct character states and polarization proposed in Serrano-Martínez (inn press). The endocranial cavities of HUE-04498 show all character states that can be considered eusuchian plesiomorphies, such as a flat caudodorsal outline of the brain hemispheres in lateral view, an intertympanic diverticula with distal expansions more developed than the central part, and a median pharyngeal sinus that is long and circular in cross-section along most of its length.

In all studied crocodylians, the nasopharyngeal ducts turn at a right angle to open ventrally through the internal choana. In HUE-04498, however, the caudalmost part of the nasopharyngeal ducts does not show the straight angle turn. Instead, these ducts show a gradual caudoventral curvature (Fig. 5.1.5), due to the ventral displacement of the internal choana (process explained by Tarsitano (1985)).

Regarding the dorsal alveolar canal, a notable feature is observed. In some alligatoroids, such as *C. crocodilus*, the caudal end of the canal opens into the olfactory region of the nasal cavity chamber, keeping its tubular structure all along its length. However, in crocodyloids, this neurovascular canal extends distally and then expands into a large cavity just rostral to the point where the septum between it and the nasal cavity chamber disappears (Fig. 5.1.5). In *G. gangeticus*, the dorsal alveolar canal opens into the olfactory region cavity, as in *C. crocodilus*. HUE-04498 shows a configuration recalling that seen in crocodyloids: the dorsal alveolar canal widens and opens separately from the olfactory region of the nasal cavity. The primitive condition may be the presence of a large cavity in the caudalmost region of the dorsal alveolar canal. Crocodyloidea retain this character state, as do some alligatoroids such as *A. mississippiensis*, while in Gavialoidea and *C. crocodilus* this enlargement of the dorsal

alveolar canal has been lost. Brochu (1999) also noticed this character, suggesting it to be a Crocodyloidea apomorphy.

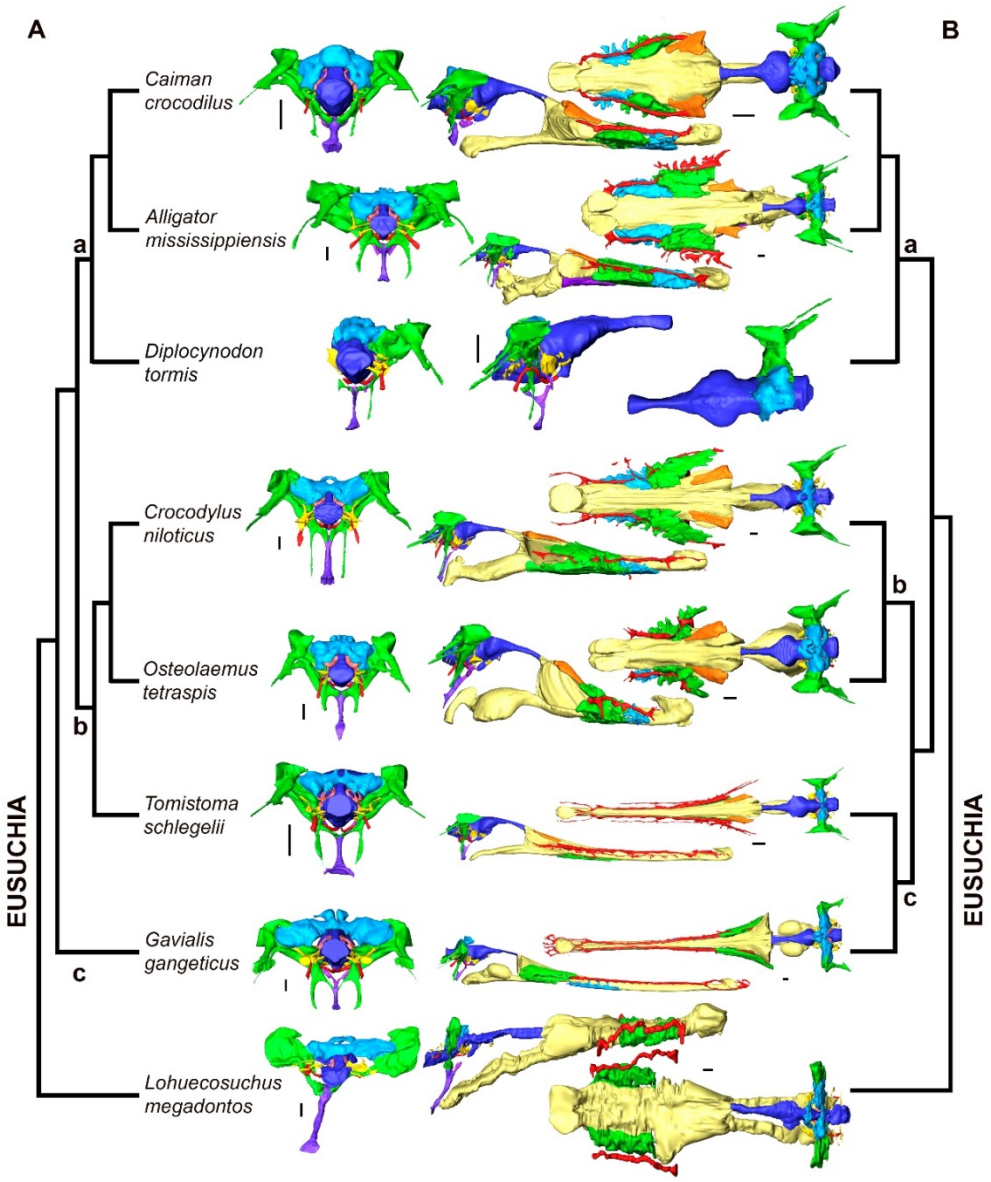

Fig. 5.1.5: Evolutionary pattern of the eusuchian brain. **A**, Phylogeny of Crocodylia based on morphological characters, modified from Brochu, (1999, 2011). **B**, Phylogeny of Crocodylia based on morphological and molecular characters, modified from Densmore and Owen, (1989) and Meganathan et al., (2010). It includes *Lohuecosuchus megadontos* (HUE-04498) and the reconstructed specimens discussed in the text. **a**, Alligatoroidea; **b**, Crocodyloidea; **c**, Gavialoidea. The images are posterior views of the brain with cranial nerves, blood vessels and inner ear, and the paratympanic sinus system (left); and right lateral (middle) and dorsal (right) views of the brain with cranial nerves, blood vessels and inner ear, the paratympanic sinus system, and the paranasal sinuses. Color key. Endocast colors were based on Witmer et al. (2008): blue, brain; yellow, cranial nerves; pink, inner ear; red, arteries. Paratympanic sinus system colors were based on Dufeau and Witmer (2015): intertympanic diverticula, blue; pharyngotympanic sinus, green; median pharyngeal recess, purple; basisphenoid diverticula, violet. Paranasal sinuses colors were based on Witmer and Ridgely (2008): nasal cavity, yellow; dorsal alveolar duct, red; postvestibular sinus, blue; antorbital sinus, green; nasolacrimal duct, orange. Scale bars equal 1cm.

On the other hand, results are not conclusive on some controversial issues within crown-group Crocodylia. As aforementioned, *T. schlegelii* has a caudal end of the dorsal alveolar canal similar to those of crocodyloids, but a short median pharyngeal sinus, as in *G. gangeticus* and the alligatoroids. The first character is in agreement with the morphological phylogenetical hypotheses that include *T. schlegelii* within Brevirostres (Fig. 5A. Brochu, 2011, 1999; Piras et al., 2010), whereas the second one it is in line with molecular phylogenetical hypotheses (Fig. 5.1.5B) in which *T. schlegelii* and *G. gangeticus* are closely related (Densmore and Owen, 1989; Meganathan et al., 2010).

Neurosensorial implications

Crocodylians are characterized by big olfactory bulbs and a sharp sense of smell (Zelenitsky et al., 2011, 2009 and references therein). Our results suggest that olfactory acuity of crocodiles is beyond that of birds and most dinosaurs (Table 5.1.1; Fig. 2 from Zelenitsky et al., 2009) (as well as beyond the outgroup taxa *Elseya dentata* and *Varanus exanthematicus*), but at the same level as the snake *Aspidites melanocephalus*. When crocodyloids and alligatoroids are considered separately, it is notable that the olfactory ratio remains relatively constant, regardless of skull-size, with crocodyloids having a slightly higher olfactory ratio than alligatoroids. With an olfactory ratio of 1.79, HUE-04498 falls between crocodyloids (average olfactory ratio = 1.82) and alligatoroids (average olfactory ratio = 1.76).

With regards to hearing, crocodiles seem to have an acoustic acuity specialized towards low frequencies (Vergne et al., 2009; Walsh et al., 2009; Brusatte et al., 2016; Pierce et al., 2017). The maximum scaled cochlear length of the studied sample is similar to that found by Walsh et al. (2009) for these taxa (-1 to -0.62). Furthermore, the minimum scaled cochlear length established for the biggest samples (-1.09 to -0.95; Table 5.1.2), are close to the average position for their hearing capability according to the regression line proposed by Walsh et al. (2009): around 700Hz (Vergne et al., 2009; Walsh et al., 2009). HUE-04498 has a small scaled EDC (-1.13), even smaller, but still similar to *A. mississippiensis* and *C. niloticus*. The hearing range of *L. megadontos* would therefore be lower than those of its extant relatives. Vergne et al. (2009) noticed that larger specimens are found to show a trend towards lower frequencies hearing.

Since *L. megadontos* has a remarkable short snout (Narváez et al., 2015), the measurements based on the rostrocaudal axis may be underestimated. However, *L. megadontos* has the largest skull width between the samples here studied, so it may be the largest specimen of this study. Therefore should not be surprising it has the lower hearing frequency. On the other hand, short cochlear size in HUE-04498 may also be explained by the compression suffered by the specimen.

The deformation of most of the brain cavity and the inner ear of HUE-04498 makes the results of some analyses, such as the encephalization quotient, the visual acuity or the balance capability less conclusive, and less distorted specimens are necessary to clarify which of this anomalous morphology is due to distortion.

Conclusion

The digital reconstruction of the holotype skull of *Lohuecosuchus megadontos* reveals an endocranial anatomy as would be expected for a taxon of its size and phylogenetical position as a basal eusuchian. A flat caudodorsal outline of the cerebral hemispheres in lateral view, large distal expansions of the intertympanic diverticula compared with the central region, and a long and circular cross-sectional median pharyngeal sinus are the most notable plesiomorphies of the endocranial cavities of *L. megadontos*. A broad caudal end of the dorsal alveolar canal is shared with crocodyloids, whereas the gradual ventral turn of the nasopharyngeal ducts becomes a right angle in more derived eusuchians.

The neurosensorial analyses are consistent with eusuchians having an acute olfactory capability and are adapted to low frequency hearing. The infered olfactory acuity of *L. megadontos* falls between that of the two major crocodylian groups: Alligatoroidea and Crocodyloidea. The inner ear of *L. megadontos* seems to be adapted to even lower frequences than extant alligatoroids and crocodyloids. The sensorial capabilities deduced from the morphology of the semicircular canals and the general shape of the brain must be considered with caution, as these structures might have been considerably deformed by diagenetic processes. Further investigations based on undeformed basal eusuchian specimens will allow to confirm the results of this study

and to provide further understanding of the neurological and sensorineural evolution of the early evolution of modern crocodiles.

Acknowledgements

We are grateful to the staff of the Centro Médico de Diagnóstico (Talavera de la Reina) and the Hospital Quirón Ruber (Madrid) for CT scanning many of the specimens analysed in this work. This article greatly benefited from comments by D. Vidal that undoubtedly improve this article. The authors want to acknowledge the valuable suggestions of two anonymous referees.

This is a contribution to a research project from the Ministerio de Economía, Industria y Competitividad, Spain [CGL2015-68363-P] and from the Junta de Comunidades de Castilla-La Mancha, Spain [DGCLM/140565]. ASM is an FPU grantee [FPU13/03362] of the Ministerio de Educación, Cultura y Deporte (Spain). FK is an ARAID Senior Researcher.

5.2 *AGARESUCHUS FONTISENSIS*

Reference: Alejandro Serrano-Martínez; Fabien Knoll; Iván Narváez; Stephan Lautenschlager; Francisco Ortega. (in Refs.). Neuroanatomical and neurosensorial analisys of the Upper Cretaceous basal eusuchian *Agaresuchus fontisensis* (Cuenca, Spain). Papers in Palaeontology.

Neuroanatomical and neurosensorial analisys of the Upper Cretaceous basal eusuchian *Agaresuchus fontisensis* (Cuenca, Spain)

Alejandro Serrano-Martínez[1*]; Fabien Knoll[2]; Iván Narváez[1]; Stephan Lautenschlager[3]; Francisco Ortega[1]

[1]Grupo de Biología Evolutiva, Universidad Nacional de Educación a Distancia, pº Senda del Rey 9, 28040, Madrid, Spain, a.serrano@ccia.uned.es, inarvaez@ccia.uned.es, fortega@ccia.uned.es;

[2]ARAID—Fundación Conjunto Paleontológico de Teruel-Dinópolis, Av. Sagunto, 44001, Teruel, Spain, knoll@fundaciondinopolis.org

[3] School of Geography, Earth and Environmental Sciences. University of Birmingham. B15 2TT, Birmingham. United Kingdom, s.lautenschlager@bham.ac.uk

[*] Corresponding author

Abstract

Agaresuchus fontisensis is an allodaposuchid crocodile from the Campanian-Maastrichtian (Late Cretaceous) of Lo Hueco (Cuenca, Spain). Allodaposuchidae is a clade of European basal eusuchians, which is considered a part of the stem-group of the crown-group Crocodylia. The holotype and paratype skulls of *A. fontisensis* were CT scanned and their internal cavities were digitally reconstructed, including those of the brain, nerves and blood vessels, as well as the paratympanic sinus system and the paranasal sinuses. The cranial endocast and pneumatic sinuses were then compared with those of other crocodyliforms. The neuroanatomy of *A. fontisensis* resembles those of other mesoeucrocodylians, sharing some morphological traits with extant crocodiles. The neurosensorial and cognitive capabilities inferred from the inner skull cavity reconstructions of *A. fontisensis* are similar to those of other eusuchians. The olfactory acuity of *A. fontisensis* is low for a crocodile, being closer to that of the alligatoroids

rather than to that of the crocodyloids. Its visual acuity is similar to that of *Lohuecosuchus megadontos*, a sympatric and coeval allodaposuchid also found in the fossil site of Lo Hueco.

Keywords: paleoneuroanatomy, *Agaresuchus fontisensis*, Eusuchia, Late Cretaceous, Spain

Institutional Abbreviations**—CRARC**: Centre de Recuperació d'Amfibis I Rèptils de Catalunya (Barcelona, Spain). **FMNH**: Field Museum of Natural History (Chicago, Illinois). **MCD:** Museu de la Conca Dellà (Lleida, Spain). **MLP**: Museo de La Plata (Buenos Aires, Argentina). **MUPA**: Museo de Paleontología de Castilla-La Mancha (Cuenca, Spain). **MZB:** Museu Zoològic de Barcelona (Barcelona, Spain). **OUVC**: Ohio University Vertebrate Collections (Athens, Ohio). **STUS:** Sala de las Tortugas "Emiliano Jiménez" de la Universidad de Salamanca (Salamanca, Spain). **TMM**: Texas Memorial Museum (Austin, Texas). **UA**: Université d'Antananarivo (Antananarivo, Madagascar). **UF**: University of Florida (Gainesville, Florida). **UMZC**: University Museum of Zoology, Cambridge (Cambridge, UK).

Anatomical Abbreviations**—am**: auditory meatus. **ant**: anterior semicircular canal**. bsd**: basisphenoid diverticula. **car**: cerebral carotid artery. **cer**: cerebrum. **co**: cochlear duct. **dac**: dorsal alveolar canal. **ef**: Eustachian foramen. **en**: external naris. **fm**: *foramen magnum*. **ic**: internal choana. **ie**: inner ear. **itd**: intertympanic diverticula. **lat**: lateral semicircular canal. **mes**: mesencephalon. **mps**: medial pharyngeal sinus. **np**: nasal passageway. **npd**: nasopharyngeal duct. **ob**: olfactory bulb. **oc**: otic capsule. **ol**: optic lobe. **ornc**: olfactory region of the nasal cavity. **ot**: olfactory tract. **pd**: parietal diverticulum. **pfo**: pituitary (hypophyseal) fossa. **pmmf**: premaxillary-maxillary foramen. **post**: posterior semicircular canal. **pros**: prosencephalon. **pss**: paranasal sinus system. **pts**: pharyngotympanic sinus. **pvvb**: paravestibular vascular bundle. **qs**: quadrate sinus. **rhomb**: rhombencephalon. **vls**: ventral longitudinal sinus. **II**: optic nerve canal. **III**: oculomotor nerve canal. **IV**: trochlear nerve canal. **V**: trigeminal nerve

canal. **V_{tymp}**: tympanic branch of trigeminal nerve canal. **VI**: abducens nerve canal. **VII**: facial nerve canal. **IX-XI**: shared canal for glossopharyngeal, vagus and accessory nerves. **X_{tymp}**: canal for tympanic branch of vagus nerve. **XII**: hypoglossal nerve paired canals.

Introduction

Allodaposuchidae is a recently established clade of basal eusuchians from the Late Cretaceous of Europe, which forms part of the stem-group of Crocodylia (Narváez et al., 2015), although there are studies placing them as a stem-group of Brevirostres (Blanco et al., 2014). As such, Allodaposuchidae is fundamental for understanding the early radiation of modern crocodiles. The allodaposuchids from the Late Cretaceous fossil site of Lo Hueco (Cuenca, Spain) are noteworthy for their completeness and relatively high number of specimens, including skulls which provide an opportunity to analyse the endocast and pneumatic cavities.

To date, two species have been described from Lo Hueco: *Agaresuchus fontisensis*, based on two complete skulls and one associated lower jaw (Narváez et al., 2016), and *Lohuecosuchus megadontos*, based in three skulls and three lower jaws (Narváez et al., 2015). *A. fontisensis* was a medium sized allodaposuchid characterized by a more longirostrine snout and different tooth morphology compared to the coeval *L. megadontos*.

Recently, the study of the inner skull cavities of *L. megadontos* has demonstrated the benefits and potential of digital reconstructions to the understanding of the neurological and neurosensorial evolution of Eusuchia (Serrano-Martínez et al., 2018). The firsts paleoneuroanatomical studies in crocodiles date from the 19th century (Hopson 1979 and references therein). However, since the first application of digital tomographic technology to crocodyliforms (Tykoski et al., 2002), studies on their inner skull cavities have increased. Most digital reconstructions of inner skull cavities have been performed on extant crocodiles (Witmer and Ridgely, 2008; Witmer et al., 2008; Gold et al., 2014; Dufeau and Witmer, 2015; Brusatte et al., 2016; Bona et al., 2017; Pierce et al., 2017; Serrano-Martínez et al., 2018). Furthermore, several analyses of fossil specimens have improved the knowledge on the inner skull cavities of extinct

eusuchians, such as the basal eusuchians *Aegisuchus witmeri* (Holliday and Gardner, 2012) and *Allodaposuchus hulki* (Blanco et al., 2015), the alligatoroids *Mourasuchus nativus* (Bona et al., 2013) and *Diplocynodon tormis* (Serrano-Martínez et al., in press) and the gavialoid *Gryposuchus neogaeus* (Bona et al., 2017). With regards to more stemward taxa, thalattosuchians are the best represented group in neuroanatomical studies based on CT technology (Fernández and Herrera, 2009; Fernández et al., 2011; Herrera et al., 2013a; Brusatte et al., 2016; Pierce et al., 2017). Exceptions include the notosuchian *Simosuchus clarki* (Kley et al., 2010).

This work aims to complement the studies of both species of allodaposuchids from Lo Hueco, analyzing the inner cavities of the two preserved skulls of *A. fontisensis*. The reconstruction of the endocranial elements of this species allows estimating its neurosensorial and cognitive capabilities and comparing them to those of extant and extinct representatives of Crocodylia. In the comparisons, particular attention will be given to the coeval and sympatric allodaposuchid, *L. megadontos*.

Material and methods

The specimens included in the present analysis are the holotype, HUE-02502 (Fig 5.2.1A-D) and paratype, HUE-03713 (Fig 5.2.1E-H) skulls of *Agaresuchus fontisensis* (Narváez et al., 2016), which are housed in the Museo de Paleontología de Castilla-La Mancha (MUPA) collection in Cuenca, Spain. HUE-02502 is a complete and well preserved skull with a slight shear deformation in the sagittal plane. HUE-03713 is also complete and well preserved but exhibits a marked lateral compression.

In order to reconstruct the inner skull cavities, HUE-02502 was scanned in a Toshiba Asteion Super 4 CT-scanner (Centro Médico de Diagnóstico Talavera, Talavera de la Reina, Spain) and with an Optima CT600 (Clínica Quirón Juan Bravo, Madrid, Spain), with a voltage of 135kV and a current of 75 mA. The caudal half of HUE-03713 was scanned in a Sinus 1.25 H80s (Centro de Diagnóstico de Cuenca, Cuenca, Spain), with a voltage of 130kV and a current of 68 mA. The inter-slice spacing was 0.33mm. The data were imported to Avizo 7.1.0 (VSG, Burlington, MA, USA) for segmentation, visualization and analysis.

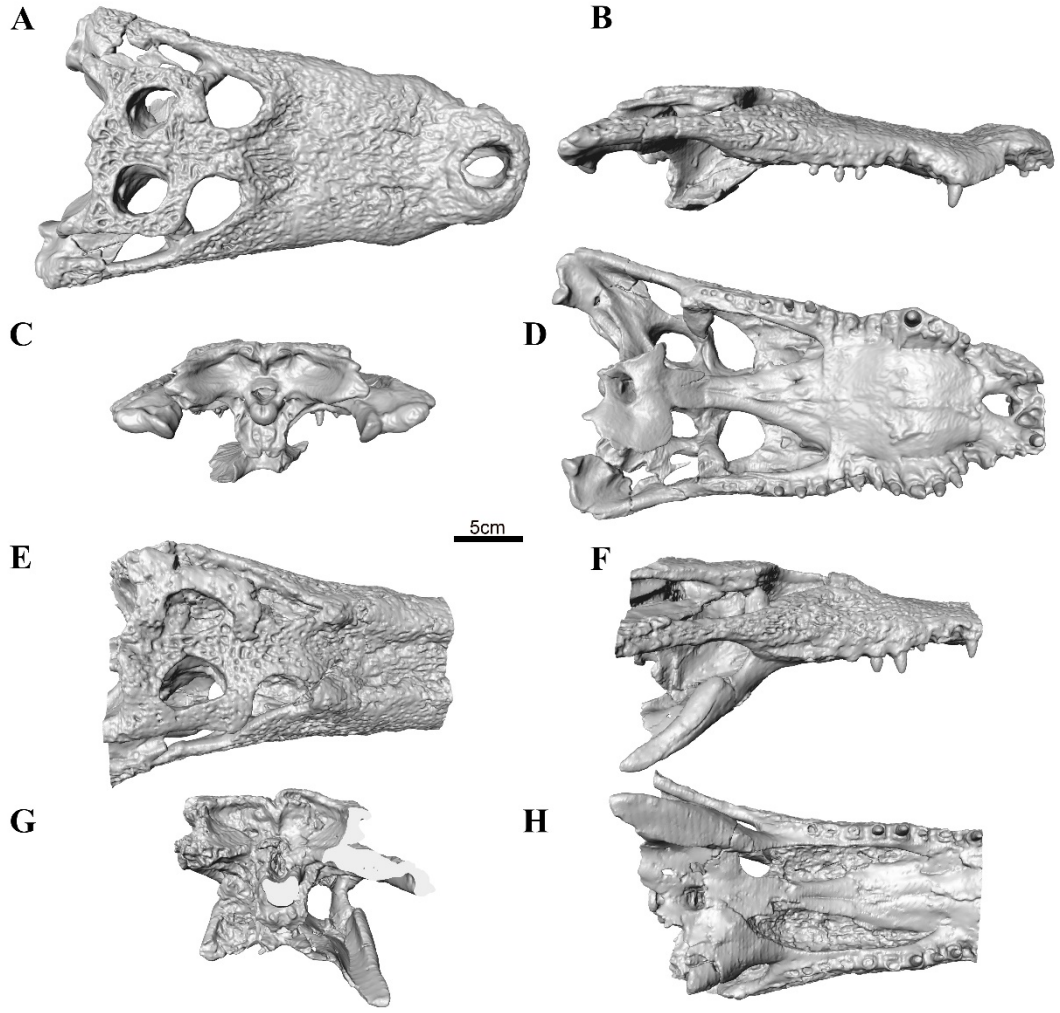

Fig. 5.2.1: Digital models of *Agaresuchus fontisensis*. **A-D**: Digital model of the holotype skull of *Agaresuchus fontisensis* (HUE-02702) in **A**, dorsal; **B,** right lateral; **C**, caudal; **D**, ventral views. **E-H**: Digital model of the paratype skull of *Agaresuchus fontisensis* (HUE-03713) in **E**, dorsal; **F**, right lateral; **G**, caudal; **H**, ventral views. See Narváez et al., (2016) for the original material.

The virtual 3D reconstruction of HUE-03713 was retrodeformed to compensate for the lateral compression suffered by the fossil. Thus, the model was laterally scaled using the "transform editor" in Avizo. Based on the proportions of HUE-02502 and the principle of symmetry, a scaling factor of 116% was applied to the X-axis. This method results in a "best-case-scenario" hypothesis (Tschopp et al., 2013; Lautenschlager and Butler, 2016; Lautenschlager et al., 2016; Vidal and Díez Díaz, 2017), which may not fully reproduce the original, *in vivo* configuration of the endocranial anatomy.

The inner skull cavities of both specimens assigned to *A. fontisensis* (HUE-02502 and HUE-03713) were compared to those of all mesoeucrocodylians for which inner

cavities have been digitally reconstructed to date. The non-neosuchian forms are represented by the notosuchian *Simosuchus clarki* (UA-8679, Kley *et al.* 2010). Although several reconstructions of inner skull cavities of thalattosuchians have been published, we decided not to include them due to their particular morphology (e.g. tubular brain shape, enlarged carotid arteries, or limited pneumaticity: see Fernández *et al.* 2011; Herrera *et al.* 2013, 2018; Brusatte *et al.* 2016; Pierce *et al.* 2017), which set them apart from other mesoeucrocodylians. Among Eusuchia, the allodaposuchids *Allodaposuchus hulki* (MCD-5139, Blanco *et al.* 2015) and *Lohuecosuchus megadontos* (HUE-04498; Serrano-Martínez *et al.* 2018) were included. Within Crocodylia, the alligatoroid sample includes the basal alligatoroid *Diplocynodon tormis* (STUS-344, Serrano-Martínez et al., in press), the alligatorine *Alligator mississippiensis* (our reconstruction based on MZB 92-0231; OUVC-9761, Witmer and Ridgely 2008; a list of another 13 specimens from Dufeau and Witmer 2015) and the caimanines *Caiman crocodilus* (our reconstruction based on caiman_crocodilus_CRARC; FMNH 73711, Brusatte *et al.* 2016) and *Mourasuchus nativus* (MLP73-IV-15-9, Bona *et al.* 2013). Crocodyloidea is represented by *Crocodylus johnstoni* (OUVC 10425, Witmer *et al.* 2008), *Crocodylus niloticus* (our reconstruction based on MZB 2003-1423), *Osteolaemus tetraspis* (our reconstruction based on MZB 2006-0039) and the phylogenetically unstable species *Tomistoma schlegelii* (our reconstruction based on TMM M-6342, www.digimorph.org). Furthermore, digital reconstructions of the gavialoids *Gavialis gangeticus* (our reconstruction based on UF118998, www.morphosource.org; MLP 602, Bona *et al.* 2017; UMZC R 5792, Pierce *et al.* 2017) and *Gryposuchus neogaeus* (MLP 68-IX-V-1, Bona *et al.* 2017) completed the comparative sample. Based on the ontogeny of *Alligator mississippiensis* (Dufeau and Witmer, 2015), the sample was divided into two size-based groups that share several features (Serrano-Martínez et al., in press). Medium-sized specimens, including *S. clarki*, *C. crocodilus*, *O. tetraspis* and *D. tormis*, have a skull length (from the caudal edge of the supraoccipital to the rostralmost tip of the premaxilla) between 100 and 300 mm. Large-sized sample includes *A. mississippiensis*, *M. nativus*, *C. niloticus*, *C. johnstoni*, *T. schlegelii*, *G. neogaeus*, *G. gangeticus*, *A. hulki*, and *L. megadontos*, with a skull length larger than 300 mm.

For the neurosensorial analyses, only the generated reconstructions of *L. megadontos*, *D. tormis, A. mississippiensis, C. crocodilus, C. niloticus, O. tetraspis, T. schlegelii* and *G. gangeticus* were taken into account.

We refer to the reconstructed bone-bounded spaces that house soft-tissue structures as if they were the structures themselves (e.g., "trigeminal nerve" instead of "endocast of trigeminal nerve canal").

Results

Neuroanatomy

The CT-data allowed to 3D reconstruct the brain cavity endocast, including the cranial nerves and carotid arteries, the paratympanic sinus system and the paranasal sinuses of HUE-02502 (Fig. 5.2.2 and 5.2.3) and HUE-03713 (Fig. 5.2.4). However, the sediment filling the inner cavities and the fossilized bone have a similar density. Therefore, some cavity boundaries, particularly those surrounding the hindbrain region, were difficult to distinguish and segment.

Brain: The brain is surrounded by the dural envelope, which often obscures the size, shape and some parts of the encephalon (Hopson, 1979; Witmer et al., 2008; Jirak and Janacek, 2017). In HUE-02502, the endocast is the best preserved cavity. It has a sigmoid morphology in lateral view, like in other eusuchians (Fig. 5.2.2D) (Witmer et al., 2008; Bona et al., 2013, 2017; Serrano-Martínez et al., 2018). The olfactory bulb connects with the brain via a long olfactory tract. The cerebrum is reniform in lateral view (Fig. 5.2.2D). The left telencephalic hemisphere is distinguishable in dorsal view as a slightly curved lump, while the right one is a bit flattened (Fig. 5.2.2E). The telencephalic region is delimited ventrocaudally by the hypophyseal fossa. The optic lobes are large (Fig. 5.2.2C), occupying 15% of the brain volume. The hindbrain has a strong sigmoid curvature in lateral view (Fig. 5.2.2D), and the reliefs of the otic capsules (Fig. 5.2.2F) and the ventral longitudinal sinus (Fig. 5.2.2F) are easily distinguishable. The hypophysis emerges from the ventral surface of the telencephalic region, in the caudal edge, and is ventrocaudally oriented. The two cerebral carotid arteries would emerge from the caudalmost part of the hypophysis and course caudally.

However, only the portions caudal to the paratympanic sinus system have been preserved. They extend caudoventrally to open at the *foramen caroticum*, on the otoccipitals (Fig. 5.2.2D).

The forebrain of HUE-03713 is less affected by the lateral compression than the hindbrain. It also shows a sigmoid outline from a lateral view (Fig. 5.2.4A). The olfactory tracts are long, and each cerebral hemisphere is clearly visible as a lateral rounded lump in dorsal view (Fig. 5.2.4B). The hindbrain has a narrow, elongate shape in dorsal view (Fig. 5.2.4B).

Cranial nerves: Canals of the optic (II), oculomotor (III), left trochlear (IV), trigeminal (V), abducens (VI), facial (VII), glossopharyngeal, vagus and accessory (IX-XI) and hypoglossal (XII) nerves have been recognized and reconstructed in HUE-02502. However, only the optic, trochlear and trigeminal nerves could be distinguished in HUE-03713.

The optic nerves are located on the ventral surface of the forebrain. They are wide but short nerves that course through the laterosphenoid. The oculomotor nerves are located dorsally from the pituitary. They are caudoventrally oriented and pass through the laterosphenoid. The trochlear nerve emerges from the posterior part of the forebrain, courses ventrally and emerges on the laterosphenoid, just rostrally to the large trigeminal foramen. As in other archosaurs, the trigeminal nerve is the largest cranial nerve. It arises from the rostral part of the hindbrain. The proximal part of the tympanic branch of the trigeminal nerve (V_{tymp}) could be distinguished. This branch emerges from the dorsal area of the trigeminal nerve as a thin and dorsally oriented nerve. Just ventrally to the trigeminal nerve, the abducens nerve arises from the rostroventral surface of the hindbrain and continues ventrally. It is the slenderest cranial nerve. The facial nerve is located in the lateroventral region of the hindbrain, caudally from the trigeminal nerve, and courses ventrolaterally. The glossopharyngeal, vagus and accessory nerves share a common, caudolaterally oriented canal, which opens at the otoccipital, dorsally from the *foramen caroticum*. The tympanic branch of the vagus nerve (X_{tymp}) splits close to the IX-XI foramen and courses dorsally. The caudalmost cranial nerves are the paired canals of the hypoglossal nerves. Both nerves also exit in the otoccipital, caudomedially from the IX-XI and close to the *foramen magnum*.

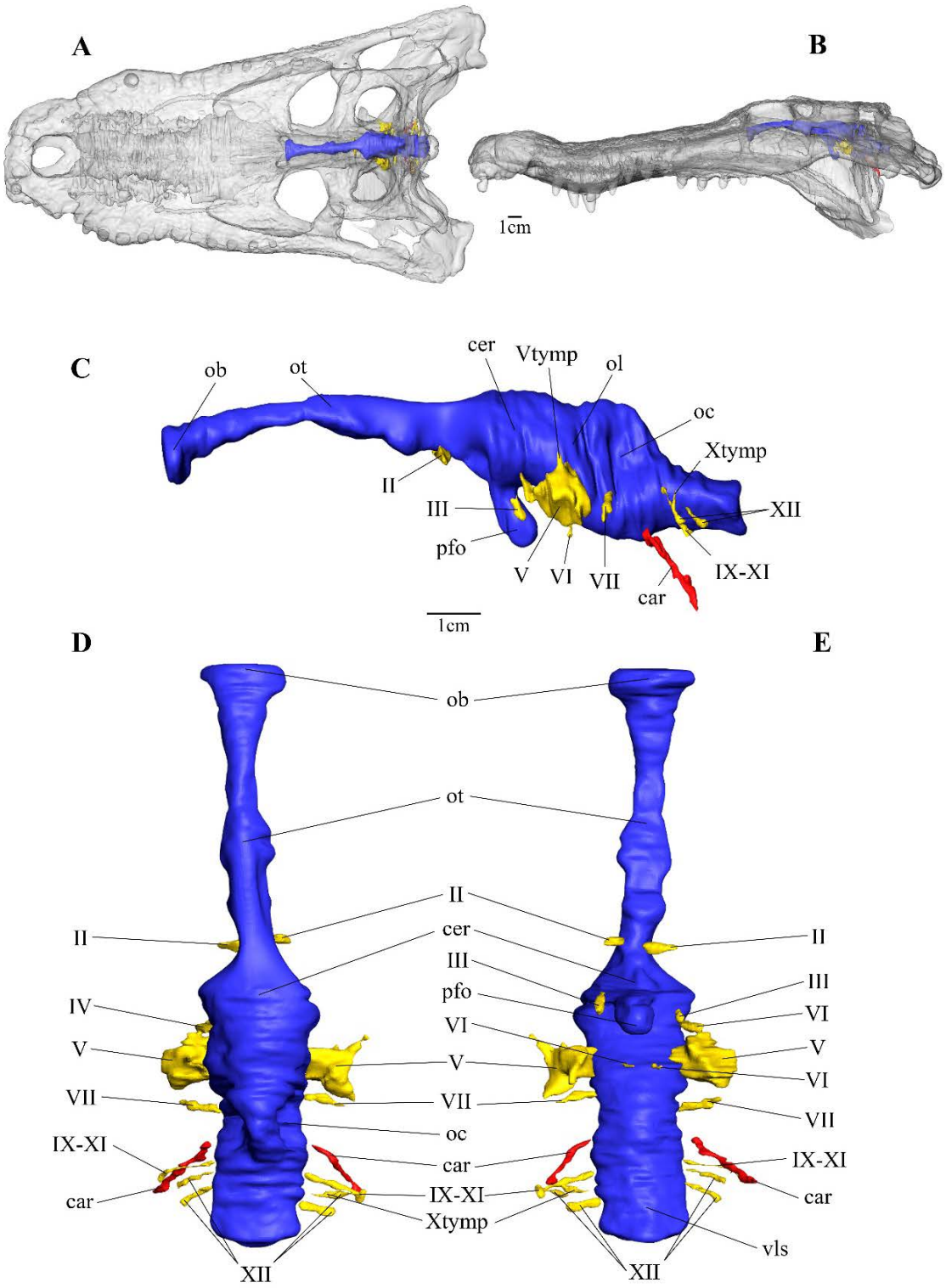

Fig. 5.2.2: Three-dimensional reconstruction of the endocranial components of the holotype of *Agaresuchus fontisensis* (HUE-02502). **A-B**: in-situ position of the brain endocast with the skull rendered semi-transparent, in **A**, dorsal; **B**, left lateral view. **C-E**: HUE-02502 brain, nerves and arteries in: **C**, left lateral; **D**, dorsal and **E**, ventral views.

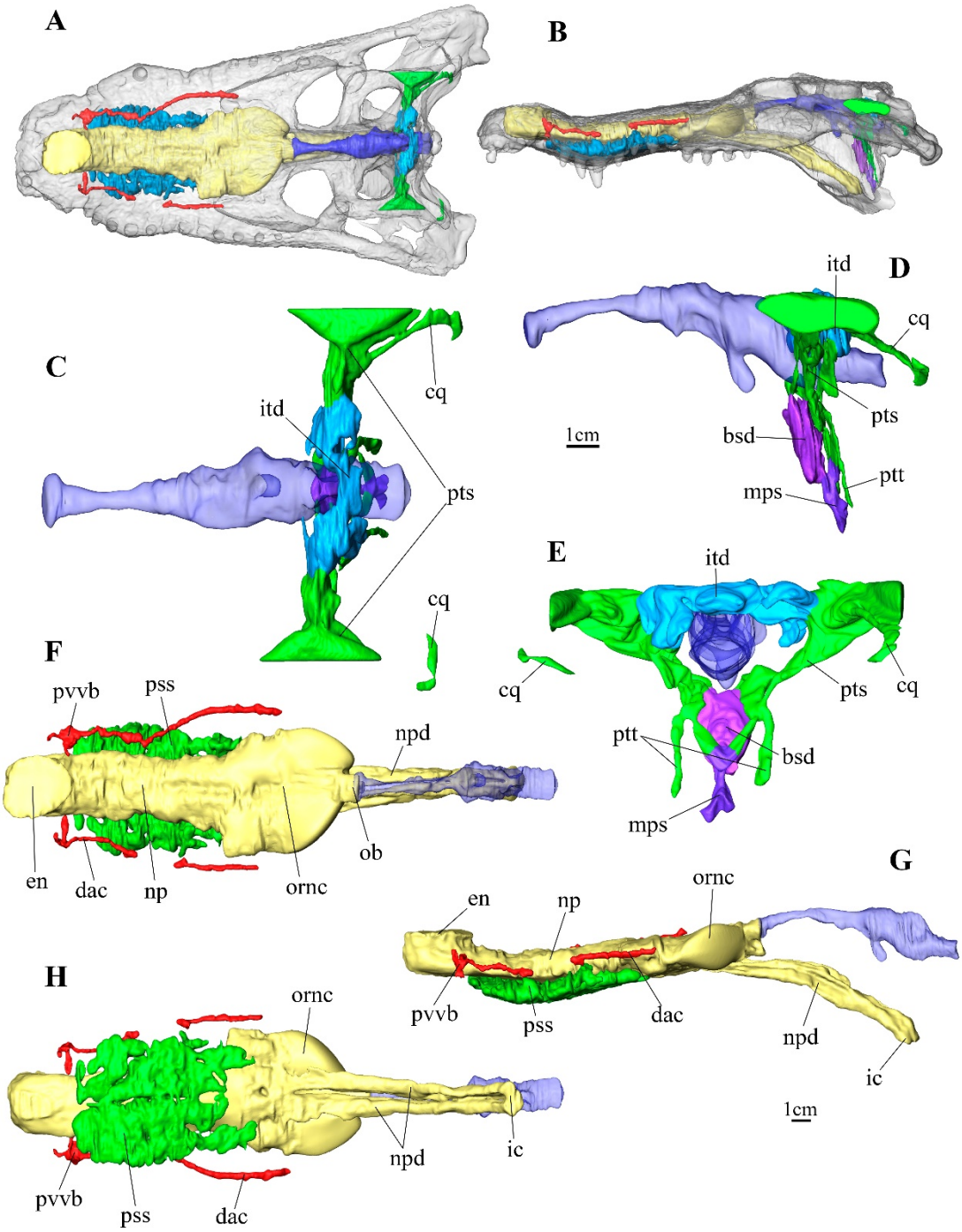

Fig. 5.2.3: Three-dimensional reconstruction of the paratympanic sinus system and paranasal structures within the braincase of the holotype of *Agaresuchus fontisensis* (HUE-02502). **A**, **B**: in-situ position of the paratympanicsinus system and paranasal structures with the skull rendered semi-transparent, in **A**, dorsal; **B**, left lateral views. **C**-**E**: the median pharyngeal and pharyngotympanic sinus systems of HUE-02502, with the brain rendered transparent, in **C**, dorsal; **D**, left lateral; **E**, caudal views. **F**-**H**: the paranasal system of HUE-02502, with the brain rendered transparent, in **F**, dorsal; **G**, left lateral; **H**, ventral views.

Inner ear and paratympanic sinus system: The inner ear is located in two lateral concavities formed by the otic capsules, in the rostral region of the metencephalon (Fig. 5.2.2D and 5.2.2E). The paratympanic sinus system is constituted by complex middle-ear diverticula that excavate bony recesses around the hindbrain (Fig. 5.2.3A and 5.2.3B). However, the inner ear is indistinguishable in both specimens, and the boundaries of the paratympanic recesses are hardly recognizable, due to the low contrast between the matrix filling the cavities and the bone.

The intertympanic diverticula form the dorsal part of the pharyngotympanic sinus, delimited laterally by the supraoccipital-otoccipital sutures. In dorsal (Fig. 5.2.3C) and caudal view (Fig. 5.2.3E), the parietal pillars delimit the lateral expansions medially, which are larger than the central region in HUE-02502. The caudal region of the right lateral expansion could not be distinguished in the CT slices. The medial region is caudally displaced. In HUE-03713, the boundaries between the intertympanic diverticula and the pharyngotympanic sinuses are indistinguishable, but they follow the same pattern as in HUE-02502, with a narrow medial region (Fig. 5.2.4D and 5.2.4F).

The pharyngotympanic sinus connects the intertympanic diverticula and the inner ear with the exterior through the external auditory meatus. The pharyngotympanic sinus also has two caudolateral passages that connect with the exterior. The siphonial tube cannot be reconstructed in HUE-02502 (Fig. 5.2.3C and 5.2.3E), while none of them can be reconstructed in HUE-03713. The right cranioquadrate passage of HUE-02502 is complete, but the left canal only preserves the distal region. This canal courses caudally, close to the auditory meatus, before opening on the caudal surface of the otoccipital. The ventral region of the pharyngotympanic sinus is tubular and ventrally oriented. The pharyngotympanic tubes are long and rostrocaudally flattened canals that extend ventrally and open between the basisphenoid and the basioccipital (Fig. 5.2.3D and 5.2.3E).

In HUE-02502, the median pharyngeal sinus connects the ventral parts of both pharyngotympanic sinuses (Fig. 5.2.3E) and course ventrally as a short single canal (Fig. 5.2.3D) that opens between the basisphenoid and the basioccipital, just between the pharyngotympanic tubes. The basisphenoid diverticula emerge from the rostral side of the median pharyngeal sinus, at midlength. It is an unusually large cavity that also connects dorsally with the pharyngotympanic sinus (Fig. 5.2.3D).

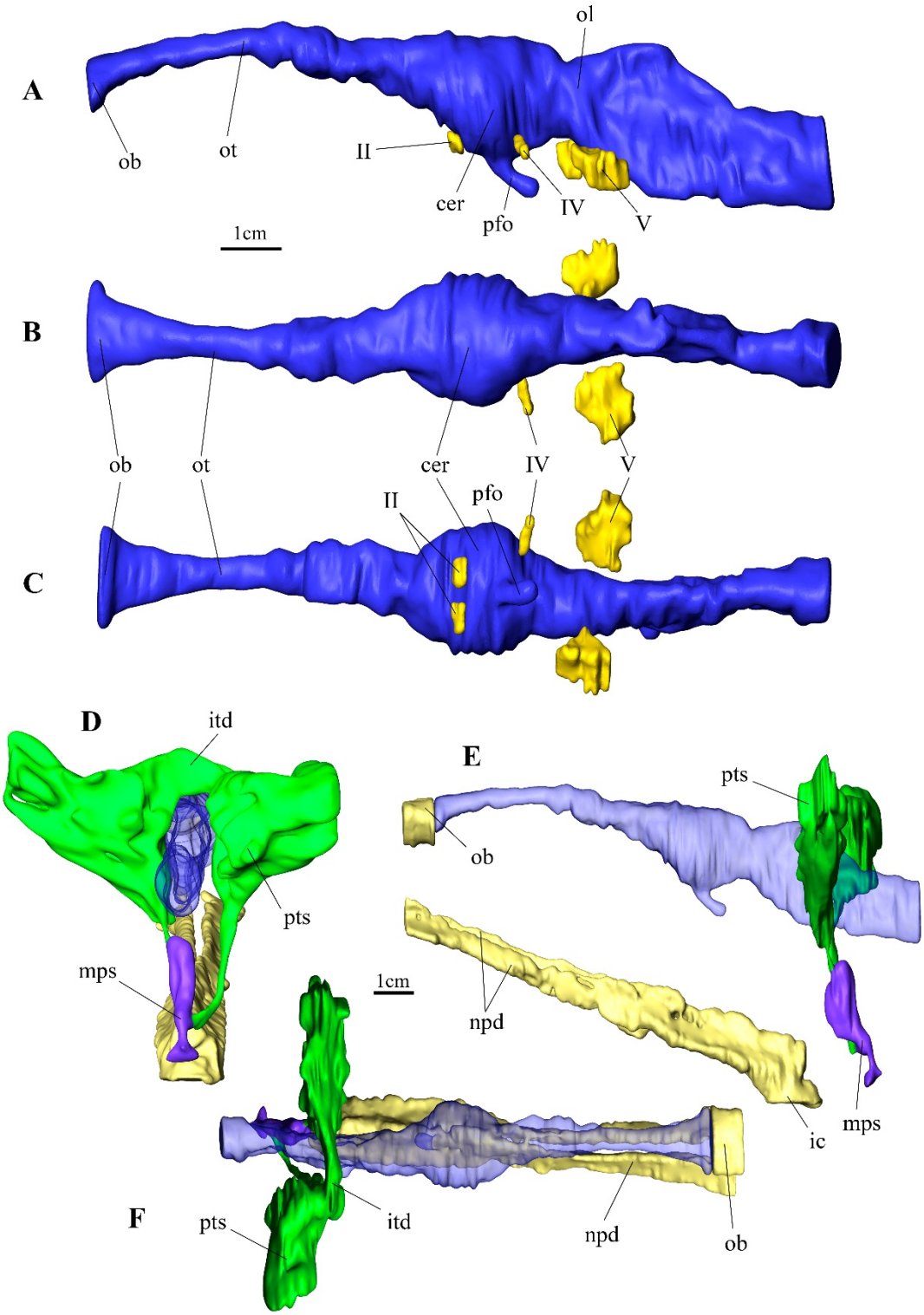

Fig. 5.2.4: Three-dimensional reconstruction of the endocranial components of the paratype of *Agaresuchus fontisensis* (HUE-03713). **A-C**: HUE-02502 brain, nerves and arteries in: **A**, left lateral; **B**, dorsal and **C**, ventral views. **D-F**: the paratympanic sinus system and the paranasal system of HUE-03713, with the brain rendered transparent, in **D**, caudal; **E**, left lateral; **F**, dorsal views.

The ventrally oriented canals that form the ventral section of the paratympanic sinus system of HUE-03713 have been substantially altered by the lateral compression (Fig. 5.2.4D): The left one is a short canal, which joins the median pharyngeal sinus close to the hindbrain. In contrast, the right canal is long, joining the median pharyngeal sinus close to its aperture to the pharynx. The median pharyngeal sinus is also a ventrally oriented canal, with a slight rostral lump at the level of the hypothetical position of the basisphenoid recess (Fig. 5.2.4E). As aforementioned, there are four connections between the pharyngotympanic sinus and the median pharyngeal sinus system, but only two were recognized in this specimen. Furthermore, due to the modified morphology of these cavities from taphonomic compression, the basisphenoid diverticula are indistinguishable from the median pharyngeal sinus. Therefore, it is not possible to determine what each canal is.

Nasal cavity and associated structures: Only the caudalmost section of HUE-03713 was CT-scanned. The olfactory bulb and the caudal region of the nasopharyngeal ducts could be reconstructed. In HUE-02502, the nasal passageway starts rostrally at the external nares, which are oval-shaped and longer than wide (Fig. 5.2.3F). From there, the nasal passageway courses ventrally, makes a 90º turn and then extends caudally. The nasal passageway has the same width over its entire length. Caudally, the passageway divides into two structures. Dorsally, it becomes wider to form the olfactory region of the nasal cavity, a large chamber limited dorsally by the frontals, and caudally by the prefrontal pillars. The olfactory bulbs emerge from the caudodorsal region of the chamber, between the prefrontal pillars, and connect with the brain via the olfactory tracts. Ventral to the olfactory region of the nasal cavity, the nasal passageway divides into the paired nasopharyngeal ducts (Fig. 5.2.3F). These canals course caudally at first, and gradually turn ventrally to open on the pterygoid via the internal choana (Fig. 5.2.3G). This curvature is also observed in HUE-03713 (Fig. 5.2.4E).

The paranasal sinus system is a complex of different cavities located ventrolaterally to the nasal passageway (Fig. 5.2.3H). However, the limits between both structures cannot be distinguished in HUE-02502. These cavities are dorsoventrally flat, and extend from the caudalmost point of the external naris to the rostral extreme of the olfactory region of the nasal cavity.

The dorsal alveolar canal is a bony cavity that houses the maxillary branches of the trigeminal nerve and the maxillary veins and arteries. This neurovascular canal courses rostrocaudally over the length of the snout, lateral to the nasal passageway and dorsal to the paranasal sinus system (Fig. 5.2.3F and 5.2.3G). The right canal could be fully reconstructed, unlike the left canal, of which the middle part could not be distinguished. The paravestibular vascular bundle is close to the external naris, in the rostral part of the canal. From this expansion emerges the medial subnarial anastomosis, which is a medially oriented canal that connects with the nasal passageway (Fig. 5.2.3F). From the paravestibular vascular bundle also emerges a ventrally oriented canal that opens onto the palate by the premaxillary-maxillary foramen (Fig. 5.2.3G). Caudally, the dorsal alveolar canal opens far from the olfactory region of the nasal cavity.

Estimation of neurosensorial capabilities

The reconstruction of the inner skull cavities of *Agaresuchus fontisensis* allows obtaining linear and volumetric measurements, which allow to estimate some of its sensorial and cognitive capabilities (exclusive of the senses of hearing and balance as the inner ear could not be reconstructed in any of the specimens).

The olfactory acuity has been found to depend on the number and size of the mitral cells, odour receptors and olfactory receptor genes (Zelenitsky et al., 2009). These factors are correlated with the absolute and relative size of the olfactory bulbs (Zelenitsky et al., 2009; Lautenschlager et al., 2012). Following the studies of Zelenitsky *et al.* (2009, 2011), olfactory ratios were calculated by comparing the greatest dimension of the olfactory bulb and the brain hemispheres, normalized by a log transformation. In the present analysis, the olfactory ratios of extant taxa were estimated as an average of 1.82 for crocodyloids, 1.76 for alligatoroids and 1.70 for gavialoids. The olfactory ratio of the basal eusuchian *Lohuecosuchus megadontos* is 1.79, falling just between alligatoroids and crocodyloids. The olfactory ratios of the *A. fontisensis* samples are 1.76 for HUE-02502 and 1.88 for HUE-03713 (Table 5.2.1).

Taxon	Olfactory bulb (mm)	Cerebral hemispheres (mm)	**Log olfactory ratio**
Al. mississippiensis	17.30	29.80	**1.76**
Ca. crocodilus	10.92	19.62	**1.75**
Cr. niloticus	20.37	30.50	**1.82**
O. tetraspis	15.43	24.90	**1.79**
T. schlegelii	19.13	28.89	**1.82**
G. gangeticus	16.65	33.29	**1.70**
L. megadontos	20.80	33.52	**1.79**
Ag. fontisensis HUE-02502	17.81	30.34	**1.77**
Ag. fontisensis HUE-03713	16.98	22.45	**1.88**

Table 5.2.1: Measurements for the olfactory capability calculations, based on Zelenitsky et al. (2011, 2009).

The visual acuity is generally estimated on the basis of eyeball size. Usually, larger eyes house more photoreceptors and sensorial cells (Hall and Ross, 2007; Schmitz, 2009; Lautenschlager et al., 2012). The eyeball size can be estimated from the orbital (sclerotic) ring (Lautenschlager et al., 2012) or from the orbit size (as proposed for lepidosaurs, Hall 2009, and birds, Hall 2008). Eusuchians lack sclerotic rings and there is no published evidence for a correlation between their optic capabilities and orbit size. However, the position of their optic lobes can be relatively well inferred from the endocast (Fig. 5.2.2C), being located in a narrowing between the cerebral hemispheres and the hypophyseal fossa and the otic capsule concavities of the rhombencephalon (Jirak and Janacek, 2017) (Fig. 2 from Jirak and Janacek 2017; Watanabe *et al.* 2018). The relative volume of the optic lobes was calculated comparing the volume of the optic lobes (Fig. 5.2.2C) in respect to the whole brain volume. The relative volume of the optic lobes in extant specimens varies between 10 and 15% in large-sized taxa, including *L. megadontos*, and between 19-22% in medium-sized taxa. The relative size of the optic lobes of HUE-02502 is 15%, being one of the greatest in the large-sized sample. In contrast, the relative size of the optic lobes of HUE-03713 is only 9% (Table 5.2.2).

Taxon	Endocast volume (mm3)	Optic lobe volume (mm3)	**Relative Volume**
Al. mississippiensis	18719.90	2467.94	**0.13**
Ca. crocodilus	4941.74	936.48	**0.19**
Cr. niloticus	24764.80	3789.03	**0.15**
O. tetraspis	11593.10	2577.36	**0.22**
T. schlegelii	19390.50	2105.72	**0.11**
G. gangeticus	38309.90	6996.52	**0.18**
L. megadontos	13604.50	1885.87	**0.14**
Ag. fontisensis HUE-02502	14696.40	2263.55	**0.15**
Ag. fontisensis HUE-03713	13515.90	1164.18	**0.09**

Table 5.2.2: Measurements for the relative size of the optic region, based on Jirak and Janacek, (2017).

Brain volume can be used to estimate cognitive capabilities, based on an equation adjusted to reptilian features, referred to as REQ (Reptile Encephalization Quotient, Hurlburt 1999). Body mass was estimated based on skull measurements (Dodson, 1975b; Webb and Messel, 1978; Platt et al., 2011). The endocast volume was obtained using the measurement tool from AVIZO, and its mass was calculated by applying a density of $1g/cm^3$ (Franzosa, 2004). The endocast houses the brain and associated tissues such as the dural envelope (Hopson, 1979; Jirak and Janacek, 2017; Watanabe et al., 2018). The respective proportions of these structures seem to vary during ontogeny (Jirak and Janacek, 2017; Watanabe et al., 2018). The relative brain volume was estimated based on a linear regression (Fig. 5) based on the crocodylian ontogenetical series published by Jirak and Janacek (2017) and Watanabe *et al.*, (2018). The REQ of the large-sized samples ranges between 0.9 and 1.2 (Table 5.2.3). The estimated brain mass of HUE-02502 would be 5.89 g, and its REQ would be 0.91. HUE-03713 has an estimated brain mass of 5.55 g, and its REQ would be 0.63, much lower than the holotype of *A. fontisensis*, extant taxa, and even the holotype of *L. megadontos* (REQ = 0.83), which is dorsoventrally compressed. This is probably due to the lateral compression suffered by the brain cavity in HUE-03713, which could not be completely corrected by the retrodeformation procedure.

Taxon	Endocast volume (cm^3)	Brain volume* (cm^3)	Body mass (g)	**REQ**
Al. mississippiensis	18.72	6.91	104328.28[1]	**0.94**
Ca. crocodilus	4.94	2.75	5887.67[1]	**1.74**
Cr. niloticus	24.76	8.38	151389.30[2]	**0.94**
O. tetraspis	11.59	4.96	20228.39[2]	**1.62**
T. schlegelii	19.39	7.08	93619.60[3]	**1.02**
G. gangeticus	38.31	11.32	170000**	**1.19**
L. megadontos	13.60	5.54	88719.46[2]	**0.82**
Ag. fontisensis HUE-02502	14.70	5.84	58107.02[2]	**0.90**
Ag. fontisensis HUE-03713	13.52	5.52	103847.04[2]	**0.62**

Table 5.2.3: Measurements for the Reptile Encephalization Quotient calculations, based on Hurlburt et al. (2003). *The brain volume was estimated introducing the data of Jirak and Janacek, (2017) in a regression plot (Fig. 4.2.2.1). The body mass was estimated using skull measurements, basing in [1](Dodson, 1975b); [2]Webb and Messel, (1978); [3]Platt et al. (2011) and **average species body mass.

Discussion

Morphological implications

The neuroanatomical structures of all previously described mesoeucrocodylians are quite similar, and in fact, braincases are generally considered to be conservative structures (Witmer and Ridgely, 2009; Knoll et al., 2012; Jirak and Janacek, 2017). *Agaresuchus fontisensis* exhibits several features considered as eusuchian plesiomorphies (Serrano-Martínez et al., 2018). In lateral view, *A. fontisensis* has a flat dorsal cerebrum outline. The flat dorsal surface of the caudal region of the cerebrum is most likely a plesiomorphy of eusuchians, which would develop into a lump of variable size in derived alligatoroids (Fig. 5.2.6) (Storrs et al. 1983; Serrano-Martínez et al., in press).

The lateral parts of the intertympanic diverticula are larger than the medial region in *A. fontisensis*. This configuration is also seen in crocodyloids, whereas in alligatoroids, the central region is larger to the detriment of the lateral parts (Fig. 5.2.6).

The median pharyngeal sinus has been demonstrated to be a variable structure (Fig. 6). Its length has been related to a "verticalization process" of the basisphenoid and basioccipital during ontogeny, that expanded the ventral region of the braincase (Brochu, 2004; Gold et al., 2014; Dufeau and Witmer, 2015). Furthermore, the length of

the section ventral to the basisphenoid diverticula relative to that of the section dorsal to them seems to also varies within the phylogeny (Gold et al., 2014; Serrano-Martínez et al., 2018). The ventral part of the median pharyngeal sinus is short in relation to the dorsal region in alligatoroids, gavialoids and *Tomistoma schlegelii*, being always less than 1.57. On the other hand, the length of the ventral section of the median pharyngeal sinus in crocodyloids and basal eusuchians, such as *L. megadontos*, is almost three times the length of the dorsal section (Serrano-Martínez et al., 2018). Although the length of the median pharyngeal sinus in HUE-02502 seems short (Fig. 5.2.3D), its ventral length relative to the dorsal one is 2.29, greater than what is seen in *A. mississippiensis*, the largest alligatoroid studied herein. However, it is lower than in *O. tetraspis*, being approximately between these two extant taxa (Fig. 5.2.5) (Serrano-Martínez et al., in press). The morphology of the pharyngotympanic sinus of HUE-03713 has been dramatically altered due to taphonomic compression. As the basisphenoid diverticula cannot be recognised, the relation of the ventral and dorsal lengths of the median pharyngeal sinus is uncertain. The length of the median pharyngeal sinus is also uncertain, due to the different morphology of the ventral regions of the pharyngotympanic sinus (Fig. 5.2.4D).

The extant taxa of our samples have caudally oriented nasopharyngeal ducts, which form a 90º angle before opening into the secondary choana. However, HUE-02502 and HUE-03713, as well as *L. megadontos*, show a gradual caudoventral curvature in the caudalmost part of the nasopharyngeal ducts, which is considered to be an eusuchian plesiomorphy (Tarsitano, 1985; Serrano-Martínez et al., 2018). Furthermore, the caudal part of the dorsal alveolar canal of both *A. fontisensis* specimens opens at a distance from the olfactory region of the nasal cavity, as in *L. megadontos*.

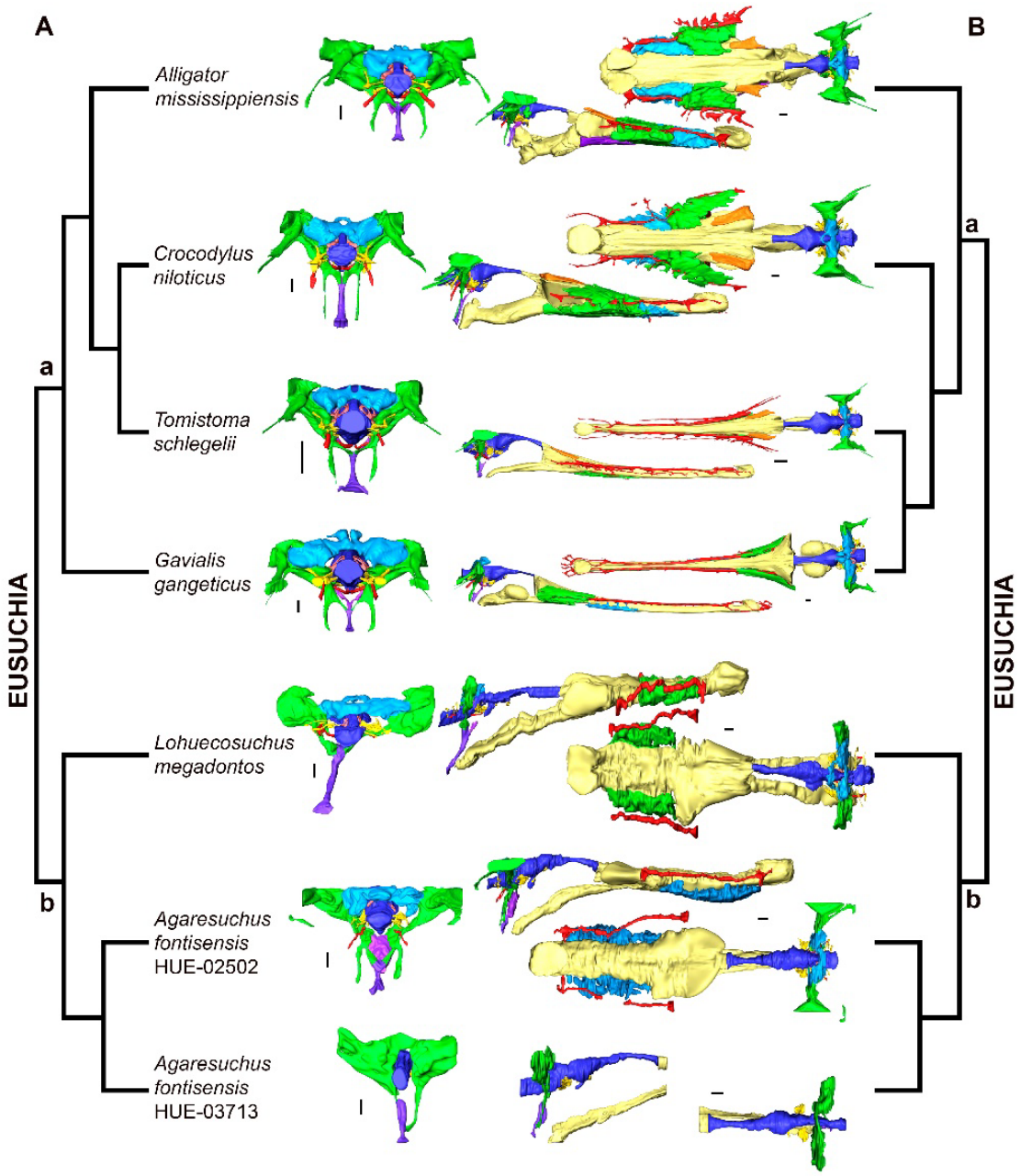

Fig. 5.2.5: Evolutionary pattern of the eusuchian brain. **A**, Phylogeny of Crocodylia based on morphological characters, modified from Brochu, (1999, 2011). **B**, Phylogeny of Crocodylia based on morphological and molecular characters, modified from Densmore and Owen, (1989) and Meganathan et al., (2010). The phylogeny includes the holotype (HUE-2502) and the paratype (HUE-03713) of *Agaresuchus fontisensis*, *Lohuecosuchus megadontos* (HUE-04498) and the reconstructed specimens of large-sized crocodylians discussed in the text. **a**, Crocodylia; **b**, Allodaposuchidae. The images are posterior views of the brain with cranial nerves, blood vessels and inner ear, and the paratympanic sinus system (left); and right lateral (middle) and dorsal (right) views of the brain with cranial nerves, blood vessels and inner ear, the paratympanic sinus system, and the paranasal sinuses. Color key. Endocast colors were based on Witmer et al., (2008): blue, brain; yellow, cranial nerves; pink, inner ear; red, arteries. Paratympanic sinus system colors were based on Dufeau and Witmer, (2015): intertympanic diverticula, blue; pharyngotympanic sinus, green; median pharyngeal recess, purple; basisphenoid diverticula, violet. Paranasal sinuses colors were based on Witmer and Ridgely, (2008): nasal cavity, yellow; dorsal alveolar duct, red; postvestibular sinus, blue; antorbital sinus, green; nasolacrimal duct, orange. Scale bars: 1cm.

Neurosensorial implications

Crocodylians are characterized by big olfactory bulbs and an acute sense of olfaction compared with other archosaurs (Zelenitsky et al., 2009, 2011; Grigg and Kirshner, 2015). In the present analysis, the olfactory ratio of crocodyloids (average olfactory ratio = 1.82) is higher than that of alligatoroids (average olfactory ratio = 1.76). *L. megadontos*, with an olfactory ratio of 1.79 (Serrano-Martínez et al., 2018), is intermediary. The olfactory ratio of HUE-02502 is 1.77, very close to that of alligatoroids and slightly lower than its allodaposuchid relative from Lo Hueco. On the other hand, HUE-03713 has a high olfactory ratio (1.88), which may actually reflect the deformation suffered by the skull that affected more intensely the proportions of the cerebrum than those of the olfactory bulb.

Sight plays an important role in crocodilian lifestyle (Garrick and Lang, 1977; Nagloo et al., 2016), which agrees with the relative complex eyes of these animals (Nagloo *et al.* 2016 and references therein). Despite the lack of comparative studies between orbit and eyeball sizes, the volume of the optic lobes can be used as a proxy to infer visual acuity. The volume of the optic lobes in HUE-02502 relative to the brain is 15%, slightly higher than in the sympatric and coeval *L. megadontos*, and higher than in *C. niloticus*, the large-sized extant specimen of our samples, which shows the largest optic lobes in relation to its brain. HUE-03713 has a very apparent low relative size of the optic lobes, probably due to the lateral compression of the endocast. As the eyesight capability in coeval and sympatric extant crocodyles is related to the photic conditions rather than to the prey selection (Nagloo et al., 2016), the similar visual acuity of *L. megadontos* and *A. fontisensis* may be due to similar environmental conditions.

The estimated REQs obtained for extant taxa (0.96-1.71) agree with the range suggested by Wharton (2002) for extant reptiles in general (REQ=0.4-2.4) and for gharials, the only crocodylian sample in her study (REQgharial=0.8-2) (Fig. 7). The REQ estimated for HUE-02502 is 0.91, similar to that of most of the large-sized specimens studied herein such as *C. niloticus* and *A. mississippiensis* (both REQs = 0.96), and higher than that of *L. megadontos* (REQ = 0.83). In contrast, the REQ estimated for HUE-03713 is 0.63, a value abnormally low, even more so than that found for *L. megadontos*, which has also suffered from taphonomical compression.

Conclusion

The holotype skull and one of the paratypes of *Agaresuchus fontisensis* have a endocranial morphology consistent with their size and their phylogenetic position as a basal eusuchian. The brain endocast shows several features considered plesiomorphies for Eusuchia, such as a flat dorsal outline of the caudal region of the cerebral hemispheres in lateral view, huge lateral expansions in the intertympanic diverticula, a posterior end of the dorsal alveolar canal separated from the olfactory region of the nasal cavity, and a ventral turn of the nasopharyngeal ducts. Other possible eusuchian plesiomorphies, such as a long and circular cross-section of the median pharyngeal sinus, cannot be asserted in these specimens. The median pharyngeal sinus is longer than those of the alligatoroids and gavialoids studied herein but does not reach the length found in crocodyloids and other allodaposuchids, such as *Lohuecosuchus megadontos*.

The infered neurosensorial capabilities of *A. fontisensis* are similar to those of other Crocodylia, including the sympatric and coeval allodaposuchid *L. megadontos*. The olfactory acuity of *A. fontisensis* is closer to that of alligatoroids, in which the olfactory ratio is slightly lower than those of crocodyloids. The visual acuity is close to the estimate for *L. megadontos*, which probably shared habitat with *A. fontisensis*. The encephalization quotient of *A. fontisensis*, which represents an estimate of its cognitive capabilities, is similar to that of the large-sized Crocodylia specimens studied herein.

Neurosensorial and morphological similarities between the inner skull cavities of *A. fontisensis* and *L. megadontos* are probably due to a combination of their phylogenetic proximity and the fact that both taxa shared the same habitat. More analyses with similar pairs of extant sympatric crocodylians, such as *Caiman yacare* and *Caiman latirostris*, could shed further light on the ecological and morphological relationships between these two allodaposuchids.

Acknowledgements

We are grateful to the staff of the Centro Médico de Diagnóstico (Talavera de la Reina), the Hospital Quirón Ruber (Madrid) and the Centro de Diagnóstico de Cuenca (Cuenca) for CT scanning the specimens analysed in this work. This article greatly

benefited from comments by D. Vidal. This is a contribution to research projects from the Ministerio de Economía, Industria y Competitividad, Spain [CGL2015-68363-P and CGL2017-89123-P] and from the Junta de Comunidades de Castilla-La Mancha, Spain [SBPLY/14180601/000074]. ASM is an FPU grantee [FPU13/03362] of the Ministerio de Educación, Cultura y Deporte (Spain). FK is an ARAID Senior Researcher.

5.3 UNASIGNED CRANIAL SAMPLES FROM LO HUECO

THE RELEVANCE OF THE MEDIAN PHARYNGEAL SINUS POSITION AND LENGTH IN THE TAXONOMIC ASSIGNATION OF BASAL EUSUCHIANS

Abstract

Crocodyliforms are one of the best represented vertebrate groups from the Late Cretaceous fossil site of Lo Hueco (Cuenca, Spain). These remains have been included into two different sympatric and synchronic species: *Lohuecosuchus megadontos* and *Agaresuchus fontisensis*. However, Lo Hueco fossil site also yielded several skulls similar to these two species, but not fitting completely in them. A set of three of indeterminate allodaposuchids from Lo Hueco was CT-scanned, and all their distinguishable inner cavities were three-dimensionally reconstructed, focusing in the ventral region of the pharyngotympanic sinus system, the best preserved structure. Our results suggest that these skulls belong to subadult specimens of *L. megadontos*, based on the relative development of their median pharyngeal sinus.

Introduction

The application of non-invasive tomographic techniques have significantly increased the neuroanatomical studies, previously restricted to the unusual appearances of casts of these internal structures due to resistant matrices, fortuitous breaks, sectioning with a saw, or latex endocasts (Witmer et al., 2008 and references therein). The CT technology allows obtaining a series of axial slices with the inner structure of the specimen. The X-ray scanner detects the differences in the density of the sample and represents them as a set of greyscale cuts (Goldman, 2007). Thus, applied to vertebrate fossils, the matrix infilling cavities can be distinguished from the mineralized tissues, if their densities are different enough. The first application of this technology to a fossil crocodyliform is attributed to Tykoski et al., (2002), and several fossil crocodylians

have been studied by those techniques since then (Brusatte et al., 2016; Bona et al., 2017; Pierce et al., 2017).

Inner skull cavities are considered conservative structures (Witmer and Ridgely, 2009; Knoll et al., 2012; Jirak and Janacek, 2017; Paulina-Carabajal and Filippi, 2017), and those of crocodyliforms follow the same pattern (Bona et al., 2017; Serrano-Martínez et al., in press). Despite its conservativeness, median pharyngeal sinus (mps) is remarkable for being one of the most changing inner skull cavities in eusuchians, suffering a verticalization process during the ontogeny (Tarsitano, 1985, 1989; Gold et al., 2014; Dufeau and Witmer, 2015). In adult eusuchians, the posterior part of the pterygoid, basisphenoid and basioccipital are ventrally elongated, increasing the height of the skull and modifying the angle of application of the jaw adductor muscles and the structure of the median pharyngeal sinus (Tarsitano, 1985, 1989). At hatchling, eusuchians have a flat braincase floor, being the median pharyngeal sinus a difuse caudorostrally oriented canal. During the first years of life, the basisphenoid grows upward, and the median pharyngeal sinus becomes a vertical canal (Tarsitano, 1985, 1989; Dufeau and Witmer, 2015). However, the median pharyngeal sinus verticalization process seems to have different development in the eusuchian lineages. Gavialoids seems to retain the primitive condition, showing a short median pharyngeal sinus (Brochu, 2004; Gold et al., 2014). Dufeau and Witmer, (2015) noticed that the verticalization in *Alligator mississippiensis* is not as marked as in *Tomistoma schlegelii* (considering it as a crocodyloid). In the morphospace proposed by Gold et al., (2014), alligatoroids tend to have shorter median pharyngeal sinuses than crocodyloids. (Serrano-Martínez et al., in press) also described this pattern. The dorsal and ventral regions from the join of the basisphenoid diverticula were compared. The ventral part of the median pharyngeal sinus in alligatoroids has a relative length always less than 75%, measured in *A. mississippiensis*, the larger alligatoroid studied. On the other hand, the relative length of the ventral part of the median pharyngeal sinus of the crocodyloids studied is, at least, three times longer than the dorsal part.

The comparison with members of the stem-group is key to understand the variation of the inner skull cavities in Crocodylia. Basal eusuchians, specifically allodaposuchids, are one of the best represented groups in the Late Cretaceous fossil site of Lo Hueco (Cuenca, Spain). Several skulls and postcranial remains from there have already been described (Narváez et al., 2015, 2016; de Celis et al., 2018), and were

classified into three different morphotypes. Two of them have been published as the new species *Lohuecosuchus megadontos* and *Agaresuchus fontisensis*. The skulls of these species were also digitally rendered, and its inner skull cavities reconstructed (Serrano-Martínez et al., 2018). The inner skull cavities of *L. megadontos* and *A. fontisensis* are very similar, showing a combination of Eusuchian plesiomorphyes and allodaposuchid apomorphyes. The third morphotype shows several but not all the morphological characters described for *L. megadontos*, being preliminarly considered as sexual dimorphism or ontogenetic variation of *Lohuecosuchus megadontos*.

The aim of this work is to complete the neuroanatomical studies of the specimens of allodaposuchids from Lo Hueco, analyzing the inner cavities of three preserved skulls from the third morphotype of skull from Lo Hueco. The reconstruction of the endocranial elements of this species allows comparing them to extant and extinct representatives of the eusuchian lineage, including *Lohuecosuchus megadontos* and *Agaresuchus fontisensis*, the other allodaposuchids from Lo Hueco.

Material and methods

Lo Hueco fossil site has yielded at least a dozen of almost complete skulls of eusuchians. The first analyses of this sample have allowed identifying two taxa of allodaposuchids: *Lohuecosuchus megadontos* and *Agaresuchus fontisensis*. However, there are some specimens whose characters difficult to assign them to one of these species.

Three of these skulls, housed in the collection of the Museo de Paleontología de Castilla-La Mancha (MuPaCLM, Cuenca, Spain), are included in the present study. A preliminary morphological analysis allows identifying them as possible representatives of *Lohuecosuchus megadontos*.

HUE-02018 (Fig. 5.3.1A and B) is a well preserved skull, lacking pterygoid wings and part of ectopterygoids. The snout is anteriorly narrow, describing an outline of skull slightly more elongate than the specimens assigned to *Lohuecosuchus megadontos*. Despite this, this specimen presents some characters shared with this species, such as a wider than long naris, a low number of alveoli in the maxillae (eleven in the left branch), with robust and hypertrophied teeth, closely spaced alveoli and narrow

interalveolar spaces; or a teardrop-shaped choana. In addition, it is possible that the maxillae bear a pair of parasagittal foramina placed in the palatal shelf, but they are collapsed. In the present analysis, the caudal half of HUE-02018 was scanned in a Sinus 1.25 H80s, with a voltage of 130kV and a current of 68 mA. The inter-slice spacing was 1.25mm.

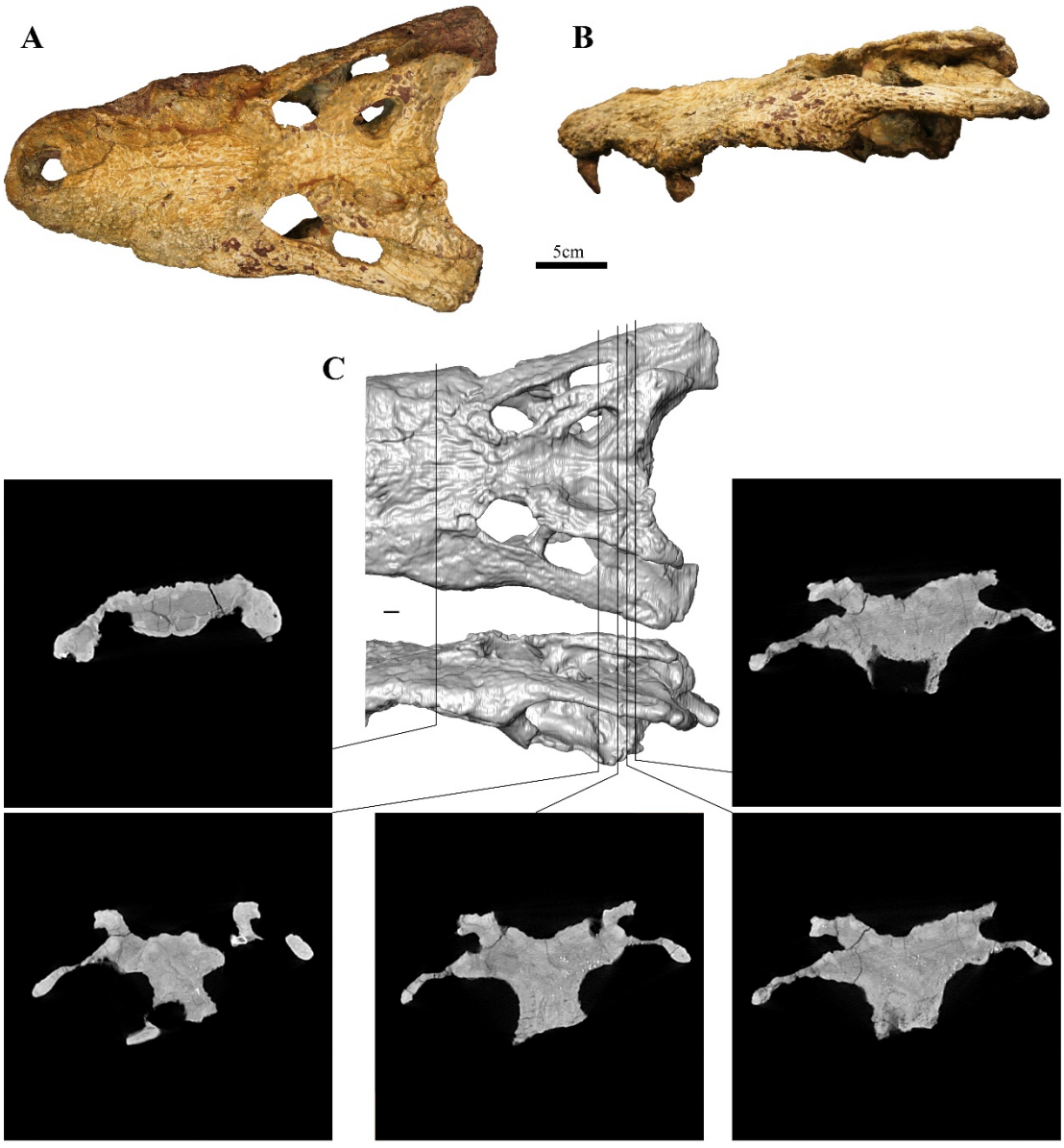

Fig. 5.3.1: Skull of HUE-02018. **A**: dorsal view of the skull. **B**: left lateral view of the skull. **C**: dorsal and left lateral views of the digital reconstruction of HUE-02018, with a series of axial slices at different levels. Scale bar equals 5cm.

HUE-02815 (Fig. 5.3.2A-D) is a nearly complete skull, with flattened skull table. Most of the braincase bones are damaged, lacking the right orbit, both jugals and quadratojugals, left quadrate and part of the left pterygoid wing. The left orbit is complete, and it is rounded with a broad postorbital bar. This specimen bears ten alveoli in the right maxillary branch and eleven in the left one. The preserved teeth are hypertrophied and close between them. The naris is wider than long and the choana has a teardrop-shaped. The specimen was scanned with an YxlonY.TU 450-D09, with a voltage of 400kV and a current of 3.75mA, and an inter-slice spacing was 0.3mm; and with a Toshiba Asteion, with a voltage of 135kV and a current of 75 mA, with an inter-slice spacing was 2mm.

HUE-08881 (Fig. 5.3.3A and B) is a nearly complete skull, lacking some regions of both jugals and quadratojugals, right postorbital, right squamosal, and pterygoid wings. This specimen has a short and broad rostrum, with a naris wider than long. Only left maxillary branch can be observed, and it has a tooth row composed by a low number of alveoli (eleven), very close between them. This specimen was scanned with an Optima CT600, with a voltage of 120kV and a current of 1 mA. The inter-slice spacing was 0.625mm.

The scan data of the three specimens were imported to ImageJ 1.49b (National Institutes of Health, USA) for artefact removal and optimizing the contrast and then into Avizo 7.1.0 (VSG, Burlington, MA, USA) for segmentation, visualization and analysis.

These reconstructions were compared to those of several reconstructions of the inner skull cavities of extant and extinct eusuchians, including the alligatoroids *Aligator mississippiensis*, *Melanosuchus niger*, *Caiman crocodilus* and the extinct *Diplocynodon tormis*; the crocodyloids *Crocodylus niloticus*, *Crocodylus moreletii*, *Osteolaemus tetraspis* and the phylogenetically conflictive *Tomistoma schlegelii*; and the gavialoid *Gavialis gangeticus*. Holotypes of the allodaposuchids *Lohuecosuchus megadontos* (HUE- 004498) and *Agaresuchus fontisensis* (HUE-02502) were also included.

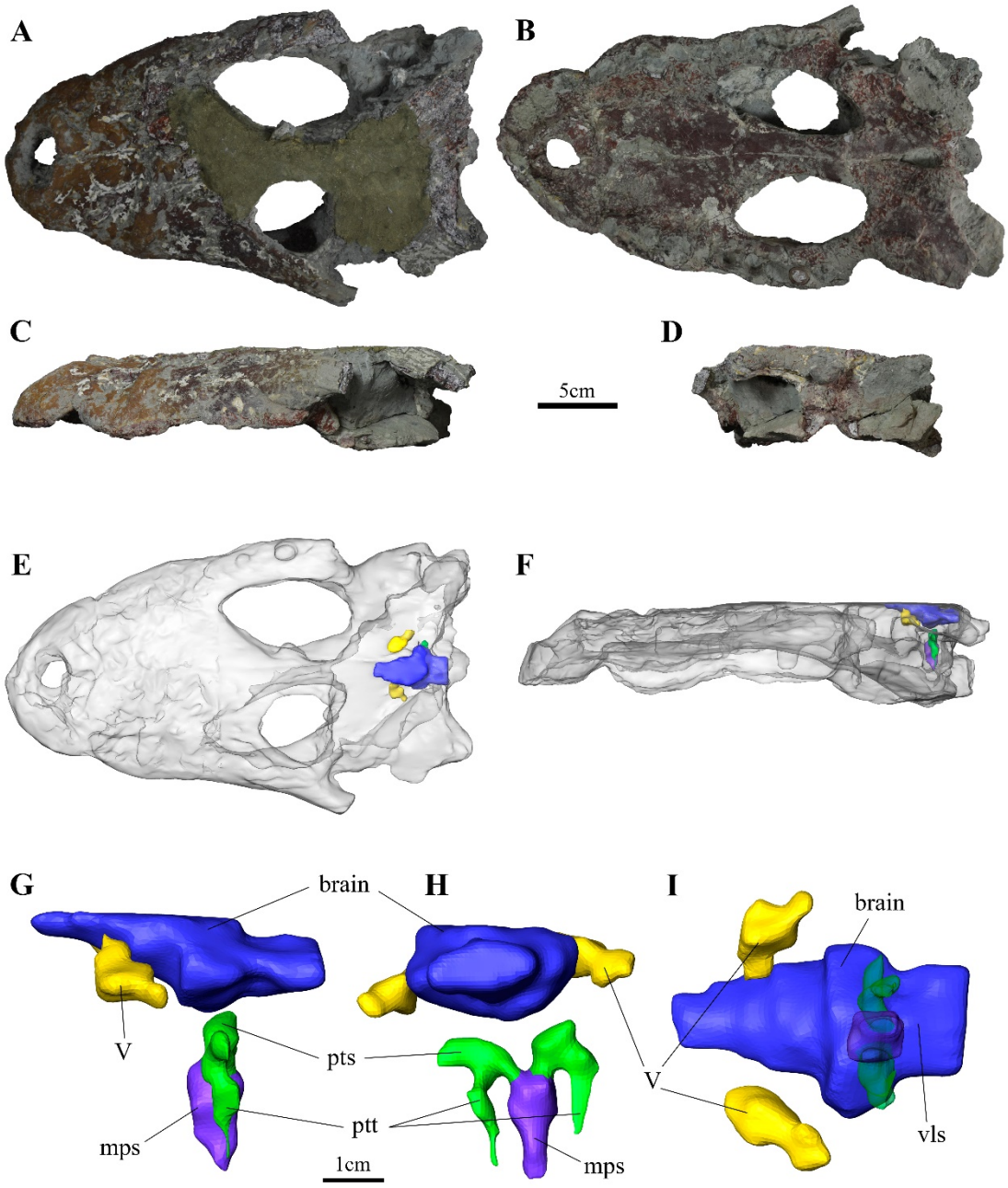

Fig. 5.3.2: Skull of HUE-02815. **A**: dorsal; **B**: ventral; **C**: left lateral; **D**: caudal views of the skull. Scale bar equals 5cm. **E**: dorsal; **F**: left lateral views of the digital reconstruction of HUE-02815, with the bones rendered transparent to visualize the inner cavities. **G**: left lateral; **H**: caudal; **I**: ventral views of the inner skull cavities of HUE-02815, including the caudoventral part of the brain, and the ventral region of the pharyngotympanic sinus system. **Abbreviations**: **mps**: median pharyngeal sinus; **pts**: pharyngotympanic sinus; **ptt**: pharyngotympanic tubes; **vls**: ventral longitudinal sinus; **V**: trigeminal nerve. Scale bar equals 1cm.

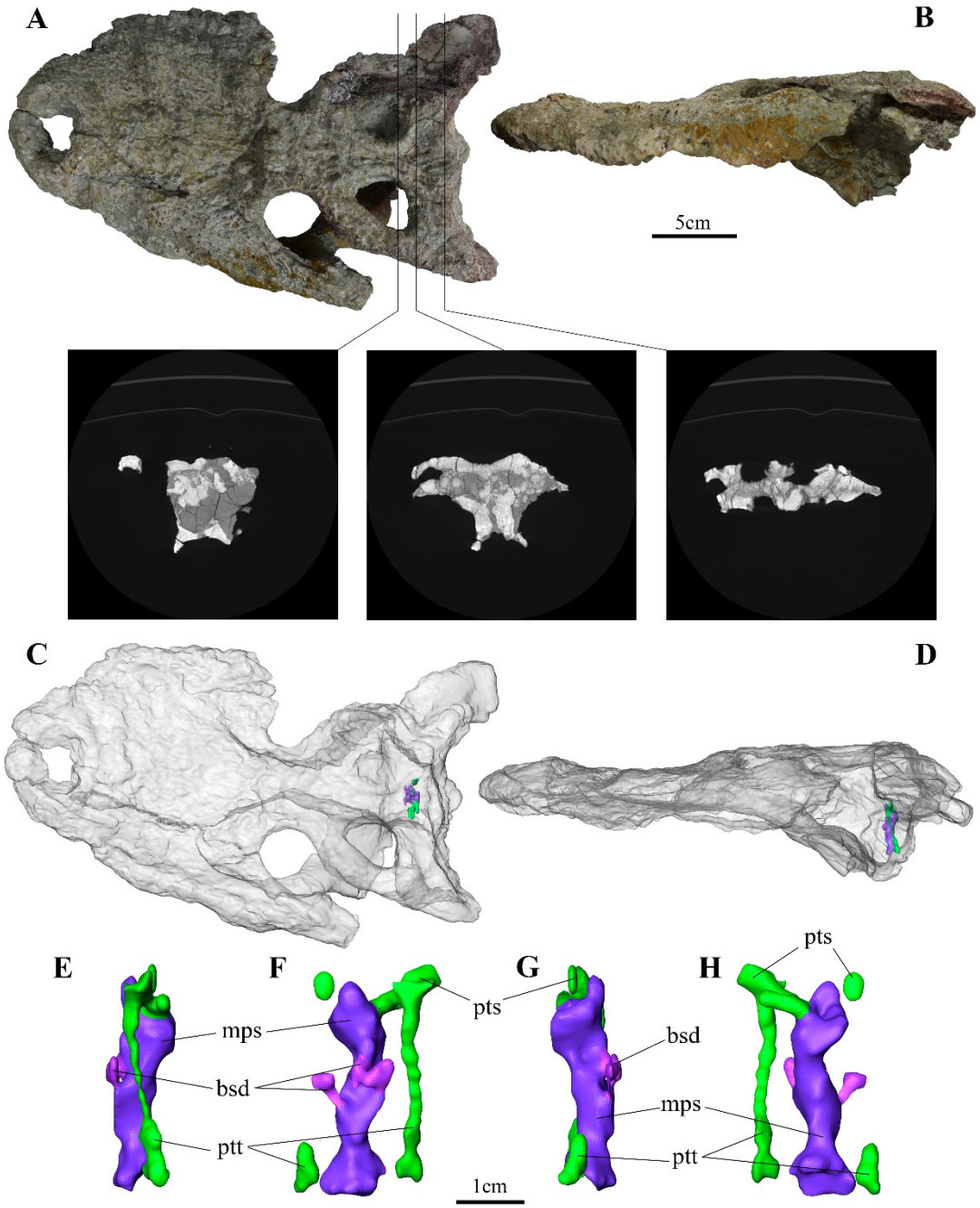

Fig. 5.3.3: Skull of HUE-08881. **A**: dorsal; **B**: left lateral views of the skull, with a series of axial slices at different levels. Scale bar equals 5cm. **C**: dorsal; **D**: left lateral views of the digital reconstruction of HUE-02815, with the bones rendered transparent to visualize the inner cavities. **E**: left lateral; **F**: rostral; **G**: right lateral; **H**: caudal views of the inner skull cavities of HUE-08881, including the ventral region of the pharyngotympanic sinus system. **Abbreviations**: **bsd**: basisphenoid diverticula; **mps**: median pharyngeal sinus; **pts**: pharyngotympanic sinus; **ptt**: pharyngotympanic tubes. Scale bar equals 1cm.

Results

HUE-02018 CT-data has an extremely low contrast between the fossilized bone and the infilling matrix (Fig. 5.3.1C). This fact made impossible to distinguish any braincase inner structure, and only the anterior region of the nasal passageway is slightly visible in some of the slices, although its boundaries are difficult to identify.

The breakage of the braincase dorsal bones only allows reconstructing part of the brain of HUE-02815 (Fig. 5.3.2E-I). The presence of a large pair of nerves, probably the trigeminal (V) pair, locates the anteriormost part of the reconstruction at the level of the hindbrain. Therefore, olfactory bulbs, olfactory tract, cerebral hemispheres and optic lobe are missing. The metencephalon, located at the dorsal part of the hindbrain between both otic capsules, is also missing, as well as the inner ear. The myelencephalon seems to be dorsoventrally compressed and still preserves the ventral longitudinal sinus. The ventral region of the pharyngotympanic sinus system is preserved too, although the contrast between the fossilized bone and the infilling matrix is also low. The ventral part of the pharyngotympanic sinuses, and the pharyngotympanic tubes and the median pharyngeal sinus could be reconstructed. The only preserved parts of the pharyngotympanic sinuses are two ventromedially oriented canals. From them, emerge the pharyngotympanic tubes, two ventrally oriented flat canals opening to the pharynx (Fig. 5.3.2H). Both pharyngotympanic sinuses merge ventrally to the brain in the median pharyngeal sinus. It is a short ventrally oriented canal located between both pharyngotympanic tubes that opens to the pharynx.

HUE-08881 CT-data has a relatively good contrast between the fossilized bone and the infilling matrix. However, the inner braincase cavities seem to be collapsed, and there is not any visible pattern to render the brain and its associated structures (Fig. 5.3.3A). On the other hand, the ventral region of the pharyngotympanic sinus system has preserved mostly intact. The ventral part of the pharyngotympanic sinus, and the pharyngotympanic tubes, the median pharyngeal sinus and the basisphenoid diverticula were recognized (Fig. 5.3.3C-H). The left pharyngotympanic tube was fully distinguished, but only the ventralmost part of the right one could be reconstructed. They are ventrally oriented thin canals, as seen in HUE-02815. The median pharyngeal sinus is rostroventrally oriented first, slightly turning caudoventrally to opens between the basisphenoid and the basioccipital. The basisphenoid diverticula emerge from the

median pharyngeal sinus at the level of the caudoventral turn. Both diverticula are laterodorsally oriented, but the left one also projects medially to connect with the median pharyngeal sinus.

Discussion

HUE-02018, HUE-02815 and HUE-08881 share several but not all the characters described as Lohuecosuchus synapomorphies, such as the hypertrophied and close between them teeth. The lower size of the three skulls (Table 5.3.1), the absence of the broad rostrum in HUE-02018 and HUE-02815 and the absence of the angular maxillary-palatine suture in HUE-02815 could be interpreted as ontogeny or sexual variability from the type specimens of *Lohuecosuchus megadontos*.

Specimen	Skull length (mm)
L. megadontos holotype (HUE-04498)	333.42
L. megadontos paratype (HUE-02920)	339.02
L. megadontos paratype (HUE-04263)	318.75
A. fontisensis holotype (HUE-02502)	327.30
A. fontisensis paratype (HUE-03713)	358.93
HUE-02815	296.90
HUE-08881	280.38

Table 5.3.1: Skull length of the samples here studied, in mm.

The length of the median pharyngeal sinus differs between the major crocodylian groups (Serrano-Martínez et al., in press). Gold et al. (2014) generate a morphospace basing one of the axis on the length of the median pharyngeal sinus. In that morphospace, alligatoroids and crocodyloids overlap, althought alligatoroids are concentrated in the “short ventral mps” part, while crocodyloids have a wider range slightly displaced to the “long ventral mps” part. These overlapping, with crocodyloids having a longer mps than alligatoroids, agree with the observed for the extant crocodylian specimens here studied (Table 5.3.2 and Fig. 5.3.4). Gharials are located between both groups, but closer to alligatoroids, as seen in Gold et al., (2014). The

allodaposuchid pattern seems to be closer to the crocodyloid one. *Lohuecosuchus megadontos* has a very long ventral mps, only exceeded by that of *Crocodylus niloticus*. *Agaresuchus fontisensis* has shorter ventral mps, but it is still longer than that of all alligatoroids studied.

Taxon	mps lenght	brain lenght	Relative mps lenght	Dorsal mps lenght	Ventral mps lenght	Dorsal/ventral ratio
A. mississippiensis	27.05	101.76	0.27	13.41	21.09	1.57
C. crocodilus	10.38	54.14	0.19	6.16	6.62	1.07
M. niger	16.75	101.18	0.17	8.04	11.74	1.46
C. niloticus	31.82	101.90	0.31	6.62	29.24	4.42
C. moreleti	17.45	80.92	0.22	8.62	11.13	1.29
O. tetraspis	24.40	76.98	0.32	8.85	25.65	2.90
T. schlegelii	119.02	603.90	0.20	58.21	94.57	1.62
G. gangeticus	16.78	134.86	0.12	9.23	15.68	1.70
D. tormis	15.47	67.54	0.23	8.64	10.31	1.19
A. fontisensis HUE-02502	20.41	110.01	0.19	8.59	16.79	1.95
L. megadontos HUE-04498	54.43	122.44	0.44	11.10	48.25	4.35
HUE-08881	-	-	-	20.03	22.40	1.12

Table 5.3.2: Comparison of the median pharyngeal sinus measurements of the samples studied, in mm.

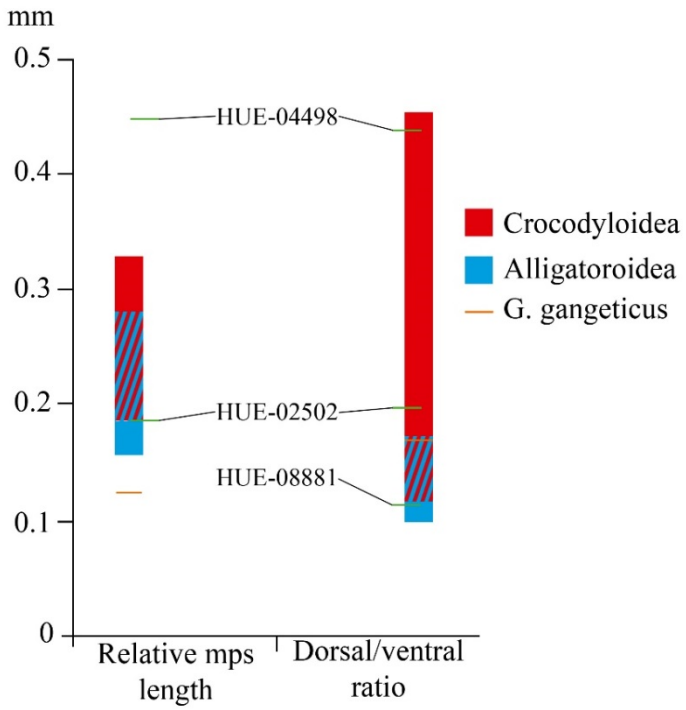

Fig. 5.3.4: Graphic with the results given in Table 5.3.2. Relative median pharyngeal sinus length and dorsal/ventral ratio of the samples here studied.

The relative length of the mps is the relation between the dorsal and the ventral part from the join of the basisphenoid diverticula. In this way, only HUE-08881, the only one that preserves the basisphenoid diverticula, could be included in the analysis. HUE-08881 has a short relative length of the ventral part of the mps, close to the alligatoroid with the shortest ventral mps, *Caiman crocodilus*. Although HUE-02815 lacks the basisphenoid diverticula, its mps is similar in size to that of HUE-08881.

In the ontogenical series of Aligator mississippiensis described by Dufeau and Witmer, (2015), mps elongates during the ontogeny. Thus, the presence of shorter mps in HUE-02815 and HUE-08881, two similar, synchronic and sympatric specimens of *Lohuecosuchus megadontos*, could be interpreted as they belong to a subadult *L. megadontos*, whose median pharyngeal sinus is not completely developed.

However, the lack of cuantitative data of HUE-02815, due to the brain is incomplete and the basisphenoid diverticula could not be reconstructed, makes its assignation as a subadult *L. megadontos* must be taken with caution.

Conclusion

The CT-scans performed on HUE-02018, HUE-02815 and HUE-08881 have not sufficient resolution to perform a complete analysis of their inner skull cavities. However, the ventral sections of the basicranium are distinguishable enough to render the ventral part of the pharyngotympanic sinus system of HUE-02815 and HUE-08881. Both median pharyngeal sinuses are short, in contrast to the condition showed by the phylogenetically related *Lohuecosuchus megadontos* and *Agaresuchus fontisensis*. HUE-02815 and HUE-08881 share several characters with those described for *L. megadontos*, but they are smaller than the type specimens. The elongation of the median pharyngeal sinus during the ontogeny in eusuchians makes plausible the assignation of HUE-02815 and HUE-08881 to subadult *L. megadontos*.

Acknowledgements

We are grateful to the staff of the Centro Médico de Diagnóstico (Talavera de la Reina), the Centro de Diagnóstico Cuenca (Cuenca) and the Hospital Quirón Ruber (Madrid) for CT scanning many of the specimens analysed in this work.

This is a contribution to a research project from the Ministerio de Economía, Industria y Competitividad, Spain [CGL2015-68363-P] and from the Junta de Comunidades de Castilla-La Mancha, Spain [DGCLM/140565]. ASM is an FPU grantee [FPU13/03362] of the Ministerio de Educación, Cultura y Deporte (Spain). FK is an ARAID Senior Researcher.

TERCERA PARTE

THIRD PART

CAPÍTULO 6: DISCUSIÓN GENERAL

GENERAL DISCUSSION

DISCUSIÓN GENERAL

Mediante la consecución de los objetivos planteados en esta tesis doctoral se han obtenido una serie de resultados de gran relevancia para el estudio de la evolución de las cavidades intracraneanas y de las capacidades neurosensoriales y cognitivas de los miembros de Crocodylia, enfocado desde la interpretación de las cavidades intracraneanas de los eusuquios basales hallados en el yacimiento de Lo Hueco.

Se discuten los resultados que permiten abordar el objetivo principal de esta tesis doctoral consistente en el análisis de la evolución de las cavidades intracraneanas y de las capacidades neurosensoriales y cognitivas de los miembros de Crocodylia desde la perspectiva de la interpretación de las cavidades intracraneanas de los eusuquios basales hallados en el yacimiento de Lo Hueco.

Como parte del proceso de análisis de las cavidades intracraneanas de los eusuquios de Lo Hueco se ha procedido a realizar un análisis exhaustivo de las cavidades de los miembros que componen el grupo corona. En este sentido, se han reconstruido y analizado las cavidades intracraneanas de representantes de los distintos linajes de cocodrilos actuales. Así, en la presente tesis doctoral se han reconstruido y estudiado los cráneos de los aligatoroideos *Alligator mississippiensis*, *Caiman crocodilus* y *Melanosuchus niger*; los crocodiloideos *Crocodylus niloticus, Crocodylus moreletii, Osteolaemus tetraspis* y *Tomistoma schlegelii*; y el gavialoideo *Gavialis gangeticus* (Capítulo 4.1). A estas reconstrucciones se ha añadido la información disponible de *Crocodylus johnstoni* (Witmer et al., 2008). Para completar la base de datos, se han incluido también las reconstrucciones de varios Crocodylia extintos, como la del aligatoroideo basal *Diplocynodon tormis*, del Eoceno medio de Salamanca (Capítulo 4.2), del aligatoroideo caimanino *Mourasuchus nativus* (Bona et al., 2013) y el gavialoideo *Gryposuchus neogaeus* (Bona et al., 2017), ambos del Mioceno de Argentina.

Se han identificado diferencias morfológicas en las cavidades intracraneanas de la muestra, aunque algunas parecen estar más relacionadas más con el tamaño de los especímenes que con una señal filogenética. Atendiendo al estudio ontogenético de Dufeau and Witmer, (2015), se han dividido los ejemplares de la muestra en aquellos con tamaño medio (subadulto sensu Dufeau and Witmer, 2015) y aquellos de gran

tamaño (adulto sensu Dufeau and Witmer, 2015). Así, *C. crocodilus*, *M. niger*, y *O. tetraspis*, cuyo cráneo no alcanza los 30cm de longitud, presentan un ángulo cercano a los 90º en la transición entre el canal olfatorio y los hemisferios cerebrales en vista dorsal, hemisferios cerebrales con morfología semiesférica y unas columnas parietales anchas. Por otro lado, los ejemplares de más de 30cm, incluyendo *A. mississippiensis*, *C. niloticus*, *T. schlegelii* y *G. gangeticus* presentan una transición más suave entre el canal olfatorio y el cerebro, unos hemisferios cerebrales con morfología cónica, y unas columnas parietales muy finas (Capítulo 4.2.1).

No obstante, se han identificado una serie de caracteres que parecen ajustarse a las propuestas filogenéticas más consensuadas del grupo (Fig. 2.1. Brochu, 1999, 2011). El encéfalo de los crocodilios es rostrocaudalmente alargado, con largos canales olfativos y una morfología sigmoidal en vista lateral (Colbert, 1946; Witmer et al., 2008; Bona et al., 2013; Dufeau and Witmer, 2015; Brusatte et al., 2016; Pierce et al., 2017; Capítulo 5.1). Los hemisferios cerebrales forman sendos abultamientos laterales en vista dorsal, sobresaliendo del perfil del encéfalo de forma muy evidente (Witmer et al., 2008; Bona et al., 2013; Brusatte et al., 2016; Capítulo 4.1). La fosa hipofisaria, localizada en la región caudoventral del cerebro, está orientada caudoventralmente (Witmer et al., 2008; Bona et al., 2013; Dufeau and Witmer, 2015; Brusatte et al., 2016; Pierce et al., 2017; Capítulo 5.1). El oído interno de los crocodilios se asemeja al del resto de arcosaurios, siendo el canal semicircular anterior el mayor de todos. Además, en crocodilios este canal semicircular está alargado dorsalmente, mientras que en crocodilomorfos basales, el canal anterior y el posterior alcanzan una longitud dorsoventral similar (Brusatte et al., 2016; Pierce et al., 2017; Capítulo 4.1). Los miembros de Crocodylia también se caracterizan por tener un basicráneo muy pneumatizado, con un gran desarrollo del sistema de senos faringotimpánicos. En el marco del desarrollo de estas cavidades, destaca la aparición de los divertículos intertimpánicos como una cavidad dorsomedial que une los dos senos faringotimpánicos (Bona et al., 2013, 2017; Capítulo 5.1).

Profundizando dentro de Crocodylia, la región posterodorsal del cerebro de crocodiloideos y gavialoideos es plana, mientras que la de los aligatoroideos presenta una convexidad de tamaño variable (Storrs et al., 1983; Capítulo 4.2.1). El desarrollo de los divertículos intertimpánicos también es diferentente en cada uno de los grandes linajes de Crocodylia. En aligatoroideos, la región central de dicha cavidad, localizada entre las dos columnas parietales, está más desarrollada que las regiones laterales. Sin

embargo, en crocodiloideos y gavialoideos, las regiones laterales son más grandes que la región central (Capítulo 4.2.1). Los eusuquios se caracterizan por un proceso de verticalización del basicráneo consistente en un desplazamiento ventral del basioccipital, basiesfenoides y pterigoides, modificando el ángulo de inserción de los músculos de la mandíbula, la orientación del cuadrado, y la forma de las cavidades contenidas en estos huesos: el canal nasofaríngeo y el seno faríngeo medio (Tarsitano, 1985, 1989). Sin embargo, este proceso afecta de forma distinta a las cavidades contenidas en estos huesos, haciendo que la longitud y morfología del seno faríngeo medio varíe en función de la ontogenia (Dufeau and Witmer, 2015) y del linaje (Gold et al., 2014; Capítulos 4.2.1, 5.1, 5.2 y 5.3). Así, los crocodiloideos tienden a mantener constante la estructura del seno faringotimpánico y de la región dorsal del seno faríngeo medio (la región dorsal a la conexión con los divertículos basiesfenoideos), siendo la parte ventral de este último la más afectada por la elongación ventral del basicráneo (que es entre 3 y 4 veces más largo que la región dorsal). Por otro lado, en los aligatoroideos, el desplazamiento de estos huesos afecta de forma similar a la región ventral del seno faringotimpánico y a ambas regiones del seno faríngeo medio, siendo la longitud de estas dos últimas subiguales (la región ventral es entre 1 y 1.5 veces más larga que la dorsal). La longitud relativa del seno faríngeo medio de los gavialoideos tiene una estructura intermedia, aunque está más próxima a la observada en los aligatoroideos (Gold et al., 2014; Capítulos 5.1, 5.2 y 5.3).

T. schlegelii, un cocodrilo de posición filogenética discutida (Meganathan et al., 2010; Brochu, 2011), presenta una longitud ventral a la cavidad basiesfenoidea no tan elevada como el resto de crocodiloideos, sigue siendo mayor que la mostrada por cualquiera de los aligatoroideos, y similar a la observada para *G. gangeticus*. Esto puede deberse a similitud filogenética, o a un grado de desarrollo ontogenético aún temprano.

El sistema de senos paranasales también es diferente en los distintos linajes de Crocodylia. En los aligatoroideos, como *C. crocodilus* y, de forma menos evidente, en *A. mississippiensis*, y en el gavialoideo *G. gangeticus*, la región caudal del canal dorsal alveolar desemboca en la parte dorsal de la región olfatoria de la cavidad nasal. En cambio, en crocodiloideos, el canal dorsal alveolar se ensancha formando una gran cavidad lateral a la región olfatoria de la cavidad nasal (Capítulos 5.1 y 5.2).

La estimación de las capacidades neurosensoriales y cognitivas a partir de las reconstrucciones de las cavidades intracraneanas de los ejemplares actuales de Crocodylia coincide con los resultados obtenidos en estudios etológicos y anatómicos de estos animales. La agudeza olfativa de los cocodrilos ha sido abordada en estudios como los de Weldon y Ferguson, (1993), Weldon et al., (1990) o Grigg and Kirshner, (2015). Darla Zelenitzsky, en sus análisis de la capacidad olfativa en aves y dinosaurios no avianos (Zelenitsky et al., 2009, 2011), relacionó el tamaño del lóbulo olfativo y la agudeza olfativa, proponiendo una serie de fórmulas para estimar la agudeza olfativa a partir de medidas lineales de las cavidades intracraneanas, en los que incluyó algunos ejemplares de *A. mississippiensis* (Zelenitsky et al., 2009 y referencias). En este estudio puede observarse el elevado grado de desarrollo del lóbulo olfativo de *A. mississippiensis* en comparación con el resto de arcosaurios. Analizando varios especímenes de Crocodylia, las capacidades olfativas son similares a las descritas por Zelenitsky et al., (09) para *A. mississippiensis*, mostrando además una correlación en función de su posición filogenética (Capítulos 5.1 y 5.2). Aunque la diferencia es ligera, los miembros de Crocodyloidea presentan un mayor desarrollo relativo del lóbulo olfativo que los aligatoroideos y gavialoideos, independientemente de su tamaño (Tablas 5.1.1 y 5.2.1).

Por otro lado, los cocodrilos poseen una alta capacidad auditiva, tanto dentro como fuera del agua, con estructuras específicas para optimizar la localización del sonido (Dufeau and Witmer, 2015; Grigg and Kirshner, 2015). En los reptiles, las capacidades auditivas pueden estimarse a partir de una serie de medidas craneales, incluyendo la longitud del conducto coclear, el órgano encargado de la audición en estos animales (Walsh et al., 2009). La cóclea de los cocodrilos es corta en relación al resto del cráneo (Fig. 2 de Walsh et al., 2009; Tabla 5.1.2), situándose su rango auditivo en una región de bajas frecuencias, lo que concuerda con los estudios etológicos (Vergne et al., 2009). La capacidad auditiva parece estar más relacionada con el tamaño de los individuos que con la posición filogenética, teniendo los ejemplares de tamaño medio una longitud coclear relativa mayor que la de los de gran tamaño (Tabla 5.1.2) adaptándose así el oído a menores frecuencias cuanto más grande es el animal.

La agudeza visual de los cocodrilos es también es elevada (Grigg and Kirshner, 2015; Nagloo et al., 2016). Generalmente se considera que la visión está relacionada con el tamaño del globo ocular (Hall, 2008, 2009 y referencias), pero no se dispone de

estudios de correlación entre el tamaño del ojo y el de la órbita u otra estructura que permita estimar la capacidad visual a partir de restos esqueléticos en cocodrilos. Atendiendo a que el lóbulo óptico de los cocodrilos es fácilmente distinguibles (Jirak and Janacek, 2017) se ha utilizado su volumen como aproximación a las capacidades visuales, lo que ya ha sido utilizado en aves (Martin et al., 2007; Torres and Clarke, 2018). En este caso, los individuos de gran tamaño tienen un volumen relativo del lóbulo óptico ligeramente menor que los de tamaño medio (Tabla 5.1.3), lo que implicaría una menor agudeza visual.

Finalmente, las capacidades cognitivas de estos animales, al igual que las del resto de reptiles no avianos, son substancialmente inferiores a las mostradas por mamíferos y aves (Jerison, 1969, 1973; Grigg and Kirshner, 2015). Hurlburt, (1996) propuso un método para comparar los coeficientes de encefalización de mamíferos, aves y reptiles. Así, el REQ (Reptile Encephalization Quotient) incluye a los quelonios, lepidosaurios y cocodrilos, situándolos en un rango entre 0.4 y 2.4. Específicamente, el REQ de los cocodrilos se sitúa en un punto intermedio, entre 0.9 y 1.5 (Hurlburt, 1996; Capítulo 4.2.2 Tabla 4.2.2.3). Entre los cocodrilos el cociente de encefalización muestra una mayor relación con el tamaño de los individuos que con su posición filogenética, situándose los de gran tamaño (REQ≈1) por debajo de los de tamaño medio (REQ≈1.65).

Las cavidades intracraneanas de *Diplocynodon tormis* son similares a las descritas para los crocodilios de tamaño medio, el grupo que le corresponde por tamaño, con un ángulo casi recto en la transición entre el canal olfatorio y los hemisferios cerebrales, hemisferios cerebrales semiesféricos y unas columnas parietales anchas.

D. tormis presenta varios de los caracteres atribuidos a las cavidades intracraneanas de los aligatoroideos, como un mayor desarrollo de la sección central de los divertículos intertimpánicos respecto a las regiones laterales, y una longitud ventral del seno faríngeo medio subigual a la longitud dorsal. Sin embargo, la superficie caudodorsal de sus hemisferios cerebrales es plana, al igual que se observa en crocodiloideos y gavialoideos. Por tanto, la aparición de la convexidad en la superficie caudodorsal del cerebro, ya descrita por Storrs et al., (1983), podría considerarse una autapomorfía adquirida por los miembros más derivados del linaje Alligatoroidea. La

combinación de caracteres de *D. tormis* es congruente con su posición filogenética como un aligatoroideo basal externo al grupo corona Alligatoridae (Fig. 2.1).

El ejemplar estudiado de *D. tormis* presenta algunas fracturas que impiden realizar con precisión algunas de las medidas volumétricas requeridas para los análisis de las capacidades neurosensoriales y cognitivas, distorsionando ligeramente los resultados. La agudeza olfativa estimada para *D. tormis* se localiza en el intervalo estimado para el resto de aligatoroideos estudiados, lo que refuerza la hipótesis de que el tamaño relativo del lóbulo olfatorio está más relacionado con la posición filogenética que con el tamaño de los individuos. El volumen relativo de los lóbulos ópticos de *D. tormis* también coincide con el calculado para el resto de crocodilios, siendo ligeramente mayor que los de los ejemplares de gran tamaño, pero sin llegar a alcanzar los de los ejemplares de tamaño medio, el rango de tamaño que le corresponde. Este mismo patrón se observa al calcular el cociente de encefalización de *D. tormis*. Si bien el REQ coincide con el rango calculado para el resto de crocodilios, es también inferior al mostrado por los ejemplares de tamaño medio.

Atendiendo a los objetivos 3, 4 y 5 de esta tesis, se han analizado representantes de Allodaposuchidae (Eusuchia no Crocodylia) de Lo Hueco, incluyendo el holotipo de *Lohuecosuchus megadontos* (HUE-04498), el holotipo y uno de los paratipos de *Agaresuchus fontisensis* (HUE-02502 y HUE-03713), y tres ejemplares del tercer morfotipo craneal de Lo Hueco (HUE-02018, HUE-02815 y HUE-08881). Las reconstrucciones de las cavidades intracraneanas de estos cocodrilos han permitido establecer la morfología general de estas cavidades en Allodaposuchidae. La mayoría de los caracteres reconocidos en los ejemplares de Lo Hueco se han interpretado previamente como sinapomorfías de Crocodylia (Capítulos 4.1 y 4.2.1). Por tanto, la presencia de un encéfalo con morfología sigmoidal en vista lateral, una superficie dorsal aplanada de los hemisferios cerebrales en vista lateral, un canal semicircular anterior alargado dorsalmente, un mayor desarrollo de las regiones laterales de los divertículos intertimpánicos con respecto a la región central, un seno faríngeo medio largo y de sección circular y una región caudal del canal alveolar dorsal amplio y alejado de la región olfativa de la cavidad nasal deberían ser considerados como sinapomorfías del clado Eusuchia en vez de sinapomorfías de Crocodylia.

Los conductos nasofaríngeos de los alodaposúquidos analizados están curvados ventralmente de forma gradual mientras que en los crocodilios estudiados se curvan ventralmente en un ángulo cerrado de 90 grados. Entre los crocodilomorfos no-eusuquios la morfología de esta estructura únicamente se conoce en los talatosuquios *Cricosaurus araucacensis* (Herrera et al., 2013b) y *Pelagosaurus typus* (Pierce et al., 2017). En ambos ejemplares, el canal nasofaríngeo está orientado rostrocaudalmente en toda su extensión, saliendo del cráneo a la faringe en una posición rostral a la fosa hipofisiaria. Los talatosuquios son un grupo de mesoeucrocodilios cuya posición filogenética es controvertida y que presentan una morfología craneal, y por lo tanto intracraneal muy diferente a la observada en el grupo corona (Fernández et al., 2011; Herrera et al., 2013b, 2018; Brusatte et al., 2016; Pierce et al., 2017). Por tanto, es necesario el análisis de algunos taxones cercanos a Eusuchia para comprobar si los caracteres aquí descritos suponen una serie de novedades evolutivas de Eusuchia, o bien son simplesiomorfías adquiridas en nodos aún más basales del linaje. En todo caso, si consideramos como primitiva la condición presente en los Thalattosuchia, la presencia de un giro ventral en la región caudal de los canales nasofaríngeos sería una apomorfía adquirida en algún punto del stem-group de Eusuchia, que, a su vez, derivaría en un giro más pronunciado en Crocodylia. Este proceso puede estar relacionado con el proceso de verticalización del basicráneo en Eusuchia descrito por Tarsitano, (1985).

No hay apenas diferencias en la morfología de las cavidades intracraneanas de los distintos ejemplares hallados en el yacimiento de Lo Hueco. La mayoría de las diferencias observadas probablemente se deben a deformaciones tafonómicas sufridas por el fósil (como el aplanamiento de la región anterior del encéfalo y el sistema faringotimpánico, o la fusión del sistema de senos paranasales y el conducto nasal en *L. megadontos*) o al bajo contraste observado entre el hueso fosilizado y el sedimento que rellena cada una de las cavidades (como el ensanchamiento de la cavidad basiesfenoidea del holotipo de *A. fontisensis*).

La diferencia más evidente en los ejemplares de Lo hueco se encuentra en la región ventral del sistema paratimpánico. En el holotipo de *A. fontisensis* la región ventral de los senos faringotimpánicos se alarga ventralmente hasta contactar con un seno faríngeo medio relativamente corto (Fig. 5.2.3) mientras que en *L. megadontos* los canales ventrales de los senos faringotimpánicos convergen justo bajo el encéfalo, y es la región ventral del seno faríngeo medio la que presenta una marcada elongación (Fig.

5.1.4). No obstante, la longitud ventral del seno faríngeo medio con respecto a la dorsal en ambos casos es superior a la de los aligatoroideos y gavialoideos.

Las capacidades neurosensoriales y cognitivas de los alodaposuquidos de Lo Hueco son similares a las descritas para Crocodylia (Capítulo 5.2.2). La agudeza olfativa estimada para *L. megadontos* y *A. fontisensis* es elevada. *L. megadontos* se sitúa en una posición intermedia entre la calculada para los crocodiloideos y los aligatoroideos. Por otro lado, el tamaño relativo del lóbulo olfativo de *A. fontisensis* se sitúa más próximo al calculado para los aligatoroideos (Tabla 5.2.1).

La capacidad auditiva estimada para *L. megadontos* es ligeramente más baja a la obtenida para los ejemplares de gran tamaño como *A. mississippiensis* y *C. niloticus*, estando su oído adaptado a menores frecuencias (Tabla 5.1.2).

El volumen relativo de los lóbulos ópticos de las especies de Lo Hueco es similar al estimado para los especímenes de gran tamaño como *A. mississippiensis*, *C. niloticus*, *T. schlegelii* y *G. gangeticus*, siendo la del holotipo de *A. fontisensis* ligeramente superior a la del holotipo de *L. megadontos*. Hay que remarcar también que la agudeza visual en especies simpátricas y sincrónicas es similar cuando se desenvuelven en condiciones fóticas similares (Nagloo et al., 2016; Capítulo 5.2).

Finalmente, los cocientes de encefalización estimados para *L. megadontos* y *A. fontisensis* son ligeramente inferiores a los obtenidos para los crocodilios de gran tamaño (Tabla 5.2.3). Esto se debe muy probablemente a la deformación sufrida por la cavidad encefálica, lo que redujo el volumen total de la misma.

Las imágenes obtenidas a partir de TAC de los tres ejemplares del tercer morfotipo craneal de Lo Hueco carecen de la resolución suficiente para realizar una reconstrucción completa de las cavidades intracraneanas, y, por tanto, de efectuar unos análisis morfológicos y de las capacidades neurosensoriales y cognitivas en detalle. Las únicas estructuras reconocibles son la región caudal del encéfalo de HUE-02815 y las regiones ventrales del sistema de senos faríngeos medios de HUE-02815 y HUE-08881. La longitud relativa de la región ventral del seno faríngeo medio de ambos especímenes es más corto que la observada en *L. megadontos* y *A. fontisensis*. Numerosos estudios proponen que el seno faríngeo medio de los crocodilios es muy corto en estadíos perinatales, y se alarga a lo largo del desarrollo (Gold et al., 2014;

Dufeau and Witmer, 2015). Esto, sumado a la presencia de similitudes en algunos caracteres morfológicos, como la presencia de dientes hipertrofiados y muy próximos entre sí (Capítulo 5.3), sugiere que estos ejemplares corresponden a especímenes subadultos de *Lohuecosuchus megadontos*.

GENERAL DISCUSSION

The completion of the main objective of this PhD Thesis has provided results with important implications in the study of the evolution of the inner skull cavities and neurosensorial and cognitive capabilities of Crocodylia, focused from the rendering of the inner skull cavities of the basal eusuchians from Lo Hueco fossil site.

The first step to analyze the inner skull cavities of the eusuchians from Lo Hueco was to make an exhaustive analysis of crown-group taxa. Several skulls from the different major lineages of Crocodylia were reconstructed in 3D from CT-Scan data and analyzed. The comparative database for this thesis included the alligatoroids *Alligator mississippiensis*, *Caiman crocodilus* and *Melanosuchus niger*; crocodyloids *Crocodylus niloticus*, *Crocodylus moreletii*, *Osteolaemus tetraspis* and *Tomistoma schlegelii*; the gavialoid *Gavialis gangeticus* (Chapter 4.1), and the reconstruction of *Crocodylus johnstoni* already published by Witmer et al., (2008). To complete the database, reconstructions of several fossil crocodylians were also included, such as *Diplocynodon tormis*, from the Middle Eocene of Salamanca (Chapter 4.2), the caimanine alligatoroid *Mourasuchus nativus* (Bona et al., 2013) and the gavialoid *Gryposuchus neogaeus* (Bona et al., 2017), both from the Miocene of Argentina.

Several morphological differences have been identified in the studied sample. Some of them seem more related to specimen size than phylogeny. Basing on the ontogenetic study of Dufeau and Witmer, (2015), the sample was divided into two categories: medium-sized specimens (subadult sensu Dufeau and Witmer, 2015) and large-sized specimens (adult sensu Dufeau and Witmer, 2015). *C. crocodilus*, *M. niger*, and *O. tetraspis*, whose skull length is less than 30cm, show nearly 90º in the transition between the olfactory tract and the cerebrum in dorsal view, semispheric cerebral hemispheres and wide parietal pillars. On the other hand, specimens with skull length over 30cm, including *A. mississippiensis*, *C. niloticus*, *T. schlegelii* and *G. gangeticus*, have a progressive transition between the olfactory tract and the cerebrum, conical cerebral hemispheres and narrow parietal pillars (Chapter 4.2.1).

However, there is a series of characters in accordance with current phylogenetical hypotheses (Fig. 2.1. Brochu, 1999, 2011). Crocodylian brain is rostrocaudally elongated, with long olfactory tracts and sigmoid shape in lateral view (Colbert, 1946;

Witmer et al., 2008; Bona et al., 2013; Dufeau and Witmer, 2015; Brusatte et al., 2016; Pierce et al., 2017; Chapter 4.1). Cerebral hemispheres are easily distinguished as a pair of lateral lumps in dorsal view (Witmer et al., 2008; Bona et al., 2013; Brusatte et al., 2016; Chapter 4.1). The hypophyseal fossa, located in the caudoventral surface of the cerebrum, is caudoventrally oriented (Witmer et al., 2008; Bona et al., 2013; Dufeau and Witmer, 2015; Brusatte et al., 2016; Pierce et al., 2017; Chapter 4.1). The inner ear of crocodylians is similar to those of other archosaurs, with the anterior canal being the largest of the three semicircular canals. Furthermore, the anterior semicircular canal is dorsally elongated in crocodylians, while in more basal crocodylomorphs the anterior and posterior semicircular canals have the same dorsal length (Brusatte et al., 2016; Pierce et al., 2017; Chapter 4.1). Crocodylians also have a very pneumatized basicranium, with a very developed pharyngotympanic sinus system. It is noteworthy the appearance of the intertympanic diverticula, a dorsomedial cavity that joins both pharyngotympanic sinuses (Bona et al., 2013, 2017; Chapter 4.1).

Within Crocodylia, crocodyloids and gavialoids have a flat caudodorsal surface of the brain, while alligatoroids develop a lump, variable in size (Storrs et al., 1983; Chapter 4.2.1). The development of the intertympanic diverticula also varies among the different crocodylian major clades. In alligatoroids, the central region of the diverticula, located between both parietal pillars, is larger than the lateral regions. However, crocodyloids and gavialoids have these lateral parts more developed (Chapter 4.2.1). Eusuchians are characterized by a verticalization process of its basicranium that consists of a ventral displacement of the basioccipital, basisphenoid and pterygoids, modifying the insection angle of the jaw muscles, the orientation of the quadrate and the shape of the cavities contained in these bones: nasopharyngeal ducts and median pharyngeal sinus (Tarsitano, 1985, 1989). However, the way this elongation affects the shape and elongation of these cavities is ontogeny (Dufeau and Witmer, 2015) and lineage dependant (Gold et al., 2014; Chapters 4.2.1, 5.1, 5.2 and 5.3). The length of the pharyngotympanic sinus and the dorsal part of the median pharyngeal sinus (dorsal to the join with the basisphenoid diverticula) are constant in Crocodyloids. Also, the ventral part of the median pharyngeal sinus is the most affected structure by the elongation of the basicranium (3-4 times larger than the dorsal region). On the other hand, the verticalization process affects the ventral region of the pharyngotympanic sinus and both regions of the median pharyngeal sinus the same way in alligatoroids:

the ventral region of the median pharyngeal sinus is between 1 and 1.5 times larger than the dorsal one. The relative length of the median pharyngeal sinus in gavialoids is somewhere between that of Alligatoroidea and Crocodyloidea, although closer to the condition showed by alligatoroids (Gold et al., 2014; Chapters 5.1, 5.2 and 5.3).

T. schlegelii, whose phylogenetic placement is under debate (Meganathan et al., 2010; Brochu, 2011), has a ventral length of the median pharyngeal sinus shorter than the other crocodyloids. However, its ventral length is still longer than those of alligatoroids, similar to that of *G. gangeticus*. This might be due to convergency, phylogenetical closeness, or an early stage ontogenetic state.

Paranasal sinus system is also different among the crocodylian lineages. In alligatoroids such as *C. crocodilus* and, in a less conspicuous way, in *A. mississippiensis*, or in the gavialoid *G. gangeticus*, the caudal region of the dorsal alveolar canal leads into the dorsal part of the olfactory region of the nasal cavity. In crocodyloids, the dorsal alveolar canal progressively widens, forming a large cavity lateral to the olfactory region of the nasal cavity (Chapters 5.1 and 5.2).

The neurosensorial and cognitive capabilities estimated for the extant representatives of Crocodylia agree with several results published in the etological and cytological studies of these animals. Olfactory acuity of crocodylians has been tested in the studies of Weldon and Ferguson, (1993), Weldon et al., (1990) or Grigg and Kirshner, (2015). Darla Zelenitzsky analyzed the olfactory acuity of birds and non-avian dinosaurs (Zelenitsky et al., 2009, 2011), including some specimens of *A. mississippiensis*. Zelenitzky related the size of the olfactory bulb and the olfactory acuity, proposing a coefficient to estimate the olfactory acuity from linear measurements of inner skull cavities (Zelenitsky et al., 2009 and references therein). This study shows the large relative size of the olfactory bulbs of *A. mississippiensis* in comparison to other archosaurs. The crocodylians studied have similar olfactory capabilities than those of *A. mississippiensis* analyzed by Zelenitsky et al., (2009), also showing a distribution corelated with their phylogenetic affinities (Chapters 5.1 and 5.2): Crocodyloids have a larger relative development of the olfactory bulb than alligatoroids and gavialoids, independently of their size (Tables 5.1.1 and 5.2.1).

Crocodylians also have an acute hearing sense, in land and underwater, with specific structures to optimize the precise localization of the sound (Dufeau and

Witmer, 2015; Grigg and Kirshner, 2015). In reptiles, the hearing capability can be estimated from some linear measurements of the inner skull cavities, such as the length of the cochlear duct, the hearing organ of these animals (Walsh et al., 2009). Crocodylian cochlear length is short in comparison with their skull length (Fig. 2 from Walsh et al., 2009; Table 5.1.2), being their hearing range specialized in lower-frequency sound, as described by etological studies (Vergne et al., 2009). Hearing capability seems to be related to the size of the specimen rather than to its phylogenetic relationships. Large-sized specimens have a smaller relative cochlear length than that of the medium-sized specimens (Table 5.1.2): the larger the crocodile, the lower is its hearing frequence range.

The visual capability of crocodylians is sharp too (Grigg and Kirshner, 2015; Nagloo et al., 2016). There are studies that relate visual acuity with the size of the eyeball (Hall, 2008, 2009 and references). However, there are not studies that correlate the size of the eyeball with the orbit or any other skeletal structure in crocodylomorphs. The optic lobe is an easily distinguishable structure in crocodylians (Jirak and Janacek, 2017), so its relative volume has been suggested as a proxy for its visual capabilities, as in birds (Martin et al., 2007; Torres and Clarke, 2018). This way, large-sized specimens have a smaller relative volume of the optic lobe than medium-sized specimens (Table 5.1.3), which may imply less visual acuity.

The cognitive capabilities of crocodylians, as those of non-avian reptiles, are substantially lower than those of mammals and birds (Jerison, 1969, 1973; Grigg and Kirshner, 2015). Hurlburt, (1996) proposed a method to compare separately the encephalization quotient of mammals, birds and reptiles. The Reptile Encephalization Quotient (REQ) includes turtles, lepidosaurs and crocodiles, and varies in a range between 0.4 and 2.4. Specifically, crocodylian REQ is in an intermediate point, between 0.9 and 1.5 (Hurlburt, 1996; Chapter 4.2.2 Table 4.2.2.3). Among crocodylians, the encephalization quotient is correlated with the size of the specimens rather than their phylogenetic position, with the large-sized specimens having a lower REQ (≈1) than that of the medium-sized samples (REQ≈1.65).

The inner skull cavities of *Diplocynodon tormis* are similar to those described for medium-sized crocodylians (as would be expeted, given its skull length), with an abrupt

transition between the olfactory tract and the cerebrum, semispheric cerebral hemispheres and wide parietal pillars.

D. tormis has several characters of the inner skull cavities attributed to alligatoroids, such as a central region of the intertympanic diverticula more developed than the lateral parts, and a ventral length of the median pharyngeal sinus subequal than the dorsal length. However, the caudodorsal surface of the cerebrum is flat, as seen in crocodyloids and gavialoids. Therefore, the appearance of a convexity on the caudodorsal surface of the cerebrum, a character mentioned by Storrs et al., (1983), would be an synapomorphy of a more inclusive clade of alligatoroids. The combination of alligatoroid synapomorphies and crocodylian symplesiomorphies is consistent with its basal alligatoroid phylogenetical position, outside crown-group Alligatoridae (Fig. 2.1).

The specimen studied of *D. tormis* has some breakages that make impossible to make with accuracy several volumetric measurements required for the neurosensorial and cognitive analyses, slightly distorting the results. The olfactory acuity estimated for *D. tormis* is close to those of the other studied alligatoroids, compatible with the hypothesis that the relative size of the olfactory bulb is related to the phylogenetic relationship rather than to the size of the specimen. The relative volume of the optic lobes of *D. tormis* is also similar to that of the extant crocodylian samples, being slightly larger than those of the large-sized specimens but not reaching those of the medium-sized specimens. Something similar happens with the encephalization quotient of *D. tormis*. Its REQ is similar to that of the crocodylian sample, but is lower than those of the medium-sized samples.

Attending to objectives 3, 4 and 5 of this PhD thesis, several allodaposuchian (non-crocodylian eusuchians) specimens from Lo Hueco have been studied, including the holotype of *Lohuecosuchus megadontos* (HUE-04498), the holotype and a paratype of *Agaresuchus fontisensis* (HUE-02502 and HUE-03713) and three specimens of the third skull morphotype from Lo Hueco (HUE-02018, HUE-02815 and HUE-08881). Reconstructions of the inner skull cavities have allowed establishing the general morphology of the inner skull cavities in Allodaposuchidae. Most of the characters showed by the Lo Hueco samples have been previously considered crocodylian synapomorphies (Chapters 4.1 and 4.2.1). Therefore, a sigmoid brain in lateral view, a

flat caudodorsal surface of the brain, a dorsally elongated anterior semicircular canal, a central region of the intertympanic diverticula less developed than the lateral regions, a long median pharyngeal sinus with a circular section and a wide caudal part of the dorsal alveolar canal separated from the olfactory region of the nasal cavity must be considered as eusuchian synapomorphies rather than crocodylian synapomorphies.

On the other hand, nasopharyngeal ducts of the allodaposuchids studied are gradually curved ventrally, while in crocodylians they turn ventrally in a 90º angle. Among non-eusuchian crocodylomorphs, the shape of these ducts has only been described in the thalattosuchians *Cricosaurus araucacensis* (Herrera et al., 2013b) y *Pelagosaurus typus* (Pierce et al., 2017). In both samples, the caudal region of the nasopharyngeal ducts is caudally oriented, emerging from the skull rostrally to the hypophyseal fossa. Thalattosuchians are a mesoeucrocodylian group whose phylogenetic position is under debate, and whose cranial shape (and therefore, the shape of its inner skull cavities) is very different from that of the crown-group (Fernández et al., 2011; Herrera et al., 2013b, 2018; Brusatte et al., 2016; Pierce et al., 2017). Therefore, more specimens closer to Eusuchia are needed to test if the aforementioned characters suppose a series of evolutionary novelties of Eusuchia, or they are symplesiomorphies acquired in even more basal nodes of the lineage. Nonetheless, if the conditions of thalattosuchians are considered plesiomorphic, the presence of a ventral turn in the caudal region of the nasopharyngeal ducts would be an apomorphy acquired in the stem-group of Eusuchia, which would derive in a more abrupt turn in Crocodylia. This whole process is probably related to the “verticalization process” of the eusuchian basicranium described by Tarsitano, (1985).

The inner skull cavities of the samples from lo Hueco are very similar between them. Most of the major differences are probably due to taphonomic deformation (such as the flattening of the anterior region of the brain and the pharyngotympanic sinus system, or the fusion of the paranasal sinus system and the nasal passageway in *L. megadontos*), or due to the low density contrast between the bone and the infilling sediment (such as the widening of the basisphenoid diverticula in the holotype of *A. fontisensis*).

The most remarkable difference among the specimens from Lo Hueco is in the ventral region of the paratympanic system. In the holotype of *A. fontisensis*, the ventral

region of the pharyngotympanic sinuses extends ventrally to join the relatively short median pharyngeal sinus (Fig. 5.2.3), while in *L. megadontos*, the ventral canals of the pharyngotympanic sinuses join together just below the brain, and the elongated structure is the ventral region of the median pharyngeal sinus (Fig. 5.1.4). Nevertheless, the relative length of the ventral región of the median pharyngeal sinus is higher in the specimens from Lo Hueco than that of alligatoroids and gavialoids.

Neurosensorial and cognitive capabilities of the allodaposuchids from Lo Hueco are similar to those described for Crocodylia (Chapter 4.2.2). The estimated olfactory acuity of *L. megadontos* and *A. fontisensis* is high, located between the range observed for both alligatoroids and crocodyloids. The relative size of the olfactory bulb of *L. megadontos* is just between the two major lineages of Crocodylia, while that of *A. fontisensis* is closer to that of alligatoroids than to those of crocodyloids (Table 5.2.1).

The hearing capability estimated for *L. megadontos* is slightly lower than that of the large-sized samples such as *A. mississippiensis* and *C. niloticus*, its ear adapted to even lower frequencies (Table 5.1.2).

The relative volume of the optic lobes of both species from Lo Hueco is similar to those estimated for the large-sized specimens such as *A. mississippiensis*, *C. niloticus*, *T. schlegelii* and *G. gangeticus*, that of *A. fontisensis* being slightly higher than that of *L. megadontos*. It is remarkable that the visual acuity of coeval and sympatric species is similar when they inhabite in places with similar photic features (Nagloo et al., 2016; Chapter 5.2).

Finally, the encephalization quotient estimated for *L. megadontos* and *A. fontisensis* is slightly lower than those obtained for the large-sized specimens (Table 5.2.3). This is probably due to the deformation suffered by the brain cavity, which reduced its total volume without affecting other linear measurements.

The CT-Scan data obtained from three specimens of the third skull morphotype of Lo Hueco lack enough resolution to render a complete reconstruction of their inner skull cavities and, therefore, to make a detailed morphological and neurosensorial analyses. The only recognizable structures are the caudal region of the brain of HUE-02815, and the ventral regions of the median pharyngeal sinus of HUE-02815 and HUE- 08881. The relative length of the ventral region of the median pharyngeal sinus in both

specimens is shorter than that of *L. megadontos* and *A. fontisensis*. Several studies propose that the crocodylian median pharyngeal sinus is short in perinatal states, and elongates as ontogeny progresses (Gold et al., 2014; Dufeau and Witmer, 2015). This feature and the presence of several skull similarities such as hypertrophied teeth, very close between them (Chapter 5.3) suggest that these samples belong to subadult specimens of *Lohuecosuchus megadontos.*

CAPÍTULO 7: CONCLUSIONES

CONCLUSIONS

CONCLUSIONES

Atendiendo a las hipótesis y objetivos planteados para la presente tesis doctoral, y en función de los resultados obtenidos, se considera que se han aportado evidencias suficientes y criterios adecuados para formular las siguientes conslusiones:

- Se confirma la presencia de una serie de caracteres en la morfología de las cavidades intracraneanas compartida por todos los Crocodylia, como la morfología alargada y sigmoidal del encéfalo, con una superficie aplanada en la región caudoventral del cerebro, una hipófisis orientada caudoventralmente, un canal semicircular anterior alargado dorsalmente, y un gran desarrollo del sistema de senos faringotimpánicos, con unas regiones laterales de los divertículos intertimpánicos más voluminosas que la región central.

- Existen una serie de caracteres autapomórficos en las cavidades intracraneanas de los linajes mayores de Crocodylia, como una convexidad en la superficie caudodorsal del cerebro y un mayor desarrollo de la región central de los divertículos intertimpánicos en aligatoroideos, y seno faríngeo medio alargado en crocodiloideos.

- Las capacidaes neurosensoriales y cognitivas inferidas para los miembros actuales de Crocodylia concuerdan con lo observado en estudios etológicos y citológicos: poseen un agudo sentido del olfato, están especializados en escuchar sonidos de baja frecuencia, y su cociente de encefalización es similar al del resto de saurópsidos no avianos.

- Las cavidades intracraneanas de *Diplocynodon tormis* presentan una mezcla de las plesiomorfías descritas para Crocodylia, como una superficie caudodorsal plana de los hemisferios cerebrales, y de las autapomorfías descritas en los representantes actuales de Alligatoroidea, como una sección central de los divertículos intertimpánicos más desarrollado que las regiones laterales y un seno faríngeo medio corto.

- Las capacidades neurosensoriales y cognitivas inferidas para *Diplocynodon tormis* coinciden con las estimadas para el conjunto de Crocodylia, siendo solo ligeramente inferiores que las del resto de especímenes de tamaño medio.

- Se confirma la presencia de las novedades evolutivas en la morfología de las cavidades intracraneanas presentes en Crocodylia en los miembros basales de Eusuchia, por lo que pasan a ser consideradas simplesiomorfías de Crocodylia.

- Las cavidades intracraneanas de *Lohuecosuchus megadontos* presentan una mezcla de las plesiomorfías descritas para Eusuchia y las sinapomorfías descritas en los representantes de Allodaposuchidae, como la presencia de una curva gradual en la región caudal de los conductos nasofaríngeos.

- Las capacidades neurosensoriales y cognitivas inferidas para *Lohuecosuchus megadontos* son similares a las de los Crocodylia de gran tamaño.

- Las cavidades intracraneanas de *Agaresuchus fontisensis* presentan una mezcla de las plesiomorfías descritas para Eusuchia y las sinapomorfías descritas en los representantes de Allodaposuchidae.

- Las capacidades neurosensoriales y cognitivas inferidas para *Agaresuchus fontisensis* son similares a las de *Lohuecosuchus megadontos* y a las de los Crocodylia de gran tamaño.

- Las cavidades intracraneanas preservadas en los representantes del tercer morfotipo craneal de Lo Hueco son ligeramente diferentes a las de *Lohuecosuchus megadontos* y *Agaresuchus fontisensis*.

- Se identifican los ejemplares del tercer morfotipo craneal de Lo Hueco como individuos subadultos de *Lohuecosuchus megadontos*.

CONCLUSIONS

Attending to the hypotheses and objectives proposed for this PhD thesis, and based on the results obtained, the evidence provided allows to reach the following conclusions:

- The following characters in the shape of the inner skull cavities shared by all Crocodylia are confirmed as such: a sigmoid brain outline in lateral view, a caudoventrally oriented pituitary, a dorsally elongated anterior semicircular canal and a very developed pharyngotympanic sinus system, with lateral regions of the intertympanic diverticula larger than the central region.

- Some characters regarding the inner skull cavities are apomorphic for the different major lineages of Crocodylia: a convexity in the posterodorsal surface of the brain and a central region of the intertympanic diverticula more developed than the central are alligatoroid synapomorphies and a long median pharyngeal sinus is a crocodyloid synapomorphy.

- Neurosensorial and cognitive capabilities inferred for extant representatives of Crocodylia agree with observations of etological and cytological studies: they have a sharp sense of olfaction, they are specialized in low-frequence hearing and their encephalization quotient is similar to that of other non-avian sauropsids

- The inner skull cavities of *Diplocynodon tormis* have a combination of crocodylian plesiomorphies, such as a flat caudodorsal surface of the brain, and alligatoroid synapomorphies, such as a central region of the intertympanic diverticula more developed than the lateral ones, and a short median pharyngeal sinus.

- Neurosensorial and cognitive capabilities inferred for *Diplocynodon tormis* are similar to those of Crocodylia, being slightly lower than those of medium-sized specimens.

- The occurrence of the evolutionary novelties in the shape of the inner skull cavities of Crocodylia is also present in basal members of Eusuchia, therefore these characters must be considered as symplesiomorphies of Crocodylia.

- The inner skull cavities of *Lohuecosuchus megadontos* have a combination of eusuchian plesiomorphies and allodaposuchid synapomorphies, such as a gradual ventral flexure in the caudal region of the nasopharyngeal ducts.

- Neurosensorial and cognitive capabilities inferred for *Lohuecosuchus megadontos* are similar to those of the large-sized members of Crocodylia.

- The inner skull cavities of *Agaresuchus fontisensis* have a combination of eusuchian plesiomorphies and allodaposuchid synapomorphies.

- Neurosensorial and cognitive capabilities inferred for *Agaresuchus fontisensis* are similar to those of *Lohuecosuchus megadontos* and those of large-sized members of Crocodylia.

- The preserved inner skull cavities of the third skull morphotype from Lo Hueco are slightly different from those of *Lohuecosuchus megadontos* and *Agaresuchus fontisensis*.

- The third skull morphotype from Lo Hueco is identified as subadult specimens of *Lohuecosuchus megadontos.*

REFERENCIAS

REFERENCES

REFERENCIAS

De Andrade, M. B., R. Edmonds, M. J. Benton, and R. Schouten. 2011. A new Berriasian species of *Goniopholis* (Mesoeucrocodylia, Neosuchia) from England, and a review of the genus. Zoological Journal of the Linnean Society 163:66–108.

von Baczko, M. B., and J. B. Desojo. 2016. Cranial anatomy and palaeoneurology of the archosaur *Riojasuchus tenuisceps* from the Los Colorados Formation, La Rioja, Argentina. PloS One 11:e0148575.

Barroso-Barcenilla, F., O. Cambra-Moo, F. Escaso, F. Ortega, A. Pascual, A. Pérez-García, J. Rodríguez-Lázaro, J. L. Sanz, M. Segura, and A. Torices. 2009. New and exceptional discovery in the Upper Cretaceous of the Iberian Peninsula: the palaeontological site of “Lo Hueco”, Cuenca, Spain. Cretaceous Research 30:1268–1278.

Benton, M. J., and J. M. Clark. 1988. Archosaur phylogeny and the relationships of the Crocodylia; pp. 295–338 in M. J. Benton and The Systematics Association (eds.), The phylogeny and classification of the Tetrapods, Volume 1: Amphibians, Reptiles, Birds. vol. 35. Clarendon Press, Oxford.

Blanco, A., E. Puértolas-Pascual, J. Marmi, B. Vila, and A. G. Sellés. 2014. *Allodaposuchus palustris* sp. nov. from the Upper Cretaceous of Fumanya (South-Eastern Pyrenees, Iberian Peninsula): Systematics, palaeoecology and palaeobiogeography of the enigmatic Allodaposuchian Crocodylians. PLoS ONE 9:1–34.

Blanco, A., J. Fortuny, A. Vicente, À. H. Luján, J. A. García-Marçà, and A. G. Sellés. 2015. A new species of *Allodaposuchus* (Eusuchia, Crocodylia) from the Maastrichtian (Late Cretaceous) of Spain: phylogenetic and paleobiological implications. PeerJ 3:e1171:1–31.

Bona, P., and A. Paulina-Carabajal. 2013. Caiman gasparinae sp. nov., a huge alligatorid (Caimaninae) from the Late Miocene of Paraná, Argentina. Alcheringa 37:462–473.

Bona, P., F. J. Degrange, and M. S. Fernández. 2013. Skull anatomy of the bizarre crocodylian *Mourasuchus nativus* (Alligatoridae, Caimaninae). The Anatomical Record 296:227–239.

Bona, P., A. Paulina-Carabajal, and Z. Gasparini. 2017. Neuroanatomy of *Gryposuchus neogaeus* (Crocodylia, Gavialoidea): a first integral description of the braincase and endocranial morphological variation in extinct and extant gavialoids. Earth and Environmental Science Transactions of the Royal Society of Edinburgh 106:235–246.

Brochu, C. A. 1999. Phylogenetics, taxonomy, and historical biogeography of Alligatoroidea. Journal of Vertebrate Paleontology 19:9–100.

Brochu, C. A. 2003. Phylogenetic approaches toward crocodylian history. Annual Review of Earth and Planetary Sciences 31:357–397.

Brochu, C. A. 2004. A new Late Cretaceous gavialoid crocodylian from Eastern North America and the phylogenetic relationships of *Thoracosaurs*. Journal of Vertebrate Paleontology 24:610–633.

Brochu, C. A. 2011. Phylogenetic relationships of *Necrosuchus ionensis* Simpson, 1937 and the early history of caimanines. Zoological Journal of the Linnean Society 163:S228--S256.

Brochu, C. A. 2013. Phylogenetic relationships of Palaeogene ziphodont eusuchians and the status of *Pristichampsus* Gervais, 1853. Earth and Environmental Science Transactions of the Royal Society of Edinburgh 103:521–550.

Bronzati, M., F. C. Montefeltro, and M. C. Langer. 2012. A species-level supertree of Crocodyliformes. Historical Biology 1–9.

Brusatte, S. L., M. J. Benton, J. B. Desojo, and M. C. Langer. 2010. The higher-level phylogeny of Archosauria (Tetrapoda: Diapsida). Journal of Systematic Palaeontology 8:3–47.

Brusatte, S. L., A. Muir, M. T. Young, S. A. Walsh, L. Steel, and L. M. Witmer. 2016. The braincase and

neurosensory anatomy of an Early Jurassic marine crocodylomorph: Implications for crocodylian sinus evolution and sensory transitions. The Anatomical Record 299:1511–1530.

Buscalioni, Á. D., F. Ortega, D. B. Weishampel, and C.-M. Jianu. 2001. A revision of the crocodyliform Allodaposuchus precedens from the Upper Cretaceous of the Haţeg Basin, Romania: its relevance in the phylogeny of Eusuchia. Journal of Vertebrate Paleontology 21:74–86.

Buscalioni, Á. D., P. Piras, R. Vullo, M. Signore, and C. Barbera. 2011. Early eusuchia crocodylomorpha from the vertebrate-rich Plattenkalk of Pietraroia (Lower Albian, southern Apennines, Italy). Zoological Journal of the Linnean Society 163:199–227.

de Celis, A., I. Narváez, and F. Ortega. 2018. Pelvic and femoral anatomy of the Allodaposuchidae (Crocodyliformes, Eusuchia) from the Late Cretaceous of Lo Hueco (Cuenca, Spain). Journal of Iberian Geology 44:85–98.

Colbert, E. H. 1946a. The Eustachian Tubes in the Crocodilia. Copeia 1946:12–14.

Colbert, E. H. 1946b. *Sebecus*, representative of a peculiar suborder of fossil Crocodylia from Patagonia. Bulletin of the American Museum of Natural History 87:1–66.

Conroy, G. C., and M. W. Vannier. 1984. Noninvasive three-dimensional computer imaging of matrix filled fossil skulls by High-Resolution Computed tomography. Science 226:456–458.

Dal Sasso, C., G. Pasini, G. Fleury, and S. Maganuco. 2017. *Razanandrongobe sakalavae*, a gigantic mesoeucrocodylian from the Middle Jurassic of Madagascar, is the oldest known notosuchian. PeerJ 5:e3481.

Delfino, M., and T. Smith. 2012. Reappraisal of the morphology and phylogenetic relationships of the middle Eocene alligatoroid *Diplocynodon deponiae* (Frey, Laemmert, and Riess, 1987) based on a three-dimensional specimen. Journal of Vertebrate Paleontology 32:1358–1369.

Delfino, M., V. Codrea, A. Folie, P. Dica, P. Godefroit, and T. Smith. 2008. A complete skull of *Allodaposuchus precedens* Nopcsa, 1928 (Eusuchia) and a reassessment of the morphology of the taxon based on the Romanian remains. Journal of Vertebrate Paleontology 28:111–122.

Densmore, L. D., and R. D. Owen. 1989. Molecular systematics of the order Crocodylia. American Zoologist 29:831–841.

Dodson, P. 1975a. Functional and ecological significnce of relative growth in Alligator. Journal of Zoology, London 175:315–355.

Dodson, P. 1975b. Functional and ecological significance of relative growth in *Alligator*. Journal of Zoology 175:315–355.

Dufeau, D. L., and L. M. Witmer. 2015. Ontogeny of the middle-ear air-sinus system in *Alligator mississippiensis* (Archosauria: Crocodylia). PloS One 10:e0137060.

Edinger, T. 1929. Die Fossilen Gehirn (J. Springer (ed.)). Springer, Julius, Berlin, 249 pp.

Edinger, T. 1938. Über Steinkeme von Him-und Ohr-Rohlen der Mesosuchier *Goniopholis* und *Pholidosaurus* aus dem Bückeburger Wealden. Acta Zoologica 19:467–505.

Edinger, T. 1975. Paleoneurology 1804-1966. An Annotated Bibliography (A. Brodal, W. Hild, J. van Limborgh, R. Ortman, T. H. Schiebler, G. Töndury, and E. Wolff (eds.)). Springer-Verlag, Berlin, 258 pp.

Erickson, B. R. 1972. *Albertochampsa langstoni* a new alligator from the Cretaceous of Alberta. Scientific Publications of the Science Museum of Minnesota 2:1–13.

Eudes-Deslongchamps, J. A. 1864. Memoires Sur Les Teleosauriens de l'epoque Jurassique Du Departement Du Calvados. Mémoires de la Société Linnéenne de Normandie 13, n°3, Normandie, 138 pp.

Ezcurra, M. D. 2016. The phylogenetic relationships of basal archosauromorphs, with an emphasis on the systematics of proterosuchian archosauriforms. PeerJ 4:e1778.

Fanti, F., T. Miyashita, L. Cantelli, F. Mnasri, J. Dridi, M. Contessi, and A. Cau. 2016. The largest thalattosuchian (Crocodylomorpha) supports teleosaurid survival across the Jurassic-Cretaceous boundary. Cretaceous Research 61:263–274.

Fernández, M. S., and Z. Gasparini. 2000. Salt glands in a Tithonian metriorhynchid crocodyliform and their physiological significance. Lethaia 33:269–276.

Fernández, M. S., and Z. Gasparini. 2008. Salt glands in the Jurassic metriorhynchid Geosaurus: Implications for the evolution of osmoregulation in Mesozoic marine crocodyliforms. Naturwissenschaften 95:79–84.

Fernández, M. S., and Y. Herrera. 2009. Paranasal sinus system of *Geosaurus araucanensis* and the homology of the antorbital fenestra of metriorhynchids (Thalattosuchia: Crocodylomorpha). Journal of Vertebrate Paleontology 29:702–714.

Fernández, M. S., A. Paulina-Carabajal, Z. Gasparini, and G. Chong Díaz. 2011. A metriorhynchid crocodyliform braincase from northern Chile. Journal of Vertebrate Paleontology 31:369–377.

Franzosa, J. W. 2004. Evolution of the Brain in Theropoda (Dinosauria). Thesis Dissertation, University of Texas at Austin, USA, 357 pp.

Garrick, L. D., and J. W. Lang. 1977. Social signals and behaviours of adult alligators and crocodiles. American Zoologist 17:225–239.

Gasparini, Z. 1971. Los Notosuchia del Cretácico de América del sur como un nuevo infraorden de los Mesosuchia (Crocodilia). Ameghiniana 1:83–103.

Gauthier, J. A., M. Kearney, J. A. Maisano, O. Rieppel, and A. D. B. Behlke. 2012. Assembling the squamate tree of life: Perspectives from the phenotype and the fossil record. Bulletin of the Peabody Museum of Natural History 53:3–308.

Gold, M. E. L., C. A. Brochu, and M. A. Norell. 2014. An expanded combined evidence approach to the *Gavialis* problem using geometric morphometric data from crocodylian braincases and Eustachian systems. PLoS ONE 9:e105793.

Goldman, L. W. 2007. Principles of CT and CT Technology. Journal of Nuclear Medicine Technology 35:115–129.

Grigg, G. C., and D. Kirshner. 2015. Biology and Evolution of Crocodylians. Cornell University Press, Ithaca, New York, 650 pp.

Hall, M. I. 2008. The anatomical relationships between the avian eye, orbit and sclerotic ring: Implications for inferring activity patterns in extinct birds. Journal of Anatomy 212:781–794.

Hall, M. I. 2009. The relationship between the lizard eye and associated bony features: A cautionary note for interpreting fossil activity patterns. Anatomical Record 292:798–812.

Hall, M. I., and C. F. Ross. 2007. Eye shape and activity pattern in birds. Journal of Zoology 271:437–444.

Herrera, Y. 2015. Metriorhynchidae (Crocodylomorpha: Thalattosuchia) from Upper Jurassic – Lower Cretaceous of Neuquén Basin (Argentina), with comments on the natural casts of the brain; pp. 159–171 in M. S. Fernández and Y. Herrera (eds.), Reptiles Extintos - Volumen en Homenaje a Zulma Gasparini. Publicación Electrónica de la Asociación Paleontológica Argentina. vol. 15.

Herrera, Y., and V. V Vennari. 2014. Cranial anatomy and neuroanatomical features of a new specimen of Geosaurini (Crocodylomorpha: Metriorhynchidae) from west-central Argentina. Historical Biology 27:33–41.

Herrera, Y., Z. Gasparini, and M. S. Fernández. 2013a. A new Patagonian species of *Cricosaurus*

(Crocodyliformes, Thalattosuchia): First evidence of *Cricosaurus* in Middle-Upper Tithonian lithographic limestone from Gondwana. Palaeontology 56:663–678.

Herrera, Y., M. S. Fernández, and Z. Gasparini. 2013b. The snout of *Cricosaurus araucanensis*: A case study in novel anatomy of the nasal region of metriorhynchids. Lethaia 46:331–340.

Herrera, Y., J. M. Leardi, and M. S. Fernández. 2018. Braincase and endocranial anatomy of two thalattosuchian crocodylomorphs and their relevance in understanding their adaptations to the marine environment. PeerJ 6:e5686.

Holliday, C. M., and N. M. Gardner. 2012. A new eusuchian crocodyliform with novel cranial integument and its significance for the origin and evolution of Crocodylia. PloS One 7:e30471.

Holloway, W. L. 2011. A Virtual Phytosaur Endocast and Its Implications for Sensory System Evolution in Archosaurs. Theses, Dissertations and Capstones, Marshall University, USA, 62 pp.

Hopson, J. A. 1977. Relative brain size and behavior in archosaurian reptiles. Annual Review of Ecology and Systematics 8:429–448.

Hopson, J. A. 1979. Paleoneurology; pp. 39–146 in R. G. Northcutt and P. Ulinski (eds.), Biology of Reptilia Volume 9. Neurology A. Academic Press, London New York San Francisco.

Hurlburt, G. R. 1996. Relative Brain Size in Recent and Fossil Amniotes: Determination and Interpretation. PhD Dissertation. Department of Zoology. University of Toronto, Toronto, 253 pp.

Hurlburt, G. R. 1999. Comparison of body mass estimation techniques, using Recent reptiles and the pelycosaur *Edaphosaurus boanerges*. Journal of Vertebrate Paleontology 19:338–350.

Hurlburt, G. R., A. B. Heckert, and J. O. Farlow. 2003. Body mass estimates of phytosaurs (Archosauria: Parasuchidae) from the Petrified Forest Formation (Chinle Group: Revueltian) based on skull and limb bone measurements. New Mexico Museum of Natural History and Science Bulletin 24:105–113.

Irmis, R. B., S. J. Nesbitt, and H. Sues. 2013. Early Crocodylomorpha; pp. 275–302 in S. J. Nesbitt, J. B. Desojo, and R. B. Irmis (eds.), Anatomy, Phylogeny and Palaeobiology of Early Archosaurs and their Kin. Geological Society, London, Special Publications, London.

Jerison, H. J. 1969. Brain evolution and dinosaur brains. The American Naturalist 103:575–588.

Jerison, H. J. 1973. Evolution of the Brain and Intelligence. Academic Press, New York and London, 482 pp.

Jirak, D., and J. Janacek. 2017. Volume of the crocodilian brain and endocast during ontogeny. PLoS ONE 12:e0178491.

Kawabe, S., T. Shimokawa, H. Miki, T. Okamoto, and S. Matsuda. 2009. A Simple and accurate method for estimating the brain volume of birds: Possible application in paleoneurology. Brain, Behavior and Evolution 74:295–301.

Kley, N. J., J. J. W. Sertich, A. H. Turner, D. W. Krause, P. M. O'Connor, and J. A. Georgi. 2010. Craniofacial morphology of *Simosuchus clarki* (Crocodyliformes: Notosuchia) from the Late Cretaceous of Madagascar. Journal of Vertebrate Paleontology 30:13–98.

Knoll, F., L. M. Witmer, F. Ortega, R. C. Ridgely, and D. Schwarz-Wings. 2012. The braincase of the basal sauropod dinosaur Spinophorosaurus and 3D reconstructions of the cranial endocast and inner ear. PloS One 7:e30060.

Koken, E. F. 1886. Über das vorkommen fossiles crocodiliden in den Wealdenbildungen Norddeutschlands und iiber die systematik der mesozoischen crocodiliden. Zeitschrift Der Deutschen Geologischen Gesellschaft 38:664–670.

Koken, E. F. 1887. Die dinosaurier, crocodiliden und sauropterygier des norddeutschen Wealden. Paleontol. Abh. 3:309–419.

Koken, E. F. 1893. Die Vorwelt Und Ihre Entwicklungsgeschichte. Hansebooks, Leipzig, 672 pp.

Lautenschlager, S. 2016. Reconstructing the past: methods and techniques for the digital restoration of fossils. Royal Society Open Science 3:160342.

Lautenschlager, S., and R. J. Butler. 2016. Neural and endocranial anatomy of Triassic phytosaurian reptiles and convergence with fossil and modern crocodylians. PeerJ 4:e2251.

Lautenschlager, S., C. A. Brassey, D. J. Button, and P. M. Barrett. 2016. Decoupled form and function in disparate herbivorous dinosaur clades. Scientific Reports 6:26495.

Lautenschlager, S., E. J. Rayfield, P. Altangerel, L. E. Zanno, and L. M. Witmer. 2012. The endocranial anatomy of therizinosauria and its implications for sensory and cognitive function. PloS One 7:e52289.

Lemoine, V. 1884. Note sur l'encéphale du gavial du Mont-Aimé, étudié sur trois moulages naturels. Bulletin de La Société Géologique de France 3:158–162.

Martin, G. R., K. J. Wilson, J. M. Wild, S. Parsons, M. F. Kubke, and J. Corfield. 2007. Kiwi forego vision in the guidance of their nocturnal activities. PLoS ONE 2.

Martin, J. E. 2010. *Allodaposuchus* Nopsca, 1928 (Crocodylia, Eusuchia), from the Late Cretaceous of southern France and its relationships to Alligatoroidea. Journal of Vertebrate Paleontology 30:756–767.

Martin, J. E., and E. Buffetaut. 2005. An overview of the Late Cretaceous crocodilian assemblage from Cruzy, southern France. Kaupia 14:33–40.

Martin, J. E., and E. Buffetaut. 2008. *Crocodilus affuvelensis* Matheron, 1869 from the Late Cretaceous of southern France: a reassessment. Zoological Journal of the Linnean Society 152:567–580.

Meganathan, P. R., B. Dubey, M. A. Batzer, D. A. Ray, and I. Haque. 2010. Molecular phylogenetic analyses of genus *Crocodylus* (Eusuchia, Crocodylia, Crocodylidae) and the taxonomic position of *Crocodylus porosus*. Molecular Phylogenetics and Evolution 57:393–402.

Mook, C. C. 1941. A new crocodilian from the Lance Formation. American Museum Novitates 1128:1–6.

Morel de Glasville, M. 1876. Sur la cavité crânienne et la position du trou optique dans le *Steneosaurus heberti*. Bulletin de La Societe Geologique de France 4:342–348.

Mueller-Töwe, I. J. 2005. Phylogenetic relationships of the Thalattosuchia; pp. 211–213 in R. Leinfelder and M. Krings (eds.), Zitteliana Series A 45. Bayerische Staatssammlung für Paläontologie und Geologie, Munchen.

Nagloo, N., S. P. Collin, J. M. Hemmi, and N. S. Hart. 2016. Spatial resolving power and spectral sensitivity of the saltwater crocodile, *Crocodylus porosus*, and the freshwater crocodile, *Crocodylus johnstoni*. The Journal of Experimental Biology 219:1394–1404.

Narváez, I., C. a Brochu, F. Escaso, A. Pérez-García, and F. Ortega. 2015. New crocodyliforms from Southwestern Europe and definition of a diverse clade of European Late Cretaceous basal eusuchians. PloS One 10:e0140679.

Narváez, I., C. A. Brochu, F. Escaso, A. Pérez-García, and F. Ortega. 2016. New Spanish Late Cretaceous eusuchian reveals the synchronic and sympatric presence of two allodaposuchids. Cretaceous Research 65:112–125.

Narváez, I., C. A. Brochu, F. Escaso, A. Pérez-García, and F. Ortega. 2017. Analysis and phylogenetic status of the eusuchian fragmentary material from Western Europe assigned to Allodaposuchus precedens. Journal of Iberian Geology 43:345–361.

Nesbitt, S. J. 2011. The early evolution of archosaurs: Relationships and the origin of major clades. Bulletin of the American Museum of Natural History 352:1–292.

Norell, M. A., J. M. Clark, and J. H. Hutchison. 1994. The Late Cretaceous alligatoroid *Brachychampsa montana* (Crocodylia): new material and putative relationships. American Museum Novitates 3116:1–26.

Ortega, F. 2008. Libro de Resumens. XXIV Jornadas de La Sociedad Espanola de Paleontologia. pp.

Ortega, F., N. Bardet, and P. M. Callapez. 2015. The biota of the Upper Cretaceous site of Lo Hueco (Cuenca, Spain). Journal of Iberian Geology 41:83–99.

Owen, F. R. S. 1842. Report on British Fossil Reptiles (R. Taylor and J. E. Taylor (eds.)). British Association for the Advancement of Science for 1841, 145 pp.

Owen, F. R. S. 1850. On the communications between the cavity of the tympanum and the palate in the Crocodilia (gavials, alligators and crocodiles). Royal Society 140:521–527.

Parrilla-Bel, J., J. i Canudo, J. Fortuny, and S. Llacer. 2016. Glándulas de la sal en Maledictosuchus riclaensis (Metriorhynchidae, Thalattosuchia) del Calloviense de la Península Ibérica. Geogaceta 59:63–66.

Paulina-Carabajal, A., and L. Filippi. 2017. Neuroanatomy of the abelisaurid theropod *Viavenator*: The most complete reconstruction of a cranial endocast and inner ear for a South American representative of the clade. Cretaceous Research.

Paulina-Carabajal, A., J. Sterli, J. A. Georgi, S. F. Poropat, and B. P. Kear. 2017. Comparative neuroanatomy of extinct horned turtles (Meiolaniidae) and extant terrestrial turtles (Testudinidae), with comments on the palaeobiological implications of selected endocranial features. Zoological Journal of the Linnean Society 180:930–950.

Pierce, S. E., M. Williams, and R. B. J. Benson. 2017. Virtual reconstruction of the endocranial anatomy of the early Jurassic marine crocodylomorph *Pelagosaurus typus* (Thalattosuchia). PeerJ 5:e3225.

Piras, P., P. Colangelo, D. C. Adams, Á. D. Buscalioni, J. Cubo, T. Kotsakis, C. Meloro, and P. Raia. 2010. The Gavialis-Tomistoma debate: The contribution of skull ontogenetic allometry and growth trajectories to the study of crocodylian relationships. Evolution and Development 12:568–579.

Platt, S. G., T. R. Rainwater, J. B. Thorbjarnarson, and D. Martin. 2011. Size estimation, morphometrics, sex ratio, sexual size dimorphism, and biomass of *Crocodylus acutus* in the coastal zone of Belize. Salamandra 47:179–192.

Pol, D., P. M. Nascimento, A. B. Carvalho, C. Riccomini, R. A. Pires-Domingues, and H. Zaher. 2014. A new notosuchian from the Late Cretaceous of Brazil and the phylogeny of advanced notosuchians. PLoS ONE 9:e93105.

Porter, W. R., J. C. Sedlmayr, and L. M. Witmer. 2016. Vascular patterns in the heads of crocodilians: blood vessels and sites of thermal exchange. Journal of Anatomy 1–25.

Puértolas-Pascual, E., J. I. Canudo, and P. Cruzado-Caballero. 2011. A new crocodylian from the late maastrichtian of spain: Implications for the initial radiation of crocodyloids. PLoS ONE 6.

Puértolas-Pascual, E., J. I. Canudo, and M. Moreno-Azanza. 2014. The eusuchian crocodylomorph Allodaposuchus subjuniperus sp. nov., a new species from the latest Cretaceous (Upper Maastrichtian) of Spain. Historical Biology 26:91–109.

Radinsky, L. B. 1968. A new approach to mammalian cranial analysis, illustrated by examples of prosimian primates. Journal of Morphology 124:167–180.

Salisbury, S. W., R. E. Molnar, E. Frey, and P. M. A. Willis. 2006. The origin of modern crocodyliforms: New evidence from the Cretaceous of Australia. Proceedings of the Royal Society B: Biological Sciences 273:2439–2448.

Schmitz, L. 2009. Quantitative estimates of visual performance features in fossil birds. Journal of Morphology 270:759–773.

Seeley, H. G. 1880. Note on the cranial characters of a large teleosaur from the Whitby Lias preserved in the Woodwardian Museum of the University of Cambridge, indicating a new species, *Teleosaurus eucephalus*. Quartery Journal of Geology Society of London 36:627–634.

Sereno, P. C., S. McAllister, and S. L. Brusatte. 2005. TaxonSearch: a relational database for suprageneric taxa and phylogenetic definitions. PhyloInformatics 8:1–21.

Serrano-Martínez, A., F. Knoll, I. Narváez, S. Lautenschlager, and F. Ortega. 2018. Inner skull cavities of the basal eusuchian Lohuecosuchus megadontos (Upper Cretaceous, Spain) and neurosensorial implications. Cretaceous Research.

Shirley, M. H., A. N. Carr, J. H. Nestler, K. A. Vliet, and C. A. Brochu. 2018. Systematic revision of the living African slender-snouted crocodiles (*Mecistops* gray, 1844). Zootaxa 4504:151–193.

Sobral, G., and J. Müller. 2016. Archosaurs and their kin: the ruling reptiles; pp. 285–326 in J. A. Clack, R. R. Fay, and A. N. Popper (eds.), Evolution of the vertebrate ear. Evidence from the fossil record. vol. 59. Springer.

Storrs, G. W., S. G. Lucas, and R. M. Schoch. 1983. Endocranial cast of an Early Paleocene crocodilian from the San Juan Basin, New Mexico. Copeia 1983:842–845.

Tarsitano, S. F. 1985. Cranial metamorphosis and the origin of the Eusuchia. Neues Jahrbuch Für Geologie Und Paläontologie Abhandlungen 170:27–44.

Tarsitano, S. F. 1989. The evolution of the Crocodilia: A conflict between morphological and biochemical data. American Zoologist 29:843–856.

Torres, C. R., and J. A. Clarke. 2018. Nocturnal giants: evolution of the sensory ecology in elephant birds and other palaeognaths inferred from digital brain reconstructions. Proceedings. Biological Sciences 285:1–8.

Tschopp, E., J. Russo, and G. Dzemski. 2013. Retrodeformation as a test for the validity of phylogenetic characters: an example from diplodocid sauropod vertebrae. Paleontologia Electronica 16:1–23.

Turner, A. H. 2015. A review of *Shamosuchus* and *Paralligator* (Crocodyliformes, Neosuchia) from the Cretaceous of Asia. PloS One 10:e0118116.

Tykoski, R. S., T. B. Rowe, R. A. Ketcham, and M. W. Colbert. 2002. *Calsoyasuchus valliceps*, a new crocodyliform from the Early Jurassic Kayenta Formation of Arizona. Journal of Vertebrate Paleontology 22:593–611.

Vergne, A. L., M. B. Pritz, and N. Mathevon. 2009. Acoustic communication in crocodilians: From behaviour to brain. Biological Reviews 84:391–411.

Vidal, D., and V. Díez Díaz. 2017. Reconstructing hypothetical sauropod tails by means of 3D digitization: *Lirainosaurus astibiae* as case study. Journal of Iberian Geology 43:293–305.

Walker, A. D. 1970. A revision of the Jurassic reptile Hallopus victor (Marsh), with remarks on the classification of crocodiles. Philosophical Transactions of the Royal Society of London. Series B, Biological Sciences 257:323–372.

Walker, A. D., D. J. Gower, M. J. Benton, and A. D. Walker. 2002. *Erpetosuchus*, a crocodile-like basal archosaur from the Late Triassic of Elgin, Scotland. Zoological Journal of the Linnean Society 136:25–47.

Walsh, S. A., P. M. Barrett, A. C. Milner, G. A. Manley, and L. M. Witmer. 2009. Inner ear anatomy is a proxy for deducing auditory capability and behaviour in reptiles and birds. Proceedings of the Royal Society 276:1355–1360.

Watanabe, A., P. M. Gignac, A. M. Balanoff, T. L. Green, N. J. Kley, and M. A. Norell. 2018. Are endocasts good proxies for brain size and shape in archosaurs throughout ontogeny? Journal of Anatomy XXX:XXX–XXX.

Webb, G. J. W., and H. Messel. 1978. Morphometric analysis of *Crocodylus porosus* from the north coast of Arnhem Land, Northern Australia. Australian Journal of Zoology 26:1–27.

Weldon, P. J., and M. W. J. Ferguson. 1993. Chemoreception in crocodylians: anatomy, natural history and empirical results. Brain Behavior and Evolution 41:239–245.

Weldon, P. J., D. J. Swenson, J. K. Olson, and W. G. Brinkmeier. 1990. The American alligator detects food chemicals in aquatic and terrestrial environments. Ethology 85:191–198.

Wever, E. G. 1971. Hearing in the Crocodilia. Proceedings of the National Academy of Sciences of the United States of America 68:1498–1500.

Wharton, D. S. 2000. An enlarged endocranial venous system in *Steneosaurus pictaviensis* (Crocodylia: Thalattosuchia) from the Upper Jurassic of Les Lourdines, France. Comptes Rendus de l'Académie Des Sciences 331:221–226.

Wharton, D. S. 2002. The Evolution of the Avian Brain. PhD Dissertation. University of Bristol, Bristol, UK., 340 pp.

Williamson, T. E. 1996. ?*Brachychampsa sealeyi* sp. nov. (Crocodylia, Alligatoroidea) from the Upper Cretaceous (Lower Campanian) Menefee Formation, Northwestern New Mexico. Journal of Vertebrate Paleontology 16:421–431.

Witmer, L. M., and R. C. Ridgely. 2008. The paranasal air sinuses of predatory and armored dinosaurs (Archosauria: Theropoda and Ankylosauria) and their contribution to cephalic structure. Anatomical Record 291:1362–1388.

Witmer, L. M., and R. C. Ridgely. 2009. New insights into the brain, braincase, and ear region of tyrannosaurs (Dinosauria, Theropoda), with implications for sensory organization and behavior. Anatomical Record 292:1266–1296.

Witmer, L. M., R. C. Ridgely, D. L. Dufeau, and M. C. Semones. 2008. Using CT to peer into the past : 3D visualization of the brain and ear regions of birds, crocodiles, and nonavian dinosaurs; pp. 67–87 in H. Endo and R. Frey (eds.), Anatomical Imaging towards a new morphology. Springer, Tokyo.

Wu, X., D. B. Brinkman, and A. P. Russell. 1996. A new alligator from the Upper Cretaceous of Canada and the relationships of early eusuchians. Palaeontology 39:351–375.

Yeh, H.-K. 1958. A new crocodile from Maoming, Kwantung. Vertebrata Palasiatica 2:241–242.

Zelenitsky, D. K., F. Therrien, and Y. Kobayashi. 2009. Olfactory acuity in theropods: palaeobiological and evolutionary implications. Proceedings of the Royal Society B: Biological Sciences 276:667–673.

Zelenitsky, D. K., F. Therrien, R. C. Ridgely, A. R. McGee, and L. M. Witmer. 2011. Evolution of olfaction in non-avian theropod dinosaurs and birds. Proceedings of the Royal Society B: Biological Sciences 278:3625–3634.